US ARMY
LABORATORY COMMAND
MATERIALS TECHNOLOGY LABORATORY

AD

MTL TR 91-44

RELATIONSHIP BETWEEN COMPOSITION, STRUCTURE, PROPERTIES, THERMO-MECHANICAL PROCESSING AND BALLISTIC PERFORMANCE OF TUNGSTEN HEAVY ALLOYS

November 1991

JAMES R. SPENCER
JAMES A. MULLENDORE

GTE Products Corporation
Towanda, PA 18848

FINAL REPORT

Contract DAAL04-86-C-0023

Approved for public release; distribution unlimited.

Prepared for
U.S. ARMY MATERIALS TECHNOLOGY LABORATORY
Watertown, Massachusetts 02172-0001

The findings in this report are not to be construed as an official Department of the Army position, unless so designated by other authorized documents.

Mention of any trade names or manufacturers in this report shall not be construed as advertising nor as an official indorsement or approval of such products or companies by the United States Government.

DISPOSITION INSTRUCTIONS

Destroy this report when it is no longer needed.
Do not return it to the originator

UNCLASSIFIED

SECURITY CLASSIFICATION OF THIS PAGE (When Data Entered)

REPORT DOCUMENTATION PAGE		READ INSTRUCTIONS BEFORE COMPLETING FORM
1. REPORT NUMBER MTL TR 91-44	2. GOVT ACCESSION NO.	3. RECIPIENT'S CATALOG NUMBER
4. TITLE (and Subtitle) RELATIONSHIP BETWEEN COMPOSITION, STRUCTURE, PROPERTIES, THERMO-MECHANICAL PROCESSING AND BALLISTIC PERFORMANCE OF TUNGSTEN HEAVY ALLOYS		5. TYPE OF REPORT & PERIOD COVERED Final Report - March 1986 - July 1991
		6. PERFORMING ORG. REPORT NUMBER
7. AUTHOR(s) James R. Spencer James A. Mullendore		8. CONTRACT OR GRANT NUMBER(s) DAAL04-86-C-0023
9. PERFORMING ORGANIZATION NAME AND ADDRESS GTE Products Corporation Chemical and Metallurgical Division Towanda, Pennsylvania 18848		10. PROGRAM ELEMENT, PROJECT, TASK AREA & WORK UNIT NUMBERS
11. CONTROLLING OFFICE NAME AND ADDRESS U.S. Army Materials Technology Laboratory Watertown, Massachusetts 02172-0001 ATTN: SLCMT-PR		12. REPORT DATE November 1991 13. NUMBER OF PAGES 222
14. MONITORING AGENCY NAME & ADDRESS(if different from Controlling Office)		15. SECURITY CLASS. (of this report) Unclassified 15a. DECLASSIFICATION/DOWNGRADING SCHEDULE

16. DISTRIBUTION STATEMENT (of this Report)

Approved for public release; distribution unlimited.

17. DISTRIBUTION STATEMENT (of the abstract entered in Block 20, if different from Report)

18. SUPPLEMENTARY NOTES

Kenneth Tauer COR

19. KEY WORDS (Continue on reverse side if necessary and identify by block number)

Tungsten alloys	Impurities	Taylor testing
Composites	Mechanical properties	
Microstructure	Thermo-mechanical processing	

20. ABSTRACT (Continue on reverse side if necessary and identify by block number)

(SEE REVERSE SIDE)

DD FORM 1 JAN 73 1473 EDITION OF 1 NOV 65 IS OBSOLETE

UNCLASSIFIED

SECURITY CLASSIFICATION OF THIS PAGE (When Data Entered)

Block No. 20

ABSTRACT

A thorough study of the W-Ni-Fe heavy alloy system was made relating composition, structure, impurity content and thermo-mechanical processing to mechanical properties. Also explored were additions of cobalt, rhenium and ruthenium to the W-Ni-Fe system. Ballistic testing was done on a wide range of alloys and processing conditions. Ballistic tests included a 20mm in-house range, 30mm Phalanx, M791(25mm Bushmaster) and XM-881 (long rod Bushmaster).

ACKNOWLEDGMENT

The author wishes to acknowledge of efforts of Dr. William Snowden and Dr. Kenneth Tauer who realized the importance of doing this work and were instrumental in securing this contact. I also appreciate Ken's guidance and suggestions during the contract .

TABLE OF CONTENTS

List of Figures

List of Tables

INTRODUCTION

Traditional tungsten heavy alloys are W-Ni-Fe or W-Ni-Cu alloys containing 88 to 98% tungsten. Cobalt is also used in these alloys but to a lesser extent. These alloys are produced by blending the elemental powders, pressing billets from the blend and then liquid-phase sintering the billets. These alloys were first developed to provide high density materials that were easy to machine but were developed with little concern for mechanical properties. Initially W-Ni-Cu alloys were most common because the low melting point of copper made these alloys easier to sinter. As the demand for alloys with good mechanical properties increased, a shift occurred from the W-Ni-Cu alloys to the W-Ni-Fe alloys. One major problem with these alloys is their sensitivity to impurities and processing conditions. For example, the unworked elongation for 90W-7Ni-3Fe reported in papers presented at the 1977 High Density Alloy Materials Conference (1) ranged from 6.6% to 42%. Unfortunately that kind of variability resulted in a lot of bad data being reported in the literature along with highly variable ballistic performance.

Over the years there has been a gradual improvement if the quality and consistency of the tungsten heavy alloys being produced. At GTE we had developed the processing techniques to consistently produce high quality tungsten heavy alloys. That combined with our capability to produce high purity tungsten powder gave us the ability to produce alloys having a repeatable high ductility indicative of high quality. Having that ability we proposed that the time had come for a broadly based study of the interrelationship between the properties of the tungsten heavy alloys and various parameters that go into the manufacture of these alloys. Such a study had never been made. We felt that such a study be useful in defining the properties. Above all, we believed that it was of primary importance that all of the materials generated in this study be under close control and that they be fully characterized to insure that valid conclusions could be drawn from the data.

The purpose of this program was to do a thorough study of tungsten heavy alloys and the interrelationship between chemical composition, impurities, thermo-mechanical processing history, structure and ballistic properties. Ballistic testing was to include a wide range of types and sizes ranging from an in house 20mm range to full scale testing.

The approaches we used in this study were as follows:

1. Develop a baseline of mechanical and ballistic properties for W-Ni-Fe alloys of 90, 93 and 96% tungsten with nickel:iron ratios of 7/3.

The W-Ni-Fe alloys were chosen over W-Ni-Cu alloys because the W-Ni-Fe alloys have superior mechanical (2) and ballistic (3,4) properties. We chose a range of tungsten contents because we felt that different ballistic applications would require different combinations of density and mechanical properties for optimum performance. Generally the 7/3 nickel:iron ratio has been shown to give the best ductility(5,6) so it was initially chosen for our baseline evaluation. Central to the success of this approach was to assure that for each alloy the material we produced had unworked ductility and impact strength as good or better than those currently being reported for those alloys.

2. Determine the effects of impurities, nickel:iron ratio, structure, and thermo-mechanical processing on the W-Ni-Fe alloys.

We were interested in looking at impurities because low levels of impurities appear to greatly affect the ductility of tungsten heavy alloys. Much of the variation in properties reported for tungsten heavy alloys is likely due to undetected differences in impurity levels. For example, we have shown that very low levels of oxygen content is a probable cause of poor ductility in a W-Ni-Fe-Cu-Co alloy (7). Some investigators (8,9) have showed marked improvements in the ductility or toughness of W-Ni-Fe alloys when quenched from above 1000°C. One explanation for this improvement is that quenching prevents impurity segregation to the tungsten-matrix boundary. For our tungsten heavy alloys we use a very high-purity tungsten powder and have not noted a dramatic effect when quenching.

While a 7/3 nickel:iron ratio appears to give the best ductility it is unclear as to what ratio might give the best ballistic performance. Subscale testing by Bloore (10) appeared to show that the best nickel:iron ratio varied depending on tungsten content. Although we have found that tungsten grain size has little effect on the mechanical properties of tungsten heavy alloys we were interested in learning if tungsten grain size affects ballistic properties. We achieved grain size differences by altering the sintering schedule and exploring the use of tungsten heavy alloy powders formed by plasma spraying. Finally as part of this approach we were interested in learning how method of working as well as the total amount of work affected mechanical and ballistic properties

3. Explore the potential for improved ballistic performance through alloy additions, novel thermo-mechanical processing and composite structures.

The alloying additions to W-Ni-Fe alloys that we wanted to look at were cobalt, rhenium and ruthenium. Cobalt additions have been the subject of many studies. Work done by GTE and elsewhere (5,11) indicate that cobalt might improve mechanical properties. Both rhenium (12) and ruthenium (13) have been shown to be effective in reducing the tungsten grain size in tungsten heavy alloys. We believed that a much finer grain size might improve ballistic performance and that the rhenium and ruthenium additions might strengthen the W-Ni-Fe matrix.

The novel thermo-mechanical treatments we used had reductions in area greater than 75% and were designed to develop material with very high tensile strengths and highly elongated tungsten grains in hopes of improving ballistic performance. Normal thermo-mechanical treatments use reductions in area of 25% or less.

Composite penetrators were designed with cores of material that we felt would perform very well against targets at 0° obliquity but are too brittle to do well against high obliquity targets. We hoped that by surrounding these cores with a ductile material improved ballistic performance could be achieved.

4. Concurrent with the other approaches tensile, impact, hardness and Taylor tests were evaluated to determine if they could be related to ballistic performance.

Some of the work on thermo-mechanical processing has been classified and is covered in a separate classified report.

SUMMARY

As a result of this program several significant findings were made. Among them were:

Nickel:Iron Ratios
The results clearly show that the optimum nickel:iron ratio for W-Ni-Fe alloys is closer to 8/2 instead of 7/3 which traditionally was thought to be the best. The 8/2 ratios have superior mechanical properties and in some cases show improved ballistic properties.

If W-Ni-Fe alloys with nickel:iron ratios of 9/1 are quenched from above 1000 °C they will have better impact properties than alloys with 8/2 nickel:iron ratios. Because they don't require quenching the 8/2 nickel:iron ratio would appear to be an optimum ratio for actual applications.

During deformation of tungsten heavy alloys defects develop between the tungsten grains and the matrix. For the 8/2 nickel:iron ratios and higher we found a dramatic decrease in the number of these defects as compared to the 7/3 ratio alloys.

Equally as important as the mechanical properties is the increased workability of the alloys with the 8/2 ratios. These alloys work harden at a slower rate and have the ability to be annealed back to as sintered properties. This enables these alloys to be repeatedly worked and annealed to achieve large reductions and still maintain good tensile properties.

Impurities
It was shown that even small levels of impurities of chromium or silicon in the tungsten powder used in heavy alloy blends may have detrimental effects on the mechanical properties of the alloys. Quenching the alloys made with the impure tungsten powder can restore mechanical properties to those made with the purer powders. This may explain why some investigators have seen improvements by quenching and we have not.

Alloying Additions
Small additions of ruthenium were shown to reduce the tungsten grain size and increase the yield strength in W-Ni-Fe alloys. These improvements came about with only a nominal loss in elongation but with a larger loss in impact strength.

Adding cobalt to the W-Ni-Fe alloys resulted in slightly finer grain sizes. At the 2% level cobalt appeared to improve impact properties.

Large Reductions in Area
Procedures were developed where swaging could be used to give tungsten heavy alloys large reductions in area. With these large reductions in area we were able to develop yield strengths much higher than traditionally swaged materials. Based on our in-house testing these heavily worked materials have superior ballistic properties.

Solid State Sintered Alloys

A procedure was developed to swage tungsten heavy alloys that had only been solid-state sintered. These alloys have a substantially different structure than standard tungsten heavy alloys. After only 70% reduction in area the results from our 20mm ballistic testing showed the solid state sintered alloys to be similar to the liquid-phase sintered alloys.

Two areas that we looked at that did not yield significant improvements in properties were plasma powders and macro-composite structures. Our findings for these were as follows.

Plasma Powders

When processed through a plasma gun tungsten heavy alloys form tungsten heavy alloy particles with very fine tungsten grains. We had hoped to processes these powders into bars while still retaining the fine tungsten grain size. We found however that at even at low temperatures the tungsten grains began to grow together in a continuous phase. Also the oxygen level in bars produced from plasma powders was too high.

Macro-Composite Structures

While we were successful in making macro-composite 20mm penetrators they had slightly poorer than average performance. The composite penetrator with the tungsten carbide core was very poor.

Ballistic Testing

Time and money limitations did not allow for the range of ballistic testing we desired to do but some findings were significant.

20mm

The 20mm ballistic testing did show that 8/2 nickel:iron ratios were better than the 7/3 ratios. It also showed that a very high oxygen content compromises ballistic performance. Probably the most significant finding was that some of our novel approaches such as ruthenium additions, solid-state sintered alloys and heavily worked materials had ballistic properties at least as good or better than the conventional materials. The heavily worked materials were among the best we tested.

30 mm Phalanx

The 30mm Phalanx showed the 93% tungsten alloy with the 8/2 nickel:iron ratio to be superior to the 7/3 nickel:iron ratio. As expected it also showed the 93% alloys to be better than the 90 or 96% alloys. Also working the alloys did not improve performance.

M791/XM-881

The results of the M-791 and XM-881 testing didn't show 8/2 alloys to be superior to 7/3 alloys. One significant finding was that a 96% tungsten alloy with a 8/2 nickel:iron ratio had the best performance of the alloys tested as a XM-881. Previously we had thought the best alloys for this penetrator would be closer to a 93% tungsten alloy.

EXPERIMENTAL PROCEDURES

Blend Preparation

Powder blends were made by sifting the elemental powders -200 mesh and then blending them for one hour in a twin shell blender. For most blends we used a GTE M-55 tungsten powder which has a FSSS of about 5μm. For the nickel and iron powders we used carbonyl powders which had particle sizes in the same range as the tungsten powder. After blending iron and nickel content were determined using atomic adsorption.

Pressing

Bars were pressed in an isostatic press using pressures of 30 ksi. Molds were tapped while being filled and sealed without evacuation. After pressing bars were about 12" long with a diameter of 0.8" and weighed 1 kilogram. Green density of these bars typically ran about 60% of theoretical density.

Sintering

Except for sintering tests using vacuum or nitrogen the sintering work was done in a Hayes three-zone open-element stoke furnace which had an effective hot zone of about 36". Bars were sintered in a bed of alumina sand in molybdenum boats. Other than in tests where we were trying to vary tungsten grain size, we used a two-step sintering schedule that we have found to give good results. The first step is a solid-state sinter in hydrogen at 1400-1420°C using a stoke rate of 12"/hr. The incoming hydrogen is bubbled through room-temperature water which results in a dew point in the hot zone of >20°C. The following table shows the sintering conditions for liquid-phase sintering which vary depending on the tungsten content of the alloy. Stoke rates for all tungsten contents were 48 in/hr. These conditions were varied as required when sintering alloys other than the standard W-Ni-Fe alloys.

Liquid Phase Sintering Conditions

Tungsten %	Sintering Temp(°C)	Atmosphere	Dew Point(°C)
90	1500	H2	>20
93	1520	H2	>20
96	1550	75N2-25H2	0

Post-Sintering Heat Treatment
After sintering all of the alloys were heat treated for three hours at 1200°C in vacuum to remove hydrogen. Other than for special tests we did not quench the alloys from the heat treating temperature.

Swaging
Prior to swaging, bars were machined to a starting diameter to assure a consistent reduction in area. Bars were soaked in a oven at 300°C for at least 1/2 hour before they were swaged. For 8 and 15% reductions in area a single pass was used. For 25% reductions in area we used a 15% pass followed by a 12% pass to achieve the desired reduction. No anneals were used between passes.

Physical and Mechanical Properties

Microstructure For microstructure evaluation we used both the Jeffries grain count and a Carl Zeiss MOP-3. Because the tungsten grains do not take up 100% of the area, the Jeffries grain count had to be corrected. In making this correction we assumed the matrix contained 25% tungsten (14).

The MOP-3, manufactured by Carl Zeiss, Inc., uses a magnetized tablet on which microphotographs are placed and then objects of interest are traced with a pen. A microprocessor in the MOP-3 determines perimeter and area of the traced object. From this data grain size, grain shape and contiguity can be determined.

Tensile Properties Our tensile properties were determined using a threaded tensile sample that had a 0.25" diameter by 1" long gauge. Samples were pulled using a cross head speed of 0.005"/min to yield and then 0.05"/min to failure. Elongation was determined by piecing the broken specimen back together and measuring the one inch gauge that had been marked on it.

Impact Test Impact tests were carried out on an instrumented pendulum -type impact tester using an unnotched 5mm square Charpy bar as the sample. In addition to total energy the system provides slope, load at yield, and maximum load.

Hardness Hardness was determined using the Rockwell C scale. Each time we determined hardness a standard block was tested and a correction factor calculated. When testing worked specimens we took the hardness on a face perpendicular to the working direction.

In a few cases we wanted to determine tungsten grain hardness so we used a Vickers indenter with a 100 g load. For worked samples, we took the hardness on a face perpendicular to the working direction.

Chemical Properties

Tungsten Powder The tungsten powders we used were analyzed for impurities by spectrographic quantitative analysis.

Nickel Powder The nickel powder we used was Inco 123. We analyzed this powder only for carbon and found it to be 580 ppm

Iron Powder We used GAF iron powder and analyzed it only for carbon which we found to be 700 ppm.

Blends The nickel and iron values in our blends were determined by atomic adsorption.

Oxygen Oxygen values in good tungsten heavy alloys are typically less than 30 ppm (7). From our experience at GTE we found that for tungsten heavy alloys vacuum fusion is the preferred method of analysis. At one time we sent tungsten heavy alloy samples for oxygen analysis to Luvak of Boylston, Massachusetts because they used vacuum fusion for oxygen analysis. When they switched to carrier gas fusion for oxygen analysis, we no longer used them for our oxygen analysis. Believing we could no longer obtain vacuum fusion analysis we looked at other techniques to see if they could be used for our oxygen analysis in this work.

Carrier gas fusion was the first method we looked at and is what we use at GTE for all our oxygen analysis. The primary problem with this method is that it requires a very small sample size and for tungsten heavy alloys it is difficult to avoid adding oxygen to the sample when preparing it for analysis. Also the method requires a nickel accelerator which adds to the variability of the analysis. The first thing we looked at was the nickel accelerator. In addition to nickel powder which is our normal accelerator, we looked at nickel wire baskets. Using only the nickel accelerator we got the following results:

Accelerator	Std. Dev (oxygen ppm)	Number of Samples
Large Basket	11	9
Small Basket	9	35
Nickel Powder	22	90

Based on these results we switched to the nickel baskets for our accelerator. Using the gage sections of tensile specimens of several different tungsten heavy alloy we cut 0.10 gram slices for oxygen analysis. We analyzed these samples as cut, acetone rinsed and acid washed. Table I contains the results for these samples and at best the analysis showed that we had 48 ppm oxygen in samples that we were confident had less than 20ppm of oxygen. The standard deviations also were too high to make this method useful in the work we had planned.

Table I Oxygen Analysis By Inert Carrier Gas Fusion

		Oxygen(ppm)	
Alloy	Condition	Average	Std. Dev.
90W-7Ni-3Fe	As-Cut	241	95
"	Acetone Washed	312	113
"	Acid Etched	133	89
93W-4.9Ni-2.1Fe	As-Cut	404	104
"	Acetone Washed	339	193
"	Acid Etched	127	84
95W-3.5Ni-1.5Fe	As-Cut	240	75
"	Acetone Washed	424	91
"	Acid Etched	127	32
96W-2.8Ni-1.2Fe	As-Cut	234	85
"	Acetone Washed	238	168
"	Acid Etched	100	30
97.3W-1.9Ni-0.8Fe	As-Cut	208	95
"	Acetone Washed	199	76
"	Acid Etched	48	29

The other method we looked at was neutron activation which was performed by IRT Corporation of San Diego, California. Neutron activation uses a large sample but because of the air delivery system used to transport the samples and the density of tungsten we had to limit our sample size to a piece 1.35" long by 0.563" in diameter. This size required the sample to be placed in poly-ethylene tubing which added to the variability of the analysis. We confirmed this variability by submitting blind samples and found the oxygen analysis to vary as much as 60% as shown in Table II.

Table II Oxygen Analysis By Neutron Activation

	First Submission		Second Submission	
Alloy	Oxygen(ppm)	±(ppm)	Oxygen(ppm)	±(ppm)
90W-7Ni-3Fe	33.4	4.5	21.4	5.3
90W-7Ni-3Fe	13.9	3.7	23.6	6.9

After we had begun our work on oxygen analysis we learned that Luvak was again using vacuum fusion for some oxygen analysis. Apparently they also found that for tungsten alloys vacuum fusion was the better method. Advantages of this method are that the sample is large enough that the surface can be filed just before analysis and the process does not require a flux. Based on our past experience with this method we decided to use it for all our oxygen work in the contract.

20mm Ballistic Testing

A key element of this contract was to set up and operate a ballistic testing range to evaluate material and screen material for further ballistic testing. The range was designed to use a 20mm gun barrel and fire penetrators with a L/D of 10/1.

The process of constructing the building, setting up the range, developing procedures and designing the penetrator package took about two years. Most of the work centered around designing the penetrator package and firing procedures to get consistent launches with yaws less than 1°. Specifications for our testing range are as follows:

20mm Range Specifications

Gun Barrel	20mm smooth bore
Gun to Target	16 ft (4.88 m)
Velocity Measurement	Light screens - 10 ft spacing (3.05 m)
Yaw Measurement	Witness Screen
Throw Weight	62 grams (2.19 oz)
Velocity	1400 m/sec max (4600 ft/sec)
Penetrator Package	4 piece sabot, pusher plate and obturator
Penetrator	0.238" x 2.38"* heminose (0.605 x 6.05 cm)
Target	1" (2.54 cm) thick High Hard Armor (MIL-A-46100) Rockwell C 48.5 to 50
Target Angle	57°

* 93% tungsten alloy - length was adjusted for other alloys to maintain constant penetrator weight

Prints for all parts of the penetrator are in the appendices of the report. Also in the appendices are the hardness and impact tests on the armor we used.

V-50 Determination: The ballistic property we determined in our range was the "V-50". Our goal was to have five shots that defeated the target and five that didn't all within a 100 ft/sec range. We considered the target to be defeated if any cracking occurred on the back of the target. We only used shots that showed no yawing as determined by a witness screen just in front of the target. The "V-50" number we report is the average of the velocity average of shots that did penetrate and the average of those that didn't penetrate.

BASELINE EVALUATION

The purpose of the baseline evaluation was to determine the mechanical properties and ballistic performance of what we believed to be the best of the W-Ni-Fe alloys. This data was essential to determine if the processing and alloying changes we made during the contract resulted in significant improvements in the properties of these alloys. Although a great deal of data exists on W-Ni-Fe alloys, much of it is flawed because these alloys are very sensitive to processing, impurities and the type of tungsten powder used.

Different targets require different combinations of density and hardness so for our baseline evaluation we looked at a range of densities and hardness. We used alloys containing 90, 93 and 96% tungsten which gave us densities from about 17.1 to 18.4 g/cc. To vary hardness we evaluated the alloys in the unworked, swaged, and aged condition. This resulted in a Rockwell C hardness range of about 30 to 45.

Initially for the baseline evaluation we intended only to look at alloys with 7/3 nickel:iron ratios because that ratio generally was assumed to be optimum for W-Ni-Fe alloys (5,6). Early in our work with nickel:iron ratios however it became clear that the 8/2 ratio had superior tensile and impact properties so we included both 8/2 and 7/3 ratios in our baseline evaluation.

The blending, pressing and sintering procedures along with the powders described in the procedure section are those which we believe yield W-Ni-Fe alloys with optimum properties. From our initial examination of the microstructure as shown in Figure 1 it appeared that the 8/2 ratio alloys were under sintered and should be sintered at a slightly higher temperature than the 7/3 alloys. This is also supported by the W-Ni-Fe phase diagram (Figure 2) which shows the liquidus temperature of the 8/2 ratio to be about 10°C higher than the 7/3 ratio. Based on these observation we decided for the 90 and 93% tungsten alloys with 8/2 ratios to use a liquid-phase sintering temperature 10°C higher than we did for the 7/3 ratios. For the 96% tungsten alloys which we normally sintered well above the liquidus temperature we used the same sintering temperature for all Ni:Fe ratios.

Unworked Properties

Figures 3 - 5 are microstructures of the as-sintered alloys included in our baseline evaluation and are typical of what we consider to be a good structure. They are pore free, have large well rounded tungsten grains, a continuous matrix, and show no obvious sign of a second phase in the matrix. The matrix in W-Ni-Fe alloys has been shown to be FCC and depending on the nickel:iron ratio, contains about 25 to 30% tungsten (14).

Table III contains the results of a test run to generate quantitative information of the microstructures. The data shows the structures to be uniform as there is no significant difference between the structures in the center and those at the mid radius. As expected there was an increase in tungsten grain size as the tungsten content of the alloy increased. During sintering much of the tungsten grain growth takes place by coalescence(15) which partly explains why the tungsten grain size increases with increasing tungsten content. Also the higher temperatures we use to sinter the alloys with higher tungsten contents probably contributed to the coarser grain size. As would be expected(16), the contiguity, a measure of the amount of tungsten-tungsten grain boundaries, increased with increasing tungsten content.

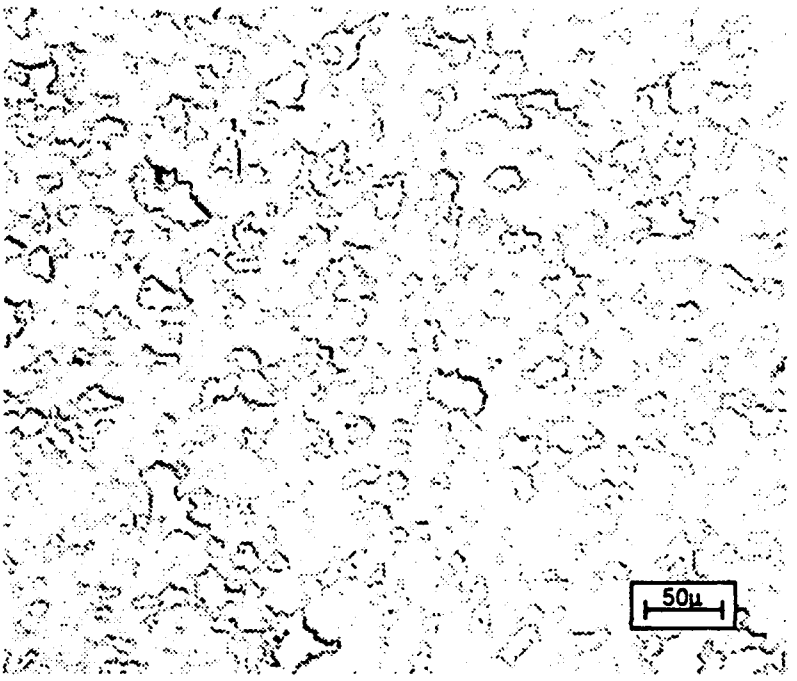

Figure 1 Under-Sintered 90W-8Ni-2Fe

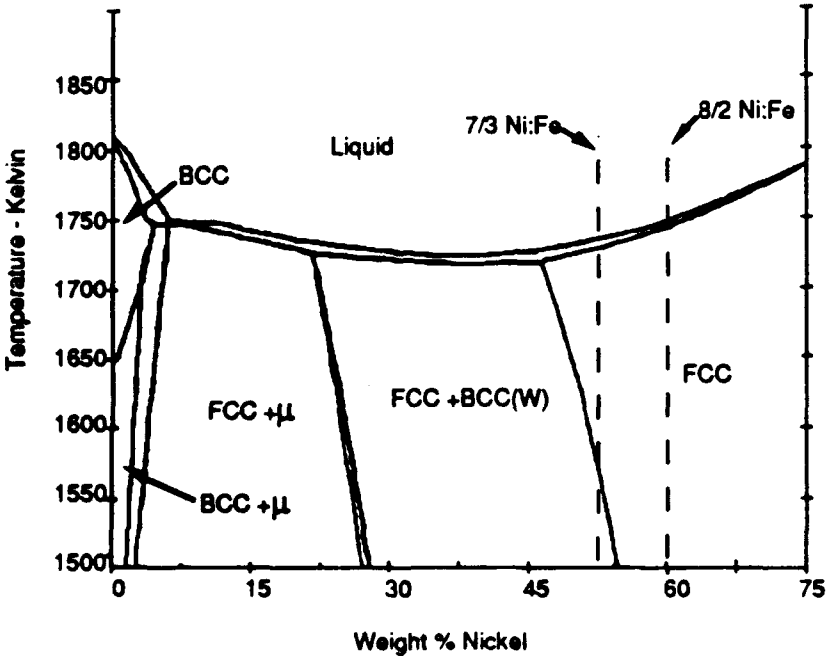

Figure 2 Phase Diagram of Ni-Fe-25W (14)

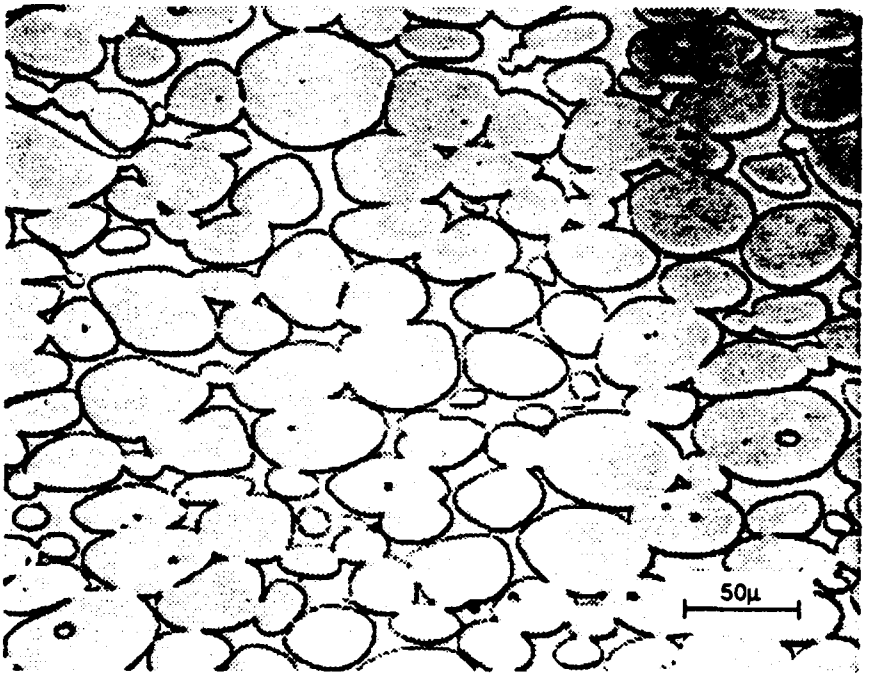

90W-7Ni-3Fe(7/3 Ni:Fe)

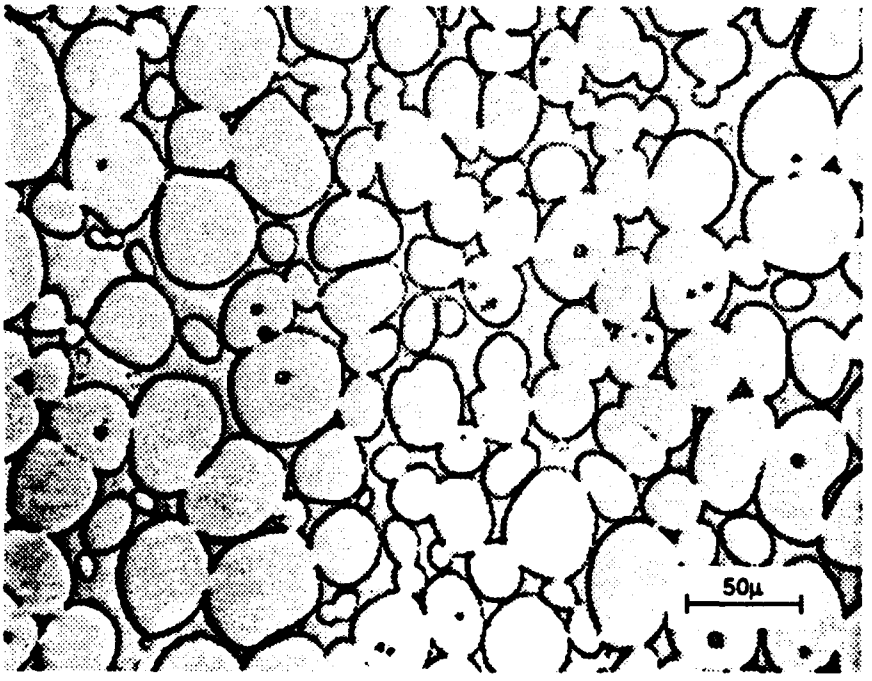

90W-8Ni-2Fe(8/2 Ni:Fe)

Figure 3 As-Sintered Microstructures of 90W-Ni-Fe Alloys

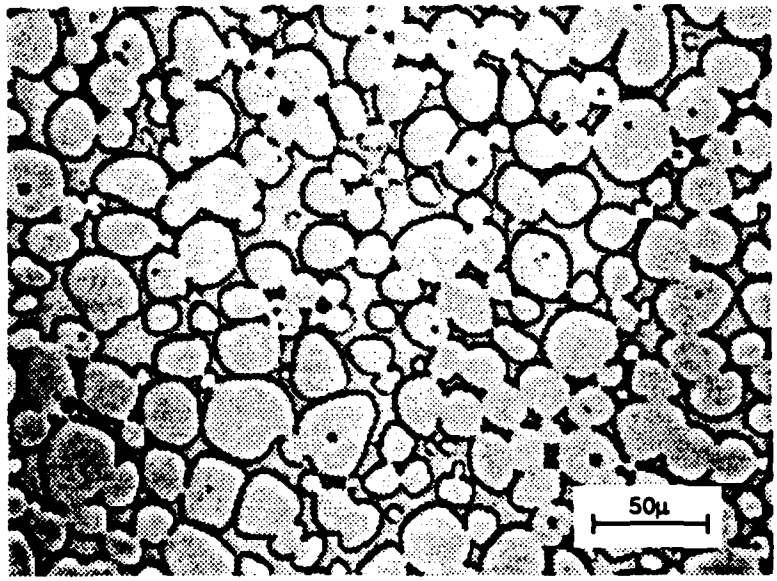

93W -4.9Ni -2.1Fe(7/3 Ni:Fe)

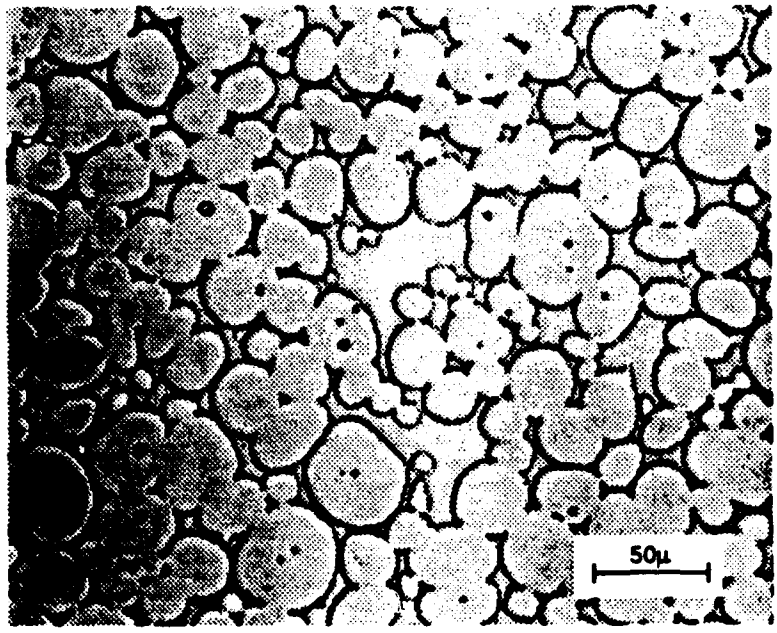

93W -5.6Ni -1.4Fe(8/2 Ni:Fe)

Figure 4 As-Sintered Microstructures of 93W-Ni -Fe Alloys

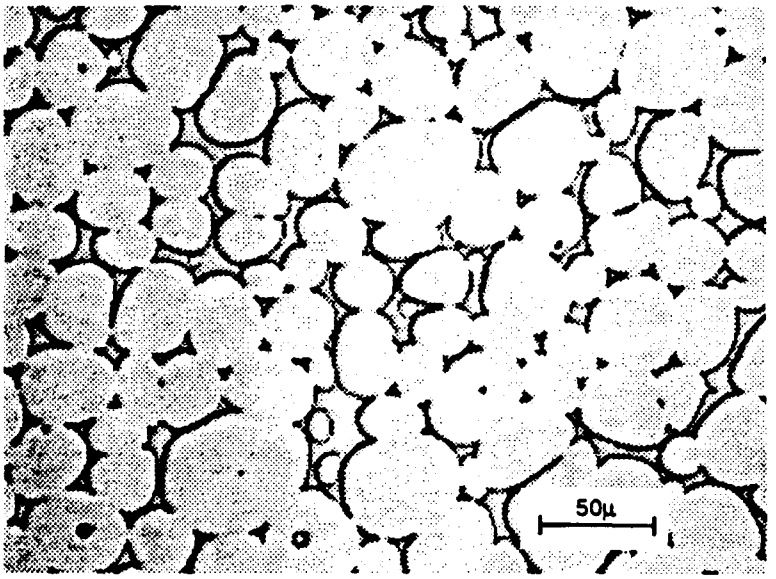

96W -2.8Ni -1.2Fe(7/3 Ni:Fe)

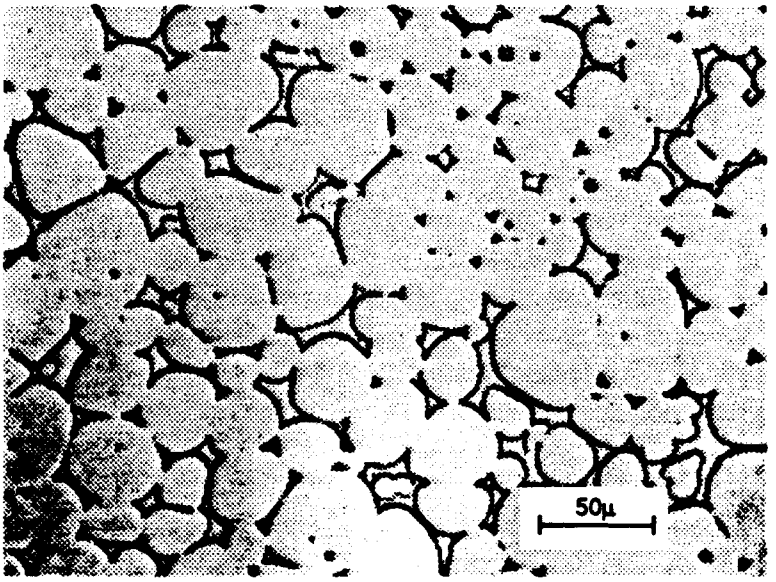

96W -3.2Ni -0.8Fe(8/2 Ni:Fe)

Figure 5 As-Sintered Microstructures of 96W - Ni -Fe Alloys

One result we did not anticipate was that the grain size of the 93 and 96% tungsten alloys with 8/2 nickel:iron ratios had a larger grain size than the corresponding alloys with 7/3 ratios. For the 93% tungsten alloys part of the grain size increase might have been due to the slightly higher sintering temperature used. Contiguity has been shown to increase with decreasing grain size(16) and probably explains why the 8/2 ratio alloys also had lower contiguities.

Table III Microstructure Evaluation of Unworked Tungsten Heavy Alloys

		Grain Count (grains/mm2)		----------MOP-3 Data---------- Diameter(μ)		Contiguity(%)	
Alloy	Ni/Fe	Center	M.R.*	Center	M.R.*	Center	M.R.*.
90W-7Ni-3Fe	7/3	2340	2280	27	28	12	12
90W-8Ni-2Fe	8/2	2310	2220	27	28	10	14
93W-4.9Ni-2.1Fe	7/3	2260	2100	30	30	18	20
93W-5.6Ni-1.4Fe	8/2	1330	1250	37	37	15	14
96W-2.8Ni-1.2Fe	7/3	1440	1390	36	36	34	30
96W-3.2Ni-0.8Fe	8/2	790	730	44	41	24	24

* Mid Radius

Table IV contains the tensile properties for the unworked alloys and represents the average of a large number of samples generated throughout the contract. The hardness and impact properties are in Table V. For the elongation and impact strengths the range and standard deviations are also given. Because the matrix is the continuous phase, hardness and yield strength vary little as the percent tungsten increases. Elongation and impact strength drop sharply with the higher tungsten contents because of the decrease in volume percent matrix and an increase in tungsten grain contiguity.

The surprising result was that the alloys with the 8/2 nickel:iron ratio appear to have superior impact properties to the 7/3 ratio alloys. For the 90W-8Ni- 2Fe alloy the ductility was so high that many of the impact samples pulled through the fixture without breaking. While the 8/2 ratio alloys had slightly lower contiguities, that alone could not explain the superior properties of these alloys. This is discussed further in the section on nickel:iron ratios.

Table IV Tensile Properties of Unworked Tungsten Heavy Alloys

Alloy	Ni/Fe	Tests	Ave. UTS(ksi)	Ave. YS(ksi)	Elongation(%) Average	Range	Std. Dev.	RIA (%)
90W-7Ni-3Fe	7/3	30	136	85	34	28-37	2.5	40
90W-8Ni-2Fe	8/2	33	140	86	38	35-43	2.3	40
93W-4.9Ni-2.1Fe	7/3	42	140	88	32	27-38	2.4	31
93W-5.6Ni-1.4Fe	8/2	41	140	87	34	27-40	3.4	31
96W-2.8Ni-1.2Fe	7/3	30	140	88	23	16-30	3.7	19
96W-3.2Ni-0.8Fe	8/2	32	141	87	25	16-30	3.4	19

Table V Hardness and Impact Energy of Unworked Tungsten Heavy Alloys

Alloy	Ni/Fe	Hardness (Rc)	Impact Energy (ft-lbs) Average	Range	Std. Dev.	Tests
90W-7Ni-3Fe	7/3	31.0	32	20-43	6.2	17
90W-8Ni-2Fe	8/2	30.0	47*	31-56	7.9	31
93W-4.9Ni-2.1Fe	7/3	31.8	19	15-26	2.7	29
93W-5.6Ni-1.4Fe	8/2	31.2	31	15-44	5.9	38
96W-2.8Ni-1.2Fe	7/3	31.6	8.1	5-14	2.0	30
96W-3.2Ni-0.8Fe	8/2	31.6	12	6-18	3.5	35

* Most bars did not break - actual impact energy would be higher

Worked Properties

After evaluating the unworked properties our next step was to evaluate these alloys after swaging 8, 15 and 25 percent. Swaging 8% is the minimum we believe we can swage and still have uniform working throughout the cross section. Much beyond 25% swaging defects can develop in the microstructure. Figures 7 - 12 are the longitudinal microstructure of the bars swaged 8 and 25%. At 25% reduction in area the 7/3 ratio alloys have some defects between the tungsten grains near the center of the bars. Figure 12 is a higher magnification than figures 6-11 showing this defect in a 96W-2.8Ni-1.2Fe alloy. It is interesting that these defects did not form in the alloys with the 8/2 ratios. This difference in the formation of defects is discussed further in the section on nickel:iron ratios.

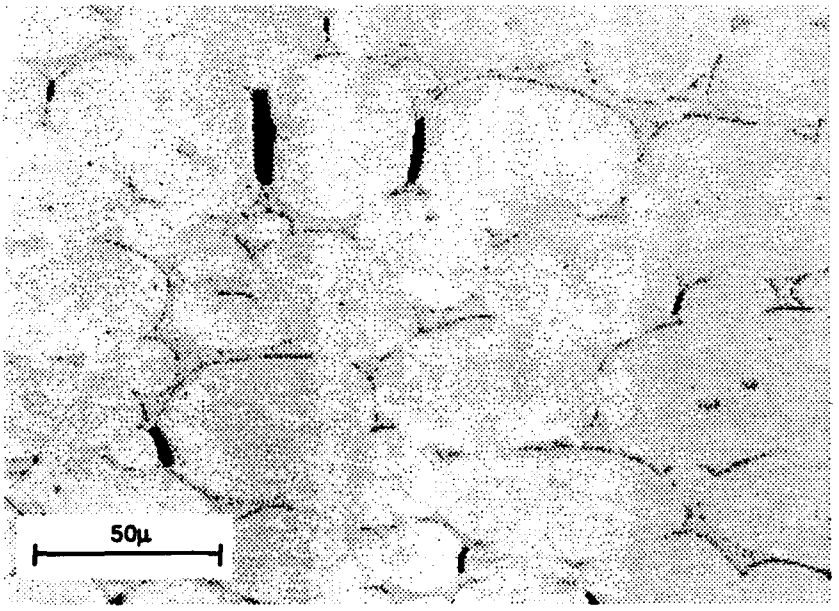

Figure 6 Defects in a 96W-2.8Ni-1.2 Fe(7/3) Swaged 25%

Table VI contains the tensile properties of the worked alloys and represent the average from 2 to 16 samples. Table VII contains the hardness and impact properties. The initial working of 8% causes a big jump in hardness and corresponding loss in elongation for all of the alloys. Beyond 8% there is only a slight increase in hardness and drop in elongation. For the same amount of work the 8/2 ratio alloys appear to have a lower hardness than the 7/3 ratio alloys. While the elongation continues to drop after the initial 8% reduction the impact properties appear to drop very little if any.

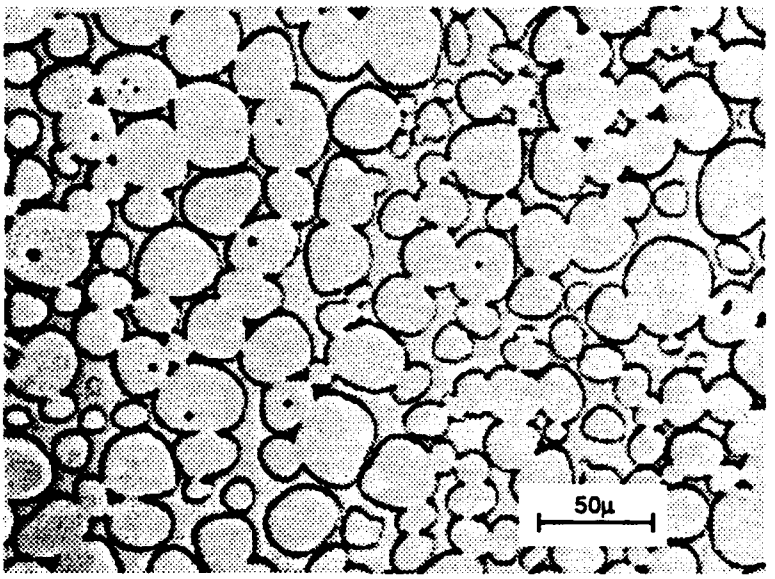

Swaged 8% RIA

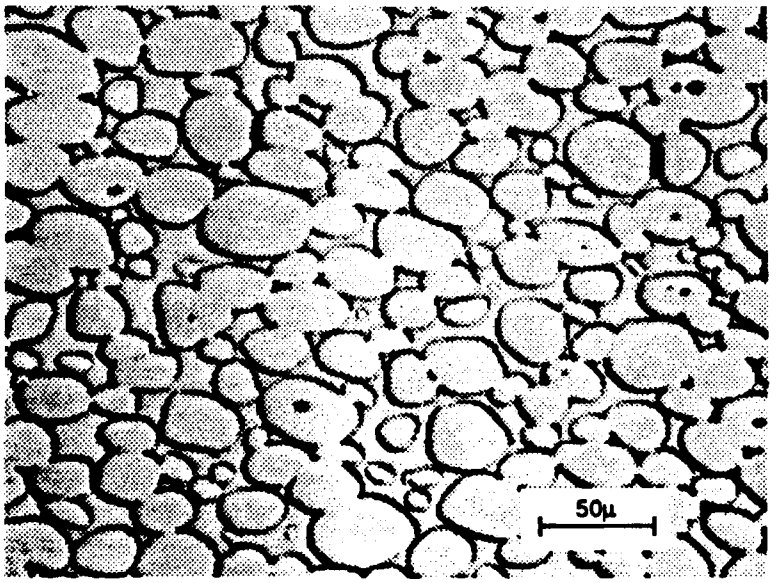

Swaged 25% RIA

Figure 7 Microstructures of Swaged 90W-7Ni-3Fe (7/3 Ni:Fe)

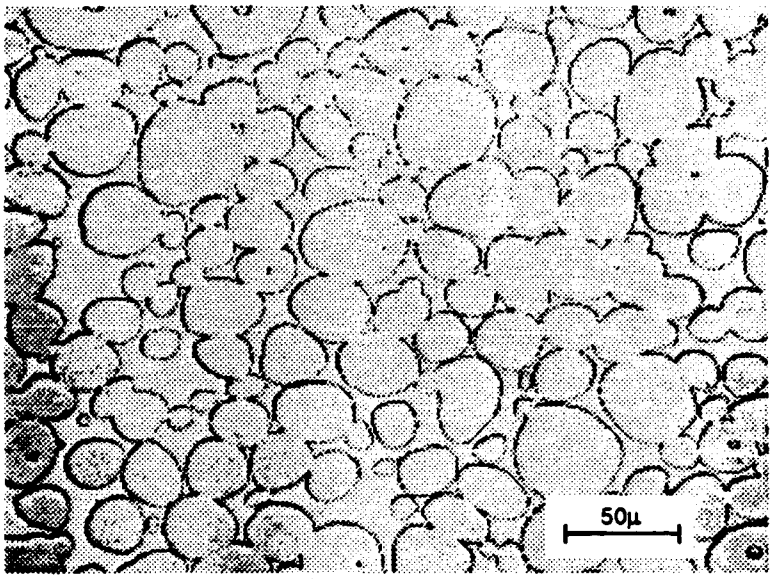

Swaged 8% RIA

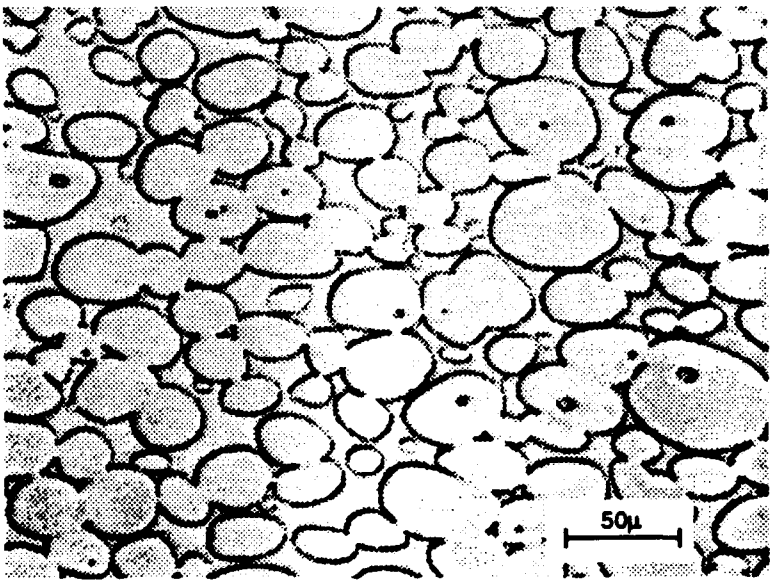

Swaged 25% RIA

Figure 8 Microstructures of Swaged 90W-8Ni-2Fe (8/2 Ni:Fe)

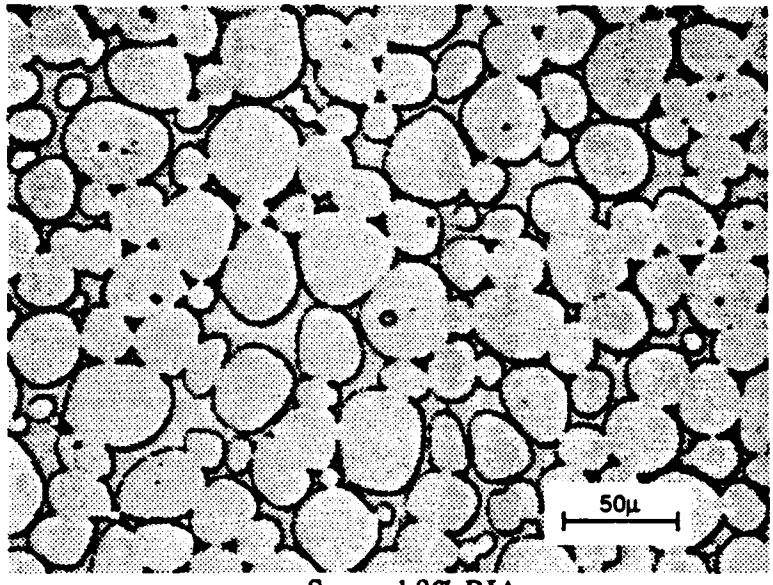

Swaged 8% RIA

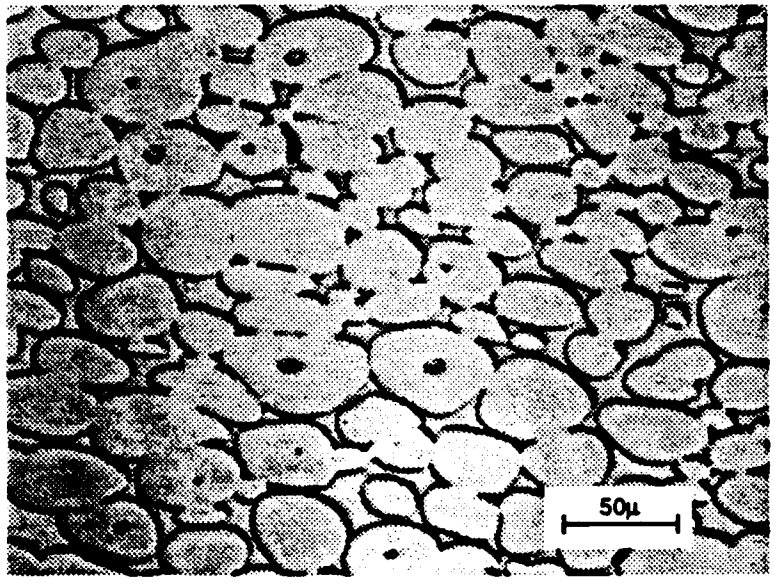

Swaged 25% RIA

Figure 9 Microstructures of Swaged 93W-4.9Ni-2.1Fe (7/3 Ni:Fe)

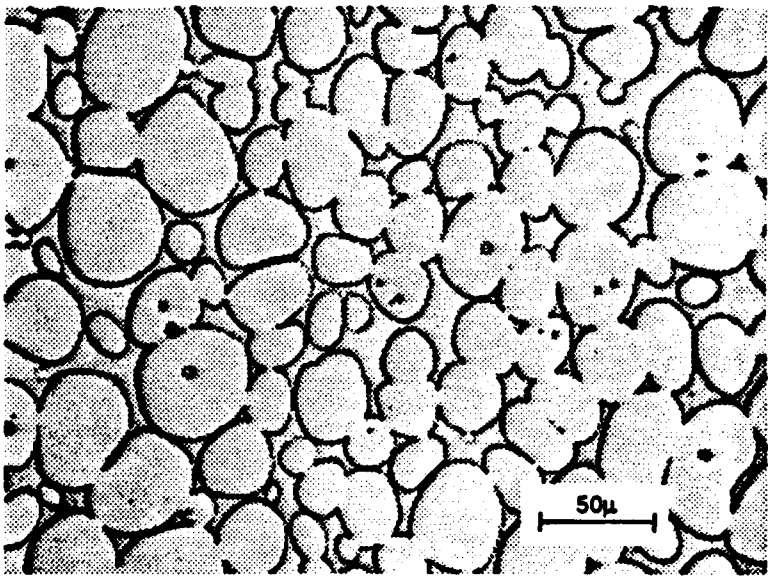

Swaged 8% RIA

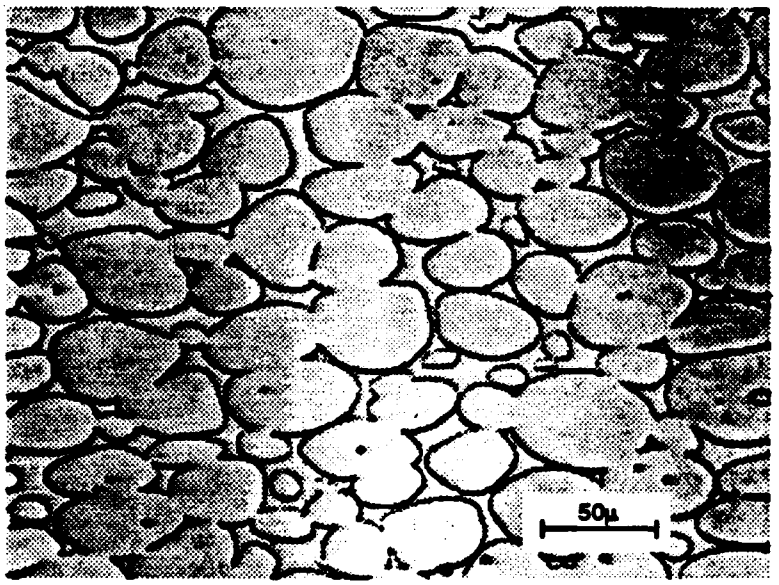

Swaged 25% RIA

Figure 10 Microstructures of Swaged 93W-5.6Ni-1.4Fe (8/2 Ni:Fe)

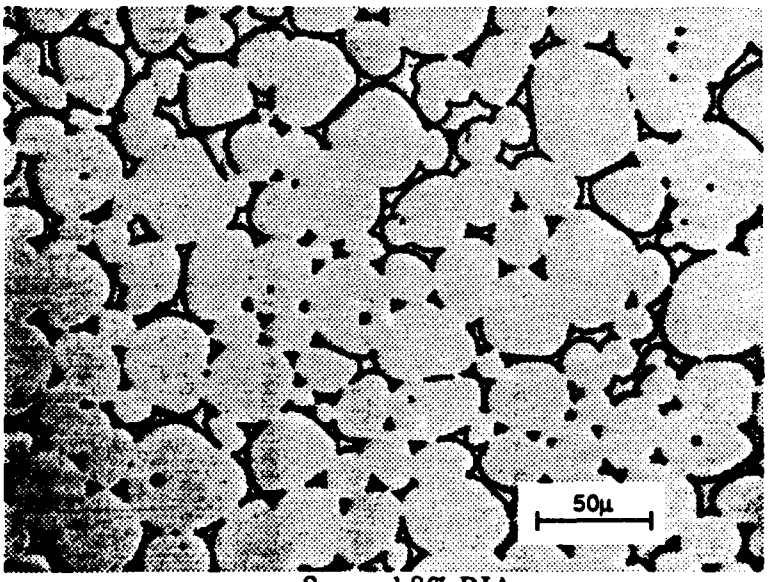

Swaged 8% RIA

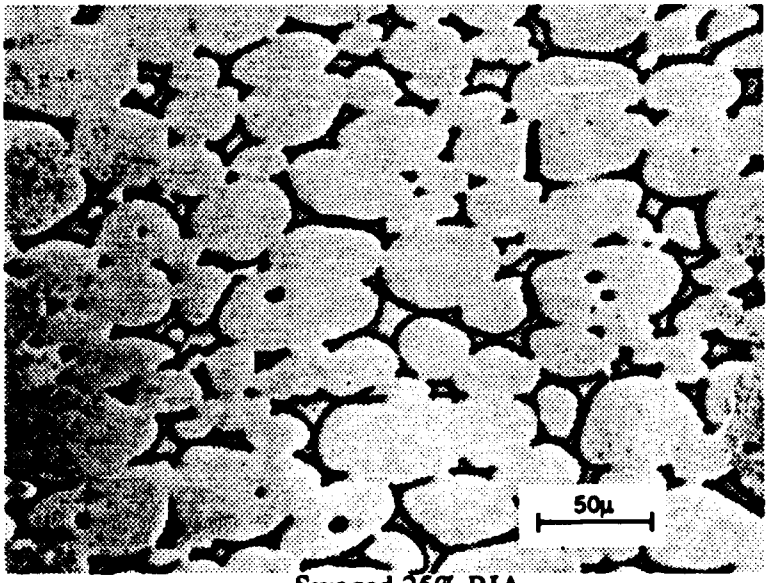

Swaged 25% RIA

Figure 11 Microstructures of Swaged 96W-2.8Ni-1.2Fe (7/3 Ni:Fe)

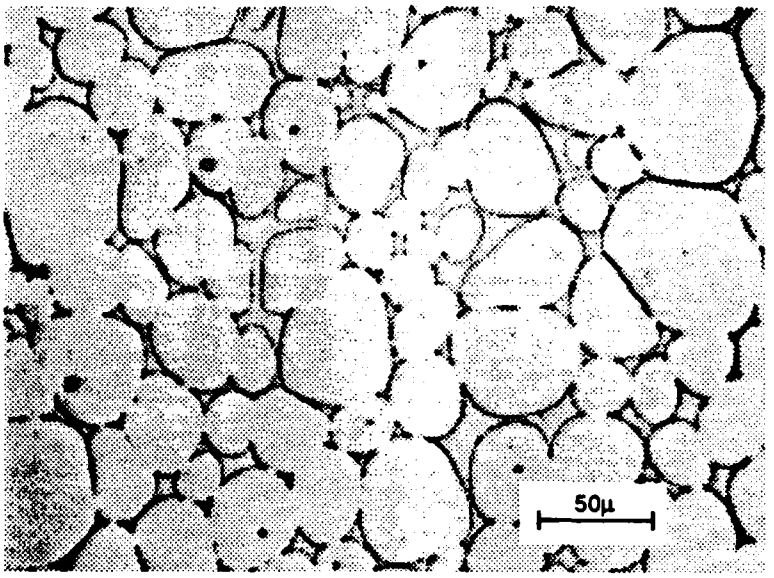

Swaged 8% RIA

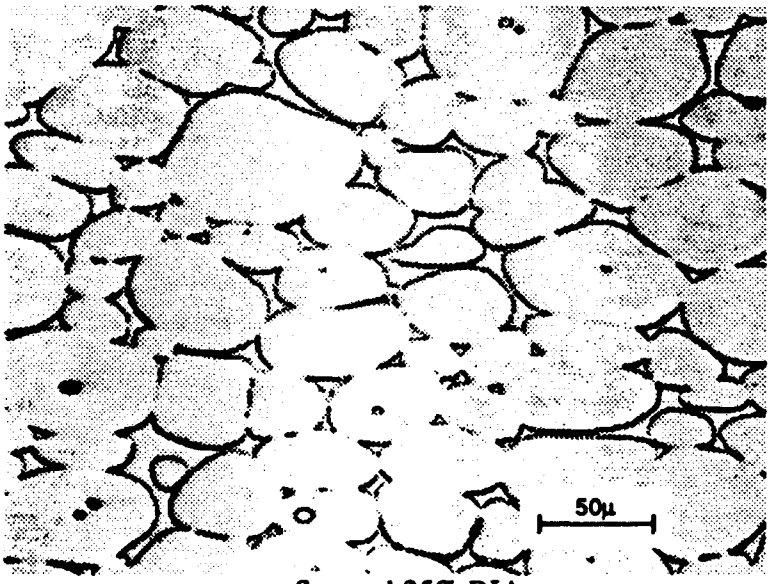

Swaged 25% RIA

Figure 12 Microstructures of Swaged 96W-3.2Ni-0.8Fe (8/2 Ni:Fe)

Table VI Tensile Properties of Swaged Tungsten Heavy Alloys

						Elongation(%)			
Alloy	Ni/Fe	%Swaged	Tests	UTS(ksi)	YS(ksi)	Ave.	Range	Std.Dev	RIA(%)
90W-7Ni-3Fe	7/3	8	2	156	143	21	19-23	2.8	35
"	"	15	6	166	153	17	15-19	1.5	32
"	"	25	4	181	171	11	10-13	1.5	24
90W-8Ni-2Fe	8/2	8	4	159	148	20	18-22	1.7	36
"	"	15	11	168	156	20	16-25	2.7	34
"	"	25	2	177	165	16	15-16	0.7	32
93W-4.9Ni-2.1Fe	7/3	8	2	161	147	17	16-18	1.4	26
"	"	15	6	169	156	12	10-13	1.5	22
"	"	25	16	183	170	11	5-14	2.5	21
93W-5.6Ni-1.4Fe	8/2	8	2	164	150	20	20	0	30
"	"	15	12	171	156	14	10-20	2.5	28
"	"	25	2	181	172	14	13-15	1.4	21
96W-2.8Ni-1.2Fe	7/3	8	4	165	153	9	7-10	1.5	14
"	"	15	12	174	161	8	6-10	1.5	12
"	"	25	2	186	178	5	5	0	5
96W-3.2Ni-0.8Fe	8/2	8	2	161	150	13	12-13	0.7	16
"	"	15	12	172	158	9	8-11	1.1	14
"	"	25	4	178	164	7	5-9	2.1	7

Table VII Impact Energy and Hardness of Swaged Tungsten Heavy Alloys

				----------Impact Energy(ft-lbs)----------			
Alloy	Ni/Fe	%Swaged	Hardness (Rc)	Average	Range	Std. Dev	Tests
90W-7Ni-3Fe	7/3	8	41.3	15	14-16	0.6	2
"	"	15	42.5	18	12-22	4.6	4
"	"	25	42.7	10	5-14	4.2	4
90W-8Ni-2Fe	8/2	8	40.1	22	18-27	4.6	4
"	"	15	40.5	26	19-31	3.9	10
"	"	25	41.7	26	22-28	2.8	4
93W-4.9Ni-2.1Fe	7/3	8	41.9	8.6	8-9	0.7	2
"	"	15	42.5	9	8-10	0.7	4
"	"	25	43.5	9.5	5-16	2.4	16
93W-5.6Ni-1.4Fe	8/2	8	38.9	17	16-17	1.5	2
"	"	15	40.3	17	10-18	3.2	10
"	"	25	42.7	17	16-18	1.5	2
96W-2.8Ni-1.2Fe	7/3	8	42.8	2.7	2-4	0.9	4
"	"	15	44.5	2.6	1-5	1.1	10
"	"	25	45	0.9	.8-1	0.1	2
96W-3.2Ni-0.8Fe	8/2	8	40.6	6.6	6-8	1.4	2
"	"	15	41.5	4.1	1-7	1.8	15
"	"	25	42.7	3.3	1-6	2.6	4

Aged and Annealed Properties

For temperatures up to 600°C there is a strain aging effect in worked tungsten heavy alloys and the material becomes harder and less ductile (17). Beyond 600°C the alloys begin to anneal and the material becomes softer and more ductile. We have found that at some point depending on the material and thermal mechanical treatment the tungsten grains will recrystallize causing a substantial loss in mechanical properties(18).

We ran a series of two hour heat treatments on worked alloys using temperatures of 400, 600, 800, 900, 1000, 1200 and 1400°C. We used two hours because we have found that little age hardening or annealing effect occur beyond two hours. Table VIII gives the results for a series of heat treatments given to the 93% tungsten alloys that had been swaged 25%. One very significant finding in this data is that the 8/2 ratio alloy could be annealed all the way back to as-sintered properties while in the 7/3 ratio alloy the tungsten grains recrystallized before the as-sintered properties were attained. This finding is graphically shown in Figures 13 and 14 which plot elongation and impact strength versus heat treat temperature. At 1200°C the 8/2 alloy has properties similar to its unworked properties, but the 7/3 properties are much lower than it's unworked properties. This is especially true for the impact strength which we have found to be very sensitive to recrystallization of the tungsten grains. Contributing to this difference may be the fewer number of defects created when swaging the 8/2 alloys compared to the 7/3 alloys. We believe the ability to anneal 8/2 ratio alloys back to as-sintered properties enhances their use in applications calling for large reductions in area. Conceivably these large reductions could be accomplished by using a series of work and anneal cycles.

Another interesting point is that there seems to be a slight path dependency for these alloys. In the intermediate strength ranges for a given yield strength those bars that had only been swaged have a lower ultimate tensile strength than those that had been swaged and annealed. This is illustrated in Figure 15 using data from Tables VI and VIII. For example, at a yield strength of 160ksi the bars that had only been swaged had an ultimate tensile strength of about 173 ksi while

Table VIII Properties of 93%W-Ni-Fe Alloys Swaged 25% and Heat Treated 2 Hours

Alloy	Ni/Fe	Heat Treat Temp(°C)	Hardness (Rc)	UTS(ksi)	YS(ksi)	Elong(%)	Impact Str. (ft-lbs)
93W-4.9Ni-2.1Fe	7/3	400	46.1	202	198	9	4.6
	"	600	47.3	210	200	5	3
	"	800	46.1	197	180	7	4.3
	"	900	42.6	183	157	12	-
	"	1000	40.4	168	133	18	9.2
	"	1200	37.3	156	116	26	9.9
	"	1400	32.6	140	93	17	1
93W-5.6Ni-1.4Fe	8/2	400	46.0	200	194	11	8.8
	"	600	46.3	207	193	5	5.8
	"	800	45.2	199	169	12	8.9
	"	900	42.8	176	149	16	11
	"	1000	39.3	169	131	25	19
	"	1200	35.6	154	110	36	35
	"	1400	33.1	145	97	21	5

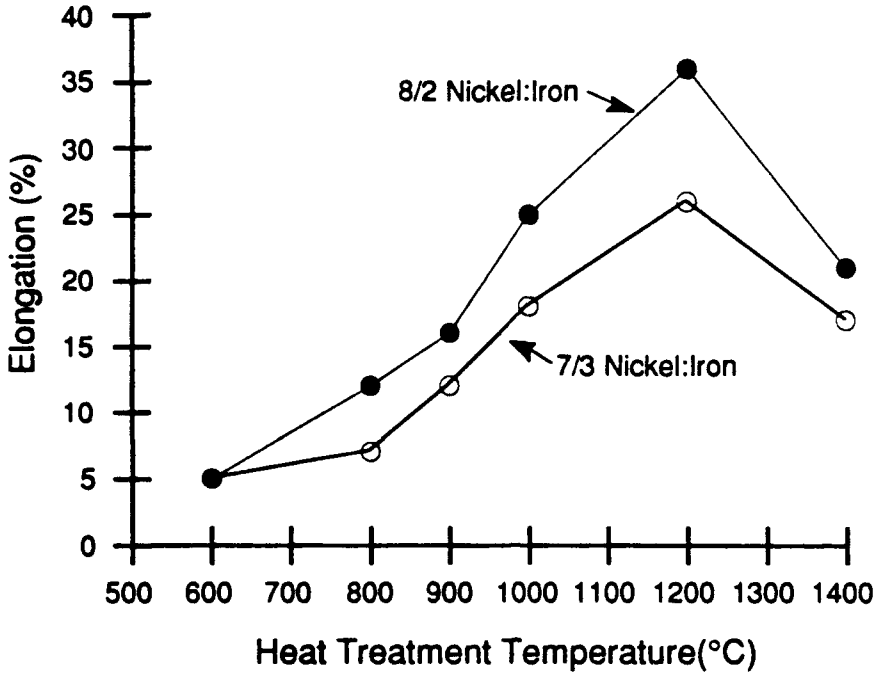

Figure 13 Elongation versus Heat Treating Temperature for 93W-Ni-Fe Alloys Swaged 25%

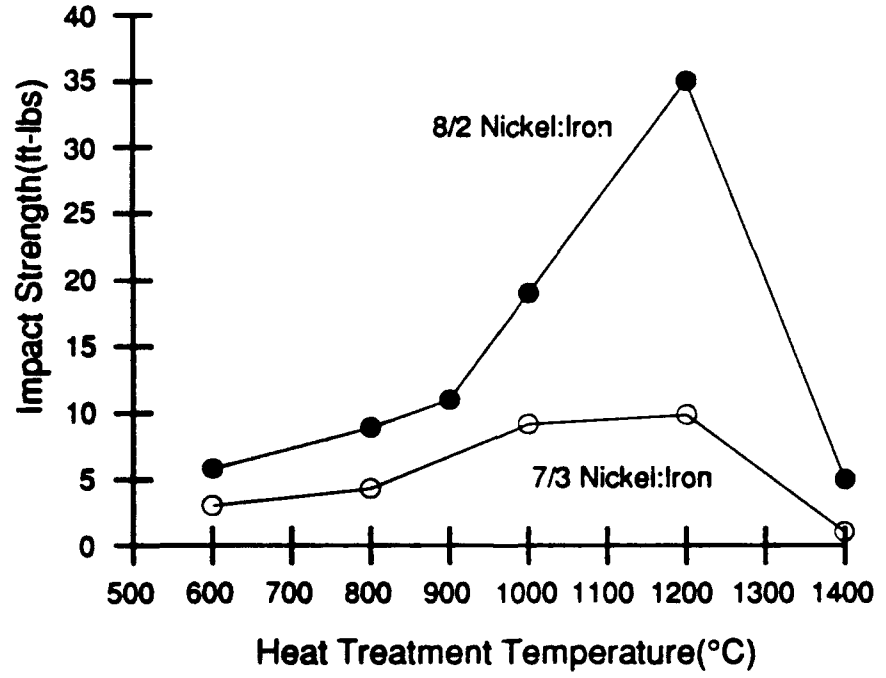

Figure 14 Impact Strength versus Heat Treating Temperature for 93W-Ni-Fe Alloys Swaged 25%

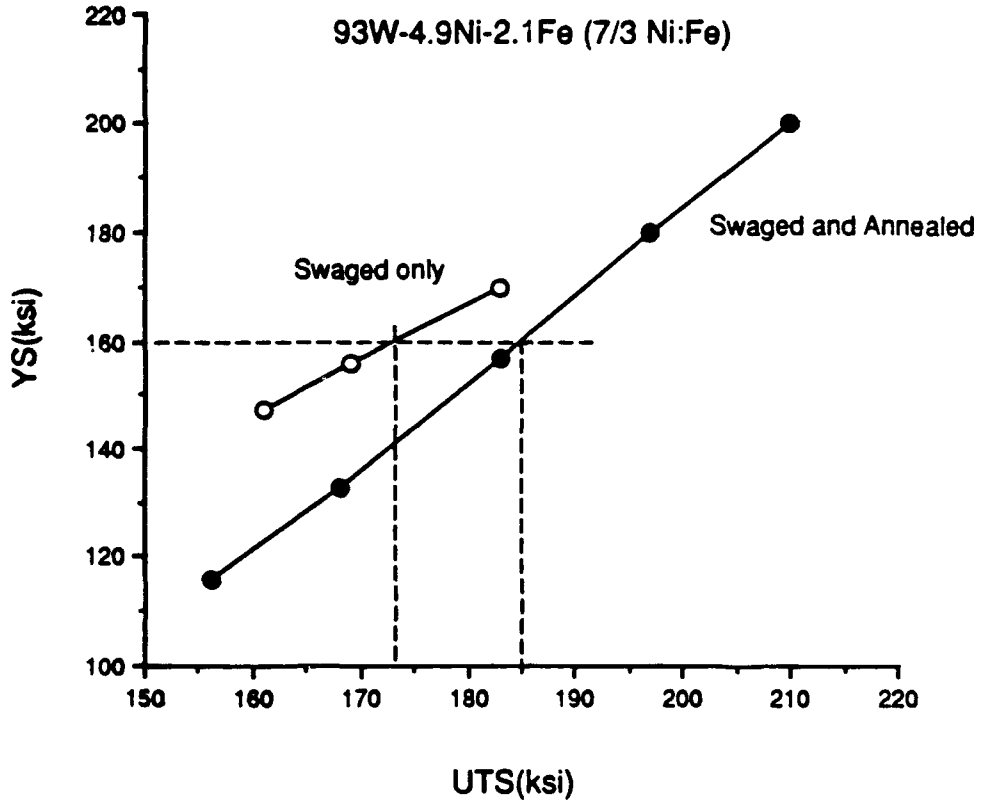

Figure 15 YS versus UTS for 93W-4.9Ni-2.1Fe Swaged 15%

those that had been swaged and annealed had an ultimate tensile strength of about 185 ksi..

Elongation Versus Hardness (EVH) Curves

One of the best methods for comparing tungsten heavy alloys are elongation versus hardness plots (EVH curves) that show the trade off of elongation for hardness. For a given alloy bands are drawn that represent the range into which good material should fall. If the values from a particular lot or source fall below these bands then that material would be suspect as to its quality. Likewise if a new alloy of similar density or a new process yield values above the band then it is likely that an improvement has been made.

Figures 16-18 are EVH curves that were drawn for the 90, 93 and 96% tungsten alloys with 7/3 and 8/2 nickel:iron ratios. The data used was taken throughout the contract and represents only conventionally processed material. The bands clearly show that the 8/2 ratio alloys are superior to the 7/3 ratio alloys.

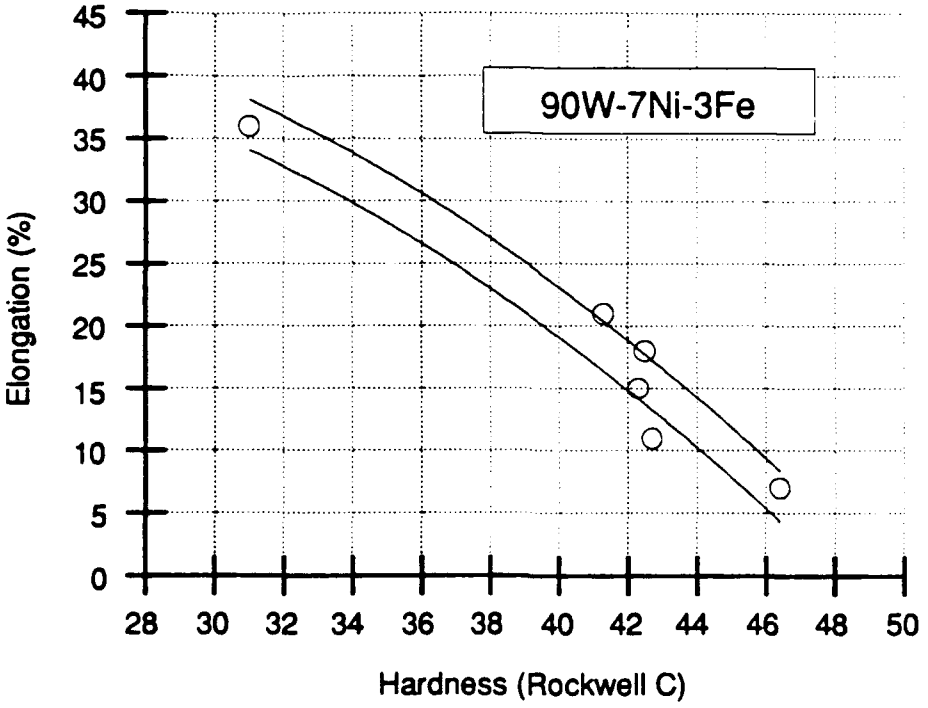

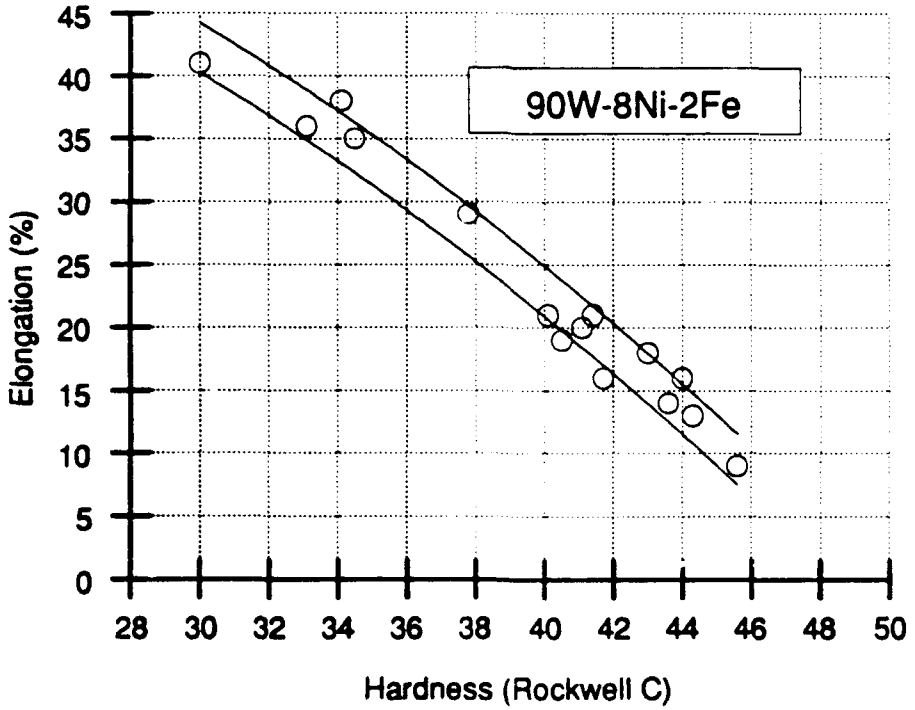

Figure 16 Elongation versus Hardness for 90W-Ni-Fe Alloys

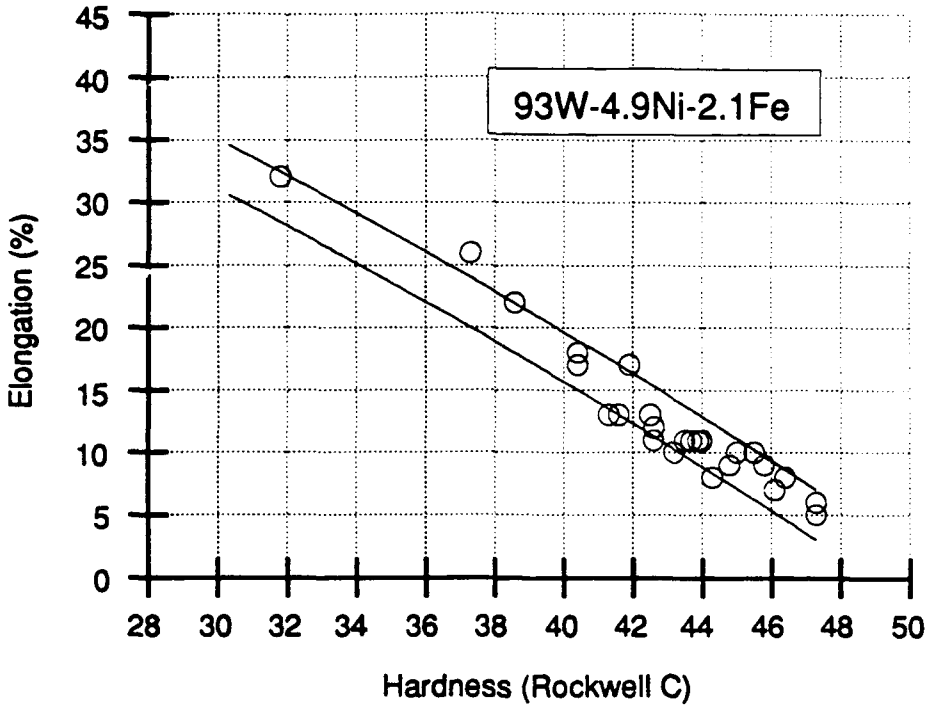

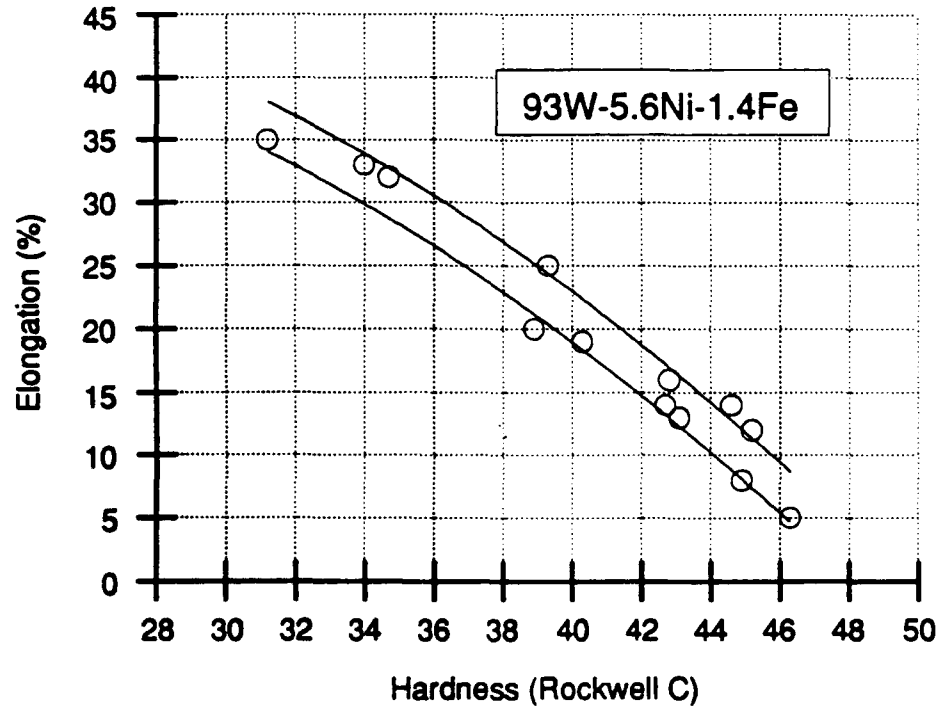

Figure 17 Elongation versus Hardness for 93W-Ni-Fe Alloys

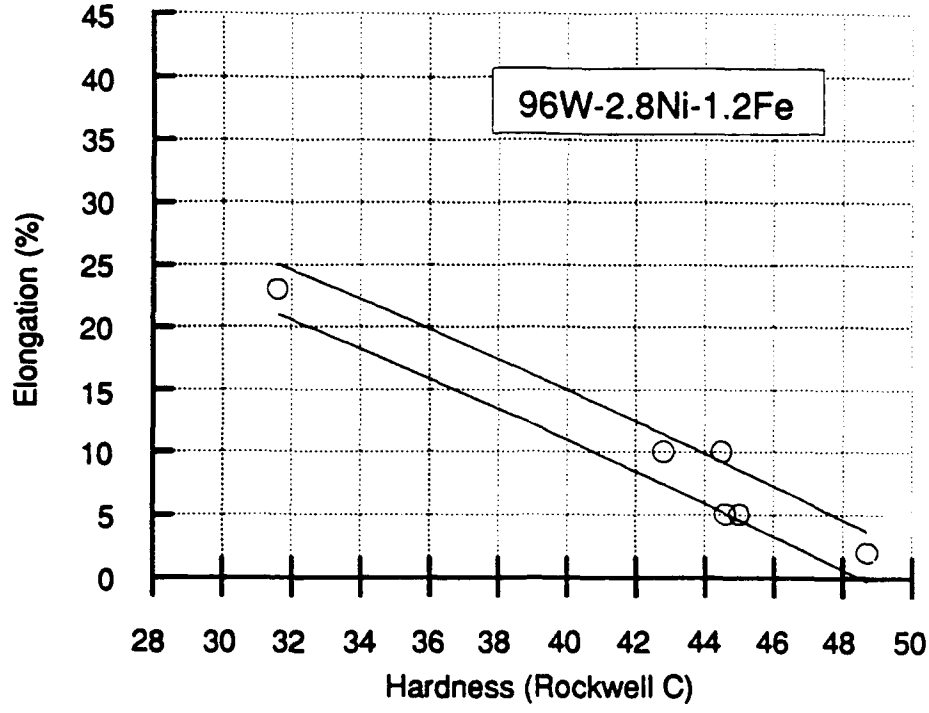

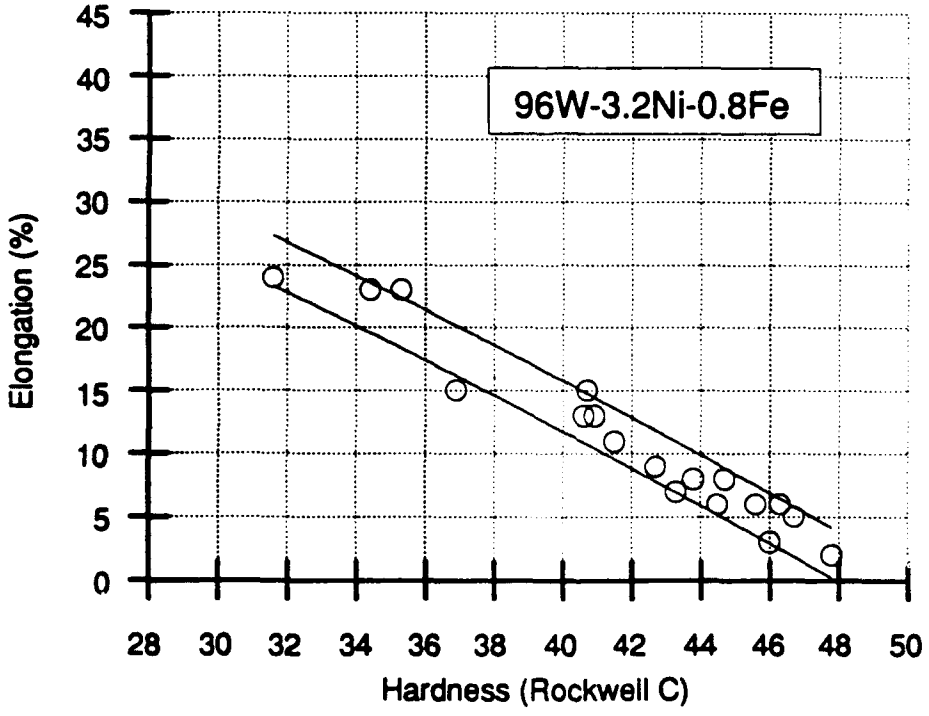

Figure 18 Elongation versus Hardness for 96W-Ni-Fe Alloys

NICKEL:IRON RATIOS

The factors which are important in determining the optimum Ni:Fe ratio for W-Ni-Fe alloys are:

1) the formation of intermetallic phases,
2) hydrogen embrittlement and
3) the strength of the tungsten-matrix boundary.

The lower limit of the Ni:Fe ratio is about 5:5 because of the formation of the μ-phase at lower ratios (Figure 2). At very high ratios nickel rich intermetallics can form(14).

Hydrogen embrittlement becomes a problem when the Ni:Fe ratio is 6:4 or higher(19). It is for this reason that in the as-sintered condition alloys with Ni:Fe ratios of 5:5 have better elongations than alloys with ratios of 6:4 and higher. After annealing to remove hydrogen the elongations of the higher ratio alloys are superior to the 5:5 ratio alloys. Based on our experience typical hydrogen levels after annealing are less than 2 ppm.

The tungsten-matrix boundary strength is important because it affects the failure mechanism during deformation. Failure can occur by a crack that propagates primarily along the tungsten-matrix boundary or by a crack that propagates primarily through the tungsten grains.

In a tensile test, for example, at some relatively low stress, voids begin to form initially at the tungsten-tungsten interfaces and then at favorably oriented tungsten-matrix boundaries. As stress increases the number of these voids increase at a rate dependent on the matrix composition. Eventually the stress reaches a point where the tungsten grains fracture. Generally the crack starts on the surface and propagates across the sample intersecting the tungsten-tungsten voids in its path. Thus if the tungsten-matrix boundary strength is low the fracture surface will show a high proportion of tungsten-matrix failures. Conversely if the boundary strength is high the fracture surface will be predominantly cleavage failures of the tungsten grains.

Generally the 7/3 ratio has been assumed (5,6) to be the optimum Ni:Fe ratio for W-Ni-Fe alloys, although no good data has been generated to support that assumption. Because that data was lacking we decided to carry out a systematic investigation of the effect on Ni:Fe ratios on mechanical and ballistic properties of W-Ni-Fe alloys.

For our first test series we prepared the following alloys using our standard processing conditions.

	Nickel/Iron				
% Tungsten	5/5	6/4	7/3	8/2	9/1
90	X	X	X	X	X
93			X	X	
96	X		X	X	

The microstructures of the 90 and 93% tungsten alloys 8/2 and 9/1 ratios appeared to be slightly under sintered so we sintered these alloys again using a sintering temperature 10°C higher than our standard temperature. This higher temperature requirement is consistent with the phase diagram (Figure 2).

Table IX contains the tensile and impact properties of the bars made for this initial test and show that the 8/2 and 9/1 nickel:iron ratios had better properties than the alloys with 7/3 ratios. The biggest effect was on the impact strength which nearly doubled in the 90% tungsten alloy when we went from the 7/3 ratio to the 8/2 ratio. The results of this test prompted us to redo our baseline evaluation using 8/2 nickel:iron ratios.

Table IX Mechanical Properties for Initial Test Series on Ni:Fe Ratios
(average of two samples)

Alloy	Ni/Fe	UTS(ksi)	YS(ksi)	Elong.(%)	Impact Energy (ft-lbs)
90W-5Ni-5Fe	5/5	133	90	23	10
90W-6Ni-4Fe	6/4	136	92	25	13
90W-7Ni-3Fe	7/3	136	85	35	30
90W-8Ni-2Fe	8/2	140	86	40	52*
90W-9Ni-1Fe	9/1	142	87	39	52*
93W-4.9Ni-2.1Fe	7/3	140	88	33	24
93W-5.6Ni-1.4Fe	8/2	140	87	35	31
96W-2Ni-2Fe	5/5	136	91	13	2.9
96W-2.8Ni-1.2Fe	7/3	140	88	24	7.8
96W-3.2Ni-0.8Fe	8/2	141	87	26	9.7

*Did not break

As stated earlier, nickel rich intermetallics can form in W-Ni-Fe alloys with high Ni:Fe ratios. Quenching can prevent or retard the formation these intermetallics (8) so we reasoned that quenching might improve the properties of the alloys with the higher nickel:iron ratios. We ran a quenching test on 96% tungsten alloys with 7/3, 8/2 and 9/1 nickel:iron ratios. In this test we quenched in oil from 1100°C and in all cases, as shown in Table X, the impact strength improved. The percent increase in impact strength increased with increasing nickel:iron ratio. After this finding we made it a point to quench alloys with nickel:iron ratios of 9/1 or greater.

Table X Effect of Quenching 96W-Ni-Fe Alloys

Ni/Fe	Condition	UTS(ksi)	YS(ksi)	Elong(%)	RIA(%)	Impact Energy(ft-lbs)
7/3	as sintered	139	86	28	22	8
7/3	quenched	140	87	29	25	11
8/2	as sintered	141	88	26	19	9
8/2	quenched	140	87	27	21	13
9/1	as sintered	142	92	22	15	10
9/1	quenched	143	90	25	18	18

Table XI is a compilation of data collected throughout the contract showing the effect of Ni:Fe ratio on mechanical properties of W-Ni-Fe alloys. In some cases the data represents the average of many tests. In generating these averages we used data that appeared to be representative and eliminated any that were caused by a defective sample. Also since the impact bars for the 90% tungsten alloys with Ni:Fe ratios of 8/2 or higher didn't break we ran a series of 8mm square test bars instead of the standard 5mm bars. These results are also included in Table XI and have been corrected to account for the differences in cross sectional area. While the impact energy is not simply related to the cross sectional area, we have found it to be a reasonable approximation. Using the data from Table XI, Figure 19 plots the impact energy versus Ni:Fe ratio for the 90, 93 and 96% tungsten.

As shown in Figure 19 there is a significant improvement in impact strength with Ni:Fe ratio. Another interesting observation we made relating to nickel:iron ratios were the number of defects forming during deformation. To quantify this phenomenon broken tensile bars were sectioned longitudinally through the fracture and the defects were counted in an area adjacent to the fracture. These results are shown in Table XII and show a large decrease in the number of defects as the Ni:Fe ratio increases.

Table XI Mechanical Properties of UnworkedW-Ni-Fe Alloys

				-------Elongation (%)--------			----Impact Energy(ft-lbs)---		
%W	Ni/Fe	UTS (ksi)	YS (ksi)	Ave.	Std. Dev.	Tests	Ave.	Std. Dev	Tests
90	5/5	133	90	23	0	2	9.8	1.6	2
"	6/4	136	92	25	0	2	13	0.4	2
"	7/3	136	85	34	2.5	30	32	6.2	17
"	"						30*	4.3*	5
"	8/2	140	86	38	2.3	40	47	7.9	31
"	"						42*	4.1*	11
"	9/1	142	87	39	1.7	9	49	7.8	6
"	"						65*	11*	5
93	7/3	140	88	32	2.4	31	19	2.7	17
"	8/2	140	87	34	3.4	31	31	5.9	38
"	9/1	139	87	35	2.7	8	33	5.5	7
96	5/5	136	91	10	3.3	6	2.4	1	8
"	7/3	140	88	23	3.7	19	8.1	2	30
"	8/2	141	87	25	3.4	19	12	3.5	35
"	9/1	142	90	22	8.6	5	11	0.5	4

*Values Converted From 8mm x 8mm Impact Bars by Ratio of Areas

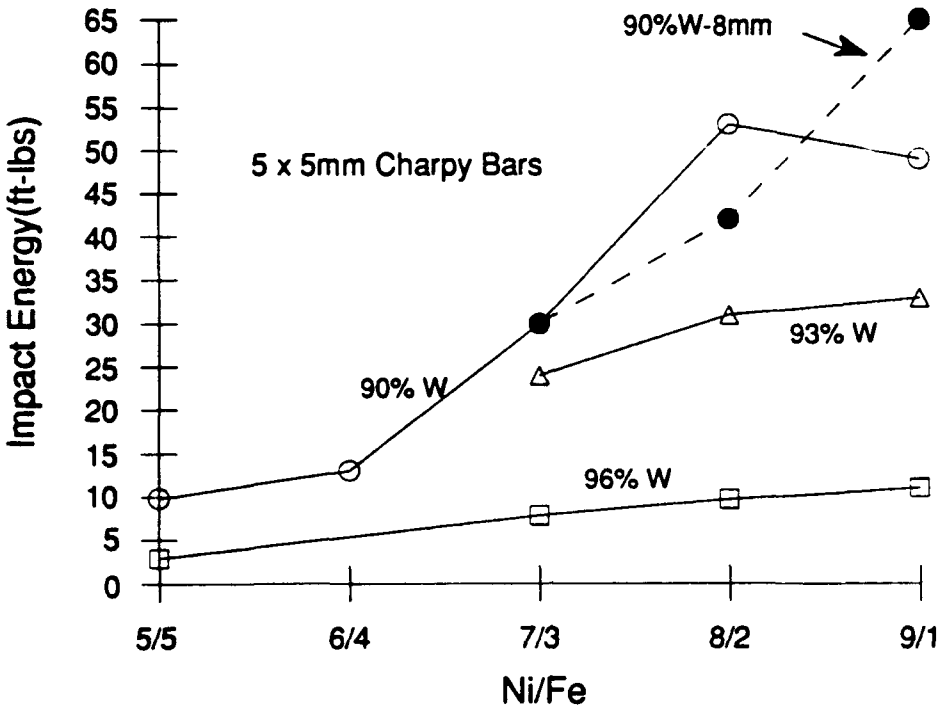

Figure 19 Impact Energy versus Ni:Fe Ratio for W-Ni-Fe Alloys

Table XII Defect Count in Tensile Samples (ave. of 4 samples)

Alloy	Ni/Fe	Average Elong. (%)	Defect Count(no./mm2)	
			Average	Range
90W-7Ni-3Fe	7/3	36	95	23-171
90W-8Ni-2Fe	8/2	40	19	8-30
90W-9Ni-1Fe	9/1*	40	8	6-10
93W-4.9Ni-2.1Fe	7/3	31	52	14-86
93W-5.6Ni-1.4Fe	8/2	36	2	2-3
96W-2.8Ni-1.2Fe	7/3	21	2	0-5
96W-3.2Ni-0.8Fe	8/2	23	1.5	0-5
96W-3.6Ni-0.4Fe	9/1*	22	1	1

* Average of 2 samples

THERMO-MECHANICAL TREATMENTS

Our standard method for working tungsten heavy alloys is swaging at a temperature of 300°C We have found that about an 8% reduction in area by swaging will produce a uniformly worked structure. We also have observed that working much above 20% reduction in area can produce defects between the tungsten grains. With these observations in mind we looked at other thermo-mechanical treatments (TMT). These included upsetting, conventional extrusion and large reductions in area using multiple swaging passes.

Upsetting and Extrusion

Our upsetting was done by placing a billet in a pressing die with a cylindrical cavity and compressing the billet until it upset and made full contact with the die wall. For extrusion we placed a slightly undersized billet (0.005-0.01" < die diameter) in a die which had a reduced opening in one end with a die angle of 15°. A small steel blank was placed on top of the billet and then the billet was extruded through the die leaving the blank in the die. For both upsetting and extrusion the billets were preheated to 300°C and coated with a lubricant. For both upsetting and extrusion tests we used 90 and 96% tungsten alloys with 7/3 Ni:Fe ratios. We didn't use the 8/2 ratio because we had completed this work prior to our findings concerning nickel:iron ratios. We used reduction in area or reduction in heights of 15 and 25%. Table XIII contains the hardness and tensile properties of the worked material. When extruding the 96% tungsten alloy the bar cracked and we could not use it for a tensile test.

For the extruded 90% alloy the properties were similar to conventionally swaged material. The upset samples had a lower than normal yield because of the Bauschinger effect. The upset 96% alloy had little ductility so we examined the microstructure but could find no defects in the structure to explain the low ductilities.

Table XIII Properties of Upset and Extruded W-Ni-Fe Alloys

Alloy	Ni/Fe	Type of Work	RIA(%) RIH(%)	Hardness (Rc)	Tensile Properties (2 tests) UTS (ksi)	YS (ksi)	Elong.(%)
90W-7Ni-3Fe	7/3	Upset	15	40.1	164	130	20
95W-2.8Ni-1.2Fe	7/3	Upset	25	41.0	190	156	0
90W-7Ni-3Fe	7/3	Extruded	15	39.7	164	151	17
"	7/3	Swaged*	15	42.5	166	153	17
"	7/3	Extruded	25	42.4	179	165	12
"	7/3	Swaged*	25	42.7	181	171	11
96W-2.8Ni-1.2Fe	7/3	Extruded	25	42.8	-----Cracked- Did Not Test-----		
"	7/3	Swaged*	25	42.8	186	178	5

* Taken From Tables VI & VII

Large Reductions in Area

We decided to look at giving tungsten heavy alloys large reductions in area by using multiple swaging passes. During our work on nickel:iron ratios we learned that the alloys with 8/2 nickel:iron ratios could be annealed back to as-sintered properties after working. This ability to anneal back to as-sintered properties is one of the reasons we wanted to look at large reductions in area. For our initial work on large reduction in areas we used 90 and 93% alloys with 8/2 nickel:iron ratios.

Using passes of 15% reduction in area we swaged these alloys at 300°C both with and without two hour 1200°C anneals between passes. We were confident that by annealing between passes we could achieve large reductions in area without cracking the bars. We were also, however, able to achieve 70% reduction in area in bars that had anneals as well as those that didn't have anneals between passes. Tables XIV and XV show how the hardness developed as the bars were swaged. Also included are tensile and impact properties at 55 and 70% reduction in area.

With no anneals between passes, the yield strength and ultimate tensile strength we achieved in the as-swaged bars were higher than in conventionally swaged material. However, the hardness and elongation generally appear to fall in line with the standard hardness versus elongation curves.

Table XIV Mecanical Properties of Swaged 90W-8Ni-2Fe (8/2)

Total Work (% RIA)	HT Between Passes*	Hardness (Rc)	UTS (ksi)	YS (ksi)	Elong(%)	Impact Energy(ft-lbs)
0	-	32.9	140	84	41	>50
15	Yes	35.3	147	101	44	>50
15	No	41.7	-	-	-	-
30	Yes	36.4	-	-	-	-
30	No	42.5	-	-	-	-
40	Yes	36.8	-	-	-	-
40	No	44.7	-	-	-	-
55	Yes	36.5	153	117	36	17
"	No	44.6	203	190	11	23
70	Yes	37	-	-	-	-
"	No	46.5	221	201	8	14

*Data is for heat-treated condition for bars heat-treated between passes

Table XV Mechanical Properties of Swaged 93W-5.6Ni-1.4Fe(8/2)

Total Work (% RIA)	HT Between Passes*	Hardness (Rc)	UTS (ksi)	YS (ksi)	Elong(%)	Impact Energy (ft-lbs)
0	-	32.2	141	88	35	30.3
15	Yes	36.7	149	106	32	29.7
"	No	40.7	-	-	-	-
30	Yes	37.7	-	-	-	-
"	No	43.4	-	-	-	-
40	Yes	37.3	-	-	-	-
"	No	45.6	-	-	-	-
55	Yes	37.7	155	120	30	2.5
"	No	46	205	190	9	5.4
70	Yes	38.2	-	-	-	-
"	No	48.6	224	210	4	2.1

* Data is for heat-treated condition for bars heat-treated between passes

One problem that is encountered with heavily worked tungsten heavy alloys is the recrystallization of the tungsten grains during annealing. Recrystallization of the tungsten grains causes a substantial drop in the impact strength. Our experience has been that an alloy worked 25%, recrystallization of the tungsten grains will occur between 1200 and 1400°C. The tungsten grains in very heavily worked material can recrystallize as low as 800°C (18). We had hoped that annealing between passes would keep the recrystallization temperature above 1200°C so that the worked bars could be annealed back to as-sintered elongations without a loss in impact strength. Despite having good elongations, the data in Tables XIV and XV shows very low impact strengths after annealing at 1200°C indicating that the tungsten grains had recrystallized. The recrystallization probably affects the impact strength more than the elongation because the new grain boundaries tend to be perpendicular to the swaging direction. Metallographic examinations also showed evidence of recrystallization.

After seeing how far we could swage the 8/2 alloys without anneals we decided to see how far a 93% tungsten alloy with a 7/3 nickel:iron could be swaged. Using the same procedures as we did with the 8/2 alloys we were able to swage to a 55% reduction in area before the bar began to crack compared to 70% for the 8/2 ratio alloy.

The bars were then given two hour heat treatments at 600, 900 and 1000°C. We limited our temperatures to 1000°C because we were certain that any higher temperatures would cause the tungsten grains to recrystallize. Table XVI contains these results. At 1000°C there is a loss in impact strength indicating recrystallization of the tungsten grains has occurred. This was metallographically confirmed as shown in Figures 20 and 21 where at 1000°C recrystallization is observed but not at 900°C.

For a given yield strength the elongations are in line with the conventionally processed alloys. With the 93% tungsten alloy we achieved a yield strength as high as 232 ksi which is much higher than can be achieved by standard swaging and aging. The corresponding impact strengths however appear to be somewhat lower than those of conventionally processed alloys.

Table XVI Properties of Heat Treated W-Ni-Fe Alloys Swaged To Large RIA's

				HT 2hrs at 600°C				HT 2hrs at 900°C				HT 2hrs at 1000°C
Alloy	Ni/Fe	RIA	Ann*	UTS (ksi)	YS (ksi)	Elong. (%)	Impact Energy. (ft-lbs)	UTS (ksi)	YS (ksi)	Elong (%)	Impact Energy(ft-lbs)	Impact Energy (ft-lbs)
90W-8Ni-2Fe	8/2	75	Y	184	175	17	8.7	169	145	25	21	14
93W-5.6Ni-1.4Fe	8/2	75	Y	188	179	9	1.9	171	146	17	5.8	3.2
93W-5.6Ni-1.4Fe	8/2	70	N	237	232	4	2.9	199	193	13	3.4	5
93W-5.6Ni-1.4Fe	8/2	55	N	230	214	3	1.9	196	171	17	11.9	2.8
93W-4.9Ni-2.1Fe	7/3	55	N	231	226	3	1.8	195	172	12	5.8	4.9

*HT Between Anneals

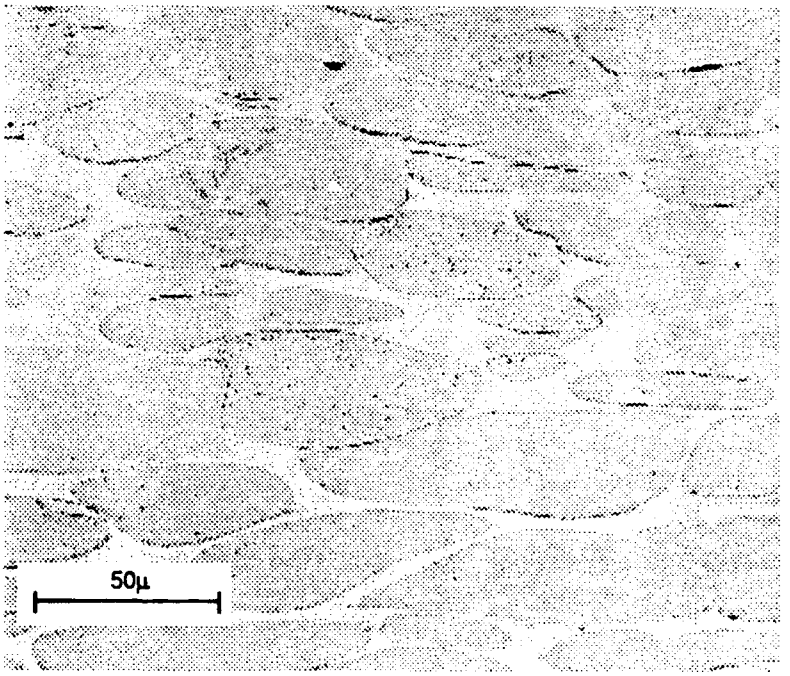

Figure 20 Heavily Worked 93W-5.6Ni-1.4Fe Heat Treated 2hrs at 900°C
(75%RIA - No Heat Treatments Between Passes)

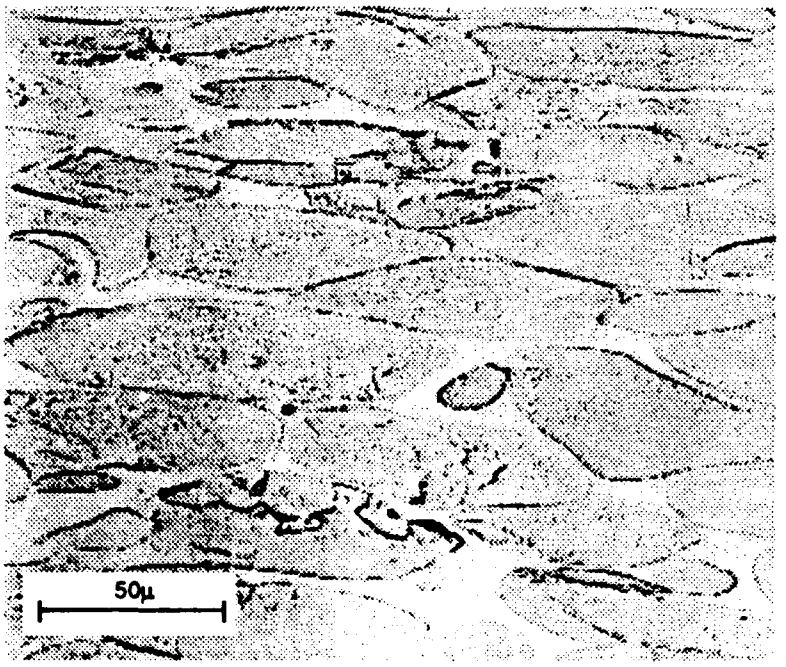

Figure 21 Heavily Worked 93W-5.6Ni-1.4Fe Heat Treated 2hrs at 1000°C
(75%RIA - No Heat Treatments Between Passes)

IMPURITIES AND OTHER EFFECTS

Impurities

Tungsten heavy alloys are very sensitive to the presence of certain impurities such as P, O, Si and S(20). These impurities can cause a wide variation in mechanical properties and alter the effects processing changes have on these alloys. We believe that differences in impurity levels are the likely cause of much of the conflicting data reported for tungsten heavy alloys in the literature. These impurities may enter the alloy with the elemental powders or during processing.

Hydrogen is the most notable impurity in tungsten heavy alloys because it embrittles the matrix and causes a substantial loss of elongation(19). It is for this reason that all of our bars are heat treated in vacuum if sintering was done in a hydrogen atmosphere. The hydrogen embrittlement effect is less for alloys with lower nickel:iron ratios. Some impurities degrade properties of tungsten heavy alloys by segregation to the grain boundaries(20). In such cases solution heat treating and quenching will often restore mechanical properties to levels expected for purer materials. Oxygen even at very low levels may degrade properties by reducing the ductility of the tungsten grains.

The chemical processing used at GTE to produce tungsten powder results in a powder that is very high purity. We feel this high purity has a lot to do with our success in making high quality tungsten heavy alloys. As a simple test for the effect of impurities we purchased a tungsten powder that appeared to be slightly lower in purity than our standard tungsten powder. The quantitative analysis of this powder (CS-1) is in Table XVII along with typical values for GTE's M-55 tungsten powder. Other than nickel and iron the only elements that appear to be significantly higher in the CS-1 powder are silicon and chromium.

Table XVII Quantitative Analysis of Tungsten Powders

	----1----						2						----3----			-------4-------		
Powder Type	Na	K	Al	Ca	Cr	Cu	Fe	Mg	Mn	Ni	Si	Sn	Mo	As	P	C	O2	S
GTE M-55	17	<10	<1	<1	3	<1	6	<1	<1	5	1	<1	<8	<5	<10	<10	390	<10
CS-1	8	10	<1	<1	116	<1	210	<1	2	95	16	<1	<8	<5	<10	<10	730	<10

1 Atomic Asorption

2 Direct Reading Spectrometer

3 Optical Emission Spectroscopy

4 Carrier Gas Fusion

Using our standard blending, pressing and sintering procedures we produced several bars from a 93W-4.9Ni-2.1Fe (7/3 Ni:Fe) blend made with the CS-1 tungsten powder. The tensile properties of these bars were similar to those made from a blend that used GTE tungsten powder. The impact properties, however, varied from 19.6 to 8.2 ft-lbs indicating that there was a problem with the CS-1 powder. We repeated the test using a 96% tungsten alloy which we felt would be more sensitive to impurities. We also included a blend made with GTE M-55 tungsten powder. All the bars from both blends were sintered and heat treated together. For both tensile and impact tests we made up five test samples and the average of these results are in Table XVIII. Also in the table are the results for the same materials quenched in oil from 1200°C after holding at that temperature for one hour.

Table XVIII Effect of Quenching on Impact Energy of 96W-2.8Ni-1.2Fe

Tungsten Powder	Condition	UTS(ksi)	YS(ksi)	Elong(%)	Impact Energy(ft-lbs)
GTE M-55	as sintered	140	87	24	9
GTE M-55	quenched	140	88	26	12
CS-1	as sintered	140	89	17	2
CS-1	quenched	136	87	26	11

While the results show only a slightly lower tensile elongation in the bars made with the CS-1 blend there was a substantial difference in impact strength. After quenching the results of both blends are similar as the CS-1 blend took a large jump and the GTE blend took only a small jump. A possible explanation of this observation is that the 1200°C anneal placed in solution certain impurities which were originally present in the tungsten/matrix boundaries. As part of this test we used Auger Spectrography to analyze the surfaces of fresh fractures of bars made from a blend using GTE M-55 tungsten powder and a blend using the CS-1 tungsten powder. We were unable, however, to detect any significant differences between these samples.

Oxygen

From past work(7) we knew that oxygen levels as low as 30 ppm can have a significant effect on mechanical properties of tungsten heavy alloys. As discussed in the procedure section obtaining good oxygen measurements in tungsten heavy alloys is difficult and it is likely that many investigators miss the role that oxygen plays in the properties of tungsten heavy alloys.

To study the effect of oxygen in tungsten heavy alloys we used several approaches to make these alloys with different oxygen levels. The first method we tried was to use blends made with a much finer tungsten powder than we normally use. Our previous experience had shown us that while using different size tungsten powders will not result in a difference in the sintered tungsten grain size, the blends made from finer tungsten powder will give sintered bars higher in oxygen. Possible causes of the difference in oxygen level may be due to the higher oxygen in the finer

tungsten powder or earlier closure of porosity during solid-state sintering of the finer powders. For our test we used both 1.3 μm and 5.2 μm GTE tungsten powder in blends of 90W-7Ni-3Fe and 96W-2.8Ni-1.2Fe. Table XIX gives the tensile, impact and oxygen results from bars sintered from these blends. Tensile and impact values are the average of two tests.

Table XIX Effect of Tungsten Particle Size on Mechanical Properties of W-Ni-Fe Alloys

Alloy	Ni/Fe	W Powder FSSS(μm)	Oxygen (ppm)	UTS (ksi)	YS (ksi)	Elong(%)	Impact Energyft-lbs)
96W-2.8Ni-1.2Fe	7/3	1.3	65	123	89	7	1.2
96W-2.8Ni-1.2Fe	7/3	5.2	8	141	89	23	4.9
90W-7Ni-3Fe	7/3	1.3	27	138	87	36	7
90W-7Ni-3Fe	7/3	5.2	8	136	87	36	29

As we expected the bars made with the blends using the finer tungsten powder had higher oxygen levels. For the 90% tungsten alloy the elongation was not effected, but the impact strength was significantly lower in the bar made with the finer tungsten powder. For the 96% tungsten alloy both impact and elongation were substantially lower in the bars made with the finer tungsten powder blends. We tried to improve the properties of the 96% alloy by quenching but unlike the test with other impurities, quenching did not improve properties.

In our next test we sintered a 96W-2.8Ni-1.2Fe alloy in dry hydrogen, wet hydrogen and in a nitrogen/hydrogen mix. Despite the differences in atmospheres we did not see a difference in oxygen levels and correspondingly we did not see any difference in mechanical properties.

In our final test we used a dry hydrogen (-20°C) clean-up at 1000°C, followed by solid-state sintering in nitrogen and liquid-phase sintering in either nitrogen or vacuum. We did this for a 90 and 96% tungsten alloys with 8/2 Ni:Fe ratios, using our normal sintering temperatures for these alloys. These sintering procedures yielded oxygen levels ranging from 100 to about 300 ppm of oxygen. As with our test using fine powders the 96% alloy ended up with higher oxygen levels than the 90% Alloy. We don't know why the 96% alloys end up with higher oxygen levels.

Table XX contains the mechanical properties and oxygen values for this test. Despite the high oxygen levels we saw only a small reduction in impact properties for the 90% tungsten alloy. For the 96% tungsten alloy that was vacuum sintered both elongation and impact strength were dramatically reduced.

One interesting observation is that in the fine powder test we used alloys with a 7/3 Ni:Fe ratio and in the last test we used alloys with 8/2 ratios. Looking at data from both tests it would appear that the 8/2 ratios are less affected by oxygen level than the 7/3 ratios. This may be related to the fewer number of defects that form during the deformation of the 8/2 alloys.

Table XX Oxygen and Mechanical Properties of W-Ni-Fe Alloys Sintered in Different Atmospheres

Alloy	Ni/Fe	Atm.	Oxygen (ppm)	UTS (ksi)	YS (ksi)	Elong(%)	Impact Energy(ft-lbs)
90W-8Ni-2Fe	8/2	Hydrogen	10	138	85	40	>50
90W-8Ni-2Fe	8/2	Nitrogen	101	136	83	36	33.3
90W-8Ni-2Fe	8/2	Vacuum	141	137	84	36	43.7
96W-3.2Ni-0.8Fe	8/2	Hydrogen	10	140	87	24	10.0
96W-3.2Ni-0.8Fe	8/2	Nitrogen	226	137	85	20	3.0
96W-3.2Ni-0.8Fe	8/2	Vacuum	302	106	85	5	0.6

Tungsten Particle Size Effects

During liquid-phase sintering of tungsten heavy alloys the tungsten particles experience considerable growth from the starting tungsten particle size. At minimum, we find that tungsten will grow to a grain size of 30 or 40 μm. Our experience has been that the starting tungsten particle size doesn't have a significant effect on the tungsten grain size. To test the effect of tungsten particle size on the properties of tungsten heavy alloys we made three blends of 93W-4.9Ni-2.1Fe using GTE tungsten powders having FSSS of 1.9, 4.05 and 5.3 μm. Oxygen levels and structures were checked both after the solid-state sintering step and after liquid-phase sintering. Table XXI contains those results. We found that the solid-state microstructure of the bar made from the finest tungsten powder had large pores compared to the other two blends. It also had the lowest density in the solid-state sintered condition.

After liquid-phase sintering the density of all the bars were similar and the bar made with the finest tungsten had the largest tungsten grain size. As we had found before the bar made with the finer tungsten had the higher oxygen levels. We did not, however, see any significant differences in the mechanical properties as shown in Table XXII. This is probably because we were using a 93% tungsten alloy and the oxygen levels were below the level where we believe it becomes a problem.

Table XXI Effect of Tungsten Particle Size on Grain Size, Density and Oxygen Content of 93W-4.9Ni-2.1Fe(7/3)

		Solid-State Sintered		Liquid-Phase Sintered			
					Grain Count(No.mm2)		
W Powder Type	Tungsten FSSS(μm)	Density (g/cc)	Oxygen (ppm)	Density (g/cc)	Center(μm)	Edge(μm)	Oxygen (ppm)
M-30	1.9	17.16	20, 45	17.73	1375(38)	1450(37)	20, 29
M-45	4.05	17.5	10, 16	17.72	1830(33)	1790(34)	11, 10
M-60	5.3	17.27	28, 44	17.73	1640(35)	1615(35)	8, 11

Table XXII Effect of Tungsten Particle Size on Mechanical Properties of 93W-4.9Ni-2.1Fe (7/3)

W Powder Type	Oxygen(ppm)	UTS(ksi)	YS(ksi)	Elong.(%)	Impact Energy (ft-lbs)
M-30	20,29	139	85	35	20
M-45	11,10	138	84	34	19
M-60	8,11	138	86	34	20

Tungsten Grain Size

Using changes in the sintering schedule as shown in Table XXIII we were able to vary the grain size in a 93W-4.9Ni-2.1Fe alloy from a Jeffries grain count of 1030 to a count of 2180. Raising the liquid-phase sintering temperature 30°C significantly lowered the grain count. Including a solid-state sintering step also had the effect of reducing the grain count. These results along with the tensile and impact properties are also contained in Table XIX and represent the average of two tests. There appears to be no effect on elongation and although the coarser grain sizes had slightly better impact properties the difference is not significant.

Table XXIII Effect of Tungsten Grain Size on Mechanical Properties of 93W-4.9Ni-2.1Fe

Presinter	Sintering Temp. (°C)	Grain Count No. mm2(μm)	UTS (ksi)	YS (ksi)	Elong. (%)	Impact Energy(ft-lbs)
Yes	1520	2180(30)	138	84	32	17
Yes	1550	1030(44)	144	86	31	22
No	1520	2210(30)	139	87	34	17
No	1550	1710(34)	139	86	33	18

QUATERNARY ALLOYS

We looked at rhenium and ruthenium additions because investigators have found that they appear to refine the tungsten grain size(12,13). Cobalt additions were examined because several studies and work done by GTE indicate that cobalt additions may improve mechanical properties(5,11) For all our work on quaternary alloys we used alloys with about 93% tungsten. Blends of these alloys were made by blending the elemental powders as we did with the W-Ni-Fe alloys.

As-Sintered Properties - Ruthenium and Rhenium Additions

Based on the references for rhenium and ruthenium additions, we believed that only small additions of these elements would be required to see a grain refinement effect. In our first series of these alloys we used 93% tungsten and added either 0.5% or 1% rhenium or ruthenium while maintaining the nickel:iron ratio at about 7/3. The 7/3 ratio was chosen because we had not yet made our finding on the 8/2 ratios.

For the first sintering test we used a sintering temperature of 1520°C which is the standard sintering temperature for the W-Ni-Fe alloys. After looking at the microstructures it appeared that these alloys were under sintered so we resintered the bars using a temperature of 1530°C which produced an acceptable microstructure.

Both rhenium and ruthenium addition resulted in a much finer tungsten grain size as shown in Table XXIV which contains the microstructural evaluation of these tests. Along with the finer grain size however, was an increase in the contiguity. The rhenium alloys also had microstructures that were not very uniform and showed a wide range in tungsten grain size. Typical microstructures of the ruthenium and rhenium alloys are shown in Figures 22 and 23.

Table XXIV Microstructure Evaluation of W-Ni-Fe-Re and W-Ni-Fe-Ru Alloys

				MOP-3 Data			
		Grain Count		Diameter(μm)		Contiguity(%)	
Alloy	Ni/Fe	Center	MR*	Center	MR*	Center	MR*
93W-4.5Ni-2.0Fe-0.5Ru	7/3	3300	3320	24	24	32	29
93W-4.2Ni-1.8Fe-1.0Ru	7/3	5030	5180	16	17	32	39
93W-4.5Ni-2.0Fe-0.5Re	7/3	2950	3110	25	24	30	30
93W-4.2Ni-1.8Fe-1.0Re	7/3	3560	3580	20	18	28	32
93W-4.9Ni-2.1Fe	7/3	2260	2100	27	28	12	12

* Mid Radius

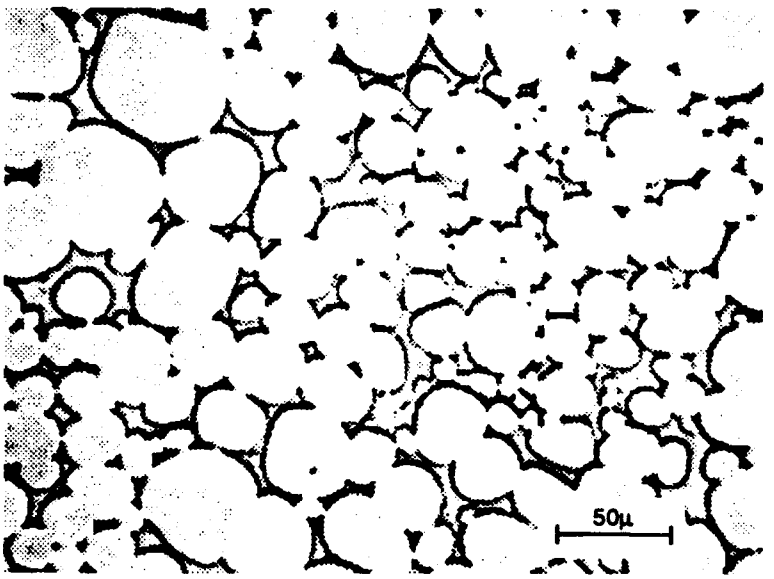

93W - 4.5Ni - 2.0Fe - 0.5Re

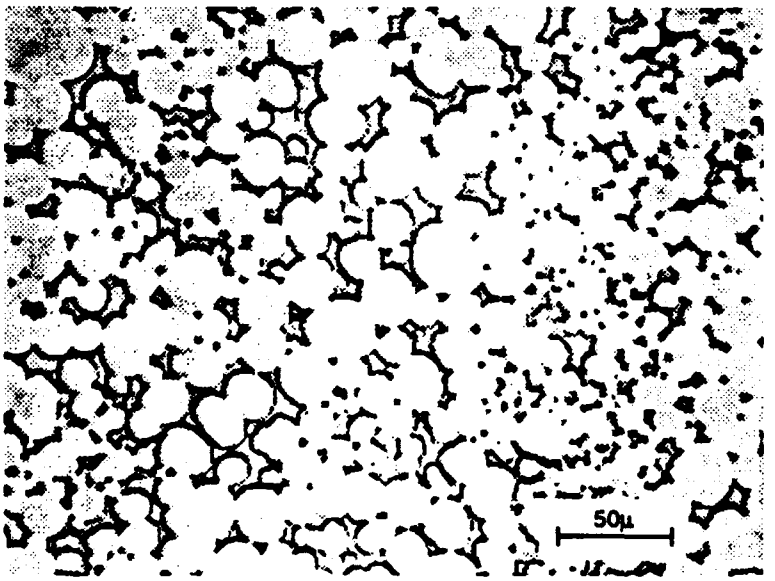

93W - 4.2Ni - 1.8Fe - 1.0Re

Figure 22 Microstructures of As-Sintered W-Ni-Fe-Re Alloys

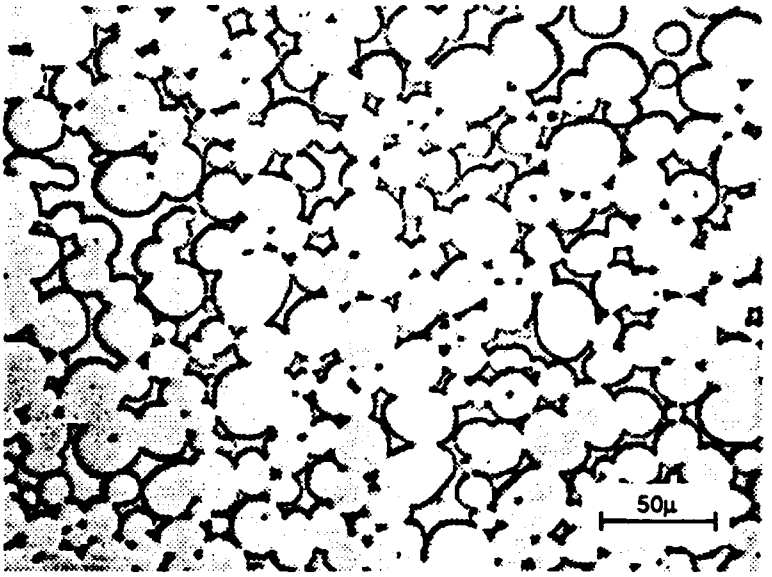

93W - 4.5Ni - 2.0Fe - 0.5Ru

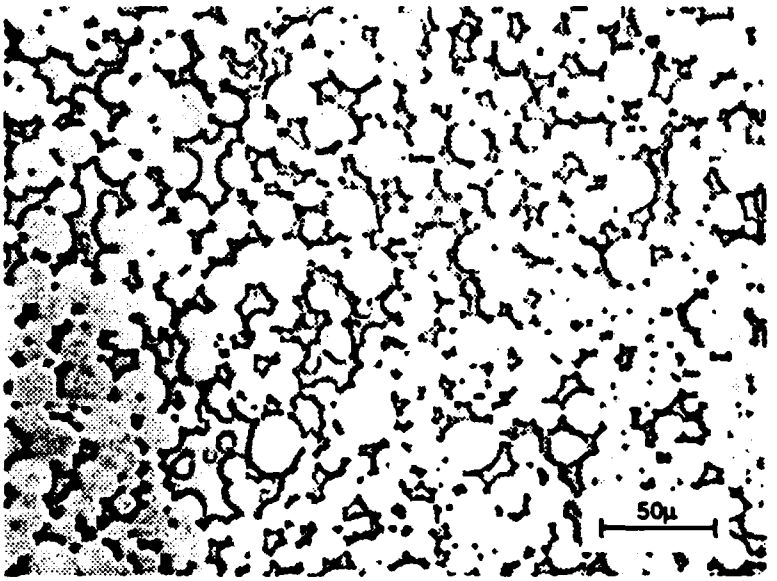

93W - 4.2Ni - 1.8Fe - 1.0Ru

Figure 23 Microstructures of As-Sintered W-Ni-Fe-Ru Alloys

Using our EDAX unit on our SEM we tried to determine if the rhenium and ruthenium were ending up in the matrix or the tungsten grains. For the 1% rhenium alloy we could not detect rhenium in either the matrix or the tungsten grains. Our detection limit for both rhenium and ruthenium is about 2 or 3%. When we examined 1% ruthenium alloy we were able to detect ruthenium in the matrix but not in the tungsten grains. These results suggested to us that the ruthenium was remaining largely in the matrix while the rhenium was not.

Because ruthenium and rhenium have much higher densities than nickel or iron, in the next series of tests we adjusted the tungsten content lower so that the theoretical density would be similar to a 93W-4.9Ni-2.1Fe alloy. Because our work on nickel:iron ratios showed the 8/2 ratios to be superior to the 7/3 ratios for our final series of tests on the rhenium and ruthenium additions we used a 8/2 nickel:iron ratios..

Table XXV summarizes the as-sintered mechanical properties for all the tests. Compared to the standard W-Ni-Fe alloys the rhenium and ruthenium alloys have higher hardnesses and yield strengths. This is likely due to a hardening effect on the matrix. The elongations are generally only a few percent lower than the standard alloys but the impact strengths are significantly reduced. At best the impact strengths for these alloys were only half of what the standard alloys were. We attributed these poor impact strength primarily to the high contiguity of the tungsten grains alloys. As would be expected, adjusting the density of these alloys by lowering the tungsten content increased the matrix volume and improved the mechanical properties.

Table XXV Mechanical Properties of W-Ni-Fe-Re and W-Ni-Fe-Ru Alloys

Alloy	Ni/Fe	(Rc)	UTS(ksi)	YS(ksi)	Elong(%)	Impact Energy(ft-lbs)
92.5W-4.9Ni-2.1Fe-0.5Re	7/3	31.0	143	88	28	12
92.5W-5.6Ni-1.4Fe-0.5Re	8/2	31.7	147	89	31	16
92W-5.6Ni-1.4Fe-1Re	8/2	32.2	152	91	28	15
93W-4.5Ni-2.0Fe-0.5Re	7/3	31.3	142	87	26	8.6
93W-4.2Ni-1.8Fe-1Re	7/3	31.2	146	91	20	4.4
92.7W-4.8Ni-2Fe-0.5Ru	7/3	31.7	149	92	29	16
92.7W-5.4Ni-1.4Fe-0.5Ru	8/2	31.9	150	90	32	16
92.4W-5.3Ni-1.3Fe-1Ru	8/2	33.7	160	97	33	17
93W-4.5Ni-2.0Fe-0.5Ru	7/3	31.9	149	93	29	11
93W-4.2Ni-1.8Fe-1Ru	7/3	32.6	160	101	21	6.2

Thermo-Mechanical Treatment - Ruthenium and Rhenium Additions

For our first series of thermo-mechanical treatments of the rhenium and ruthenium alloys we swaged the 0.5% rhenium and ruthenium alloys with 7/3 nickel:iron ratios to a 25% reduction in area. These alloys where those that we adjusted the tungsten content so they had a density similar to a 93W-4.9Ni-2.1Fe alloy. We then gave them a series of heat treatments for two hours at temperatures between 400 and 1400°C. Table XXVI gives the hardness, tensile and impact results for these tests.

Table XXVI Mechanical Properties of W-Ni-Fe-Ru and W-Ni-Fe-Re
(Swaged 25% and Heat Treated 2hrs)

Alloy	H.T. Temp.(°C)	Hardness (Rc)	UTS (ksi)	YS (ksi)	Elong.(%)	Impact Energy (ft-lbs)
92.7W-4.8Ni-2Fe-0.5Ru	As Swaged	44.4	189	178	9	6.4
"	400	46.9	-	-	-	-
"	600	49.6	226	215	5	1.2
"	800	48.0	-	-	-	-
"	900	45.7	198	172	7	4.4
"	1000	42.6	-	-	-	-
"	1200	38.0	165	118	21	7.5
"	1400	31.0	139	89	12	1.4
92.5W-4.9Ni-2.1Fe-0.5Re	As Swaged	43.6	180	169	10	6.7
"	400	43.5	-	-	-	-
"	600	45.4	209	199	0	-
"	800	44.9	-	-	-	-
"	1000	38.7	-	-	-	-
"	1200	36.3	157	112	20	-
"	1400	30.2	137	86	13	-

In Figure 24 the hardness values for the rhenium and ruthenium alloys are plotted along with data from a standard W-Ni-Fe alloy. The ruthenium alloy developed a maximum hardness of 49 Rc which is higher than we ever achieved with W-Ni-Fe alloys. One interesting result was that although the rhenium alloy swaged to a hardness similar to the ruthenium alloy, the presence of the rhenium appears to have suppressed the aging effect while the presence of ruthenium enhanced the effect.

At 600°C the ruthenium alloy developed a yield strength of 215 ksi which is higher than any conventionally processed W-Ni-Fe alloys. Although the impact strength was only about 1 ft-lb the elongation was a reasonable 4-5%. The rhenium alloy generally had poor properties.

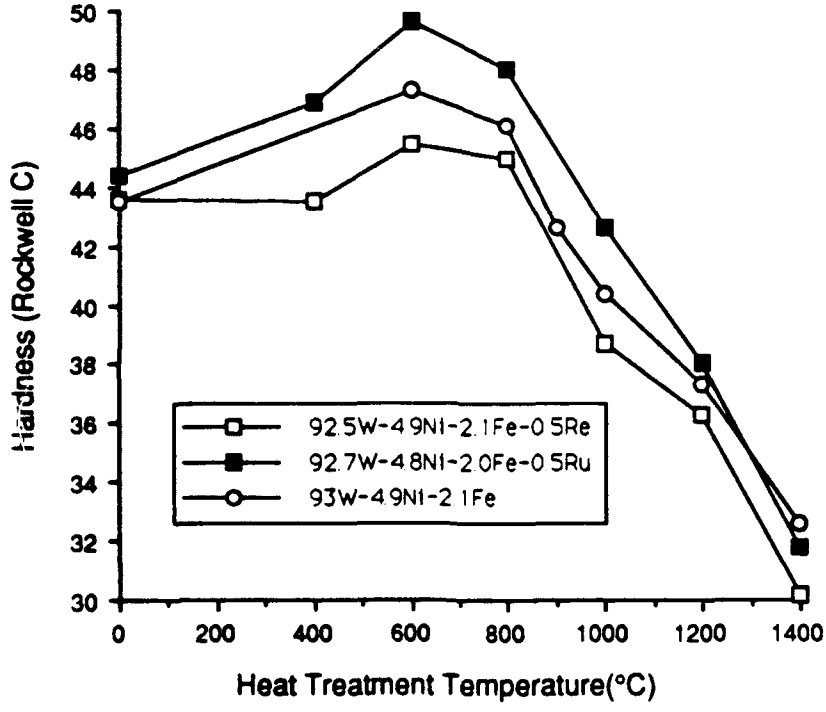

Figure 24 Effect of Heat Treating Temperature on Hardness of W-Ni-Fe-Re and W-Ni-Fe-Ru Alloys Swaged 25%

Depending on the amount of work and annealing temperature the tungsten grains in tungsten heavy alloys can recrystallize during annealing(18). Once the tungsten grains recrystallize there is a substantial loss in impact strength and elongation. Typically tungsten heavy alloys swaged 25% will recrystallize in a range of 1200 to 1400°C. We had thought that the presence of rhenium or ruthenium might raise the recrystallization temperature of the tungsten grains but the loss of tensile elongation and impact strength at 1400°C indicates that there is little difference in the recrystallization temperature.

Because the 0.5% ruthenium alloy with the 7/3 nickel:iron ratio looked so good we decided to produce several bars of a 0.5% ruthenium alloy with an 8/2 nickel:iron ratio. We planned to use this material for our in-house ballistic testing. This time we swaged the bars to a 15% reduction in area and ran a series of heat treatments for two hours at temperatures between 400 and 1400°C. The data for this test is shown in Table XXVII. Based on the hardness versus elongation curves this alloy definitely had better mechanical properties than the ruthenium alloy with the 7/3 nickel:iron ratio, but not better than the 93W-5.6Ni-1.4Fe(8/2). These curves are shown in Figure 25.

Table XXVII Mechanical Properties of Swaged and Heat Treated 92.7W-5.4Ni-1.4Fe-0.5Ru

RIA(%)	Heat Treatment	Hardness (Rc)	UTS (ksi)	YS (ksi)	Elong. (%)	RIA(%)	Impact Energy (ft-lbs)
0	none	32.1	149	91	26	33	23.7
15	none	43.1	181	164	14	25	15.5
15	400C-2hrs	44.9	-	-	-	-	-
15	600C-2hrs	47.5	207	196	9	10	5.5
15	900C-2hrs	45	195	163	12	12	9
15	1000C-2hrs	42.5	-	-	-	-	-
15	1200C-2hrs	38.1	164	116	28	29	21.4
15	1400C-2hrs	36.1	156	106	28	23	18.2

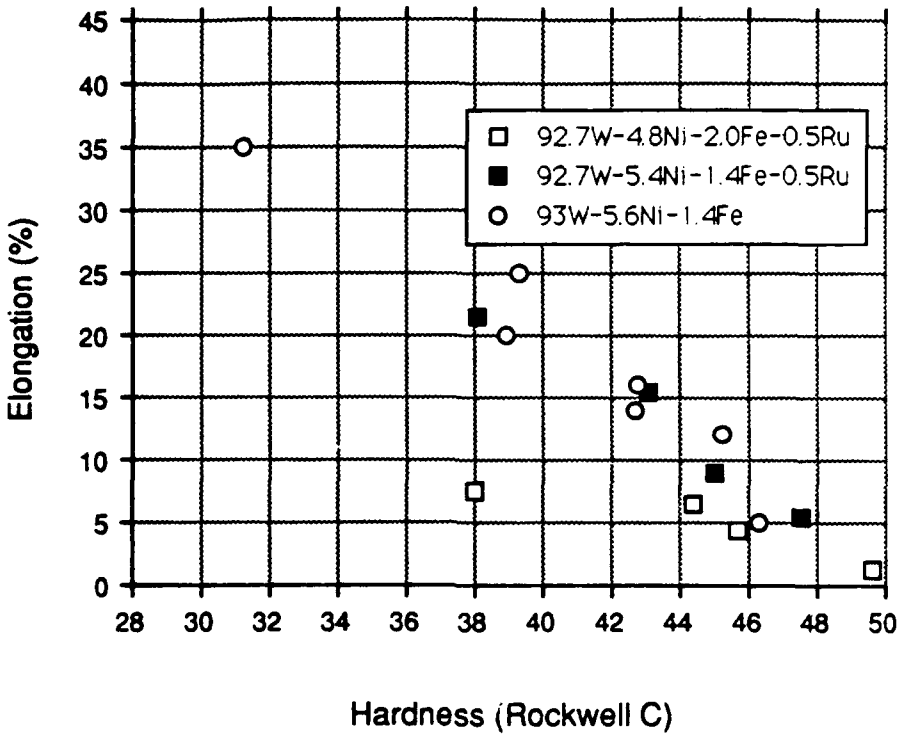

Figure 25 Elongation versus Hardness For W-Ni-Fe-Ru Alloys

W-Ni-Fe-Co Alloys

Unlike the ruthenium and rhenium additions which refined the tungsten grain size, we expected the cobalt to alloy with the matrix and cause changes in the matrix that would hopefully improve the mechanical properties of the alloys(5,11). For our initial test of W-Ni-Fe-Co alloys we used 0.5, 1.0 and 1.5% cobalt in a 93% tungsten alloy with the nickel:iron ratio set at about 7/3. We made the blends of these alloys as we did for the W-Ni-Fe alloys and sintered them at the same temperature. Later we extended the range of alloys to include 2 and 3% cobalt alloys with both 7/3 and 8/2 nickel:iron ratios.

Table XXVIII shows the results of the microstructural evaluation. For the 0.5 to 1.5% cobalt alloy the grain size appears to be finer than those of the W-Ni-Fe alloys. The 2 and 3% cobalt alloys had a coarser grain size than the lower percent cobalt alloys. This difference might be due to a difference in sintering temperature as the 2 and 3% alloys were sintered sometime after the lower percent alloys were sintered. As shown in Figure 26 the 3% cobalt alloys both had a large finger-like structure running through the matrix which we believe to be twining. X-ray diffraction analysis of the 3% cobalt alloy also revealed the presence of the μ-phase.

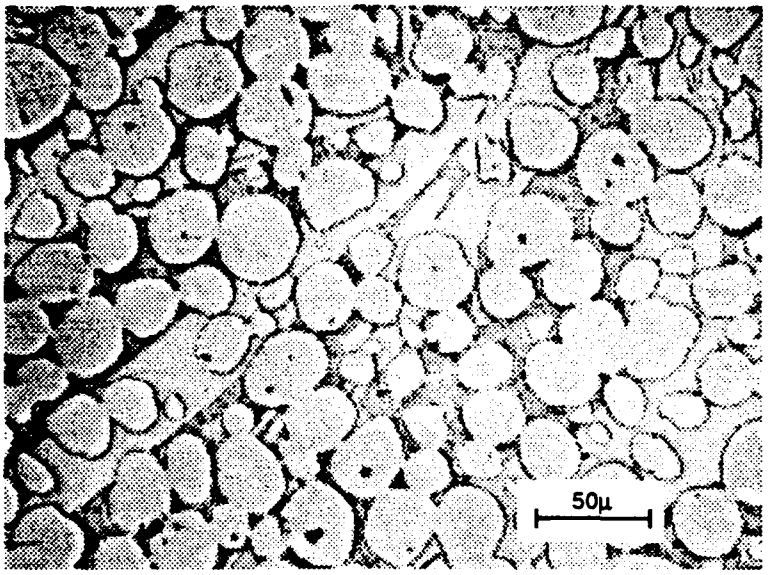

93W - 2.6Ni -1.4Fe - 3Co

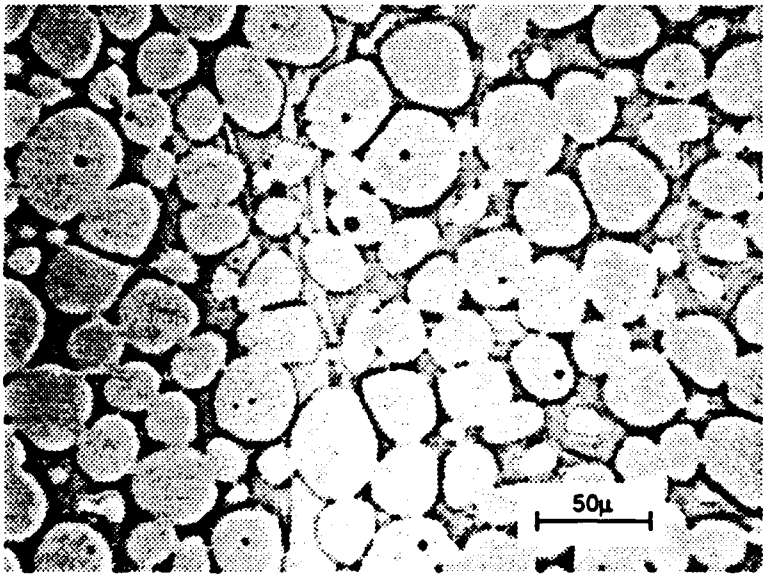

93W - 3.2Ni - 0.8Fe - 3Co

Figure 26 Microstructures of As-Sintered W-Ni-Fe-Co Alloys

Table XXVIII Microstructure Evaluation of W-Ni-Fe-Co Alloys

				MOP-3 Data			
		-Grain Count--		-Diameter(μm)--		------Contiguity(%)-----	
Alloy	Ni/Fe	Center	M.R.	Center	M.R.	Center	M.R.
93W-4.5Ni-2.0Fe-0.5Co	7/3	2180	2240	28	29	22	21
93W-4.2Ni-1.8Fe-1.0Co	7/3	2480	2440	28	28	21	17
93W-3.8Ni-1.7Fe-1.5Co	7/3	2240	2110	30	31	21	20
93W-3.6Ni-1.4Fe-2.0Co	7/3	1790	1830	–	–	–	–
93W-4.0Ni-1.0Fe-2.0Co	8/2	1680	1700	–	–	–	–
93W-3.6Ni-1.4Fe-3.0Co	7/3	1790	1720	–	–	–	–
93W-3.2Ni-0.8Fe-3.0Co	8/2	1530	1590	–	–	–	–

Table XXIX contains the impact and tensile results for the cobalt alloys. Elongations of all but the 3% cobalt alloys are similar to those of the standard W-Ni-Fe alloys. What is most interesting are the impact properties. At the low cobalt levels the impact strengths are lower than standard W-Ni-Fe alloys but at the 2% cobalt level the impact properties are superior to W-Ni-Fe alloys. The jump in impact strength at 2% cobalt might be partly do to the coarser grain size, but could not totally explain the improved properties. The μ-phase and twining present in the 3% cobalt alloys is obviously responsible for the poor properties of these alloys. We quenched the 3% alloys from 1200°C but the properties did not improve.

Table XXIX Mechanical Properties of W-Ni-Fe-Co Alloys

Alloy	Ni/Fe	UTS(ksi)	YS(ksi)	Elong(%)	Impact Energy(ft-lbs)
93W-4.5Ni-2Fe-0.5Co	7/3	141	87	32	17
93W-4.2Ni-1.8Fe-1Co	7/3	144	88	34	19
93W-3.8Ni-1.7Fe-1.5Co	7/3	145	89	34	21
93W-3.6Ni-1.4Fe-2Co	7/3	145	91	34	38
93W-4Ni-1Fe-2Co	8/2	145	92	34	37
93W-2.6Ni-1.4Fe-3Co	7/3	----------Very Brittle----------			
93W-3.2Ni-0.8Fe-3Co	8/2	----------Very Brittle----------			

PLASMA SPRAYED POWDERS AND SOLID-STATE SINTERED BARS

Plasma Sprayed Powders

GTE has a process where tungsten heavy alloy blends can be fed through a plasma spray gun to melt them and form tungsten heavy alloy powders. The particle size is in the 20 to 40 μm range with each particle being a miniature heavy alloy system as shown in Figure 27. Because the time that the particles are in the liquid-phase is so short the tungsten particles do not grow and remain at about 5 μm. It was our plan to use these powders develop a tungsten heavy alloy with a very fine grain size.

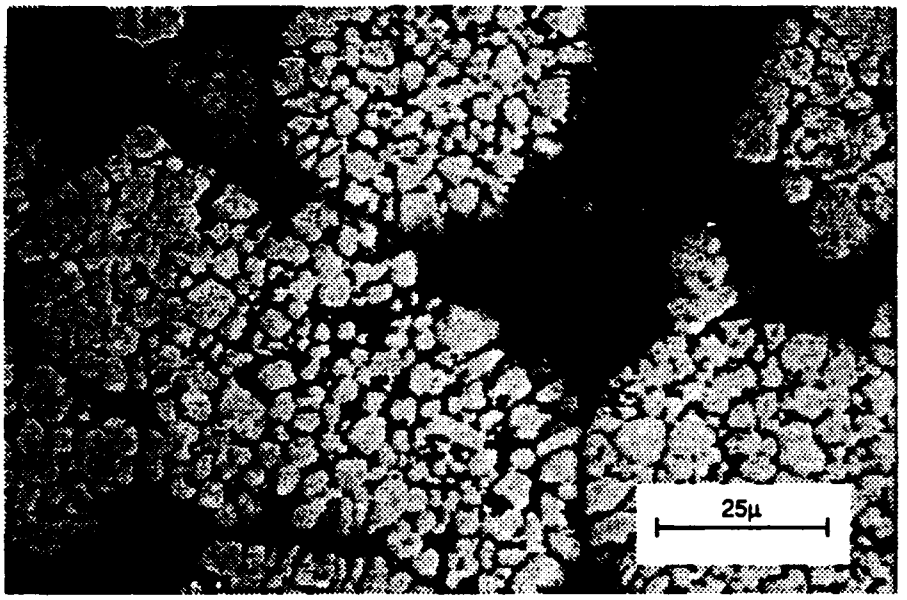

Figure 27 Microstructure of Plasma Sprayed W-Ni-Fe Powder

Using a GTE proprietary process we plasma sprayed a 91.3W-6.3Ni- 2.4Fe alloy. This composition was taken from previous work at GTE on plasma sprayed tungsten heavy alloys. This composition was determined on the powders after plasma spraying. We isostatically pressed these powders and solid-state sintered them in dry hydrogen (-20°C) at temperatures of 800, 1000 and 1200°C. We examined them for structure to see if the fine tungsten grain size was maintained. What we found was that even at 1000°C the tungsten grains were beginning to grow together into a continuous network. Figure 28 shows the 91.1W-6.3Ni-2.4Fe alloys sintered at 1200°C.

With growth already occurring during solid-state sintering we knew we would not be able to retain the fine grain size during liquid phase sintering. The only possibility would have been to use a very low sintering temperature along with a mechanical means to consolidate the alloys. Another problem we encountered with the plasma sprayed powders was the oxygen levels. Table XXX contains the oxygen results of the sintering tests and tend to show a lot of variation. The lowest values were about 70 ppm which is still much higher than is required for high quality tungsten heavy alloys. We believe anything over about 30 ppm oxygen is detrimental to tungsten heavy alloys.

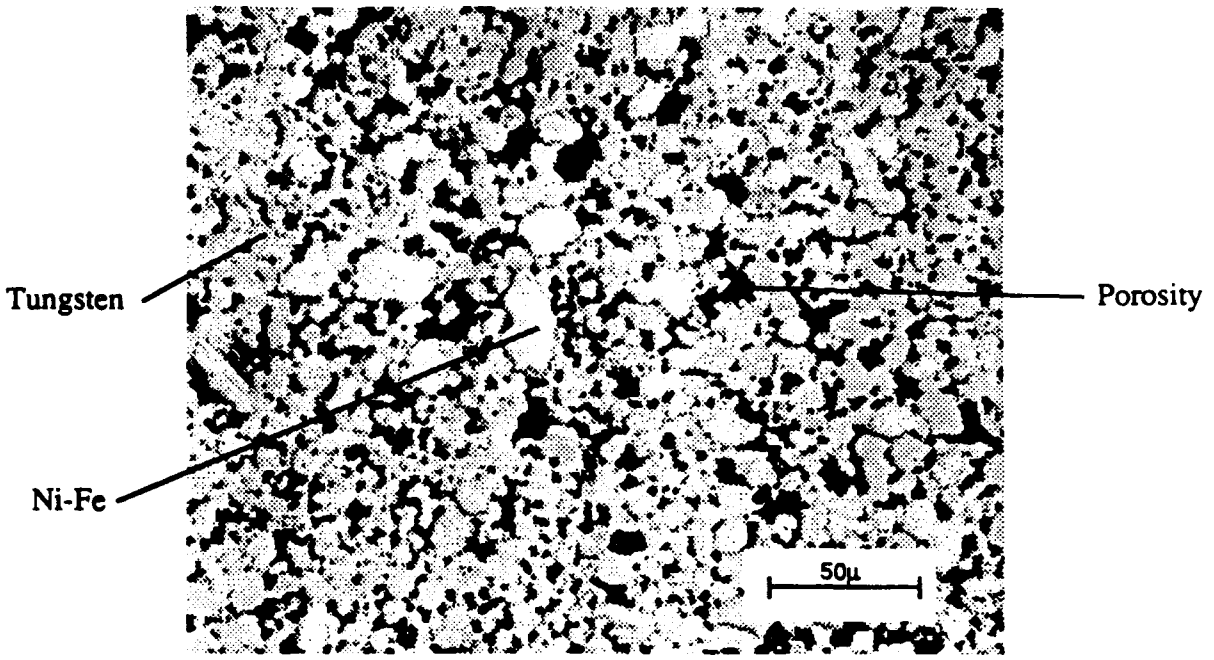

Figure 28 Microstructure of Plasma Sprayed W-Ni-Fe Powder Sintered 2hrs at 1200°C

Table XXX Effect of Sintering Temperature on Oxygen in Sintered Compacts of Plasma Sprayed Powders

ALLOY	Sintering Temp. (°C)	Oxygen (ppm)
91.3W-6.3Ni-2.4Fe	800	89
"	1000	212
"	1200	75
91.7W-8.3Ni	800	90
"	1000	175
"	1200	173

Based on the results of these tests we decided it would not be fruitful to pursue the plasma sprayed powders any further given the time limitations under this contract.

Solid-State Sintered Alloys

As a replacement for the plasma powder activity we looked at swaging a tungsten heavy alloy that had only been solid-state sintered. Unlike a liquid-phase tungsten heavy alloy the microstructure of a solid-state sintered alloy has a continuous tungsten phase with a grain size similar to the particle size of the tungsten powder used in the blend. Figure 1 is an example of a solid state sintered structure. For our standard blends this would mean a grain size of about 5 μm. With solid-state sintering full density cannot be achieved but will be in the range of 95 to 98% of theoretical density. Using solid state sintered material we hoped to produce a fine grain material and therefore improved properties.

The alloy we elected to use was 90W-8Ni-2Fe. We took bars of this alloy that had only been solid-state sintered and swaged them 8% at 900°C. We chose 900°C because we have found that when heavy alloys are worked above about 700°C they will not strain age. The bars were to be reheated during swaging and we didn't want them to age during the reheats. Also we have found that swaging at temperatures much above 900°C will cause defects to form between the tungsten grains and matrix. We believe these defects form because of the large difference in the yield strength between the tungsten grains and matrix. After the initial swaging we annealed the bar at 1200°C to reduce its hardness and increase ductility. We gave the bar two more swaging passes of 15% at 900°C. After each swaging pass we annealed the bar at 1200°C.

At this point the bars had been swaged about 33% and had sufficient ductility to run a tensile test which gave us a 12% elongation with a 112 ksi yield strength. The bar could now be worked at the normal swaging temperature of 300°C. Additional bars were processed to supply material for 20mm ballistic testing. Reduction in area of the bars used for ballistic testing was about 75%.

MACRO-COMPOSITES

High L/D penetrators require material with high density to penetrate the target, high elastic modulus to prevent bending between plates and good toughness to avoid fracturing during penetration. While tungsten and its alloys have a high modulus they may lack the toughness to make the best penetrator. To improve toughness in tungsten heavy alloys the tungsten content can be reduced but this lowers density and penetrating ability. One possible solution to this problem is to use tungsten alloys in macro-composite penetrators that have a shell made of a tough lower density material around a core made of a harder and higher density material.

We looked at three types of composites in this contract all of which used an unworked 93W-5.6Ni-1.4Fe (8/2 Ni:Fe) alloy as the shell material. For one core material we used a 96W-3.2Ni-0.8Fe(8/2 Ni:Fe) alloy that had been swaged and aged to make it as hard as possible. The second material we used was tungsten carbide-6% cobalt. While tungsten carbide is not as dense as tungsten heavy alloys it has shown excellent performance against 0° obliquity targets. Because it is very brittle, it does poorly against high obliquity targets. The third core material we looked at was swaged pure tungsten rod which is higher in density and has a higher yield strength than any tungsten heavy alloy. Swaged tungsten rod is brittle although not quite as brittle as tungsten carbide. Swaged tungsten rod will show a yield point where the tungsten carbide will not.

For our composite penetrators we used 0.187" diameter core and a 0.238" diameter shell that were made for testing in our 20mm range. These diameters were chosen to give equal volumes of the core and shell material. To make these composites oversize shells were prepared with a 0.187" diameter drilled through them. Cores that were longer than required were placed in the shells and then bonded to the cores. This bonding was done either by a light swaging pass (<5%) or brazing with pure copper. The composites were then turned to the final diameter by chucking on the protruding ends of the cores to guarantee a concentric composite.

The only way we could evaluate our composites for mechanical properties was to run impact tests on bars the same diameter (0.238") as the penetrators Table XXXI contains the impact values we determined for the composites along with comparison data of standard alloys tested using a .238" diameter sample. As can be seen from the data all of the composites had poor impact properties. Despite having a very ductile shell, the composite with the 96% tungsten core had impact energies similar to the all 96% tungsten samples. Because previous experience(18) had shown us that material with poor impact properties could have good ballistic performance we used the three composite variations for 20mm ballistic testing.

Table XXXI Impact Energy of Macro-Composites

Core Material	Bonding	Impact Energy(ft-lbs)*
Swaged Tungsten	Copper Braze	1.1
"	Silver Braze	1.1
"	Swaged	1.7
"	Swaged 5% and Heat Treated 2hrs at 1000°C	1.5
Tungsten Carbide	Copper Braze	1.2
96W-3.2Ni-0.8Fe(8/2) Swaged and aged	Copper Braze	3.1

Alloy	Condition	Impact Energy(ft-lbs)*
93W-5.6Ni-1.4Fe(8/2)	Unworked	51
96W-3.2Ni-0.8Fe(8/2)	Swaged 15%	5.7
"	Swaged 15% and Aged 4hrs at 400°C	2.6

* .238" diameter impact bars

BALLISTIC AND TAYLOR TESTING

One of the goals of the contract was to relate the mechanical properties of tungsten heavy alloys to ballistic performance. With the number and variety of ballistic tests run, however, we were not able to show strong correlations of ballistic properties to mechanical properties. We were able to show some dependence on alloying, thermomechanical processing and density. The ballistic tests and Taylor tests are reported in this section.

Taylor Tests

Taylor tests were done for us by the University of Denver. The test impacts cylinders against a steel plate at velocities between 260 and 700 fps from which dynamic yield strengths are determined. The hoop strain at the onset of radial cracking is also determined. Table XXXII contains a summary of the test results.

Figure 29 plots the dynamic yield versus the hardness for all the samples tested. Two distinct relations seem to be evident with the 8/2 Ni:Fe ratios having a higher dynamic yield for a given hardness than the 7/3 Ni:Fe ratios. Interestingly when the worked 7/3 ratio alloys are given a thermal treatment after working they fall into the curve for the 8/2 ratio alloys. Figure 30 is a similar plot which plots dynamic yield versus tensile yield.

Table XXXII Taylor Tests

% W	Ni/Fe	Percent Swaged	Heat Treatment	Hardness (Rc)	UTS (ksi)	YS (ksi)	Elong. (%)	Dynamic Yield (ksi)	Hoop Strain at unset of cracking
90	7/3	0	none	29	137	86	35	148	0.3
90	7/3	15	none	42.5	166	153	18	199	0.22
93	7/3	0	none	31	139	88	37	164	0.26
93	7/3	8	15hrs @ 500°C	43	181	170	8	245	0.16
93	7/3	15	none	42.5	169	156	13	198	0.19
93	7/3	25	8hrs @ 800°C	44.1	191	173	9	247	0.16
93	7/3	25	8hrs @ 1400°C	30.9	137	87	18	186	<0.5
93	8/2	0	none	29.6	139	85	36	170	0.28
93	8/2	15	none	40.9	171	156	19	243	0.25
96	7/3	0	none	31.8	141	87	21	167	0.18
96	7/3	15	none	44.5	174	161	10	189	0.12
96	8/2	0	none	30.9	140	87	23	190	0.22
96	8/2	15	none	41.5	172	158	11	241	0.16

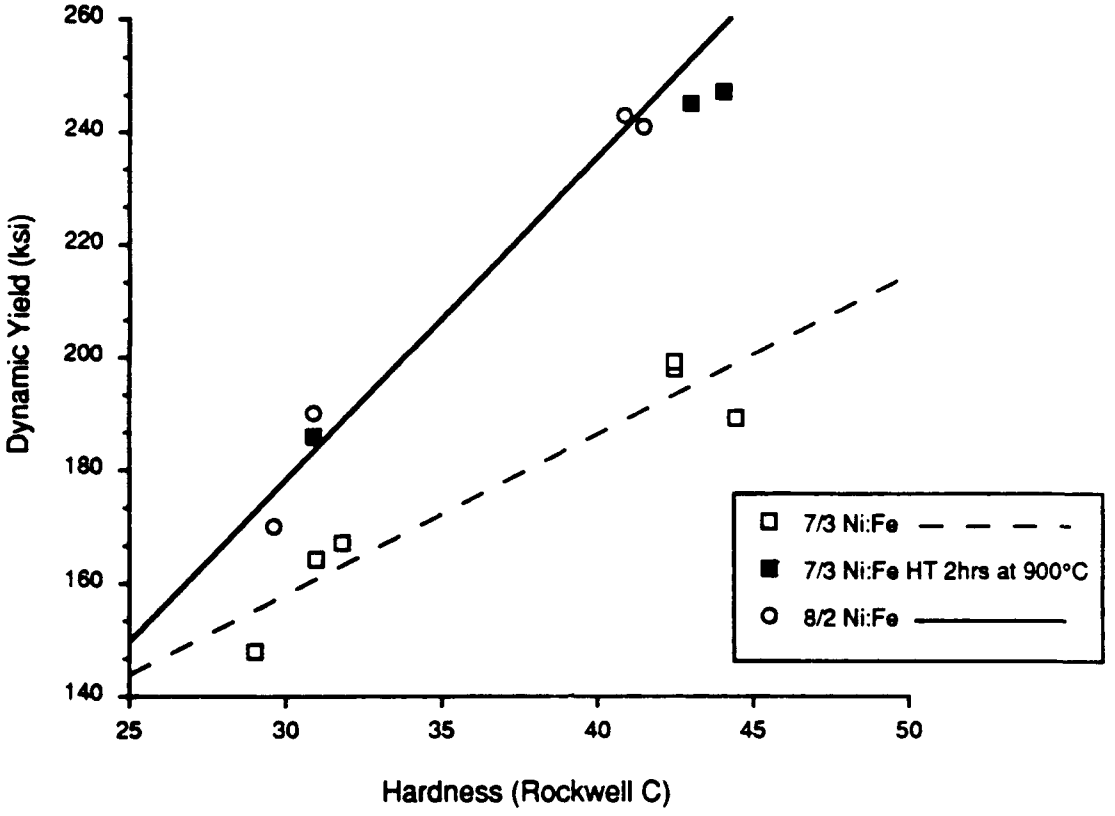

Figure 29 Taylor Test Dynamic Yield Versus Hardness For W-Ni-Fe Alloys

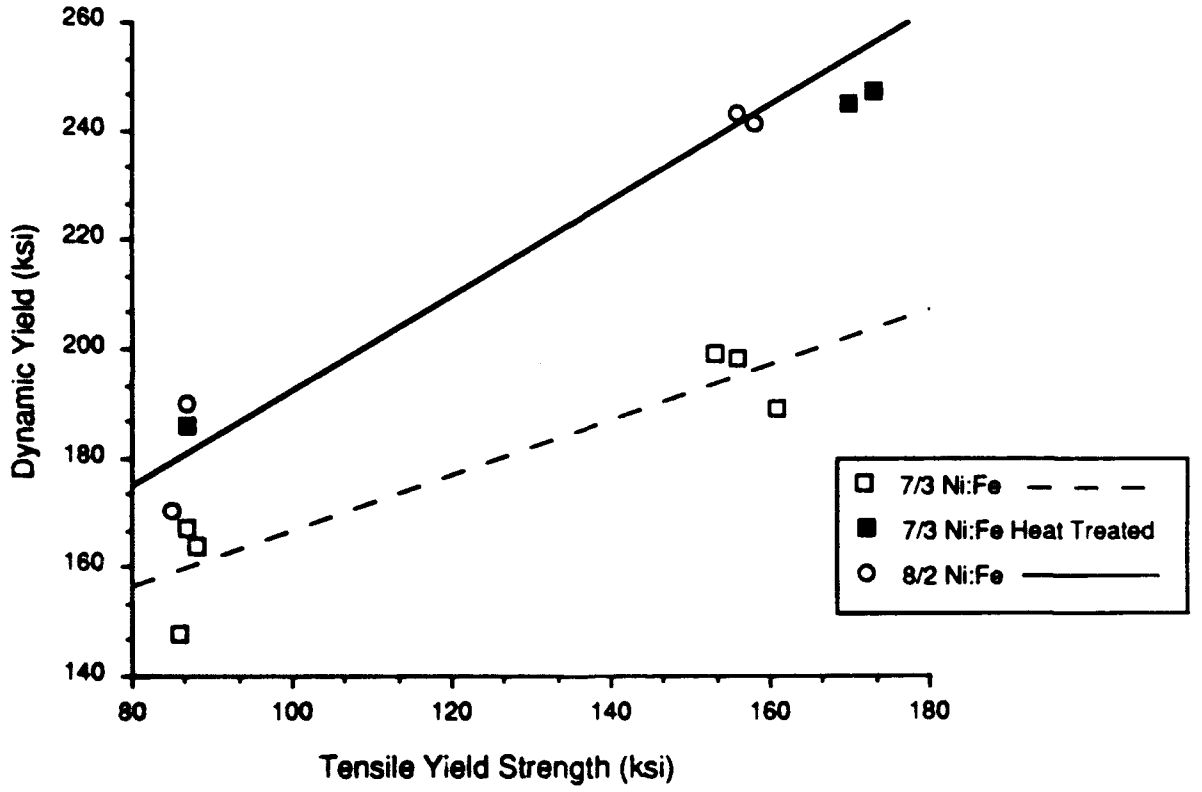

Figure30 Taylor Test Dynamic Yield Versus Tensile Yield For W-Ni-Fe Alloys

Another parameter that is generated from the test is the hoop strain at which cracking is first observed. Figure 31 shows a plot of the critical hoop strain versus the tungsten content. It shows the greater resistance to cracking of the 8/2 alloys.

The full report from the University of Denver is in the appendices.

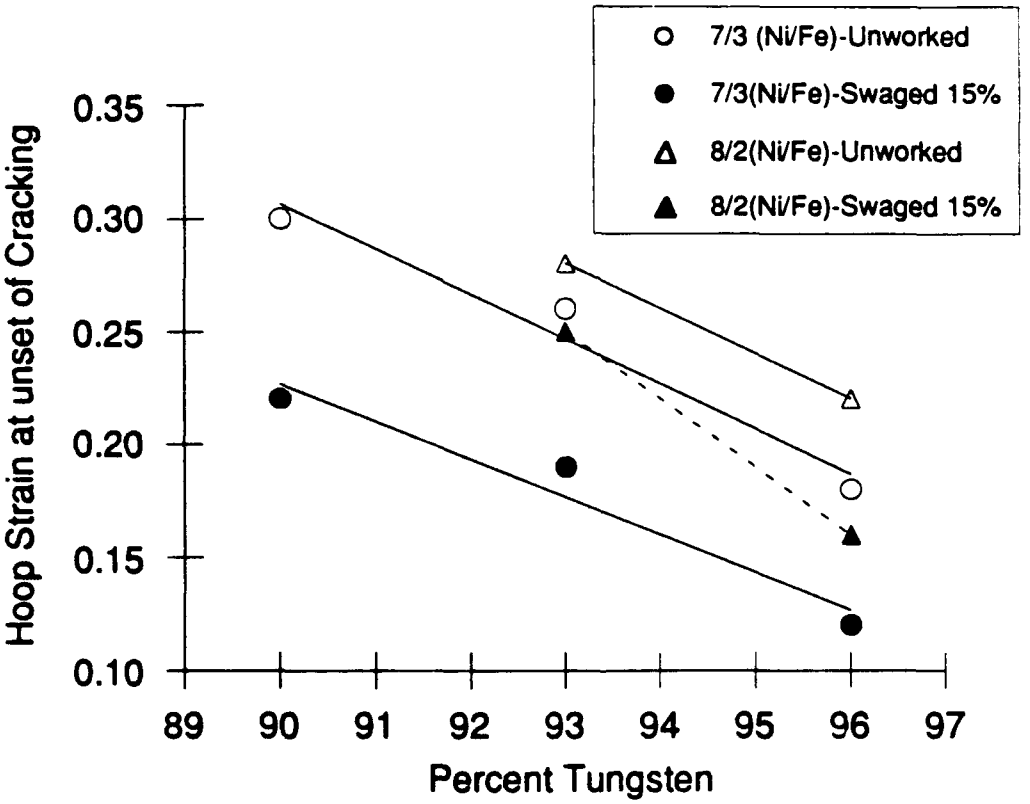

Figure 31 Taylor Test Hoop Strain at The Start of Cracking Versus Percent Tungsten

20mm Ballistic Tests

Table XXXIII contains all the results for V-50 determinations in our 20mm range. Table XXXIV is a streamlined version of Table XXXIII with the data for the W-Ni-Fe listed in order of increasing V-50. Table XXXV lists the test results by increasing V-50 for 90, 93 and 96% tungsten alloys. Also included are the mechanical properties of the alloys. No attempt was made to calculate any correlation coefficients for these results as we believe they would be very misleading.

Consider for example the impact energy. The impact energy increases as;

1. lower tungsten content is used
2. less work is put into the material
3. a higher Ni/Fe ratio is used

The lower tungsten content will raise the V50 as will less work. Higher Ni/Fe ratios , however, will lower the V50. Thus there is no simple relation of the impact energy to the V50 and calculating a correlation coefficient would only confuse the issue. The same problem exist for any property that is used.

Although it is difficult to draw hard conclusions, looking at Table XXXIV several interesting observations can be made about the W-Ni-Fe Alloys.

1. For the 93% W Alloys
    - 10 out of 10 of the 8/2 Ni:Fe alloys had lower than average V-50's
    - 2 out of 5 of the 7/3 Ni:Fe alloys had lower than average V-50's
    - Heavily working the 7/3 Ni:Fe alloys Makes it similar to the 8/2 Ni:Fe Alloy
    - The 9/1 Ni:Fe ratio didn't appear to be superior to the 8/2 ratio alloy

   Within the 8/2 alloys
    - 4 out of the 6 lowest V-50's were heavily worked(large RIA)

2. Best Overall (lowest V-50) was a 96%W (high density) alloy with a 8/2 Ni:Fe ratio
3. Best of each alloy sequence(90,93 &96% W) were all 8/2 Ni:Fe ratios
4. 6 out of the 9 as sintered alloys had higher than average V-50's
5. Best of the 90% W alloys(low density) are the heavily worked 8/2 Ni:Fe alloys
6. The highest V-50 was an alloy with a 5/5 Ni:Fe ratio

Based on these observations, it appears for the W-Ni-Fe alloys that large reductions in area, higher densities and 8/2 Ni:Fe ratios improve ballistic performance. One cautionary note should be presented here. In doing the ballistic testing the 8/2 alloys were tested first and the7/3 alloys at a later date. The possibility thus exists that some other factors may have affected the results, notably the armor plate used. We did measure the hardness and impact strength of the armor and could find no significant differences. However, the possibility of a change should be considered.

High oxygen levels also proved to be detrimental to ballistic performance. Using data from Table XX, figure 32 plots 20mm V50 results versus oxygen content. This figure definitely shows that very high oxygen levels are detrimental to ballistic performance It is interesting to note that the 8/2 ratio alloys that occur near the bottom of Table XXXIV (higher V-50) are from this high oxygen test.

The tests showed that the composite penetrator with the tungsten carbide core to be very poor and the others to have V-50's slightly higher than the average.

One of the most important findings to come out of the 20mm testing is that some of the novel materials we developed during this contract were at least as comparable to standard alloys. These include the ruthenium alloy, the solid-state sintered alloy and a 93W-7Ni alloy. If these alloys were given very large reductions in area it is possible that they may show superior performance.

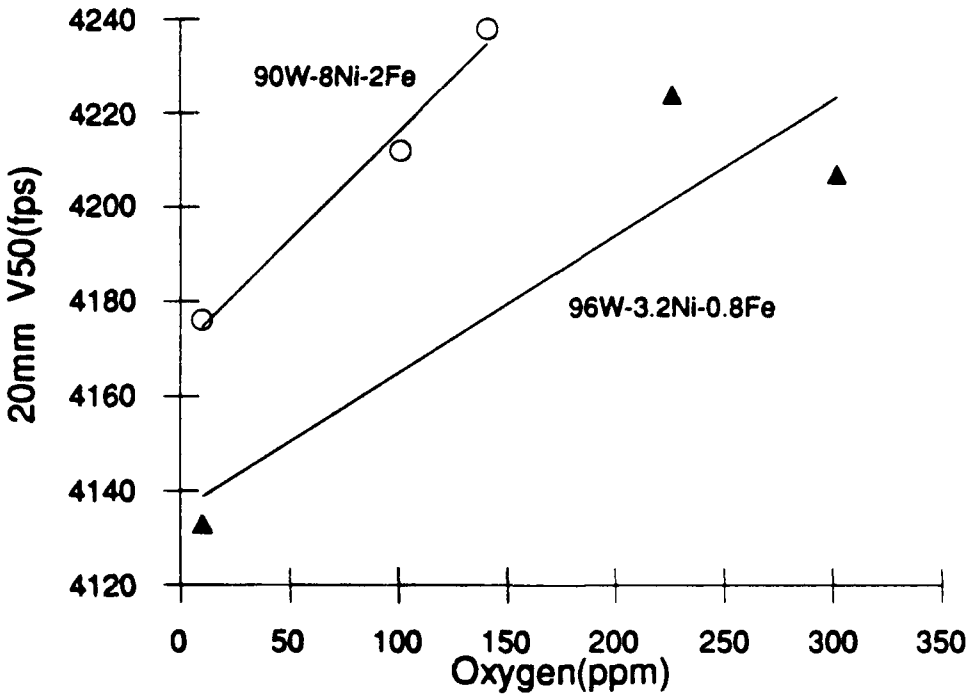

Figure 32 20mm V50 Versus Oxygen Content for W-Ni-Fe Alloys With 8/2 Ni:Fe Ratios

Table XXXIII 20mm Ballistic Tests - Arranged by Alloy

Sample	Alloy	Ni/Fe	% Worked	HT*	Heat Treatment	V-50 (ft/sec)	Std.Dev	Range	
D-3062	WHA/W Composite	-	0			4219	43	134	
D-3063	WHA/WHA Composite	-	0			4232	13	34	
D-2557	90W-5Ni-5Fe	1/1	0			4309	12	45	
D-2451	90W-7Ni-3Fe	7/3	0			4257	22	79	
D-2698	"	7/3	15			4239	36	111	
D-2697	"	7/3	15		Aged 400°C	4200	34	113	
D-2102	90W-8Ni-2Fe	8/2	0			4176	16	50	
D-2715	"	8/2	0			4212	26	97	Sintered in N2
D-2716	"	8/2	0			4238	24	87	Sintered in Vacuum
D-2103	"	8/2	15			4117	25	99	
D-2104	"	8/2	15		Aged 400°C	4174	54	165	
D-2558	"	8/2	55	N		4233	53	142	
D-3070	"	8/2	75	Y	Aged 500°C	4104	58	176	
D-3071	"	8/2	75	Y	Annealed 900°C	4115	54	139	
D-3215	92.7W-5.4Ni-1.4Fe-0.5Ru	8/2	15		400°C	4132	35	109	
D-2559	93W-4.9Ni-2.1Fe	7/3	0			4198	25	87	
D-2560	"	7/3	15			4248	52	176	
D-3214	"	7/3	15		Aged 400°C	4210	23	67	
D-2561	"	7/3	15		Aged 400°C	4207	31	106	
D-3083	"	7/3	70	N	Aged 500°C	4088	63	209	

*HT - Heat Treated Between Passes?

Table XXXIII 20mm Ballistic Tests (cont.) - Arranged by Alloy

Sample	Alloy	Ni/Fe	% Worked	HT*	Heat Treatment	V-50 (ft/sec)	Std.Dev	Range	
D-2105	93W-5.6Ni-1.4Fe	8/2	0			4121	23	92	
D-2106	"	8/2	15			4145	19	67	
D-2107	"	8/2	15		Aged 400°C	4059	28	89	
D-3216	"	8/2	15		Aged 400°C	4115	43	118	
D-3215	"	8/2	15		Aged 400°C	4132	35	109	
D-3084	"	8/2	70	N	Aged 500°C	4102	39	136	
D-3082	"	8/2	70	N	Annealed 900°C	4046	60	195	
D-3085	"	8/2	75	N	Aged 500°C	4096	63	225	
D-3086	"	8/2	75	N	Annealed 900°C	4063	47	175	
D-3087	"	8/2	75	N	Annealed 900°C	4071	88	270	
D-3217	"	8/2	75	Y		4097	29	87	Solid State Sintered
D-3212	93W-6.3Ni-0.7Fe	9/1	15		Aged 400°C	4127	20	50	
D-3213	93W-7Ni	10/0	15		Aged 400°C	4112	23	64	
D-2634	96W-2.8Ni-1.2Fe	7/3	0			4196	10	36	
D-2635	"	7/3	15			4202	16	53	
D-2704	"	7/3	15			4246	28	92	
D-2705	"	7/3	15		Aged 400°C	4274	30	105	
D-2551	96W-3.2Ni-0.8Fe	8/2	0			4133	46	155	Sintered in N2/H2
D-2452	"	8/2	0			4174	47	123	Sintered in Wet H2
D-2453	"	8/2	0			4202	48	137	Sintered in Dry H2
D-2717	"	8/2	0			4207	15	41	Sintered in Vacuum
D-2718	"	8/2	0			4224	15	46	Sintered in N2
D-2100	"	8/2	15			4039	22	77	
D-2101	"	8/2	15		Aged 400°C	4029	72	256	

*HT - Heat Treated Between Passes?

Table XXXIV 20mm Ballistic Data by Increasing V-50

Misc.	90% Tungsten 8/2Ni:Fe	90% Tungsten 7/3 Ni:Fe	93% Tungsten 8/2Ni:Fe	93% Tungsten 7/3 Ni:Fe	96% Tungsten 8/2Ni:Fe	96% Tungsten 7/3 Ni:Fe
					4029 S&A	
					4039 SW	
			4046 LR			
			4059 SW			
			4063 LR			
			4071 S&An			
				4088 LR		
4090 (Ave - Std. Dev)						
			4096 LR			
			4102 LR			
	4104 LR					
				4110 SW		
4112 (93W 6/4 Ni:Fe)						
	4115 LR		4115 S&A			
	4117 SW					
			4121 AS			
4127 (93W 9/1Ni:Fe)SW						
			4132 S&A			
					4133 AS	
			4145 SW			
4161 (Average)						
	4174 S&A				4174 AS	
		4176 AS				
						4196 AS
				4198 AS		
					4202 AS	4202 SW
				4207 S&A		
4232 (Ave+Std. Dev.)						
	4233 LR					
		4239 SW				
						4246 SW
				4248 SW		
		4257 AS				
4309 (90W 5/5Ni:Fe)AS						4274 SW

AS	As Sintered
SW	Swaged
S&A	Swaged and Aged
S&An	Swaged and Annealed
LR	Large RIA

Table XXXV 20mm Ballistic Tests and Mechanical Data

Sample	Alloy	Ni/Fe	V-50 (ft/sec)	Hardness (Rc)	UTS(ksi)	YS(ksi)	Elong(%)	Impact Energy(ft-lbs)
D-2557	90W-5Ni-5Fe	1/1	4309	29.0	133	90	23.0	9.8
D-2451	90W-7Ni-3Fe	7/3	4257		135	84	31.0	38.0
D-2698	90W-7Ni-3Fe	7/3	4239	40.3	167	157	15.0	20.0
D-2697	90W-7Ni-3Fe	7/3	4200	41.7	178	168	12.0	13.0
D-2102	90W-8Ni-2Fe	8/2	4176	30.7	141	86	38.0	55.0
D-2715	90W-8Ni-2Fe	8/2	4212	29.4	136	82	36.0	33.0
D-2716	90W-8Ni-2Fe	8/2	4238	30.7	137	84	36.0	44.0
D-2103	90W-8Ni-2Fe	8/2	4117	40.6	173	160	20.0	28.0
D-2104	90W-8Ni-2Fe	8/2	4174	43.0	182	172	13.0	14.5
D-2558	90W-8Ni-2Fe	8/2	4233	44.1	203	190	11.0	23.0
D-3070	90W-8Ni-2Fe	8/2	4104		184	175	17.0	8.7
D-3071	90W-8Ni-2Fe	8/2	4115		169	145	25.0	21.0
D-2559	93W-4.9Ni-2.1Fe	7/3	4198	29.3	140	90	33.0	27.0
D-2560	93W-4.9Ni-2.1Fe	7/3	4248	41.9	177	165	12.0	7.5
D-3214	93W-4.9Ni-2.1Fe	7/3	41i0		187	178	7.0	5.7
D-2561	93W-4.9Ni-2.1Fe	7/3	4207	40.8				
D-3083	93W-4.9Ni-2.1Fe	7/3	4088					
D-3215	92.7W-5.4Ni-1.4Fe-0.5Ru	8/2	4132	45.5	211	201	6.0	6.0
D-2105	93W-5.6Ni-1.4Fe	8/2	4121	31.3	141	86	28.0	27.0
D-2106	93W-5.6Ni-1.4Fe	8/2	4145	41.4	175	160	13.0	12.0
D-2107	93W-5.6Ni-1.4Fe	8/2	4059		185	172	14.0	11.0
D-3216	93W-5.6Ni-1.4Fe	8/2	4115					
D-3215	93W-5.6Ni-1.4Fe	8/2	4132	45.5	211	201	6.0	6.0
D-3084	93W-5.6Ni-1.4Fe	8/2	4102	49.6				
D-3082	93W-5.6Ni-1.4Fe	8/2	4046	45.0	199	183	13.0	3.4
D-3085	93W-5.6Ni-1.4Fe	8/2	4096		188	179	9.0	1.9
D-3086	93W-5.6Ni-1.4Fe	8/2	4063		171	146	17.0	5.8
D-3087	93W-5.6Ni-1.4Fe	8/2	4071					
D-3212	93W-6.3Ni-0.7Fe	9/1	4127	43.5	191	177	14.0	9.1
D-3213	93W-7Ni	10/0	4112					
D-2634	96W-2.8Ni-1.2Fe	7/3	4196	31.7	140	86	29.0	13.0
D-2635	96W-2.8Ni-1.2Fe	7/3	4202		174	160	16.0	17.0
D-2704	96W-2.8Ni-1.2Fe	7/3	4246	43.8	193	178	6.0	2.0
D-2705	96W-2.8Ni-1.2Fe	7/3	4274	43.8	193	178	6.0	2.0
D-2551	96W-3.2Ni-0.8Fe	8/2	4133	31.6	140	86	26.0	15.0
D-2452	96W-3.2Ni-0.8Fe	8/2	4174	31.4	140	89	26.0	16.0
D-2453	96W-3.2Ni-0.8Fe	8/2	4202	31.5	140	88	28.0	14.0
D-2717	96W-3.2Ni-0.8Fe	8/2	4207	30.7	106	85	5.0	1.4
D-2718	96W-3.2Ni-0.8Fe	8/2	4224	31.3	137	85	20.0	3.0
D-2100	96W-3.2Ni-0.8Fe	8/2	4039	41.4	175	164	10.0	4.6
D-2101	96W-3.2Ni-0.8Fe	8/2	4029	44.1	189	176	8.5	1.9

30 mm Phalanx

The Phalanx 30 mm testing was done by Olin against the X-1 array at 4100 ft/sec.. The following alloys were tested:

Alloy	Condition
90W-8Ni-2Fe(8/2)	Unworked
"	Swaged 15%
"	Swaged 15% and Aged 400°C -2hrs
93W-4.9Ni-2.1Fe(7/3)	Unworked
93W-5.6Ni-1.4Fe(8/2)	Unworked
96W-3.2Ni-0.8Fe(8/2)	Unworked

Table XXXVI summarizes the results and Figures 33 and 34 plot the individual shots against residual velocity and mass. These plots were made by listing the test results by decreasing residual velocity or mass and giving the highest value a Y value of 1.0 and the lowest value a Y value of 0.0. Tests in between are given proportional Y values. In evaluating these plots the lines falling to the right are the better performing materials. Although several shots were lost to yaw problems it did appear that the 96% tungsten alloy was too brittle and experienced excessive breakup through the target.

The results also show that for the 93% alloys the 8/2 ratio performed better than the 7/3 ratio. Finally the results show that even with working and aging we could not get the 90% alloy to work as well as the 93% alloys.

The full report from Olin on the 30mm Phalanx testing is in the appendix.

Table XXXVI 30mm Phalanx Testing Against The X-1 Array

				Average Entrance		Average Exit	
Alloy	Ni/Fe	Condition	Ave. Mass(g)	Vel.(fps)	Yaw(°)	Vel.(fps)	Res. Mass(g)
90W-8Ni-2Fe	8/2	unworked	269.9	4179	1.8	3491	247
"	8/2	swaged 15%	269.6	4147	3	2804	239
"	8/2	swaged 15% & aged	270.9	4173	2.1	3194	210
93W-4.9Ni-2.1Fe	7/3	unworked	277.2	4115	2.9	2903	233
93W-5.6Ni-1.4Fe	8/2	unworked	278	4154	2.3	3340	223
96W-3.2Ni-0.8Fe	8/2	unworked	287.6	4171	3	2966	157

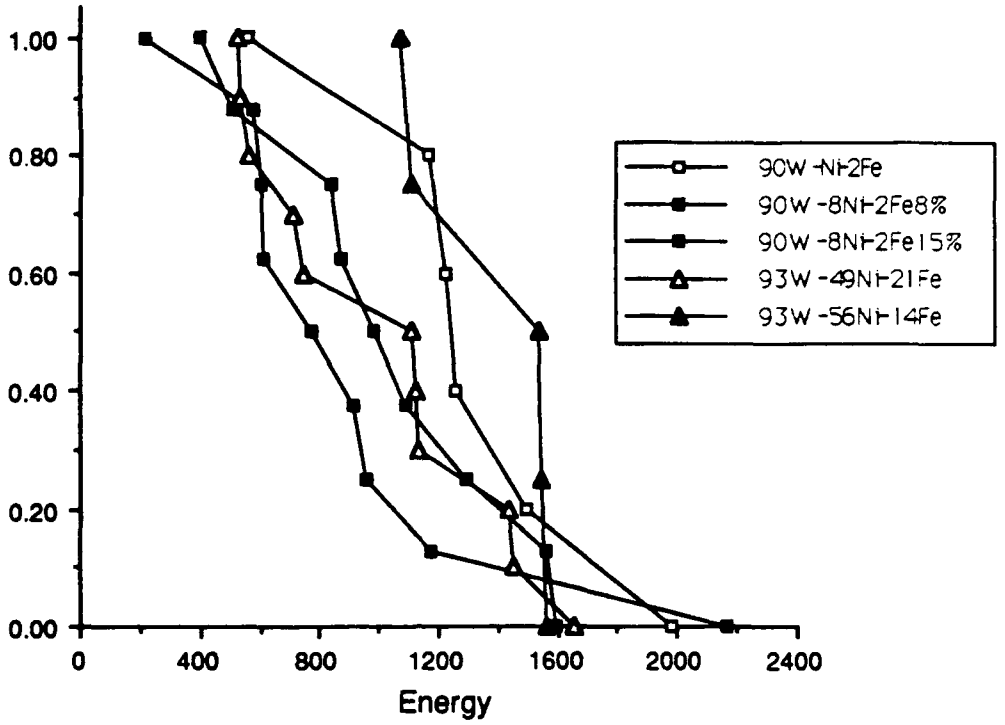

Figure 33 Residual Velocity for 30mm Phalanx Penetrators Against The X-1 Plate Array

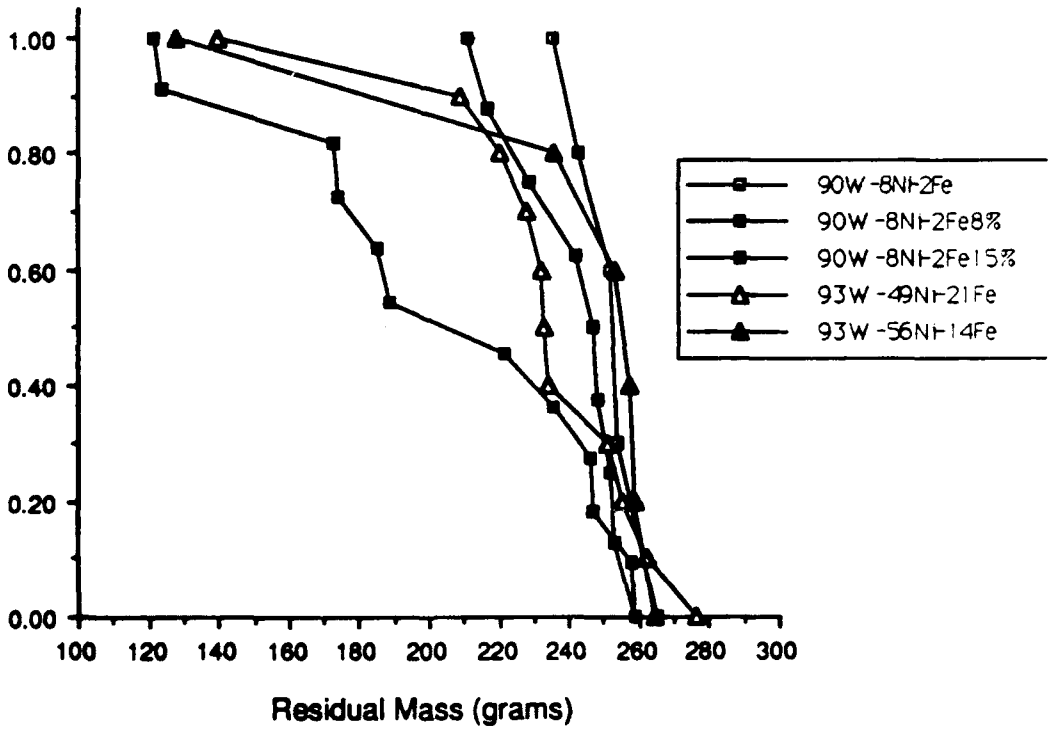

Figure 34 Residual Mass for 30mm Phalanx Penetrators Against The X-1 Plate Array

M791

We tested a variety of 96% tungsten alloys and one 93% tungsten alloy as a M791 penetrator against rolled homogenous armor and high hard armor. The tests were done for us by Aerojet. Results of these tests are in Table XXXVII. Because the actual V-50's are classified, the data shown has been normalized to the swaged 96W-2.8Ni-1.2Fe alloy using 1000 as a base. There is little differences between the alloys and the data doesn't show any obvious trend. The full report is attached to the classified report of thermo-mechanical processing from Battelle

Table XXXVI I M791 Ballistic Results

Alloy	Ni/Fe	Condition	Armor	V50*	Spread
96W-2.8Ni-1.2Fe	7/3	Swaged 8%	RHA	1011	38
"	7/3	Swaged 15%	"	1000	27
"	7/3	Swaged 15%-Aged**	"	989	35
96W-3.2Ni-0.8Fe	8/2	"	"	1018	25
93W-4.9Ni-2.1Fe	7/3	"	"	1022	34
96W-2.8Ni-1.2Fe	7/3	Swaged 15%	HHA	1000	36
96W-3.2Ni-0.8Fe	8/2	Swaged 15%-Aged**	"	1000	41
93W-4.9Ni-2.1Fe	7/3	Swaged 15%-Aged**	"	995	33

* V50 data normalized to 96W-2.8Ni-1.2Fe Swaged 15%

** Aged 4hrs at 400°C

XM-881

For the XM-881 we tested 93% tungsten alloys with 7/3 and 8/2 Ni:Fe ratios and a 96% alloy with a 8/2 ratio. These tests were also run by Aerojet and the results are in Table XXXVIII. The V-50's are also classified so the data has been normalized to the 93W-4.9Ni-2.1Fe alloy swaged 15%.

For the 93% tungsten alloys it appears that the 7/3 might be slightly better although the difference could not be shown to be significant. We tested 93W-5.6Ni-1.4Fe alloys with different mechanical properties but they do not relate to the small differences we saw in the V-50's. properties, but they do not relate to the small differences we saw in the V-50's. The most interesting result was that of the 96W-3.2Ni-0.8Fe alloy. Against the rolled homogenous armor it was as good as the 93% alloys and against the high hard armor it was the best.

Table XXXVIII XM881 Ballistic Results

Alloy	Ni/Fe	Condition	Armor	V50**	Spread
93W-4.9Ni-2.1Fe	7/3	Swaged 15% - Aged*	RHA	1000	37
93W-5.6Ni-1.4Fe	8/2	"	"	1029	33
"	8/2	Swaged 20% - Aged*	"	1043	34
"	8/2	Swaged 15% - Aged* Then 900°C for 2 hr	"	1063	42
96W-3.2Ni-0.8Fe	8/2	Swaged 15% - Aged*	"	1010	42
93W-4.9Ni-2.1Fe	7/3	Swaged 15% - Aged*	HHA	1000	29
93W-5.6Ni-1.4Fe	8/2	"	"	1010	30
93W-5.6Ni-1.4Fe	8/2	Swaged 10% - Aged*	"	1001	35
"	8/2	Swaged 20% - Aged*	"	1017	32
"	8/2	Swaged 15% - Aged* Then 900°C for 1 hr	"	1011	33
96W-3.2Ni-0.8Fe	8/2	Swaged 15% - Aged*	"	964	29

*Aged 4hrs at 400°C

**V50 normallized to 93W-4.9Ni-2.1Fe Swaged 15%

APPENDIX

20 mm Ballistic Testing

Taylor Anvil Tests

Olin 30mm Phalanx Testing

20 mm Ballistic Testing

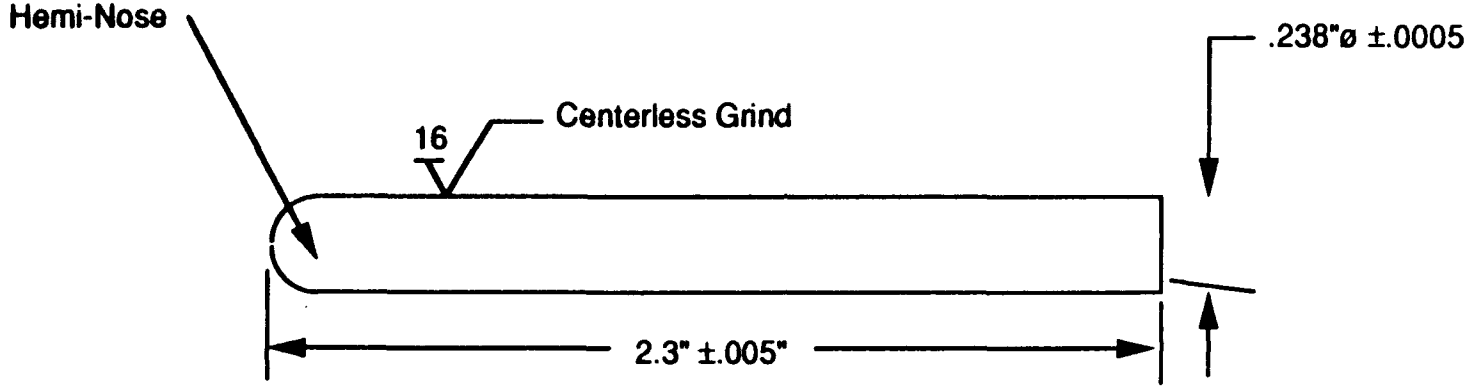

GTE 20mm Penetrator

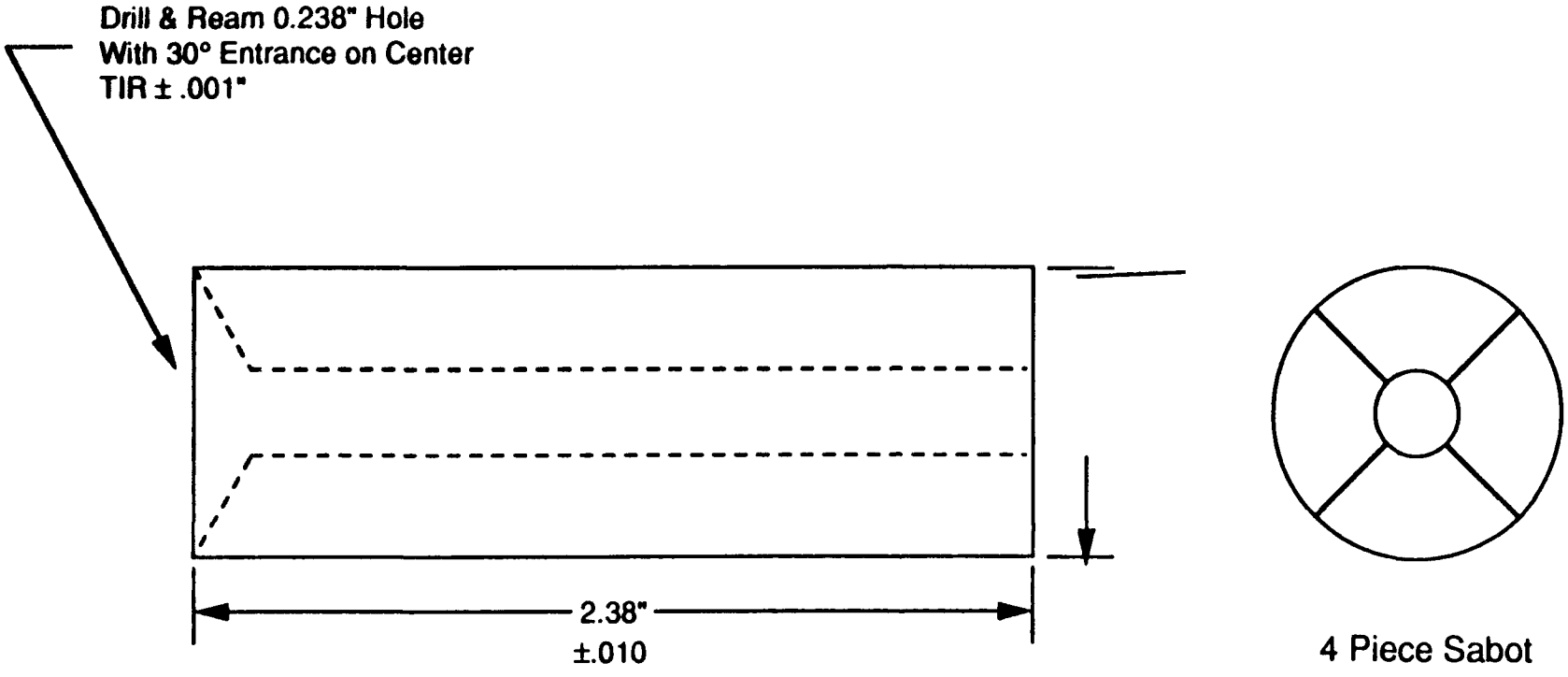

GTE 20mm Sabot

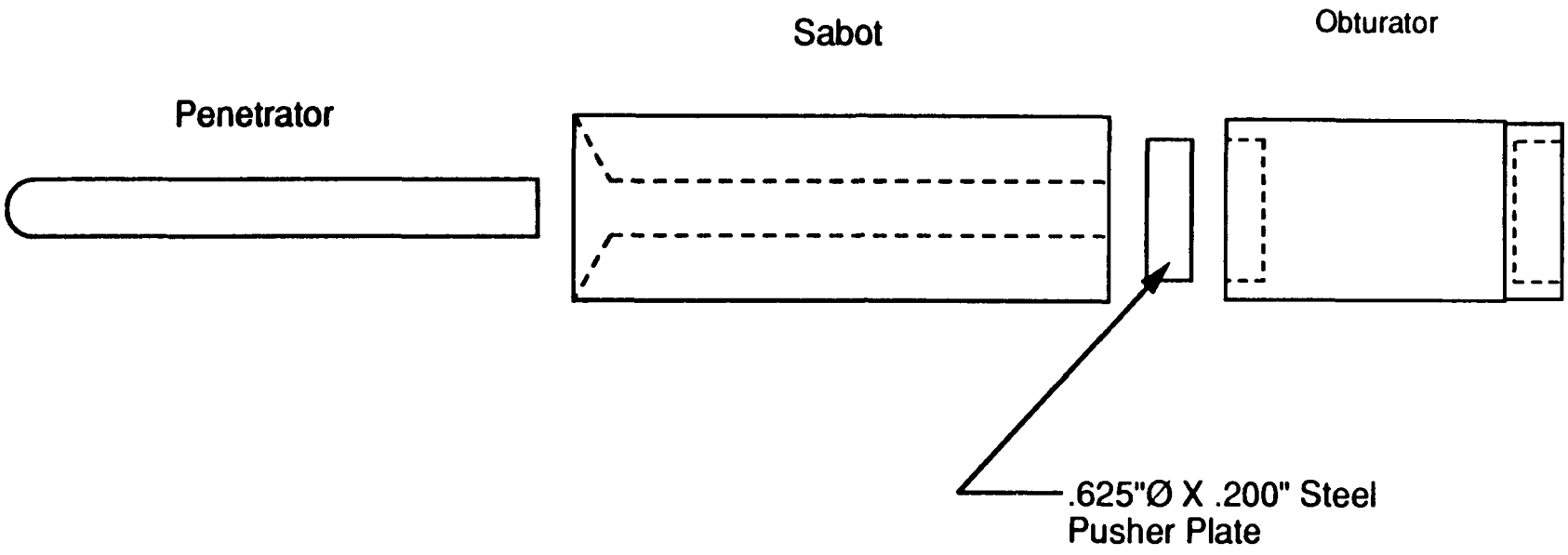

GTE 20mm Assembly

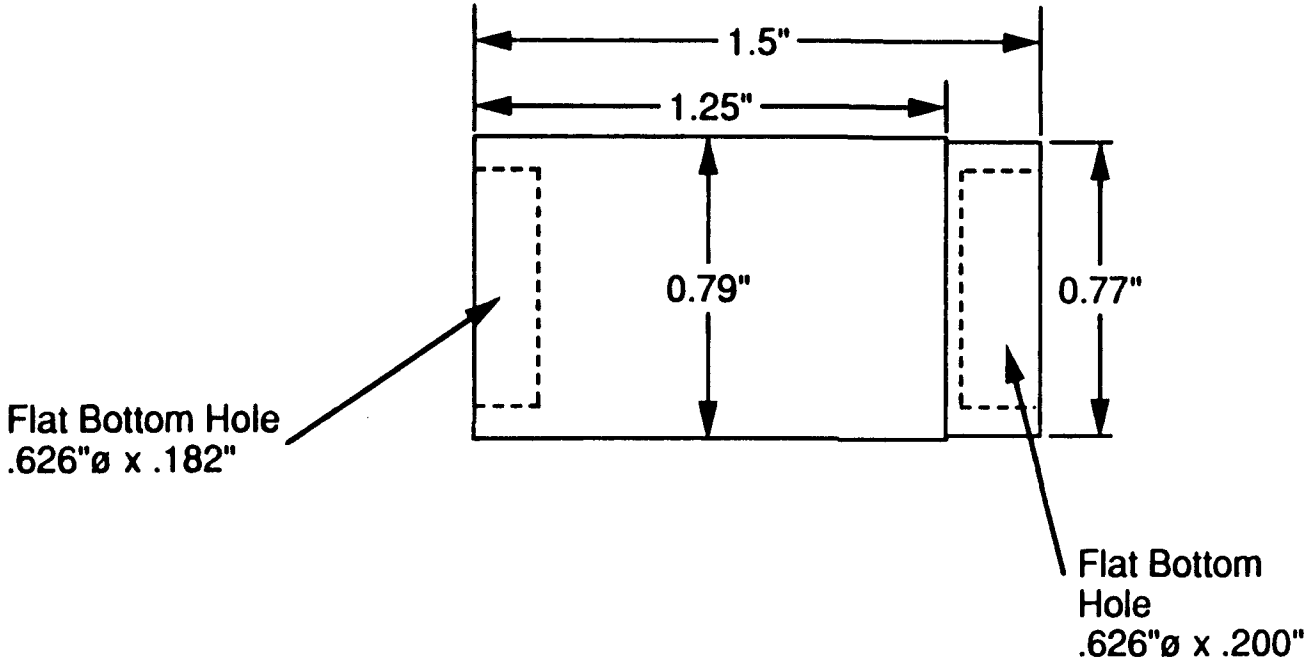

GTE 20mm Obturator

Hardness and Impact Energy of Armor Used in 20mm Tests

	Impact Energy(ft-lbs)		Hardness(Rc)	
Piece Number	Longitutinal	Transverse	Longitutinal	Transverse
1	16.7	15.6	49.1	49.1
2	15.8	15.4	48.4	50.8
3	18.9	12.8	48.8	48.2
4	19.3	11.2	48.9	48.3
5	-	-	-	-
6	18.0	11.5	48.0	48.1
7	-	-	-	-
8	15.0	13.3	49.2	49.3
9	-	-	-	-
10	18.2	12.0	49.7	49.2
11	13.0	15.3	48.6	47.8
12	21.1	15.3	48.4	48.3
13	-	-	-	-
14	-	-	-	-
15	11.7	21.9	50.7	49.5
18	21.2	-	49.0	-

Taylor Anvil Tests

INTERIM REPORT
(March through May, 1988)

TAYLOR ANVIL TESTS OF TUNGSTEN ALLOYS

Richard H. Zernow
Jerome D. Yatteau

Applied Research Associates, Inc.
7114 West Jefferson Avenue
Suite 305
Lakewood, Colorado 80235

25 May 1988

GTE Products Corporation
Chemical and Metallurgical Division
Hawes Street
Towanda, Pennsylvania 18848

ARA Contract Number 5491

Table 1. Summary of Taylor Anvil Test Results

Taylor Anvil Test Results

Mtl Type	Work	Rockwell Hardness (Rc)	Brinell Hardness (bhn) *	Static Ultimate Strength (ksi)	Static Yield Strength (ksi)	Static Percent Elong.	Average Sigma (ksi)	Hoop Strain At Crack Velocity (in./in.)
D628	Unworked	29.0	279	137	96	35	148	0.30
D630	Unworked	31.0	294	139	88	37	164	0.26
D632	Unworked	31.8	300	141	87	21	167	0.18
D1670	Unworked	29.6	283	139	85	36	170	0.28
D300	Swage 25%	30.9	293	137	87	18	186	< 0.05
D1672	Unworked	30.9	293	140	87	23	190	0.22
D633	Swage 15%	44.5	415	174	161	10	189	0.12
D629	Swage 15%	42.5	395	166	153	18	199	0.22
D631	Swage 15%	42.5	395	169	156	13	198	0.19
D1673	Swage 15%	41.5	386	172	158	11	241	0.16
D1671	Swage 15%	40.9	380	171	156	19	243	0.25
D224	Swage 8%	43.0	400	181	170	8	245	0.16
D329	Swage 25%	44.1	410	191	173	9	247	0.15

* Equivalence between bhn and Rc based upon steel

Taylor Anvil Test Samples

Sample ID	Alloy	Ni/Fe	Thermo-Mechanical Treatment
D-628	90W-7Ni-3Fe	7/3	As Sintered
D-630	93W-4.9Ni-2.1Fe	7/3	As Sintered
D-632	96W-2.8Ni-1.2Fe	7/3	As Sintered
D-1670	93W-5.6Ni-1.4Fe	8/2	As Sintered
D-300	93W-4.9Ni-2.1Fe	7/3	Swaged 25% Heat Treated 8hrs at 1400°C
D-1672	96W-3.2Ni-0.8Fe	8/2	As Sintered
D-633	96W-2.8Ni-1.2Fe	7/3	Swaged 15%
D-629	90W-7Ni-3Fe	7/3	Swaged 15%
D-631	93W-4.9Ni-2.1Fe	7/3	Swaged 15%
D-1673	96W-3.2Ni-0.8Fe	8/2	Swaged 15%
D-1671	93W-5.6Ni-1.4Fe	8/2	Swaged 15%
D-224	93W-4.9Ni-2.1Fe	7/3	Swaged 8% - Aged 15hrs at 500°C
D-329	93W-4.9Ni-2.1Fe	7/3	Swaged 25% Annealed 8hrs at 800°C

$$\sigma_c = - \rho_c U_c V_i / [k \log(L_e/L_o)] \quad (3)$$

where:
- V_i is the impact velocity,
- U_p is the bulk sound speed in the anvil,
- A/Ao is the ratio of the post-impact to pre-impact crossectional areas of the impacted face,
- L_e is the length of the rear undeformed portion of the post-impact specimen,
- L_o is the pre-impact length of the specimen.

MEASUREMENTS

Figure 1 shows two typically deformed Taylor anvil test specimens. The specimen on the left impacted at 545 ft/sec while the specimen on the right impacted at 375 ft/sec. Figure 2 shows a comparator photograph of a deformed Taylor anvil test specimen. Values of A/Ao for use in equations 1 and 2 could be easily determined by measuring the diameter of the impacted face before and after the test. The exact length of the undeformed remainder, L_e, is difficult to discern from the comparator photograph because of the gradual change in slope with distance from the impacted end. A hardened steel measurement die, figure 3, with an inside diameter ground to 0.4710-inch was therefore fabricated to measure L_e. The deformed specimens were gently turned into the die and the point of interference was used to mark the extent of the undeformed remainder.

TEST RESULTS

Table 1 summarizes the results of the first 13 tungsten material variations presented in ascending order of dynamic yield strengths. Plots of dynamic yield strength vs impact velocity for individual test specimens within each material variation, may be found in Appendix A. These plots also show which impacts resulted in radial cracks on the impact face. Figure 4 and 5 show dynamic yield strength plotted against material hardness in terms of the Rockwell C scale and Brinell scale, respectively. Figure 5 also compares the current data with a formula from Reference 1 that correlates dynamic strength data for uniaxial stress conditions from several sources for steel, titanium and aluminum alloys, with their Brinell hardness.

$$\sigma_c = 568 * \text{bhn} \quad (4)$$

It can be seen that this Brinell hardness formula continues to provide a good representation for the current Taylor anvil test results. The three groups referenced in figures 4 and 5 are detailed in table 2. Group 1 is characterized by lower dynamic and static yield strengths and correspondingly lower Brinell hardness values. Group 2 and 3, while having similar Brinell hardness values and similar static yield strengths, have different values for dynamic yield strength. This separation of groups remains apparent in figure 6 which shows dynamic vs static yield strengths, with a reference trace of dynamic equal to static yield strength.

Figure 7 shows hoop strain at the onset of radial cracking, plotted against percent elongation. This figure shows that the group 1 specimens tend to

exhibit greater static ductility than dynamic ductility, while groups 2 & 3 show greater dynamic ductility than static ductility. Plots of hoop strain versus impact velocity for each of the test specimens may be found in Appendix B.

Figure 8 compares the plastic wave velocity for the current tungsten alloys, as determined from equation 2, with the following formula.

$$U_C = 63 * (bhn / 0.638)^{1/2} \quad (5)$$

Equation 5, derived from formulas in reference 1, correlates dynamic work hardening coefficients for uniaxial stress for steel, titanium and aluminum alloys. Figure 9 is a reprint of a figure found in reference 2 and shows equations 4 and 5 and their relationships to previous DRI/GTE tungsten alloy Taylor anvil tests, tungsten alloy torsion tests and DU-.75Ti torsion tests. The comparison of figures 8 and 9 show that the current data is consistent with previous results and also indicate that equation 5 could be slightly adjusted to more accurately represent the relationship.

Appendix C contains details of each of the individual test specimens and their associated measurements. To illustrate the criteria used to comment on the degree of cracking, figure C-1 shows a specimen with 'VERY SLIGHT' cracking. The cracks are very small and found only on the walls of the specimen. Figure C-2 shows a specimen with 'SLIGHT' cracking, and exhibits small cracks that extend slightly into the impacted face. Figure C-3 shows a specimen with 'SEVERE' cracking. The cracks are large, extend well into the impacted face and have opened, producing gaps in the circumference. Figure C-4 shows the impact surface of the previous three specimens. This figure provides a better view of the gaps in the cracks of specimens classified as 'SEVERE',(specimen on left). It also shows how the cracks in specimens classified as 'SLIGHT', (middle specimen) extend into the impacted face while the cracks in specimens classified as 'VERY SLIGHT', (specimen on right) do not extend into the impacted face.

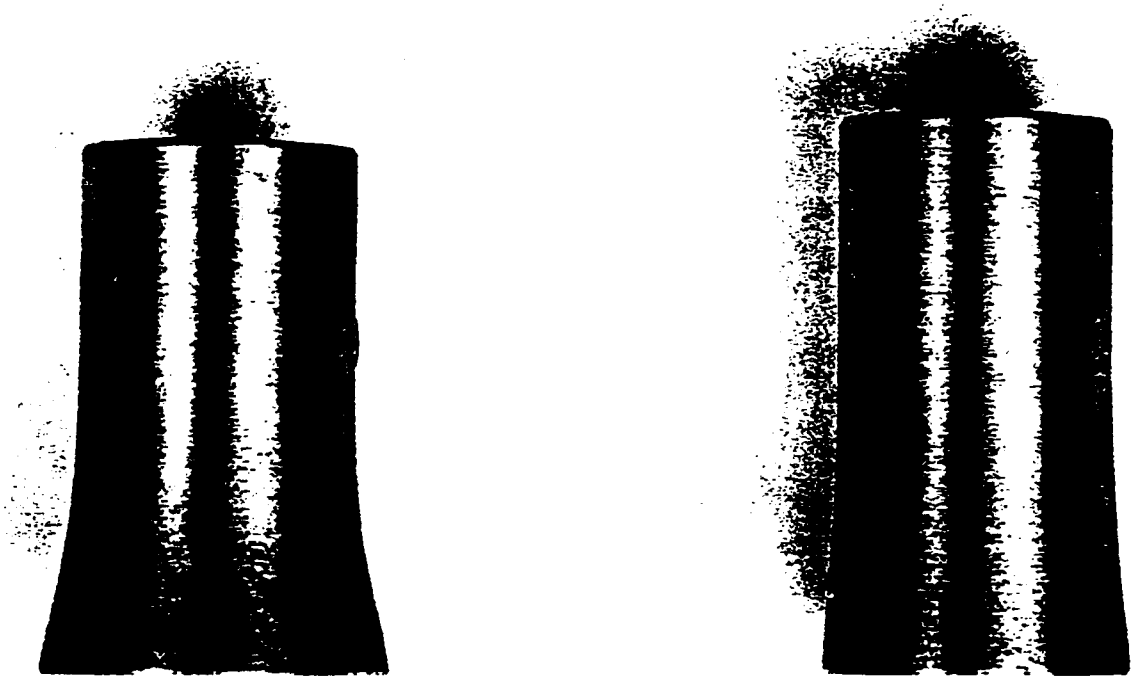

Figure 1. Two Typically Deformed Taylor Anvil Specimens Vi of Left Specimen, 545 ft/sec, Vi of Right Specimen, 375 ft/sec

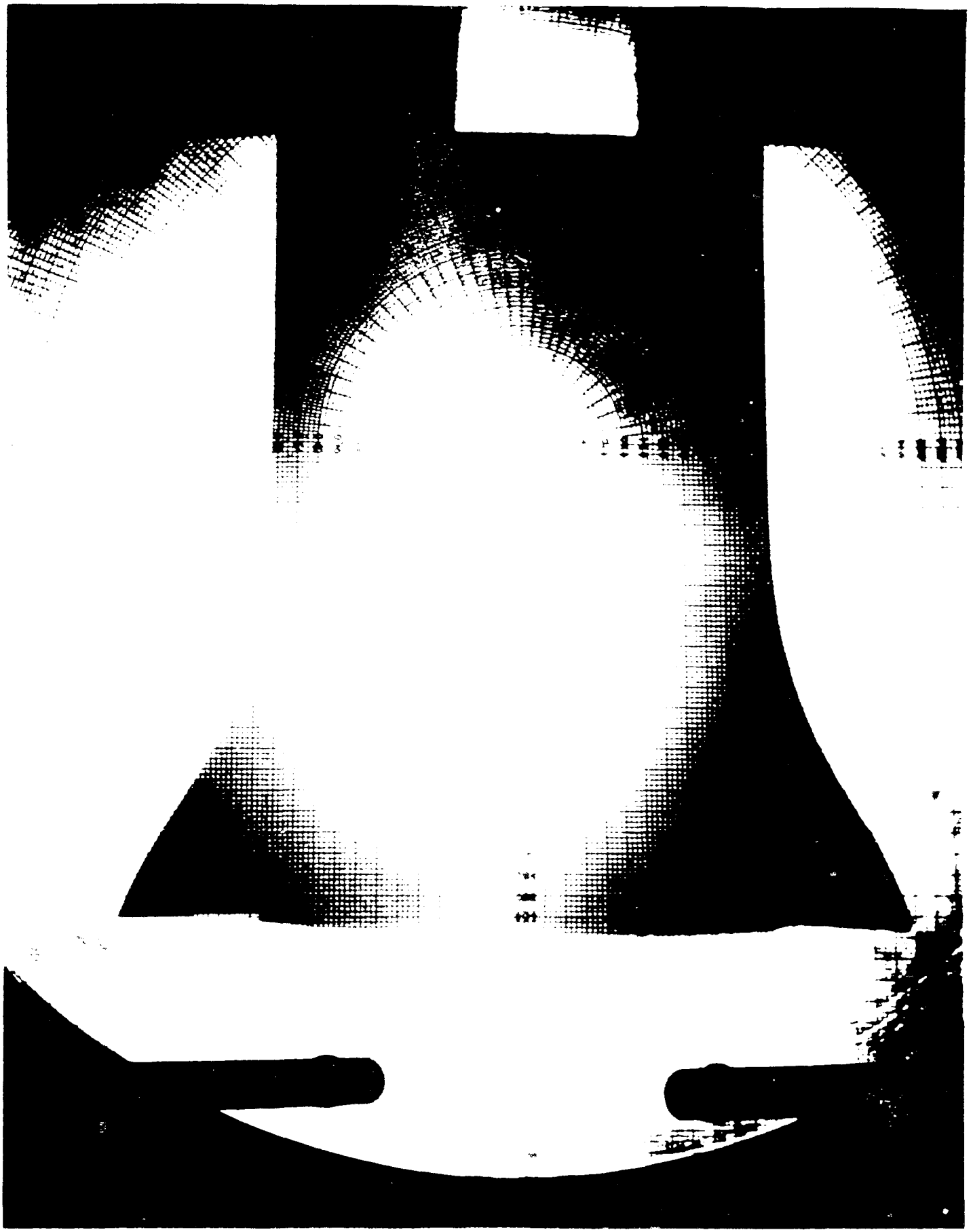

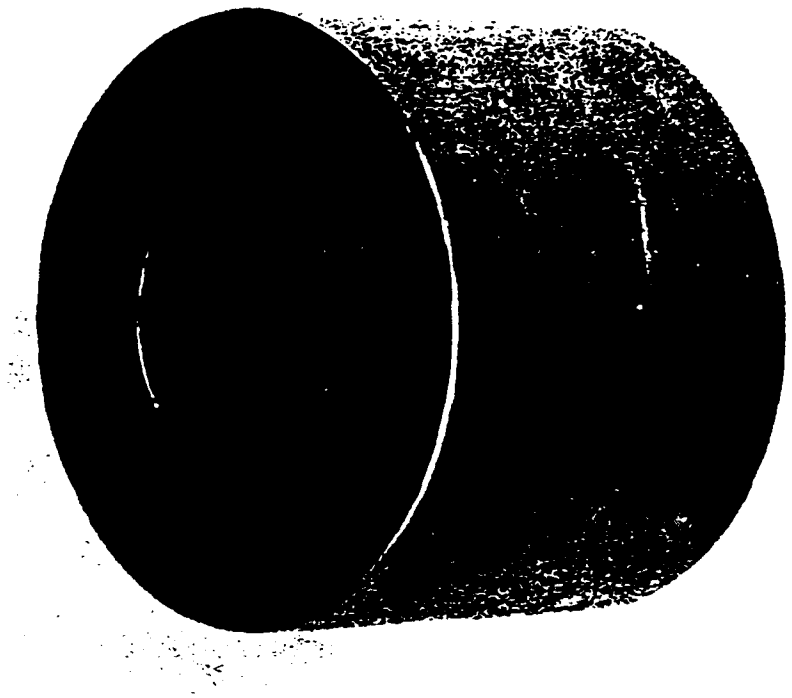

Figure 3. Hardened Steel Measurement Die.
I.D. = 0.4710-inch

Table 1. Summary of Taylor Anvil Test Results

Taylor Anvil Test Results

Mtl Type	Work	Rockwell Hardness (Rc)	Brinell Hardness (bhn) *	Static Ultimate Strength (ksi)	Static Yield Strength (ksi)	Static Percent Elong.	Average Sigma (ksi)	Hoop Strain At Crack Velocity (in./in.)
D628	Unworked	29.0	279	137	86	35	148	0.30
D630	Unworked	31.0	294	139	88	37	164	0.26
D632	Unworked	31.8	300	141	87	21	167	0.18
D1670	Unworked	29.6	283	139	85	36	170	0.28
D300	Swage 25%	30.9	293	137	87	18	186	< 0.05
D1672	Unworked	30.9	293	140	87	23	190	0.22
D633	Swage 15%	44.5	415	174	161	10	189	0.12
D629	Swage 15%	42.5	395	166	153	18	199	0.22
D631	Swage 15%	42.5	395	169	156	13	198	0.19
D1673	Swage 15%	41.5	386	172	158	11	241	0.16
D1671	Swage 15%	40.9	380	171	156	19	243	0.25
D224	Swage 8%	43.0	400	181	170	8	245	0.16
D329	Swage 25%	44.1	410	191	173	9	247	0.16

* Equivalence between bhn and Rc based upon steel

Taylor Anvil Test Samples

Sample ID	Alloy	Ni/Fe	Thermo-Mechanical Treatment
D-628	90W-7Ni-3Fe	7/3	As Sintered
D-630	93W-4.9Ni-2.1Fe	7/3	As Sintered
D-632	96W-2.8Ni-1.2Fe	7/3	As Sintered
D-1670	93W-5.6Ni-1.4Fe	8/2	As Sintered
D-300	93W-4.9Ni-2.1Fe	7/3	Swaged 25% Heat Treated 8hrs at 1400°C
D-1672	96W-3.2Ni-0.8Fe	8/2	As Sintered
D-633	96W-2.8Ni-1.2Fe	7/3	Swaged 15%
D-629	90W-7Ni-3Fe	7/3	Swaged 15%
D-631	93W-4.9Ni-2.1Fe	7/3	Swaged 15%
D-1673	96W-3.2Ni-0.8Fe	8/2	Swaged 15%
D-1671	93W-5.6Ni-1.4Fe	8/2	Swaged 15%
D-224	93W-4.9Ni-2.1Fe	7/3	Swaged 8% - Aged 15hrs at 500°C
D-329	93W-4.9Ni-2.1Fe	7/3	Swaged 25% Annealed 8hrs at 800°C

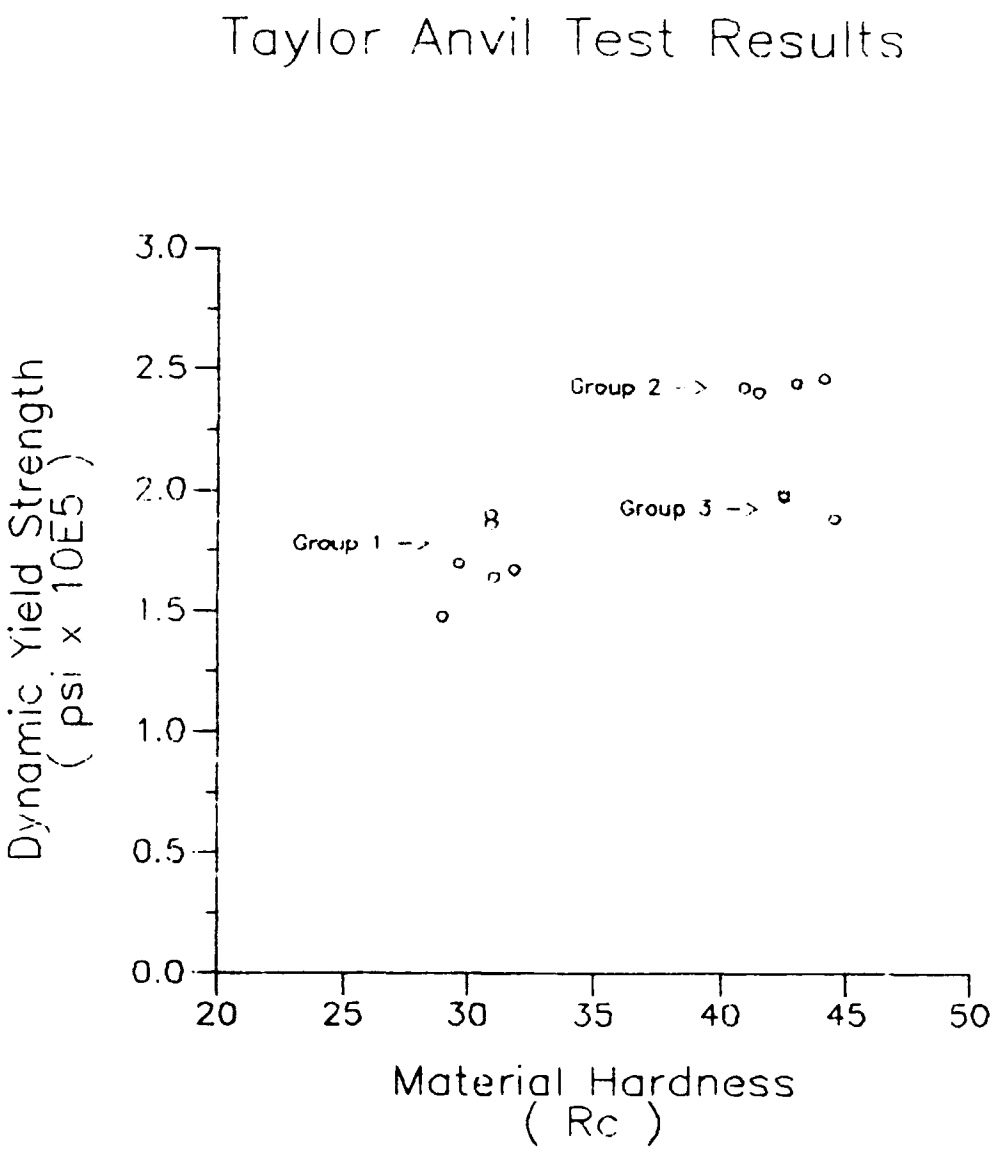

Figure 4. Dynamic Yield Strength versus Rockwell 'C' Scale Hardness

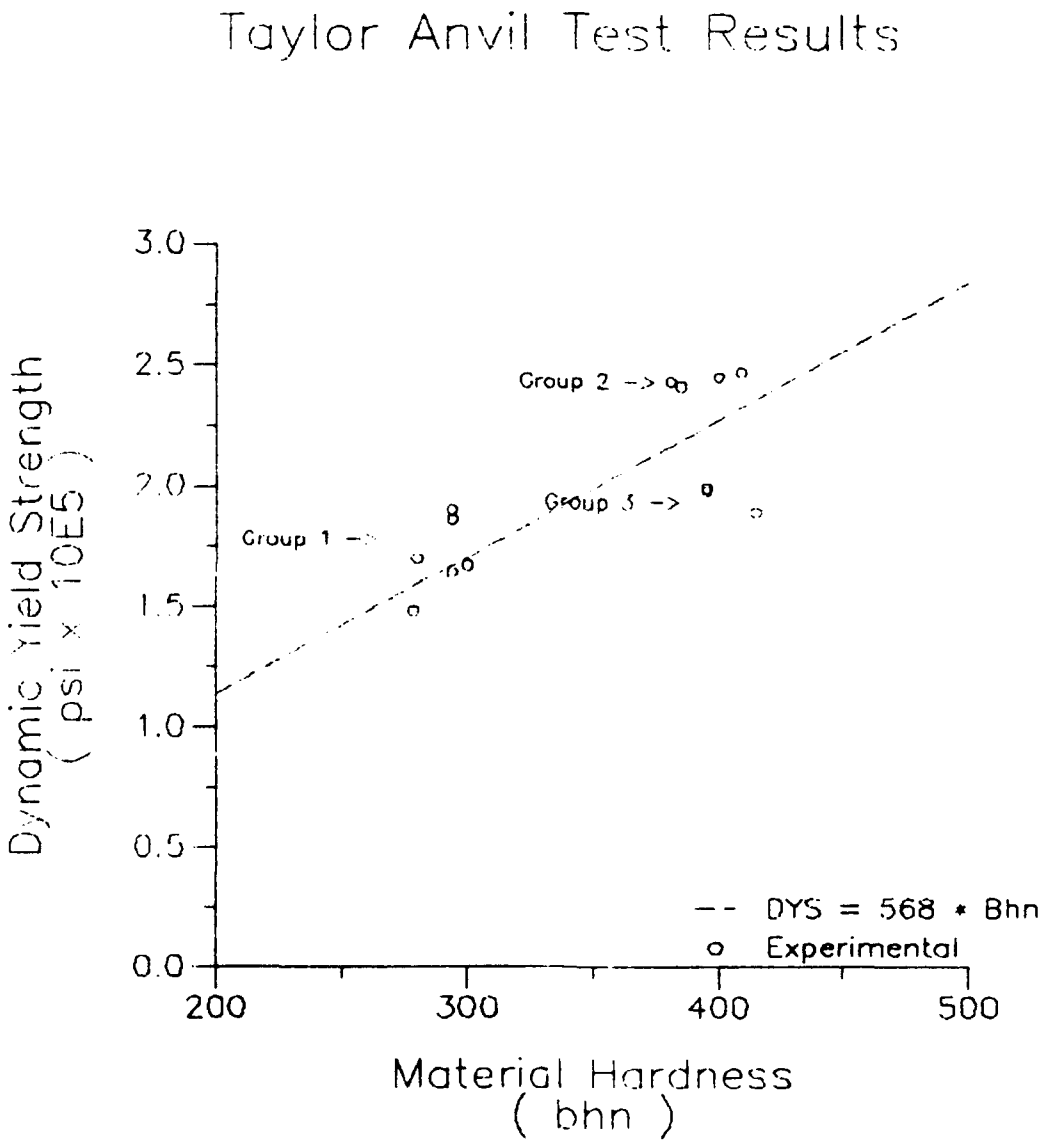

Figure 5. Dynamic Yield Strength versus Brinell Hardness

Table 2. Grouped Taylor Anvil Test Results

Taylor Anvil Test Results

	Mtl Type	Work	Rockwell Hardness (Rc)	Brinell Hardness (bhn) *	Static: Ultimate Strength (ksi)	Static: Yield Strength (ksi)	Static: Percent Elong.	Average Sigma (ksi)	Hoop Strain At Crack Velocity (in./in.)
Group 1	D628	Unworked	29.0	279	137	86	35	148	0.30
	D630	Unworked	31.0	294	139	88	37	164	0.26
	D632	Unworked	31.8	300	141	87	21	167	0.19
	D1670	Unworked	29.6	283	139	85	36	170	0.28
	D300	Swage 25%	30.9	293	137	87	19	186	< 0.05
	D1672	Unworked	30.9	293	140	87	23	190	0.22
Group 2	D1673	Swage 15%	41.5	386	172	158	11	241	0.16
	D1671	Swage 15%	40.9	380	171	156	19	243	0.25
	D224	Swage 8%	43.0	400	181	170	8	245	0.16
	D329	Swage 25%	44.1	410	191	172	9	247	0.16
Group 3	D633	Swage 15%	44.5	415	174	161	10	199	0.12
	D631	Swage 15%	42.5	395	169	156	13	198	0.19
	D629	Swage 15%	42.5	395	166	153	19	199	0.22

* Equivalence between bhn and Rc based upon steel

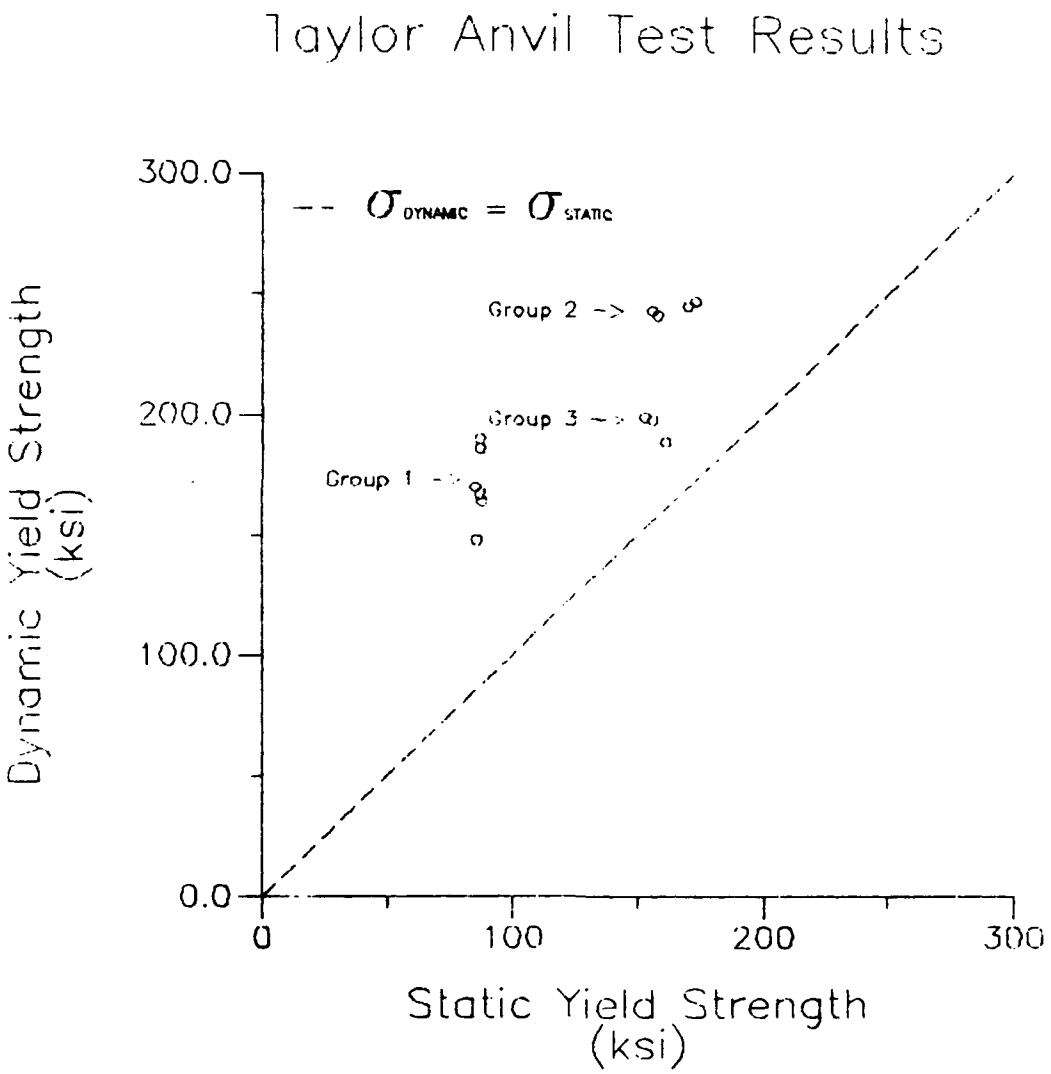

Figure 6. Dynamic Yield Strength versus Static Yield Strength

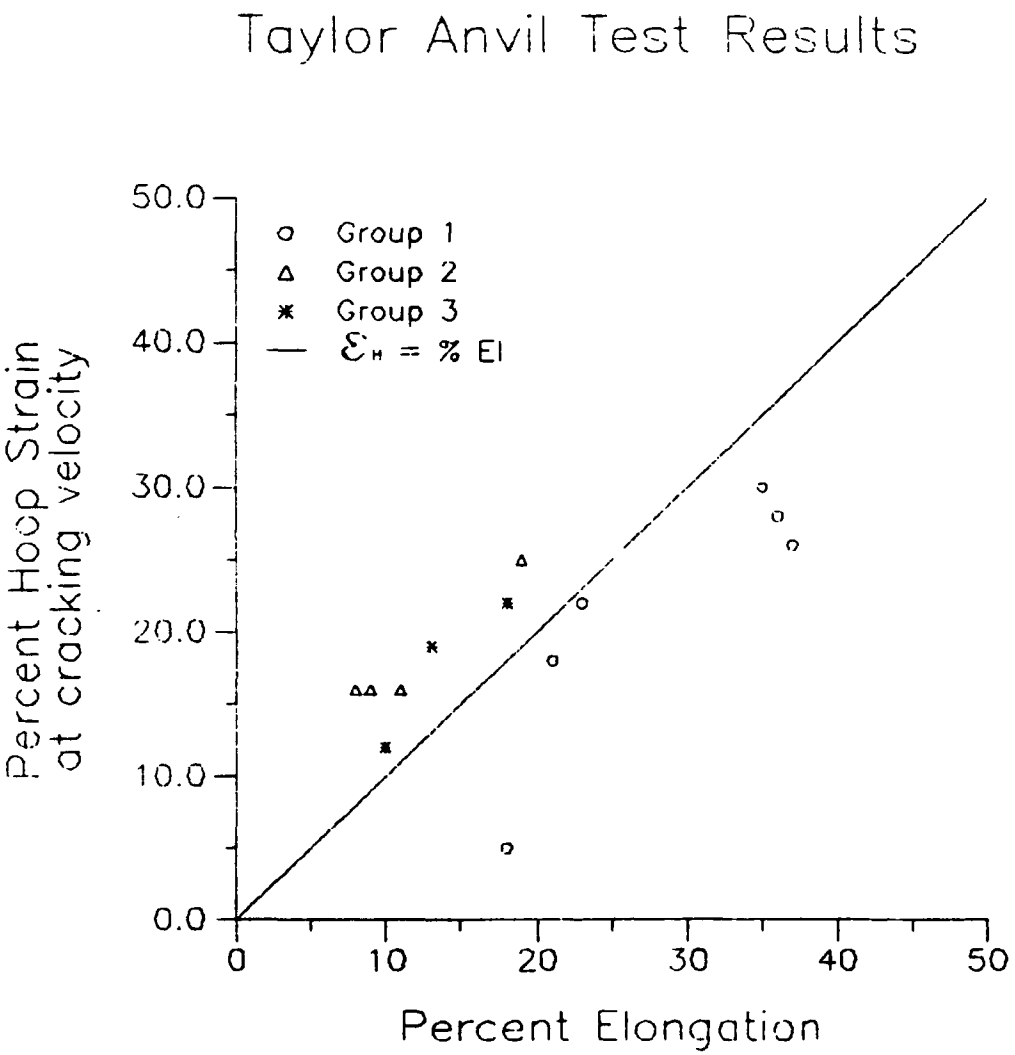

Figure 7. Hoop Strain at Onset of Radial Cracks versus Percent Elongation

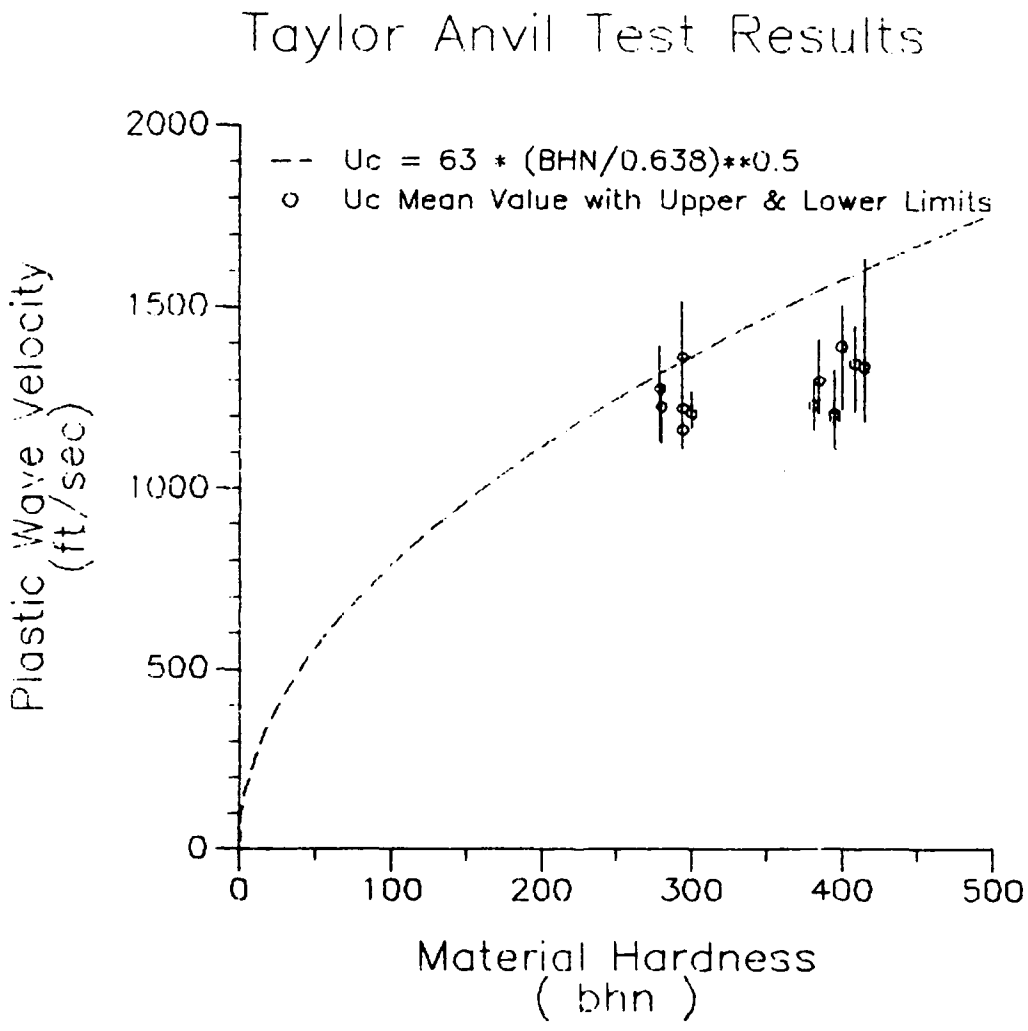

Figure 8. Plastic Wave Velocity versus Material Hardness

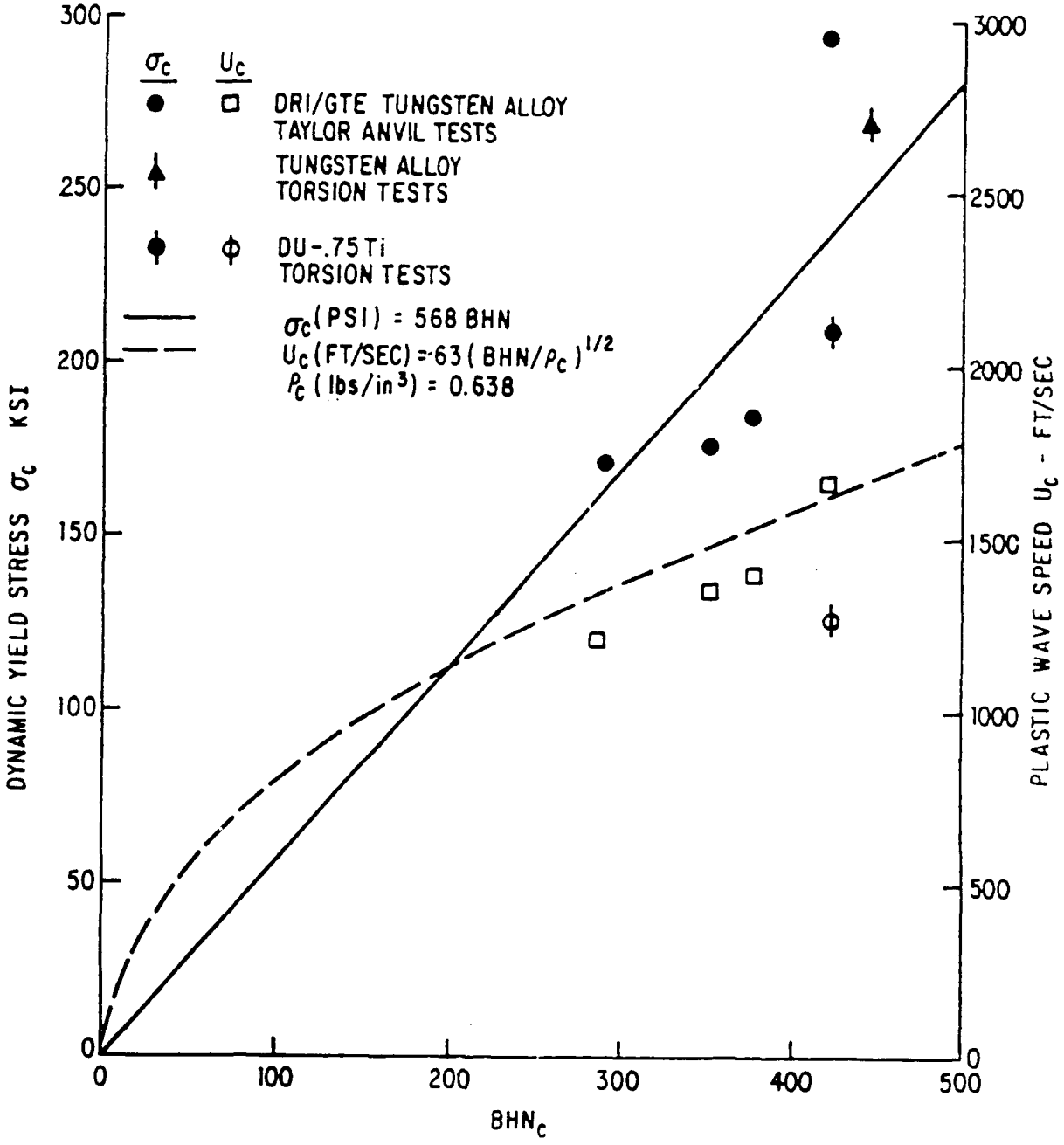

Figure 9. Dynamic Material Properties for Tungsten and Uranium Alloys

REFERENCES

1. Recht, R. F., "Taylor Ballistic Impact Modeling Applied to Deformation and Mass Loss Determinations." Int. J. Engng. Science, Vol. 16, pp 809-827, 1978.

2. Naval Surface Weapons Center. "Improved Multiple Plate Penetration Model for Spin-Stabilized Projectiles" by J. D. Yatteau, Denver Research Institute. Dahlgren, Virginia, NSWC, March 1986. (NSWC/DL TR 86-03; publication UNCLASSIFIED).

APPENDIX A

Taylor Anvil Test Results

Specimen: D628

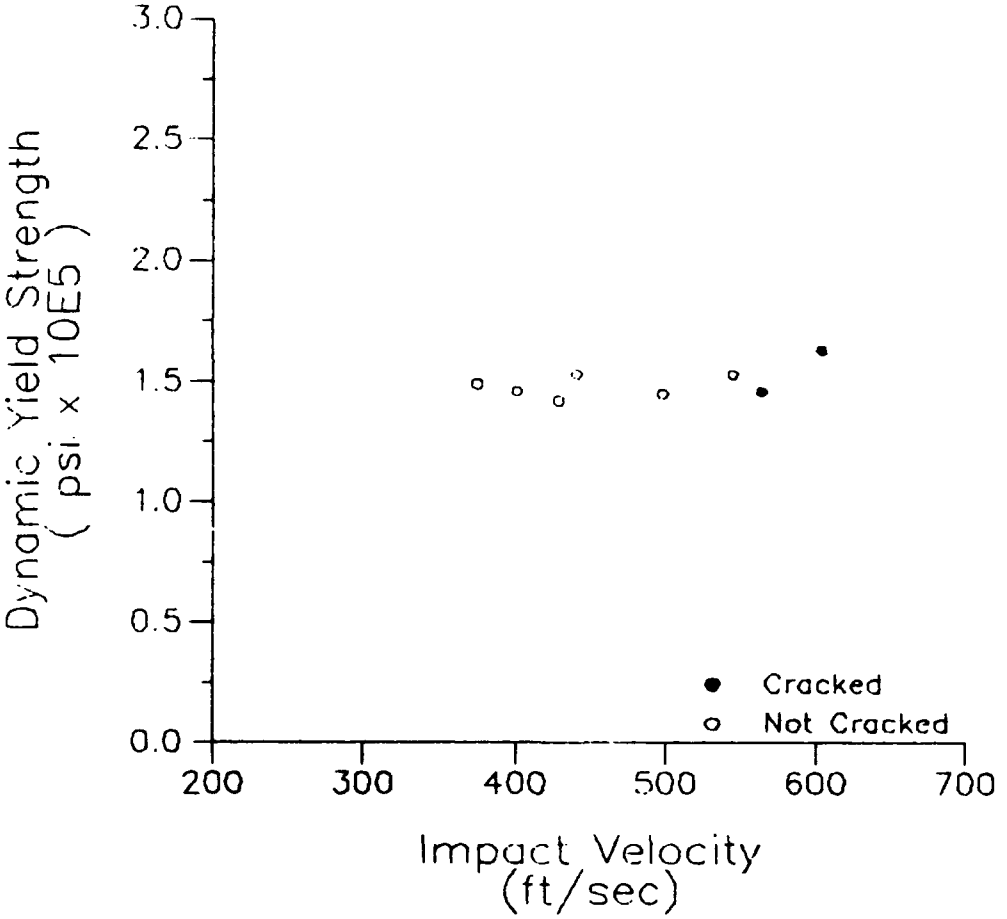

Taylor Anvil Test Results

Specimen: D630

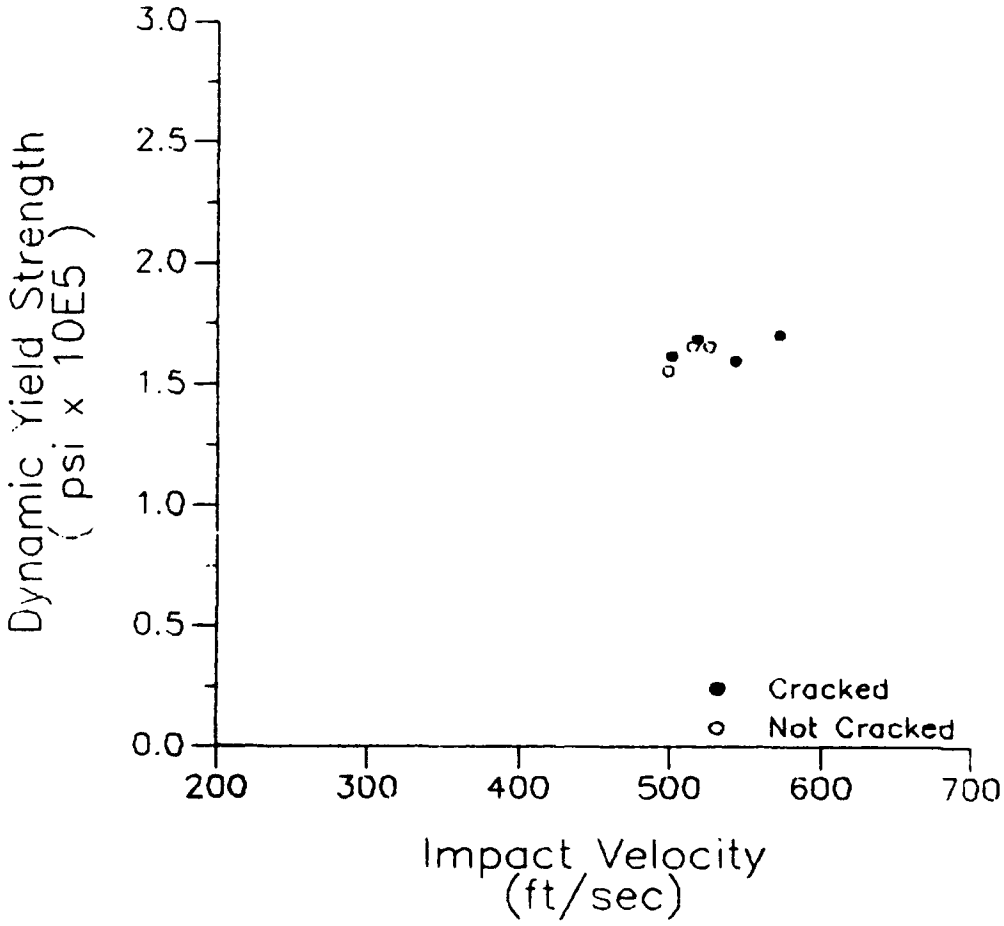

Taylor Anvil Test Results

Specimen: D632

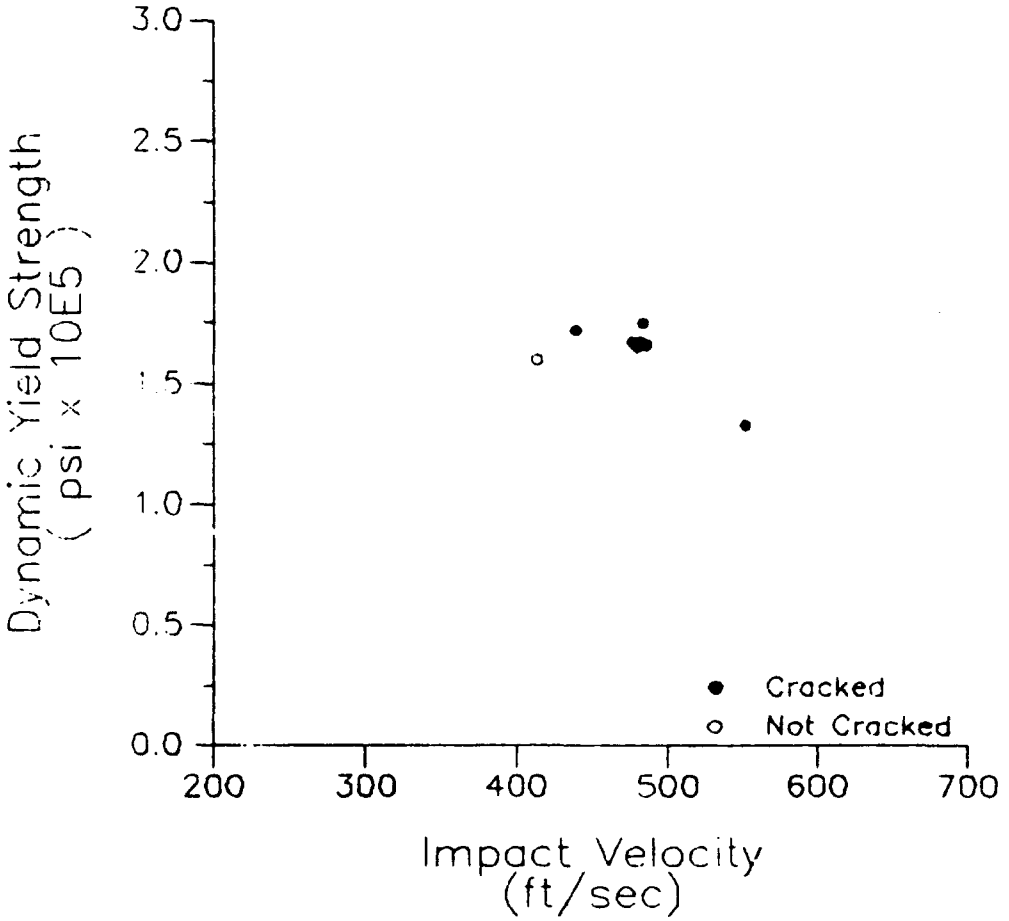

Taylor Anvil Test Results

Specimen: D1670

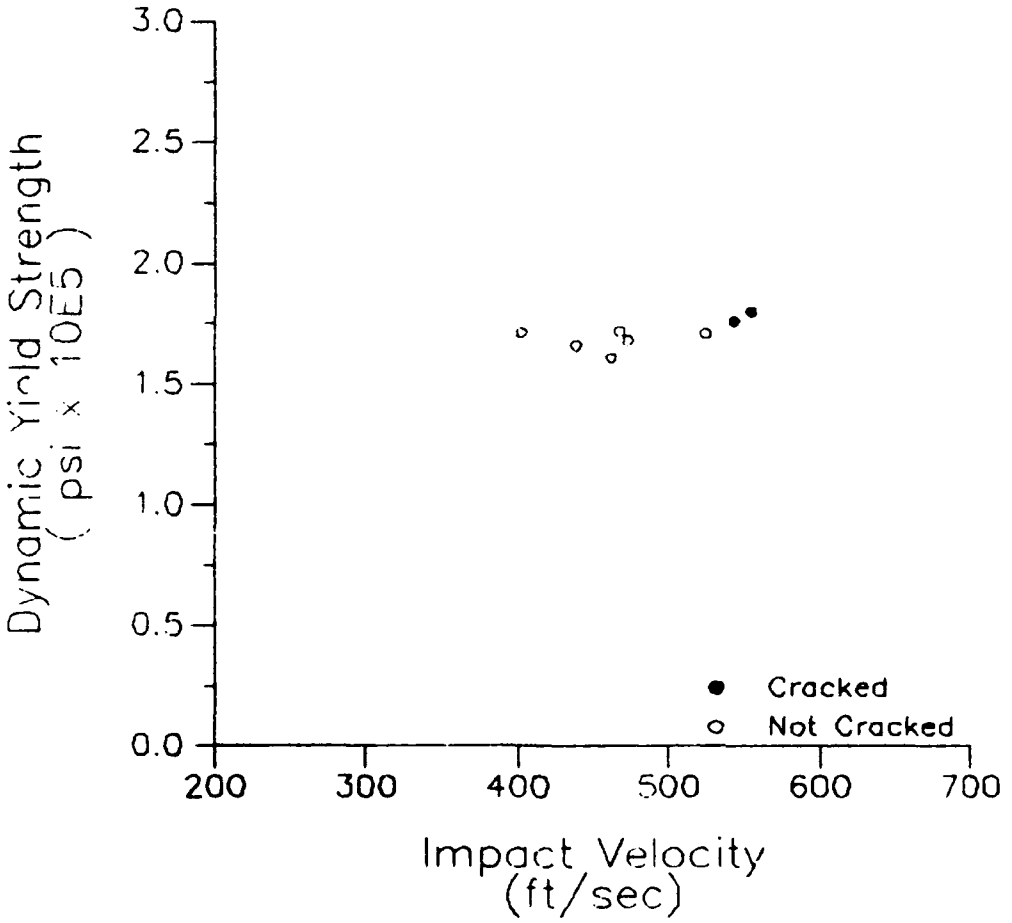

Taylor Anvil Test Results

Specimen: D300

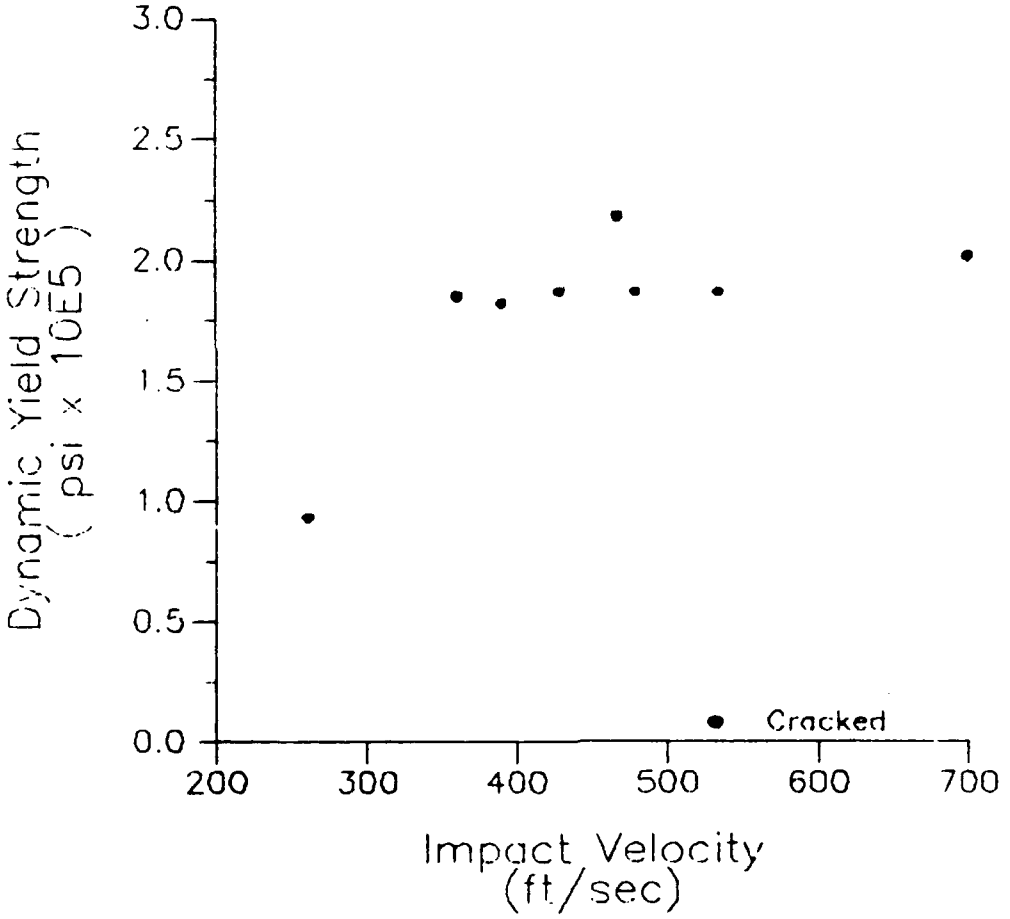

Taylor Anvil Test Results

Specimen: D1672

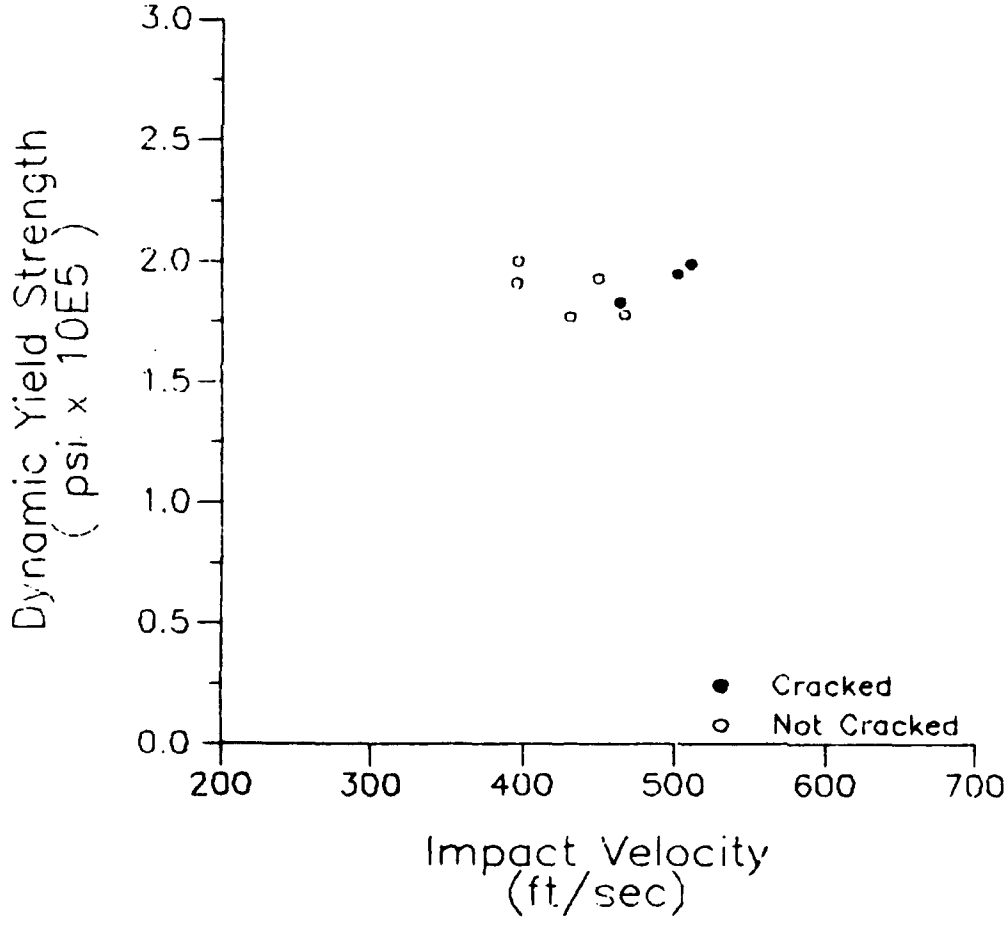

Taylor Anvil Test Results

Specimen: D633

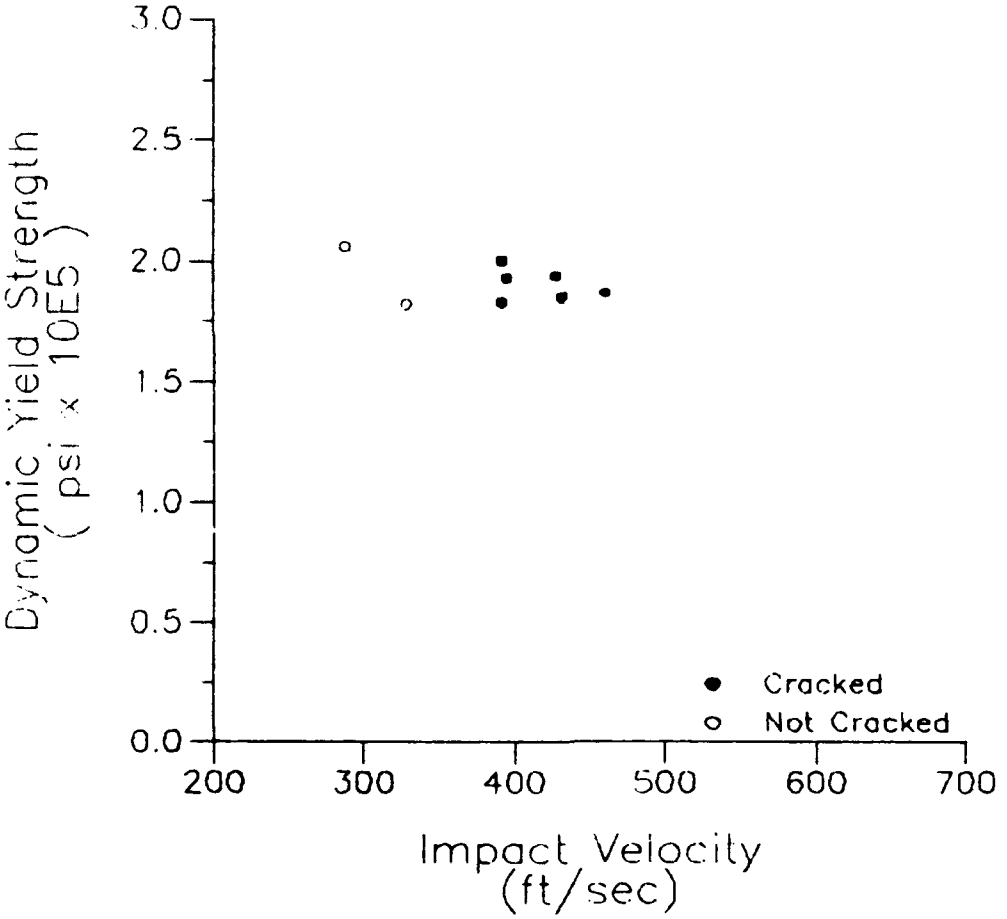

Taylor Anvil Test Results

Specimen: D629

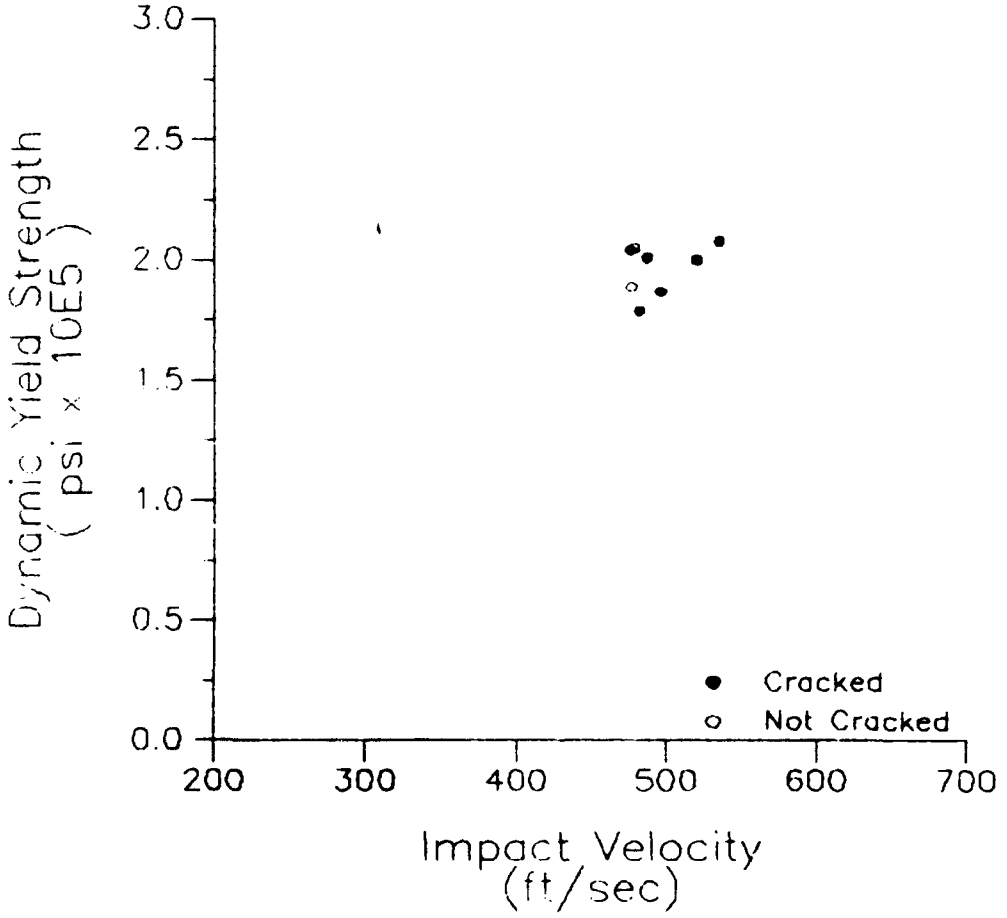

Taylor Anvil Test Results

Specimen: D631

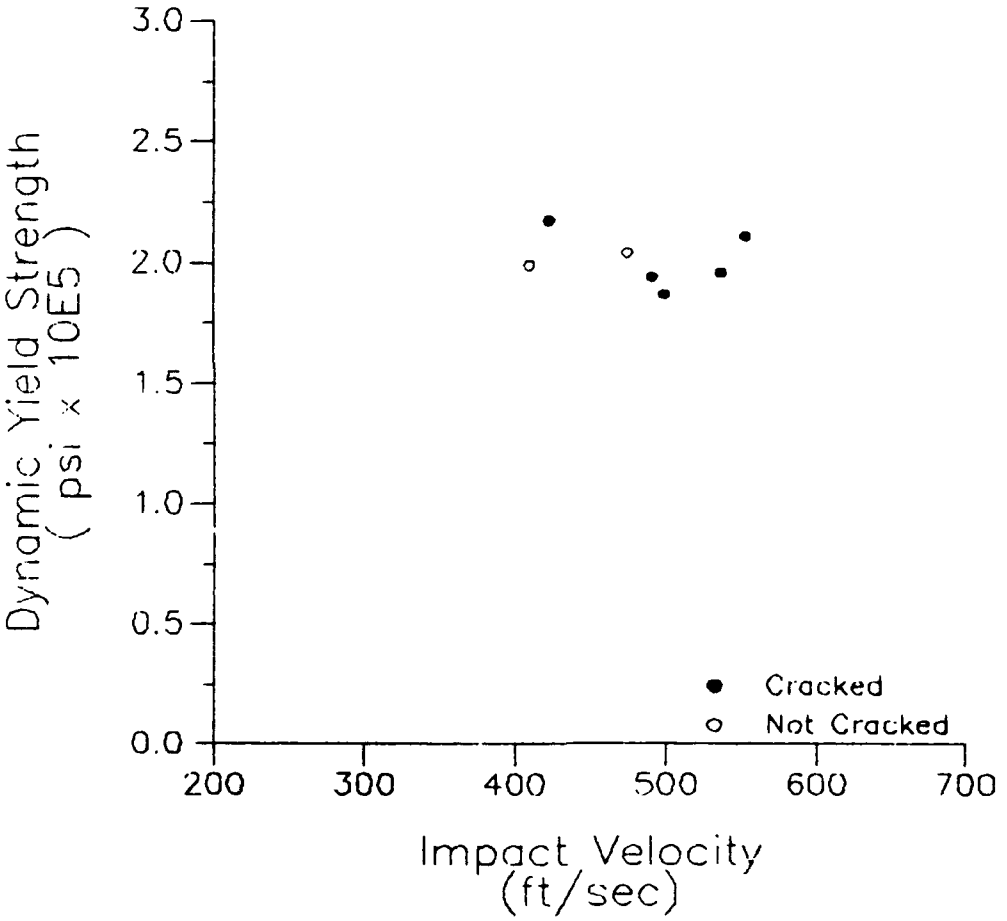

Taylor Anvil Test Results

Specimen: D1673

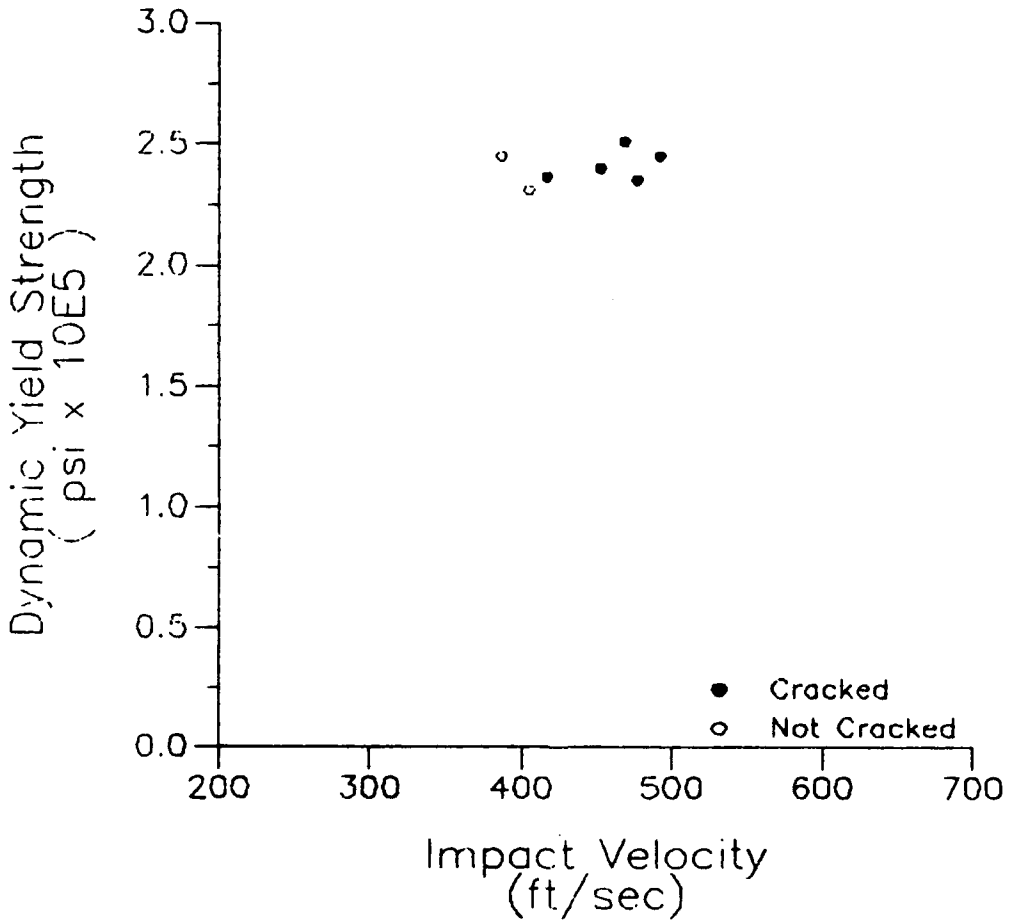

Taylor Anvil Test Results

Specimen: D1671

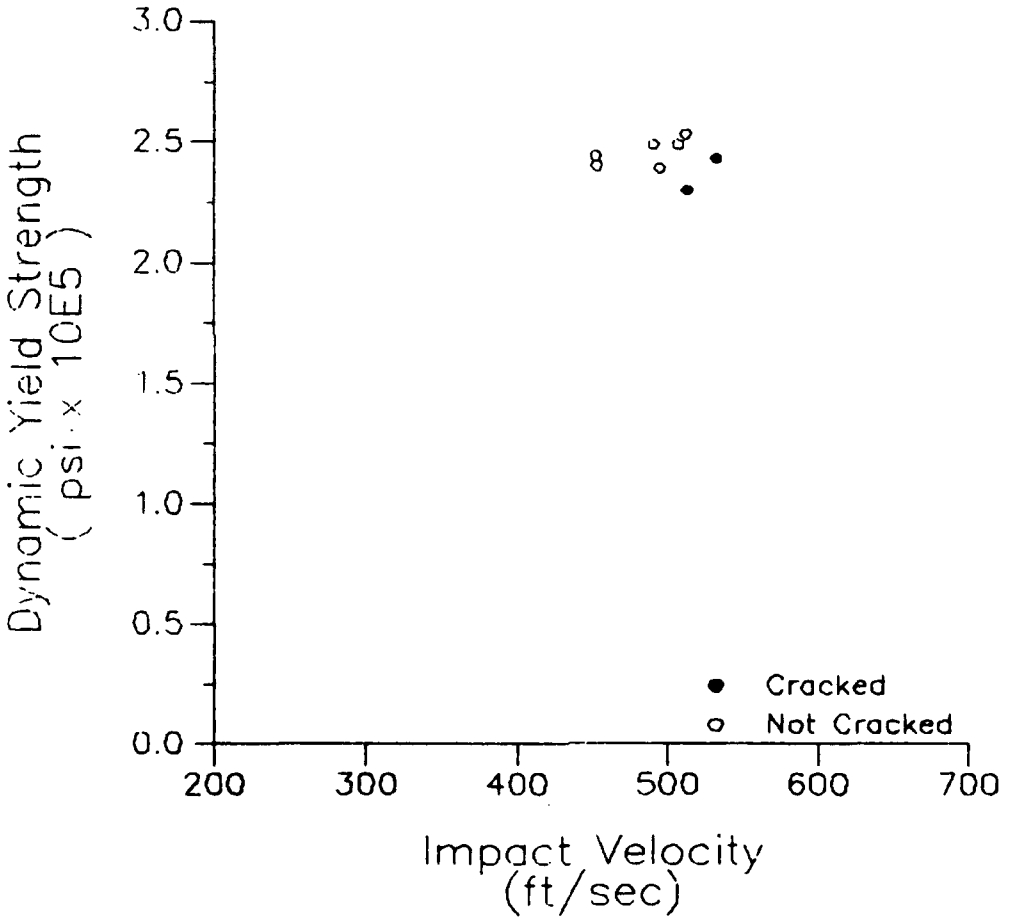

Taylor Anvil Test Results

Specimen: D224

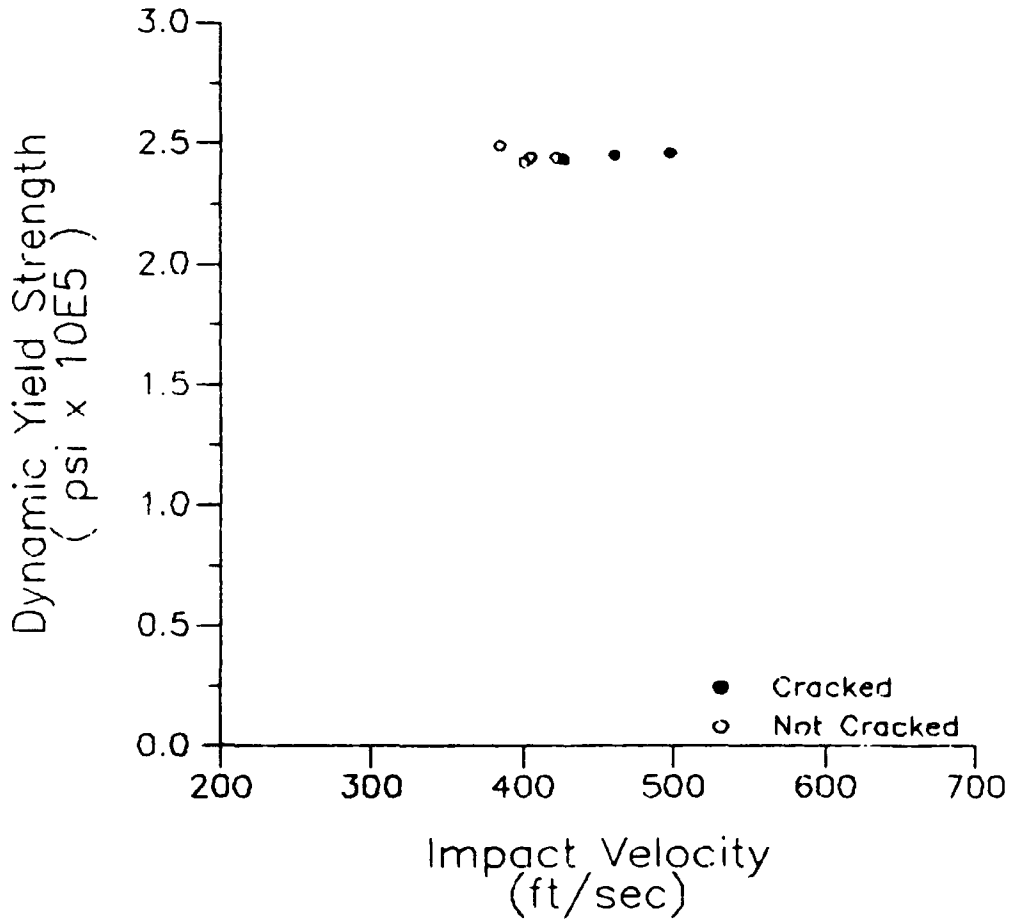

Taylor Anvil Test Results

Specimen: D329

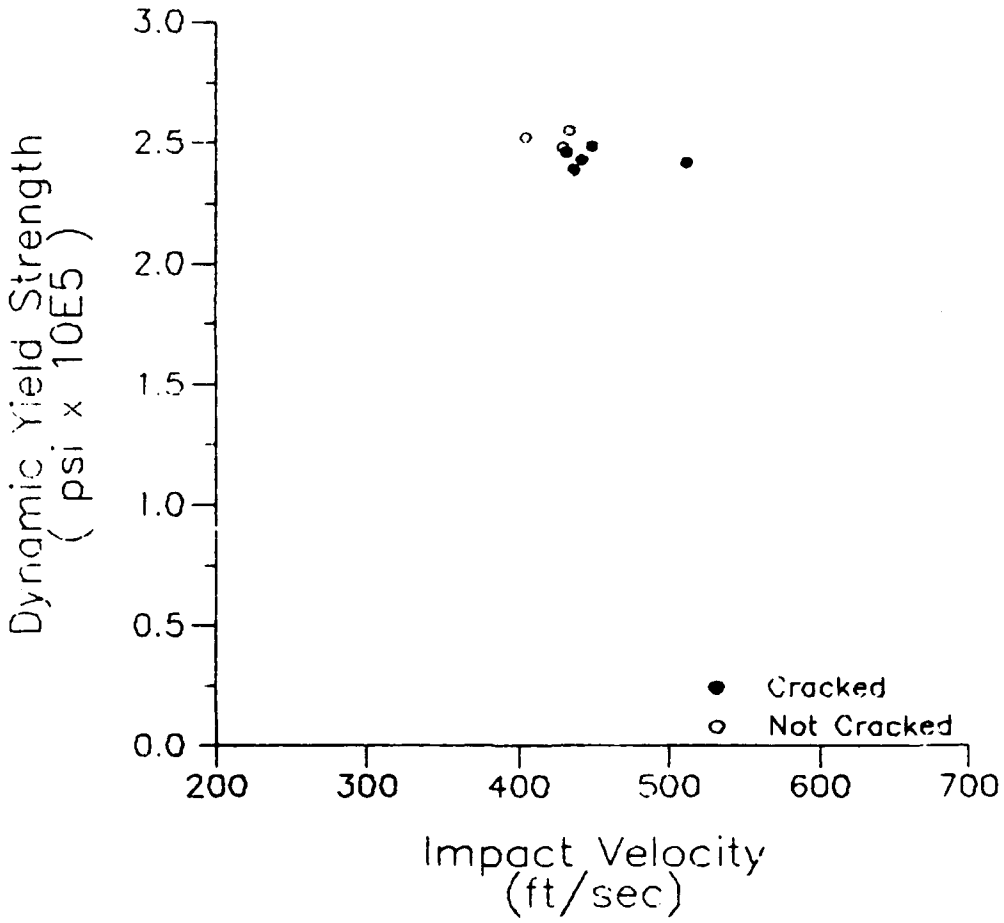

APPENDIX B

Taylor Anvil Test Results

Specimen: D628

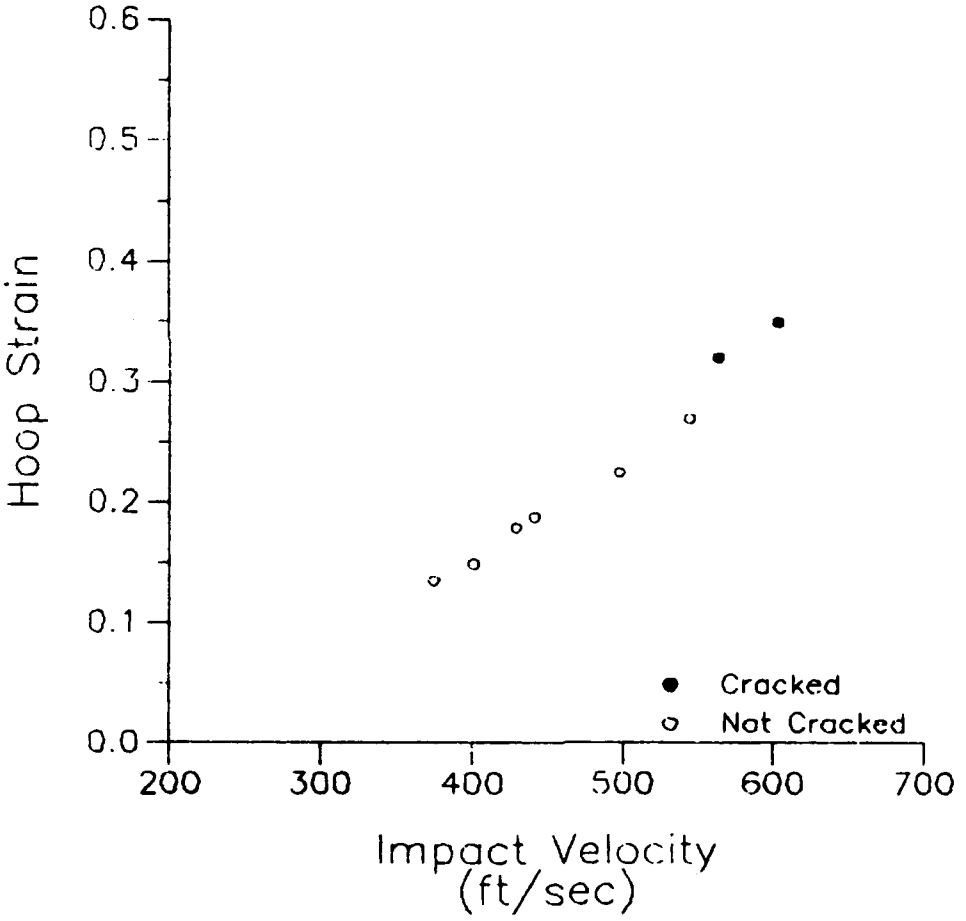

Taylor Anvil Test Results
Specimen: D630

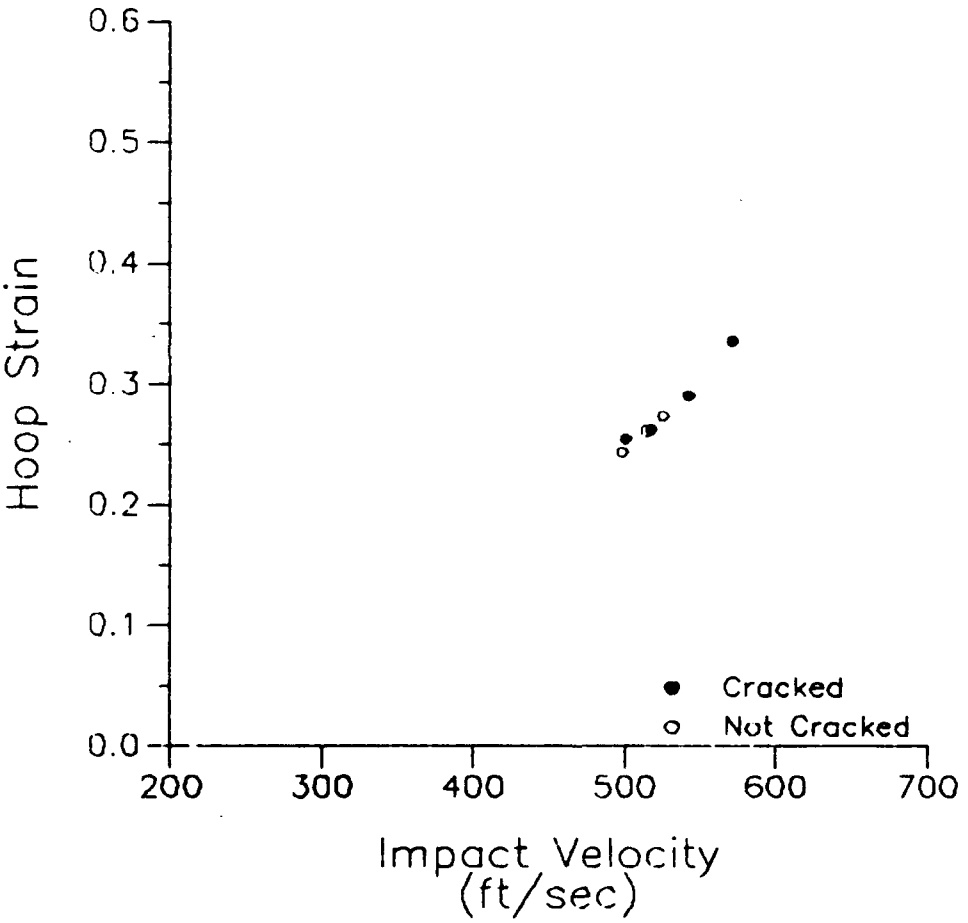

Taylor Anvil Test Results
Specimen: D632

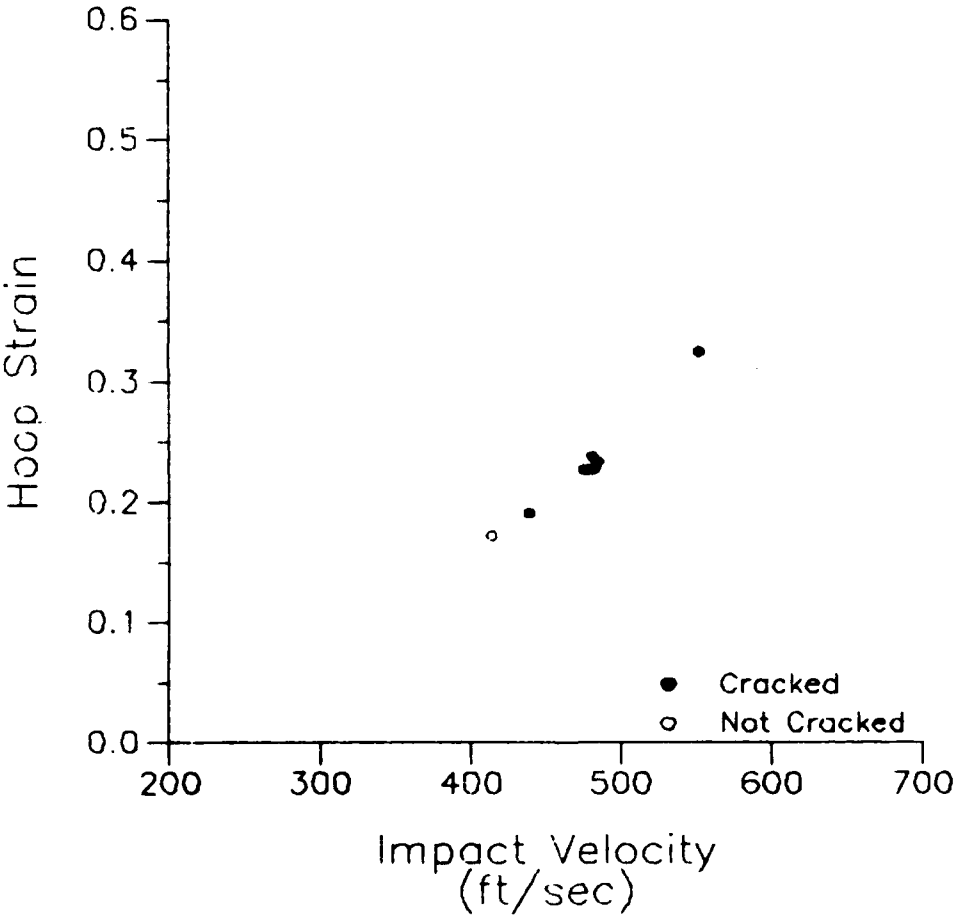

Taylor Anvil Test Results
Specimen: D1670

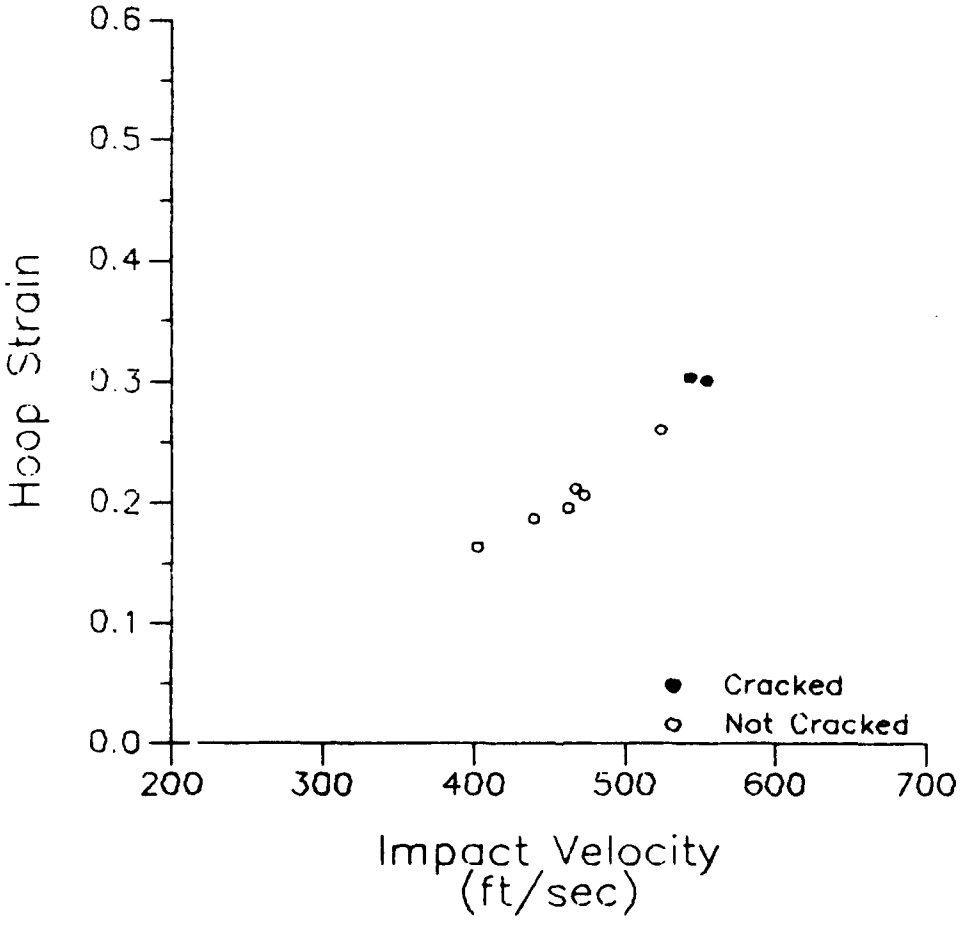

Taylor Anvil Test Results
Specimen: D300

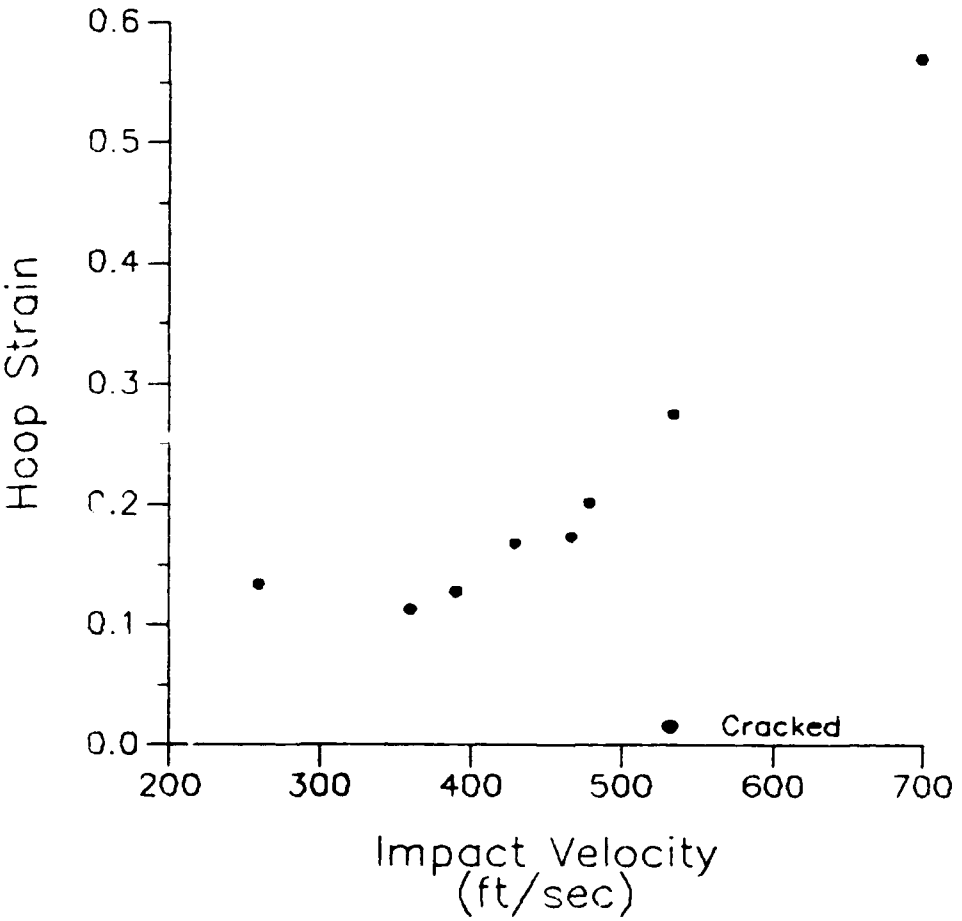

Taylor Anvil Test Results
Specimen: D1672

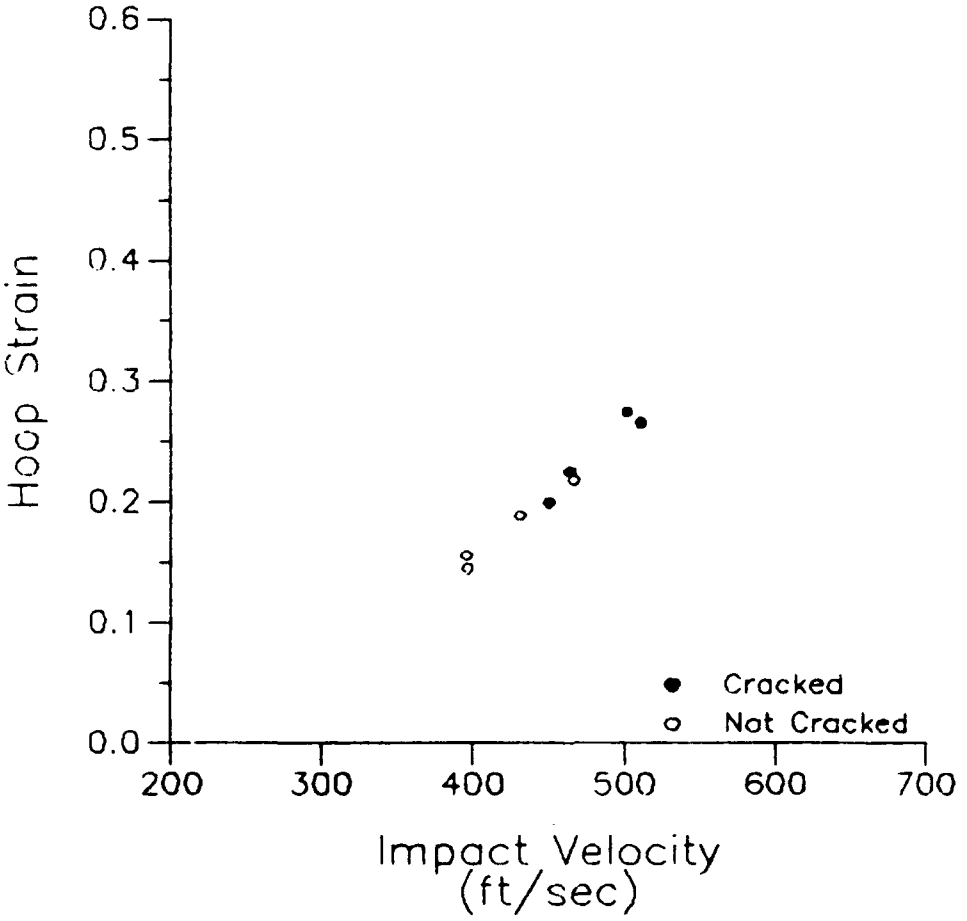

Taylor Anvil Test Results
Specimen: D633

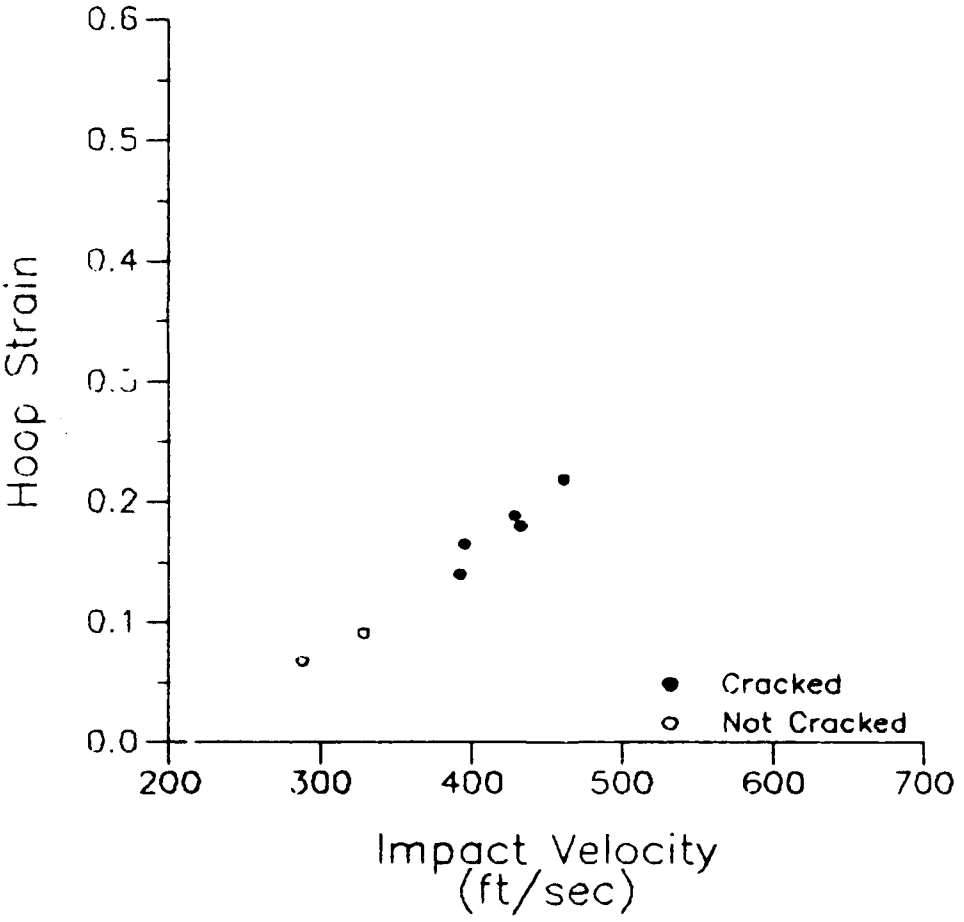

Taylor Anvil Test Results
Specimen: D629

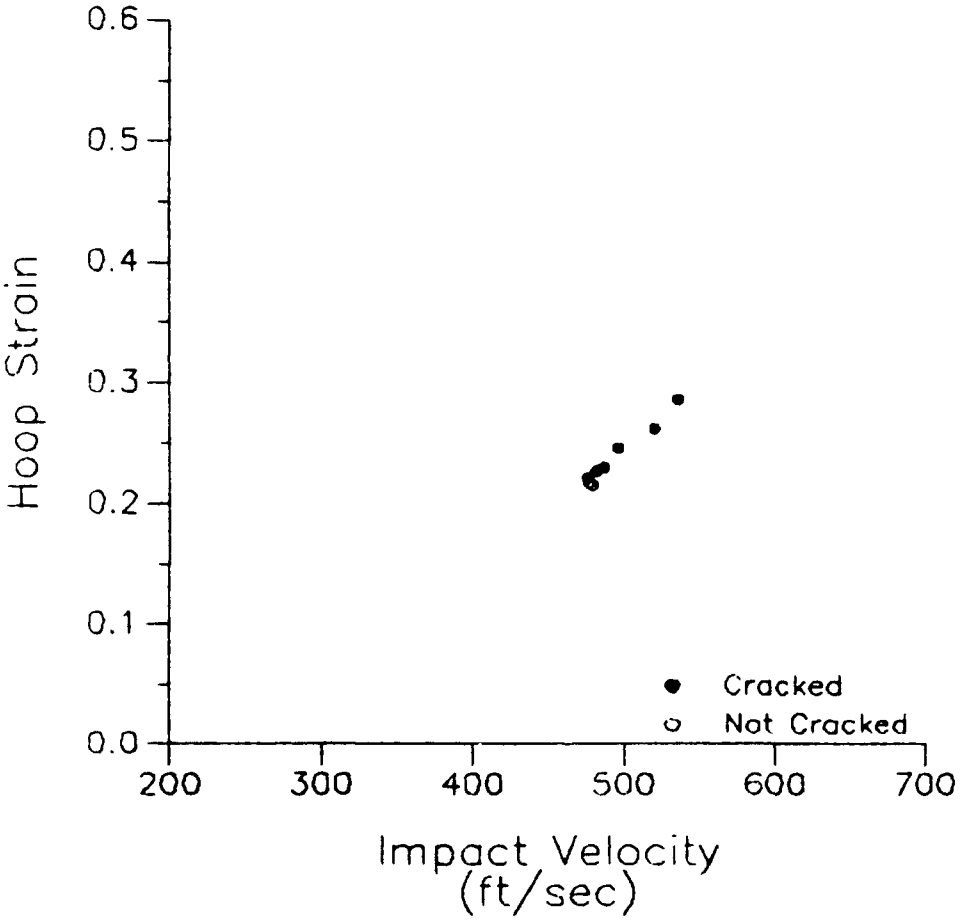

Taylor Anvil Test Results
Specimen: D631

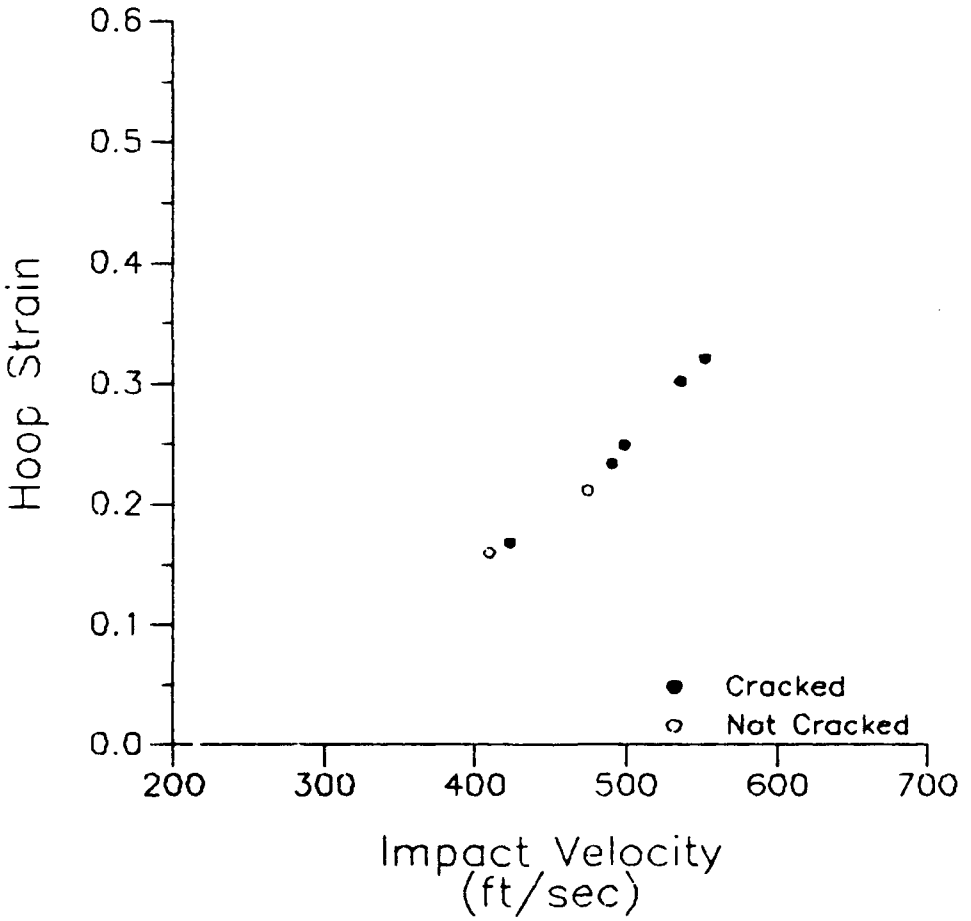

Taylor Anvil Test Results
Specimen: D1673

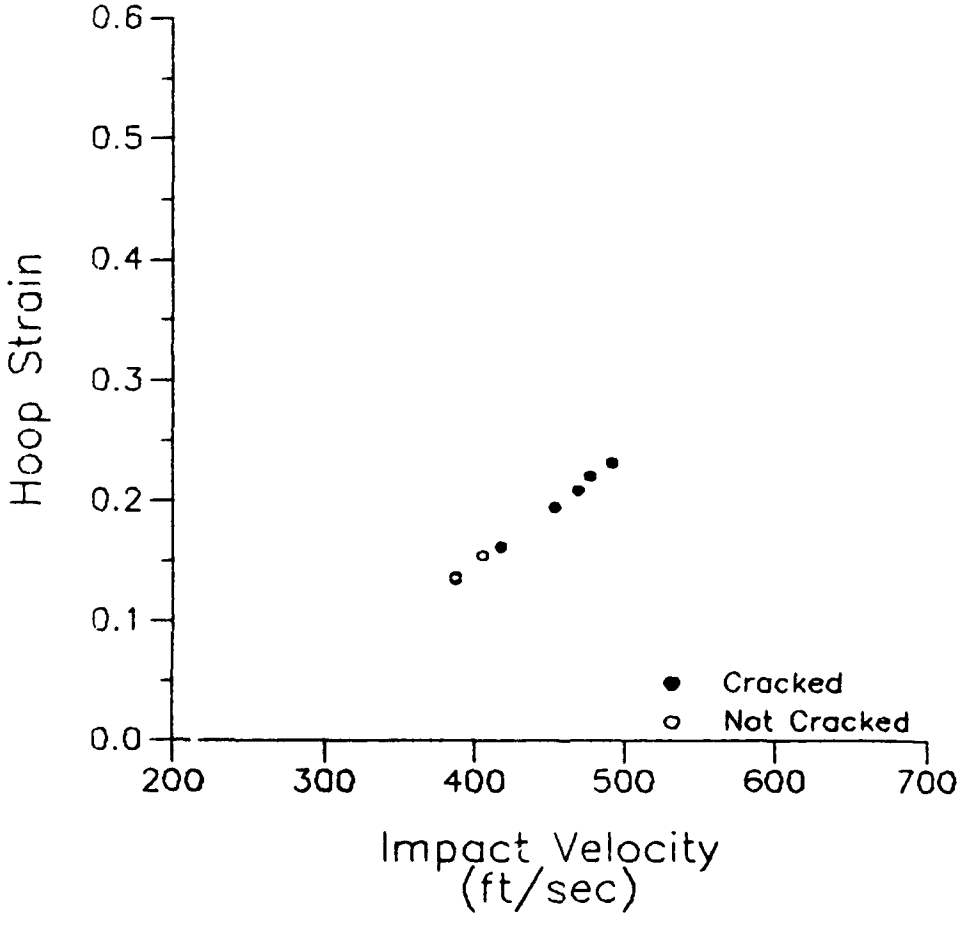

Taylor Anvil Test Results
Specimen: D1671

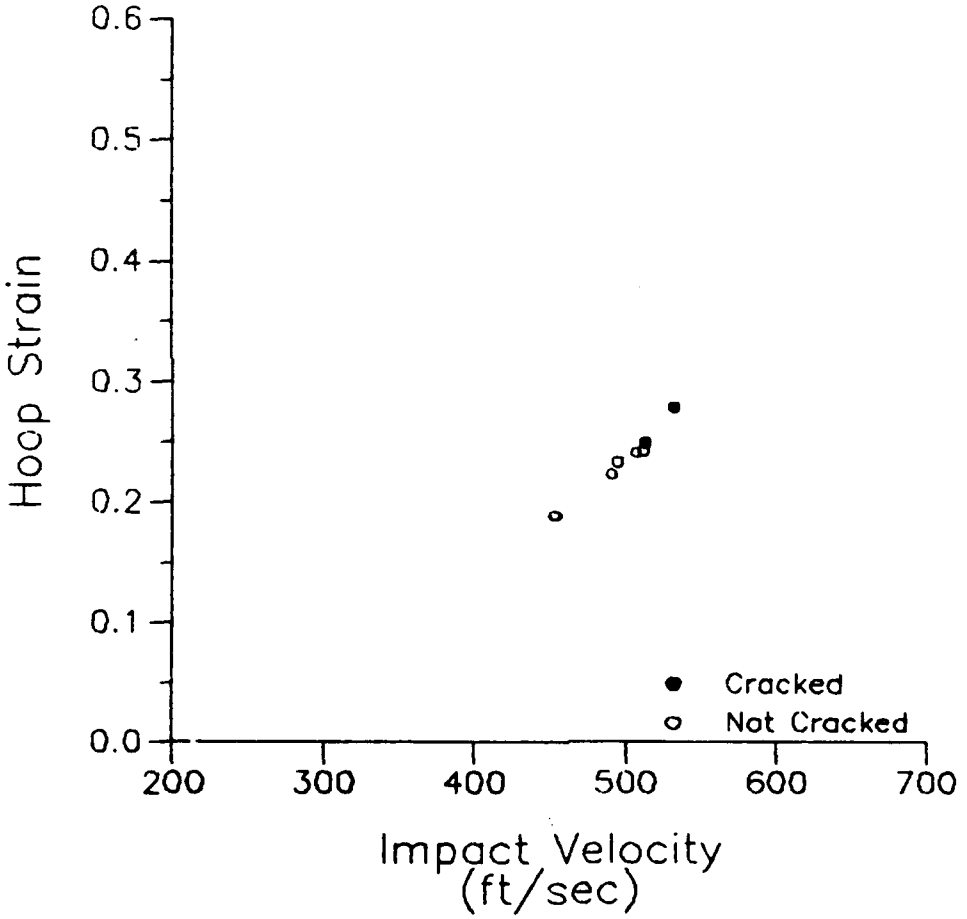

Taylor Anvil Test Results
Specimen: D224

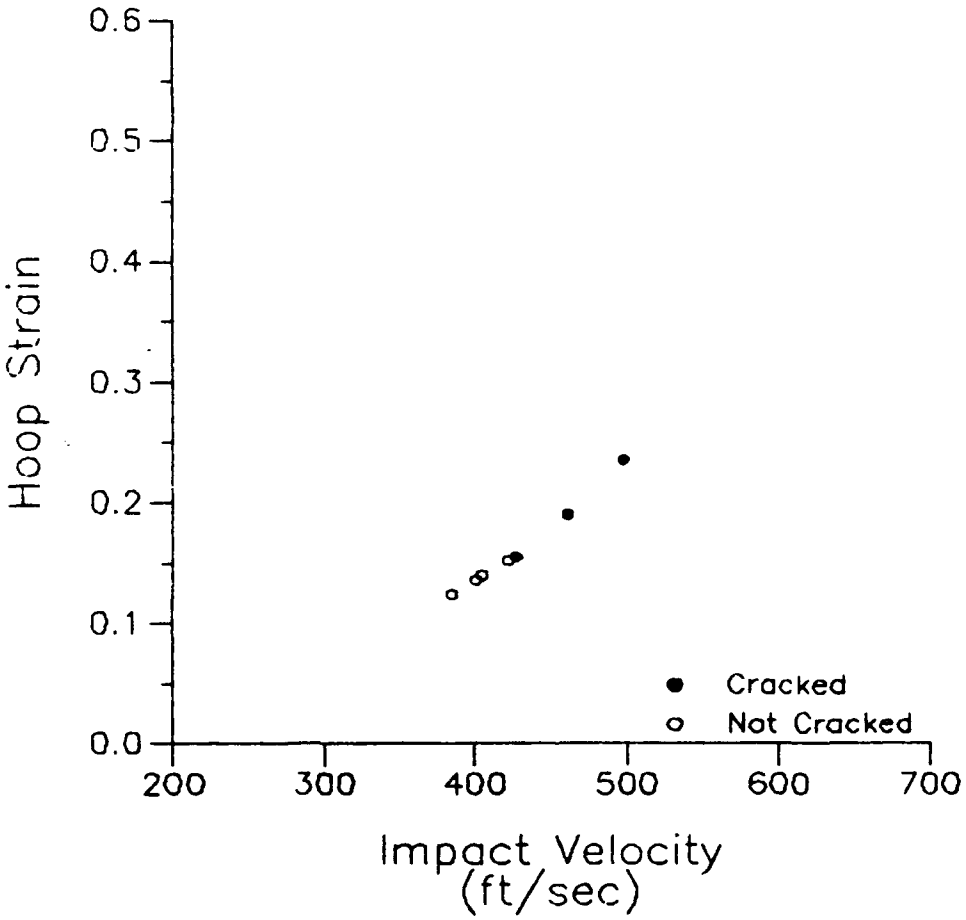

Taylor Anvil Test Results
Specimen: D329

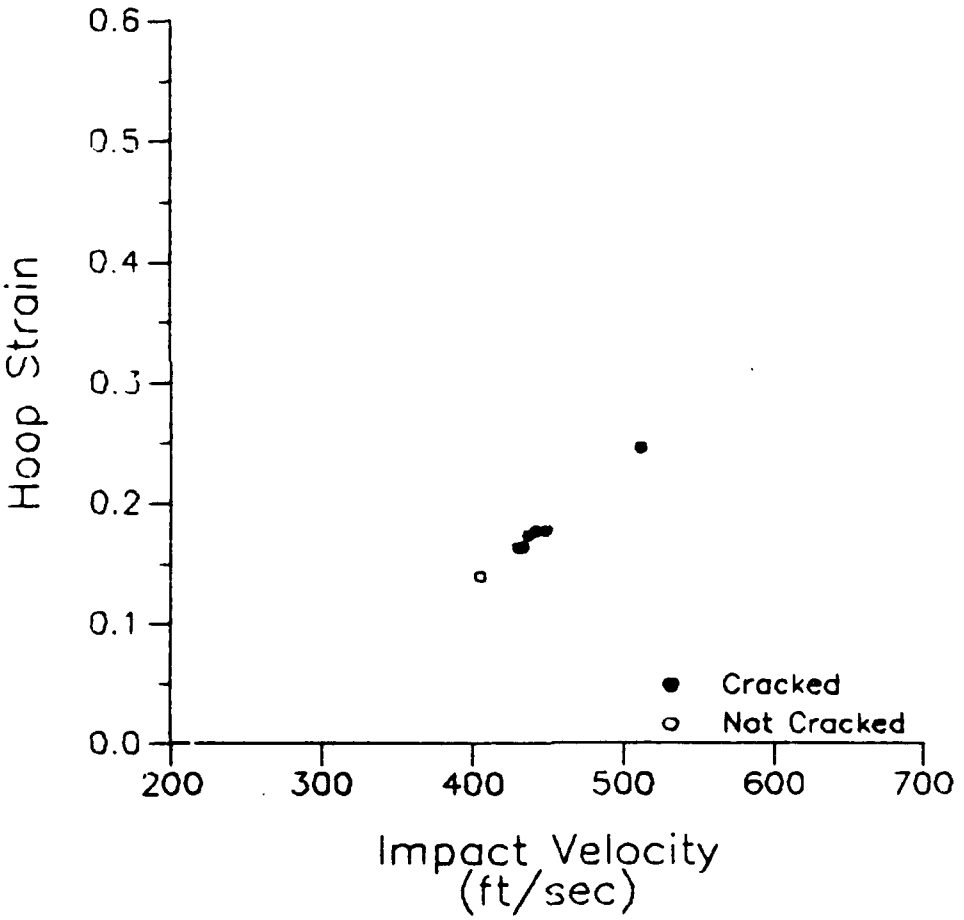

Taylor Anvil Specimens
Data Sheet

Shot No.	Mtl Type	Work	Weight (grams)	Mtl Density (#/in^3)	Hardness Rc	Brinell Hardness (bha) *	Static Ultimate Strength (ksi)	Static Yield Strength (ksi)	% Elong	Impact Velocity (fps)	Cracked (Y/N)	Comment	Lo (in)	Le (in)	Bo (in)	β (in)	Δ/Ao	h	Vc (fps)	Sigca (psi)	Hoop Strain	Average Sigca (psi,*10E5)	Percent Difference from mean	
100	D630	Unworked	775.5	0.6379	31.0	294	139	88	37	499	N		1.0002	0.4845	0.4702	0.5950	1.548	1.182	1193	1.56E+05	0.244	1.64	5%	
96	D630	Unworked	774.7	0.6374	31.0	294	139	88	37	501	Y	Very Slight	1.0004	0.4835	0.4701	0.5960	1.575	1.176	1165	1.62E+05	0.255		9%	
97	D630	Unworked	774.5	0.6371	31.0	294	139	88	37	515	N		1.0010	0.4805	0.4700	0.5930	1.592	1.179	1175	1.66E+05	0.262		1%	
102	D630	Unworked	774.0	0.6371	31.0	294	139	88	37	518	Y	V.Slt & Yawed	1.0006	0.4845	0.4702	0.5949	1.590	1.179	1176	1.69E+05	0.263		3%	
101	D630	Unworked	774.7	0.6372	31.0	294	139	88	37	526	N		1.0003	0.4765	0.4702	0.5990	1.623	1.178	1164	1.66E+05	0.274		1%	
99	D630	Unworked	775.0	0.6378	31.0	294	139	88	37	543	Y	Very Slight	1.0005	0.4535	0.4703	0.6070	1.666	1.176	1155	1.60E+05	0.291		3%	
98	D630	Unworked	772.9	0.6366	31.0	294	139	88	37	572	Y	Slight	1.0011	0.4705	0.4700	0.6200	1.785	1.169	1112	1.71E+05	0.336		4%	
63	D631	Savage 15%	775.2	0.6371	42.5	395	169	156	13	410	N		1.0023	0.5045	0.4699	0.5450	1.345	1.203	1329	1.99E+05	0.160	1.98	0%	
62	D631	Savage 15%	776.2	0.6389	42.5	395	169	156	13	423	Y	1 Edge/Severe	1.0009	0.6015	0.4699	0.5490	1.365	1.201	1317	2.17E+05	0.160		9%	not used
58	D631	Savage 15%	776.1	0.6381	42.5	395	169	156	13	475	N		1.0007	0.5595	0.4702	0.5700	1.470	1.191	1248	2.04E+05	0.212		3%	
81	D631	Savage 15%	774.1	0.6369	42.5	395	169	156	13	480	Y	B.G. - BROKEN	1.0004	0.7635	0.4701		0.000	1.000	0	0.00E-06	-1.000		-100%	not used
84	D631	Savage 15%	775.3	0.6378	42.5	395	169	156	13	491	Y	Slight	1.0002	0.5405	0.4702	0.5800	1.522	1.185	1209	1.94E+05	0.234		-2%	
61	D631	Savage 15%	775.0	0.6364	42.5	395	169	156	13	499	Y	Slight	1.0034	0.5335	0.4701	0.5870	1.559	1.180	1179	1.87E+05	0.249		-6%	
59	D631	Savage 15%	775.0	0.6362	42.5	395	169	156	13	536	Y	Severe	1.0022	0.5395	0.4702	0.6120	1.694	1.170	1119	1.96E+05	0.302		1%	
60	D631	Savage 15%	774.1	0.6370	42.5	395	169	156	13	552	Y	Severe	1.0007	0.5555	0.4700	0.6210	1.746	1.169	1106	2.11E+05	0.321		6%	
24	D632	Unworked	666.5	0.6612	31.5	[illegible]	141	87	21	414	N		1.0004	0.5095	0.4703	0.5510	1.373	1.201	1275	1.60E+05	0.172	1.67	5%	
91	D632	Unworked	669.9	0.6615	31.9	[illegible]	141	87	21	439	Y	Very Slight	1.0007	0.5205	0.4700	0.5600	1.420	1.197	1241	1.72E+05	0.191		3%	
26	D632	Unworked	666.2	0.6612	31.6	[illegible]	141	87	21	456	Y	Slight	1.0003	0.4935	0.4703	0.5770	1.505	1.189	1192	1.87E+05	0.227		2%	
94	D632	Unworked	666.2	0.6615	31.8	[illegible]	141	87	21	479	Y	Very Slight	1.0003	0.4865	0.4702	0.5770	1.506	1.190	1198	1.85E+05	0.227		1%	
25	D632	Unworked	666.0	0.6610	31.8	[illegible]	141	87	21	481	Y	Slight	1.0003	0.4975	0.4703	0.5820	1.531	1.185	1170	1.67E+05	0.238		-9%	
92	D632	Unworked	666.0	0.6615	31.5	[illegible]	141	87	21	483	Y	Very Slight	1.0009	0.5035	0.4700	0.5770	1.507	1.191	1205	1.75E+05	0.228		5%	
93	D632	Unworked	666.7	0.6617	31.9	[illegible]	141	87	21	485	Y	Very Slight	1.0000	0.4865	0.4704	0.5800	1.520	1.189	1192	1.68E+05	0.233		-1%	
95	D632	Unworked	665.9	0.6615	31.6	[illegible]	141	87	21	552	Y	Moderate	1.0003	0.3855	0.4701	0.6230	1.756	1.172	1093	1.33E+05	0.325		21%	not used
14	D633	Savage 15%	802.0	0.6602	44.5	415	174	161	10	288	N		1.0007	0.6155	0.4701	0.5820	1.140	1.287	1818	2.06E+05	0.068	1.89	9%	not used
13	D633	Savage 15%	801.7	0.6593	44.5	415	174	161	10	329	N		1.0005	0.5615	0.4702	0.5130	1.190	1.250	1635	1.82E+05	0.091		-4%	
12	D633	Savage 15%	803.6	0.6607	44.5	415	174	161	10	392	Y	Very Slight	1.0007	0.5485	0.4702	0.5380	1.299	1.220	1394	1.83E+05	0.140		-3%	
15	D633	Savage 15%	802.5	0.6600	44.5	415	174	161	10	392	Y	Very Slight	1.0004	0.5765	0.4702	0.5380	1.299	1.220	1394	2.00E+05	0.140		6%	
38	D633	Savage 15%	803.9	0.6602	44.5	415	174	161	10	395	Y	Slight	1.0019	0.5915	0.4702	0.5400	1.350	1.198	1258	1.93E+05	0.165		2%	
37	D633	Savage 15%	805.9	0.6624	44.5	415	174	161	10	420	Y	Slight	1.0010	0.5725	0.4702	0.5590	1.413	1.194	1225	1.94E+05	0.189		3%	
11	D633	Savage 15%	802.3	0.6582	44.5	415	174	161	10	432	Y	Very Slight	1.0020	0.5455	0.4704	0.5550	1.392	1.201	1277	1.85E+05	0.180		-2%	
39	D633	Savage 15%	804.3	0.6612	44.5	415	174	161	10	481	Y	Severe	1.0000	0.5455	0.4701	0.5730	1.486	1.188	1187	1.87E+05	0.219		-1%	
21	D1670	Unworked	777.5	0.6411	29.6	293	139	85	36	402	N		1.0030	0.5405	0.4698	0.5450	1.352	1.190	1290	1.71E+05	0.163	1.70	0%	
22	D1670	Unworked	775.0	0.6399	29.6	283	139	85	36	439	N		1.0003	0.5115	0.4693	0.5570	1.409	1.194	1267	1.66E+05	0.187		-3%	
40	D1670	Unworked	784.3	0.6396	29.6	283	139	85	36	462	N		1.0106	0.4845	0.4698	0.5620	1.431	1.196	1282	1.61E+05	0.196		-6%	
42	D1670	Unworked	767.1	0.6379	29.6	283	139	85	36	467	N		0.9958	0.5105	0.4687	0.5680	1.469	1.188	1232	1.72E+05	0.212		1%	
41	D1670	Unworked	774.2	0.6388	29.6	283	139	85	36	473	N		1.0001	0.4895	0.4695	0.5660	1.453	1.194	1270	1.68E+05	0.206		-2%	
44	D1670	Unworked	779.8	0.6396	29.6	283	139	85	36	524	N		1.0061	0.4805	0.4695	0.5920	1.590	1.183	1194	1.71E+05	0.261		0%	
23	D1670	Unworked	781.4	0.6427	29.6	283	139	85	36	543	Y	Slight	1.0032	0.4935	0.4694	0.6120	1.700	1.173	1124	1.76E+05	0.304		3%	
43	D1670	Unworked	780.6	0.6390	29.6	283	139	85	36	554	Y	Very Slight	1.0102	0.4935	0.4690	0.6100	1.692	1.176	1152	1.80E+05	0.301		6%	

* Equivalence between bha and Rc based upon steel

Taylor Anvil Specimens
Data Sheet

Shot No	Rd Type	Work	Weight (grains)	Density (g/cc)	Hardness Rc	Brinell Hardness (kg/mm²)	Ultimate Strength (ksi)	Yield Strength (ksi)	% Elong	Impact Velocity (fps)	Cracked (Y/N)	Comment	Lo (in)	Le (in)	Do (in)	D (in)	A/A₀	k	Uc (fps)	Stress (psi)	Hoop Stress	Average Sigma	Percent Difference Sigma mean	
16	B224	Swage 0%	770.3	0.6366	43.0	400	181	170	8	385	N		1.0036	0.6285	0.4690	0.5270	1.251	1.229	1586	2.49E+05	0.124	2.45	2%	
35	B224	Swage 0%	771.6	0.6351	43.0	400	181	170	8	401	N		1.0032	0.6275	0.4692	0.5330	1.290	1.222	1456	2.42E+05	0.120		1%	
18	B224	Swage 0%	769.8	0.6378	43.0	400	181	170	8	405	N		1.0032	0.6305	0.4693	0.5350	1.300	1.219	1442	2.44E+05	0.146		0%	
19	B224	Swage 0%	769.3	0.6363	43.0	400	181	170	8	422	N		1.0002	0.6215	0.4689	0.5400	1.326	1.215	1412	2.44E+05	0.153		0%	
17	B224	Swage 0%	770.0	0.6361	43.0	400	181	170	8	427	Y	Very Slight	1.0017	0.6185	0.4691	0.5420	1.335	1.214	1402	2.43E+05	0.155		1%	
36	B224	Swage 0%	770.5	0.6335	43.0	400	181	170	8	461	Y	Very Slight	1.0053	0.6185	0.4691	0.5500	1.415	1.199	1311	2.45E+05	0.196		0%	
20	B224	Swage 0%	769.9	0.6354	43.0	400	181	170	9	490	Y	Slight	1.0024	0.6125	0.4689	0.5790	1.525	1.186	1220	2.46E+05	0.225		1%	
8	B300	Swage 25%	770.7	0.6378	30.9	293	137	87	18	280	Y	Slight	1.0019	0.5595	0.4684	0.5310	1.285	1.155	1015	9.32E+04	0.136	1.86	50%	not used
9	B300	Swage 25%	770.1	0.6371	30.9	293	137	87	18	360	Y	Very Slight	1.0000	0.5665	0.4689	0.5220	1.239	1.231	1514	1.85E+05	0.113		-0%	
45	B300	Swage 25%	769.9	0.6356	30.9	293	137	87	18	390	Y	Very Slight	1.0017	0.5415	0.4690	0.5290	1.272	1.226	1486	1.82E+05	0.125		2%	
10	B300	Swage 25%	769.8	0.6366	30.9	293	137	87	18	429	Y	Slight & Taved	1.0019	0.5475	0.4685	0.5470	1.363	1.204	1336	1.87E+05	0.169		1%	
7	B300	Swage 25%	769.6	0.6360	30.9	293	137	87	18	467	Y	Very Slight	1.0033	0.5585	0.4684	0.5500	1.379	1.213	1401	2.18E+05	0.173		18%	not used
47	B300	Swage 25%	767.4	0.6357	30.9	293	137	87	16	479	Y	Slight	1.0013	0.5185	0.4683	0.5620	1.445	1.198	1290	1.87E+05	0.202		1%	
46	B300	Swage 25%	770.1	0.6363	30.9	293	137	87	18	534	Y	Slight	1.0017	0.5095	0.4688	0.5980	1.627	1.179	1175	1.87E+05	0.276		1%	
1	B300	Swage 25%	770.1	0.6369	30.9	293	137	87	18	760	Y	Severe	1.0020	0.4855	0.4685	0.7360	2.468	1.155	1039	3.02E+05	0.571		9%	not used
77	B329	Swage 25%	768.8	0.6376	44.1	414	191	173	9	402	N		1.0012	0.6265	0.4681	0.5330	1.297	1.221	1450	2.52E+05	0.134	2.49	1%	
72	B329	Swage 25%	770.2	0.6341	44.1	414	191	173	9	432	N		1.0053	0.6315	0.4688	0.5450	1.352	1.208	1369	2.48E+05	0.161		1%	
78	B329	Swage 25%	769.1	0.6353	44.1	414	191	173	9	432	Y	Very Slight	1.0020	0.6255	0.4686	0.5450	1.353	1.209	1373	2.46E+05	0.164		-0%	
76	B329	Swage 25%	766.4	0.6334	44.1	414	191	173	9	434	N		1.0040	0.6365	0.4682	0.5450	1.355	1.208	1371	2.55E+05	0.164		3%	
74	B329	Swage 25%	771.6	0.6354	44.1	414	191	173	9	437	Y	Slight/Taved	1.0020	0.6215	0.4695	0.5510	1.377	1.202	1329	2.39E+05	0.177		-3%	
75	B329	Swage 25%	769.6	0.6354	44.1	414	191	173	9	442	Y	Slight	1.0017	0.6235	0.4696	0.5520	1.385	1.201	1323	2.43E+05	0.177		-1%	
79	B329	Swage 25%	768.1	0.6341	44.1	414	191	173	9	449	Y	Slight	1.0052	0.6245	0.4682	0.5510	1.385	1.204	1342	2.49E+05	0.177		1%	
73	B329	Swage 25%	771.5	0.6361	44.1	414	191	173	9	512	Y	Slight/Severe	1.0034	0.5995	0.4688	0.5840	1.562	1.184	1215	2.42E+05	0.246		2%	
5	B620	Unworked	749.2	0.6165	29.0	279	137	86	35	375	N		1.0015	0.5135	0.4698	0.5230	1.287	1.206	1394	1.49E+05	0.129	1.48	1%	
6	B620	Unworked	750.6	0.6178	29.0	279	137	86	35	401	N		1.0016	0.4875	0.4698	0.5400	1.321	1.203	1371	1.46E+05	0.143		-1%	
4	B620	Unworked	752.5	0.6217	29.0	279	137	86	35	429	N		1.0005	0.4695	0.4691	0.5530	1.390	1.191	1284	1.42E+05	0.179		4%	
3	B620	Unworked	748.8	0.6160	29.0	279	137	86	35	441	N		1.0015	0.4825	0.4690	0.5580	1.411	1.188	1275	1.53E+05	0.188		4%	
48	B620	Unworked	749.2	0.6162	29.0	279	137	86	35	490	N		1.0007	0.4365	0.4701	0.5760	1.501	1.166	1258	1.45E+05	0.225		-2%	
49	B620	Unworked	749.5	0.6162	29.0	279	137	86	35	545	N		1.0000	0.4315	0.4702	0.5970	1.612	1.180	1217	1.53E+05	0.270		4%	
2	B620	Unworked	749.5	0.6155	29.0	279	137	86	35	564	Y	Very Slight	1.0015	0.4225	0.4703	0.6210	1.744	1.167	1133	1.46E+05	0.320		-2%	
50	B620	Unworked	748.1	0.6142	29.0	279	137	86	35	604	Y	Slight	0.9965	0.4305	0.4702	0.6350	1.824	1.160	1144	1.63E+05	0.350		10%	not used
87	B629	Swage 15%	749.6	0.6167	42.5	395	166	153	10	476	Y	Very Slight	1.0007	0.5745	0.4700	0.5740	1.492	1.181	1223	2.04E+05	0.221	1.99	3%	
80	B629	Swage 15%	748.5	0.6159	42.5	395	166	153	10	477	N		1.0007	0.5455	0.4700	0.5720	1.481	1.183	1241	1.89E+05	0.217		-5%	
82	B629	Swage 15%	747.4	0.6150	42.5	395	166	153	10	479	N		1.0021	0.5675	0.4699	0.5710	1.477	1.184	1253	2.05E+05	0.215		3%	
83	B629	Swage 15%	749.2	0.6167	42.5	395	166	153	10	482	Y	Very Slight	1.0000	0.5285	0.4701	0.5770	1.507	1.179	1216	1.79E+05	0.227		-10%	not used
88	B629	Swage 15%	748.6	0.6158	42.5	395	166	153	10	487	Y	Very Slight	1.0010	0.5635	0.4700	0.5780	1.512	1.180	1219	2.01E+05	0.230		1%	
84	B629	Swage 15%	751.1	0.6175	42.5	395	166	153	10	496	Y	Very Slight	1.0000	0.5415	0.4702	0.5860	1.553	1.175	1185	1.87E+05	0.246		-6%	
85	B629	Swage 15%	748.0	0.6155	42.5	395	166	153	10	526	Y	Very Slight	1.0007	0.5475	0.4700	0.5930	1.592	1.175	1193	2.00E+05	0.262		0%	
86	B629	Swage 15%	748.5	0.6164	42.5	395	166	153	10	535	Y	Slight	1.0007	0.5585	0.4698	0.6040	1.653	1.171	1157	2.08E+05	0.289		5%	

* Equivalence between Rhn and Rc based upon steel

Taylor Anvil Specimens
Data Sheet

Shot No.	Bil Type	Work	Weight (grains)	Bil Density (lb/in^3)	Hardness Rc	Brinell Hardness (5kg) *	Ultimate Strength (ksi)	Yield Strength (ksi)	% Elong	Impact Velocity (fps)	Cracked (Y/N)	Comment	Lo (in)	Lf (in)	Do (in)	D (in)	d/do	k	Vo (fps)	Energy (psi)	Final Strain	Average Sigma (psi *10E5)	Percent Difference from mean
90	B1671	Swage 15%	777.9	0.6401	40.9	380	171	156	19	453	N		1.0008	0.6255	0.4683	0.5570	1.415	1.198	1.96	2.44E+05	0.189	2.43	0%
54	B1671	Swage 15%	778.2	0.6407	40.9	380	171	156	19	454	N		1.0075	0.6195	0.4683	0.5570	1.415	1.198	1293	2.40E+05	0.189		1%
56	B1671	Swage 15%	779.5	0.6407	40.9	380	171	156	19	491	N		1.0162	0.6165	0.4685	0.5733	1.496	1.191	1244	2.49E+05	0.223		2%
53	B1671	Swage 15%	780.9	0.6416	40.9	380	171	156	19	495	N		1.0072	0.6055	0.4689	0.5786	1.519	1.187	1220	2.39E+05	0.233		2%
57	B1671	Swage 15%	777.6	0.6402	40.9	380	171	156	19	501	N		1.0087	0.6125	0.4688	0.5810	1.532	1.187	1217	2.49E+05	0.241		2%
51	B1671	Swage 15%	777.9	0.6406	40.9	380	171	156	19	512	N		1.0041	0.6135	0.4676	0.5810	1.542	1.188	1225	2.53E+05	0.242		4%
55	B1671	Swage 15%	786.9	0.6480	40.9	380	171	156	19	513	Y	Slight	1.0064	0.5855	0.4693	0.5860	1.559	1.185	1227	2.30E+05	0.249		-5%
52	B1671	Swage 15%	778.7	0.6400	40.9	380	171	156	19	532	Y	Slight	1.0083	0.6025	0.4685	0.5990	1.635	1.178	1163	2.43E+05	0.279		-0%
34	B1672	Unworked	805.5	0.6623	30.9	293	140	87	23	396	N		1.0053	0.5705	0.4689	0.5620	1.336	1.207	1304	1.91E+05	0.156	1.90	1%
33	B1672	Unworked	804.6	0.6602	30.9	293	140	87	23	397	N		1.0040	0.5705	0.4699	0.5380	1.311	1.217	1375	2.00E+05	0.145		6%
29	B1672	Unworked	804.9	0.6641	30.9	293	140	87	23	431	N		1.0038	0.5595	0.4694	0.5500	1.417	1.196	1233	1.77E+05	0.189		-6%
28	B1672	Unworked	802.2	0.6623	30.9	293	140	87	23	456	Y	Slight	1.0025	0.5535	0.4689	0.5620	1.437	1.196	1230	1.93E+05	0.199		2%
32	B1672	Unworked	806.8	0.6610	30.9	293	140	87	23	464	Y	Slight	1.0098	0.5445	0.4692	0.5750	1.502	1.186	1171	1.83E+05	0.225		-3%
30	B1672	Unworked	803.6	0.6611	30.9	293	140	87	23	467	N		1.0019	0.5205	0.4697	0.5720	1.483	1.191	1204	1.78E+05	0.210		-6%
31	B1672	Cracked	799.2	0.6625	30.9	293	140	87	23	502	Y	Slight/Severe	1.0040	0.5515	0.4675	0.5960	1.625	1.176	1116	1.95E+05	0.275		3%
27	B1672	Uncracked	809.0	0.6700	30.9	293	140	87	23	522	Y	Slight	1.0021	0.5375	0.4684	0.5930	1.603	1.184	1149	1.99E+05	0.266		5%
87	B1673	Swage 15%	809.7	0.6637	41.5	*	172	150	11	397	N		1.0059	0.6435	0.4689	0.5370	1.208	1.225	1414	2.45E+05	0.135	2.41	2%
60	B1673	Swage 15%	811.6	0.6649	41.5	*	172	150	11	397	N		1.0109	0.6455	0.4689	0.5330	1.292	1.227	1440	2.45E+05	0.127		1%
88	B1673	Swage 15%	812.0	0.6652	41.5	*	172	150	11	465	N		1.0068	0.6255	0.4694	0.5420	1.333	1.213	1336	2.31E+05	0.155		-4%
71	B1673	Swage 15%	807.3	0.6615	41.5	340	172	150	11	417	Y	Slight	1.0048	0.6255	0.4691	0.5450	1.350	1.211	1329	2.36E+05	0.162		2%
89	B1673	Swage 15%	811.9	0.6642	41.5	340	172	150	11	453	Y	Slight	1.0083	0.6175	0.4696	0.5610	1.427	1.200	1261	2.40E+05	0.195		0%
70	B1673	Swage 15%	805.1	0.6611	41.5	340	172	150	11	469	Y	Slight	1.0109	0.6275	0.4681	0.5660	1.462	1.196	1241	2.51E+05	0.209		4%
65	B1673	Swage 15%	809.7	0.6637	41.5	340	172	150	11	477	Y	Very Slight	1.0072	0.6035	0.4694	0.5730	1.490	1.197	1215	2.35E+05	0.221		-3%
66	B1673	Swage 15%	806.6	0.6625	41.5	340	172	150	11	492	Y	Slight	1.0069	0.6095	0.4691	0.5700	1.518	1.192	1209	2.45E+05	0.232		1%

* Equivalence between Rhb and Rc based upon steel

Figure C-1. Tungsten Alloy Taylor Anvil Specimen Exhibiting "VERY SLIGHT" Cracking on the Impact Edges

APPENDIX C

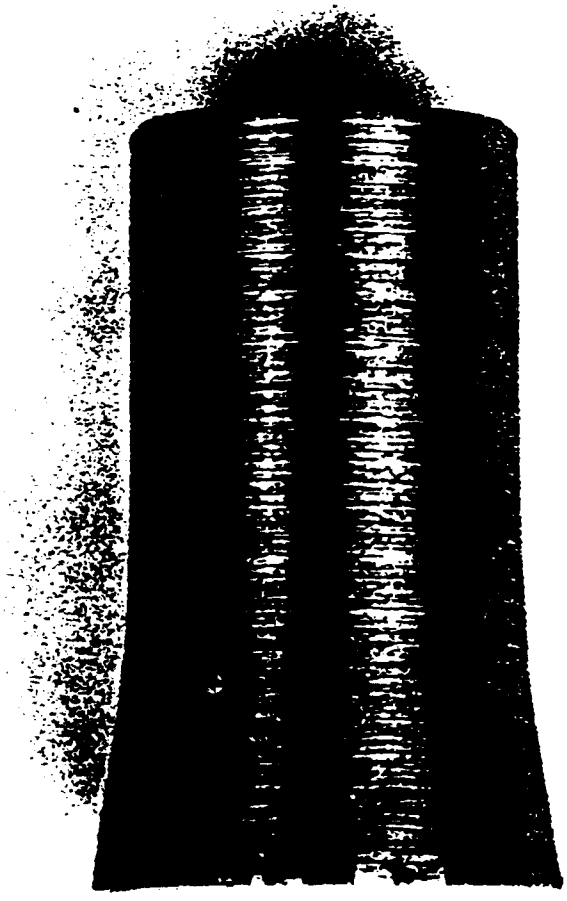

Figure C-2. Tungsten Alloy Taylor Anvil Specimen Showing "SLIGHT" Cracking on the Impact Edges

Figure C-3. Tungsten Alloy Taylor Anvil Specimen Showing "SEVERE" Cracking on the Impace Edges and Face

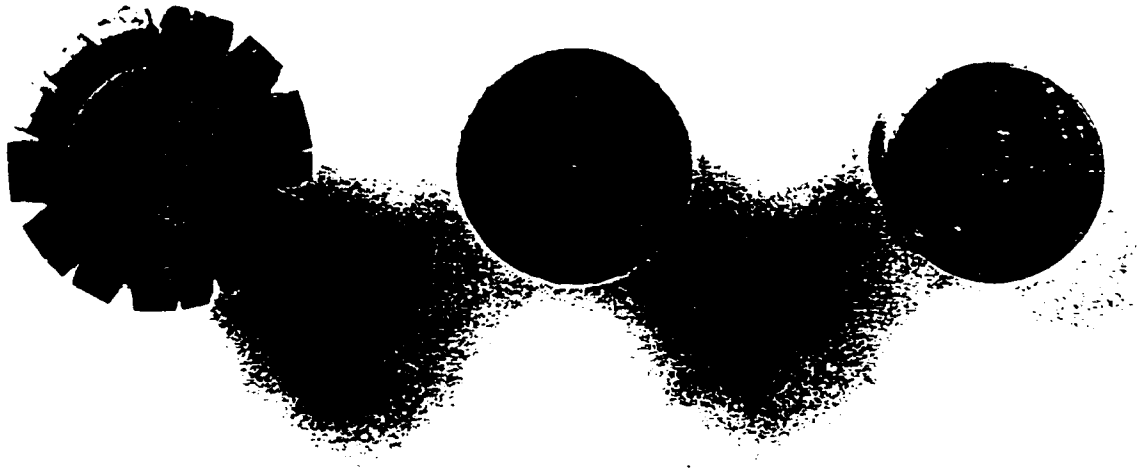

Figure C-4. Impact Surface of Tungsten Alloy Taylor Anvil Specimens Showing, Left to Right, "SEVERE" Cracking, "SLIGHT" Cracking and "VERY SLIGHT" Cracking

Olin 30mm Phalanx Testing

PRELIMINARY REPORT

FOR

GTE TUNGSTEN PENETRATOR EVALUATION

PREPARED FOR:

GTE SYLVANIA
PURCHASE ORDER 21160

BY:

KATHY GOWINS
MAY 1988

OLIN CORPORATION - MARION OPERATIONS

RESEARCH AND DEVELOPMENT

MARION, ILLINOIS

ABSTRACT

This report describes the initial test and evaluation of the GTE-Sylvania tungsten penetrators submitted to Olin Corporation in accordance with Sylvania Purchase Order No. 21160. Twenty-two tungsten penetrators have been tested to date against the X-1 plate array.

1.0 INTRODUCTION

This report describes the preliminary testing of GTE-Sylvania tungsten penetrators submitted to Olin Corporation in accordance with the Sylvania Purchase Order No. 21160.

The scope of work for that purchase order includes the following:

1. Assembly of the penetrators in Olin supplied test sabots.
2. Testing against the X-1 plate array at entrance velocities greater than 1220 meters per second with penetrator soft recovery.
3. Data acquisition, summary, analysis, and reporting.

The first partial delivery, received 17 February 1988, contained six groups of penetrators manufactured to Olin Drawing No. 8001466, see Figure 1. See Table I for a description of the penetrators along with Olin assigned serial numbers.

The preliminary evaluation used two to six penetrators from each group for a total of 22 tests against the X-1 plate array, see Figure 2.

2.0 TEST SETUP

The test setup used (see Figure 3) measured penetrator impact velocity, yaw angle and exit velocity. Plywood bundles were positioned behind the array for recovery of the penetrator or penetrator fragments. The plywood bundle was placed as close to the target as the equipment would allow at approximately three feet behind the target frame. Six penetrators were not recovered as a result of exit from the top of the plywood bundle or the back of the bundle (3 each). A second plywood bundle was added to the setup after the third failure to stop the penetrator.

NOTES:
1. SPEC. MIL-A-2550 APPLIES

REVISIONS			
REV	DESCRIPTION	DATE	APPROVED

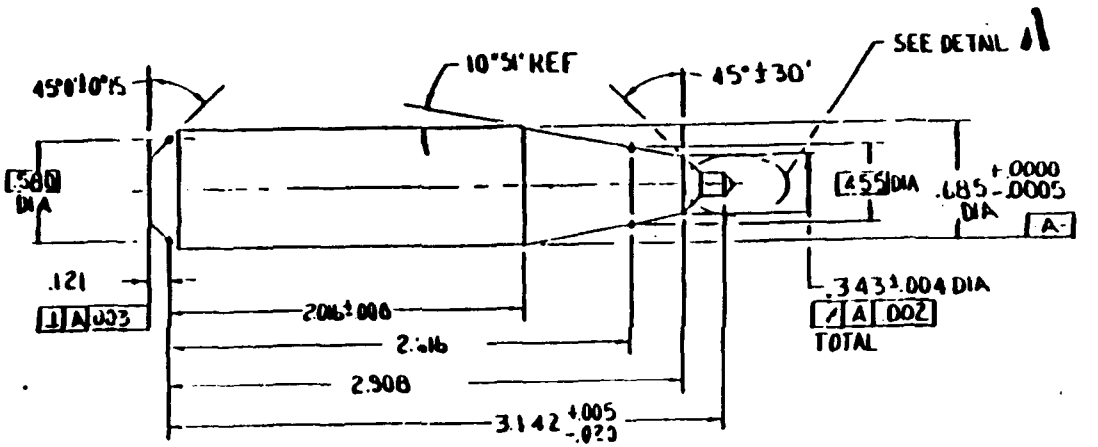

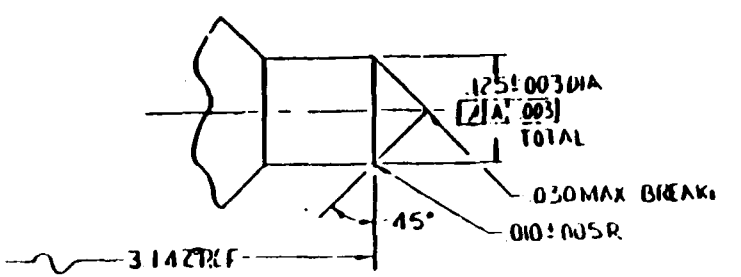

FIGURE 1

QTY REQD	NOMENCLATURE OR DESCRIPTION	IDENTIFYING NUMBER	DOCUMENT NUMBER	FSCM NUMBER	MATERIAL OR NOTE
1	ASSY	-1			

UNLESS OTHERWISE SPECIFIED — CONTRACT NO — Olin ORDINANCE PRODUCTS MARION, IL 62959

DR C.O. — PENETRATOR, 30 MM APDS

SIZE C — FSCM NO 14578 — DRAWING NO 8001466 — REV

SCALE 5/1 — SHEET 1 OF 1

NEXT ASSY — USED ON — APPLICATION — APPROVED — DATE

FIGURE 1

TABLE I.

MATERIAL	TYPE	QUANTITY	P/N	OLIN S/N
WN008FU	WHA-1069	9	924321-1	100-108
WN308FU	WHA-1078	10	924321-2	200-209
WN608FU	WHA-1071	9	924321-3	300-308
WN307FU	WHA-1053	10	924321-4	400-409
WN008FH	WHA-1069	10	924321-5	500-509
WN008FH	WHA-1069	10	924321-6	600-609

Material Supplied to Olin

Material	Blend	Alloy	Ni/Fe	Thermo-Mechanical Treatment
WN-008FU	WHA-1069	90W-8Ni-2Fe	8/2	As Sintered
WN-308FU	WHA-1078	93W-5.6Ni-1.4Fe	8/2	As Sintered
WN-608FU	WHA-1071	96W-3.2Ni-0.8Fe	8/2	As Sintered
WN-307FU	WHA-1053	93W-4.9Ni-2.1Fe	7/3	As Sintered
WN-008FH	WHA-1069	90W-8Ni-2Fe	8/2	Swaged 15%
WN-008FH	WHA-1069	90W-8Ni-2Fe	8/2	Swaged 15% - Aged 4hrs at 400°C

X-1 PLATE ARRAY

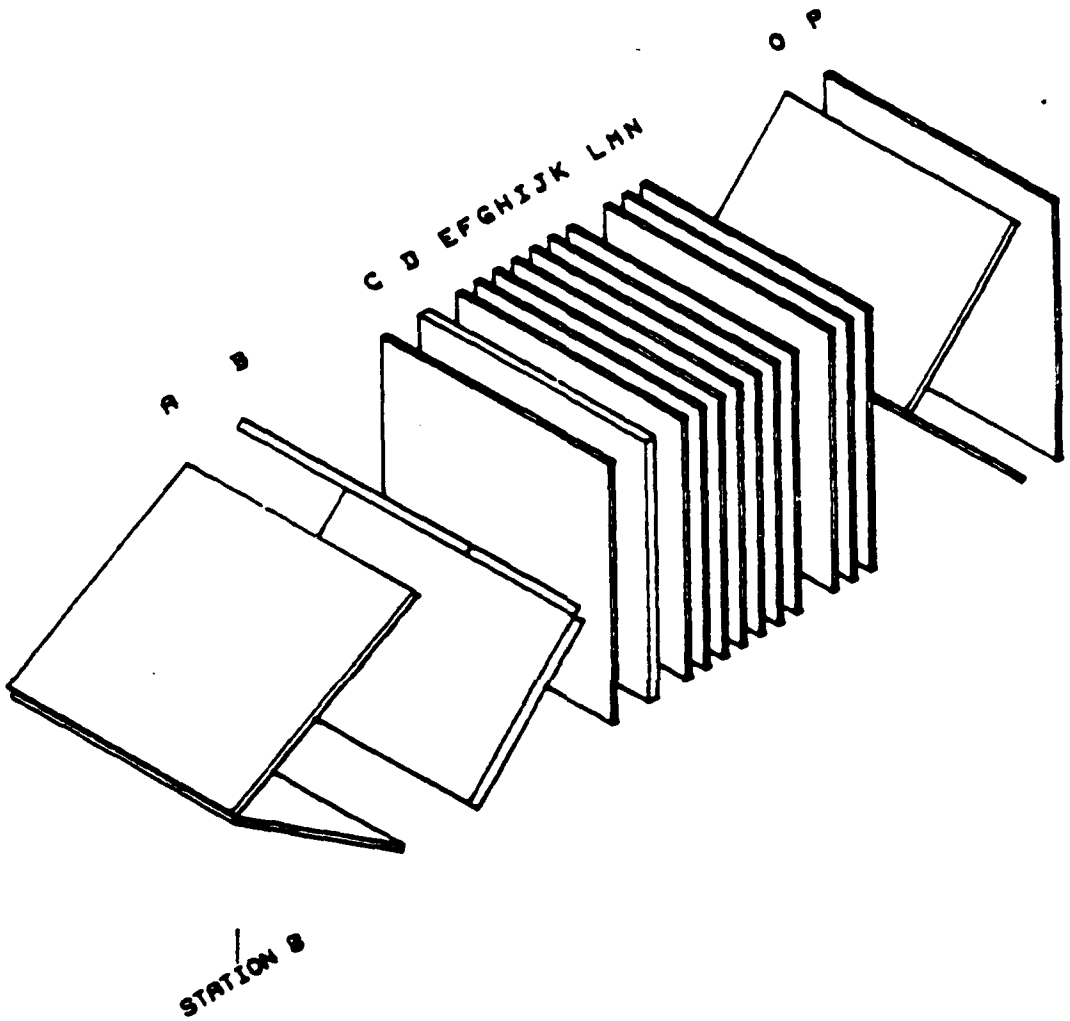

PLATE	THICKNESS IN.	THICKNESS MM	STATION NUMBER IN.	STATION NUMBER MM	OBLIQUITY DEGREES	MATERIAL
A	.300	7.620	0.000	0.000	60.000	G-10 GRP
B	.500	12.700	18.400	467.360	45.000	2024-T3 AL
C	.250	6.350	20.400	518.160	0.000	MILD STEEL
D	.500	12.700	22.400	568.960	0.000	2024-T3 AL
E	.250	6.350	24.400	619.760	0.000	2024-T3 AL
F	.250	6.350	25.400	645.160	0.000	2024-T3 AL
G	.250	6.350	26.400	670.560	0.000	2024-T3 AL
H	.250	6.350	27.400	695.960	0.000	2024-T3 AL
I	.250	6.350	28.400	721.360	0.000	2024-T3 AL
J	.250	6.350	29.400	746.760	0.000	2024-T3 AL
K	.250	6.350	30.400	772.160	0.000	2024-T3 AL
L	.250	6.350	32.400	822.960	0.000	2024-T3 AL
M	.250	6.350	33.400	848.360	0.000	2024-T3 AL
N	.250	6.350	34.400	873.760	0.000	2024-T3 AL
O	.250	6.350	36.400	924.560	45.000	MILD STEEL
P	.250	6.350	44.400	1127.760	0.000	2024-T3 AL

FIGURE 2

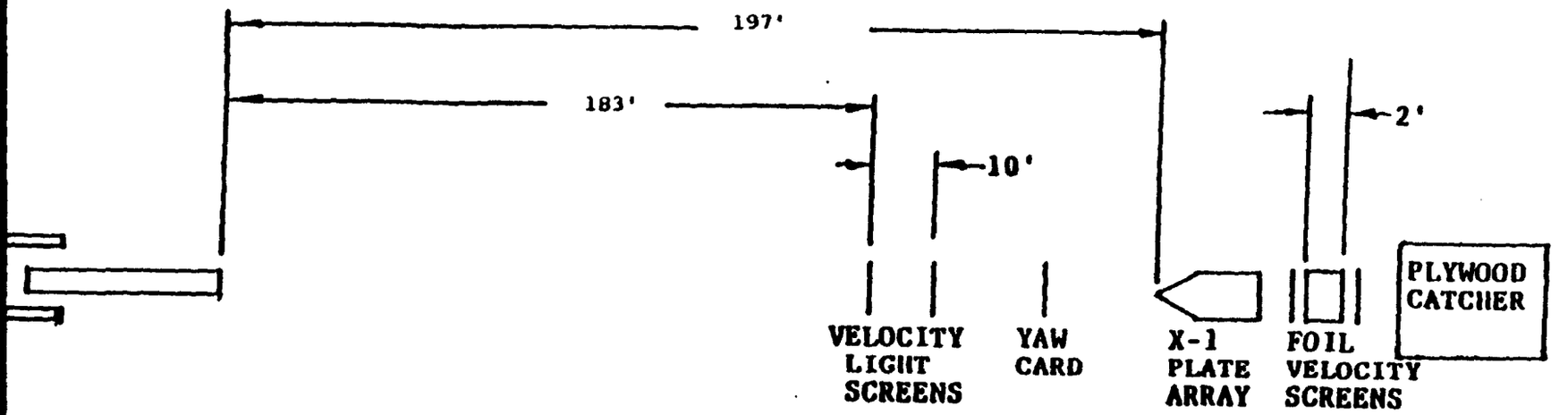

Typical Test Set-Up

FIGURE 3

3.0 PERFORMANCE

The initial tests used four GTE penetrators from Group WHA-1069 with the test sabot and pusher plug manufactured in accordance with Figures 4 and 5. The measured yaw at impact resulted in reinspection of the parts, which showed a loose fit between the sabot and penetrator. The outside diameter at the back of the sabot after assembly was outside the drawing limits which caused difficulty in chambering. An immediate corrective modification to the sabot was made to include shortening the overall length by .035 inch and machining the outside diameter after assembly to maintain concentricity and improve base fit.

During the test yaw angles were measured using orthogonal x-rays taken at the target entrance. The angles were measured between the flight path of the penetrator and flight lines on the x-rays for both the horizontal and vertical views. The two angles were then combined for the true angle of yaw. Figure 6 provides the details for this calculation. Exit velocity for all penetrators and an estimate of residual mass of the unrecovered penetrators were calculated from the flash x-rays taken at the plate array exit. The measured distance between the two penetrator images divided by the time difference (200 microseconds) gives the exit velocity of the penetrator. The residual mass of the penetrator is calculated by measuring one of the images. The difference between the image width and the actual penetrator diameter gives a percent enlargement of the image versus the actual.

3.1 S/N 100-105, TYPE WHA-1069

All six penetrators of this series entered the plate array with entrance velocities over 4000 fps. Table II lists the test data of each round of this series. Two rounds were no-tests as a result of frame hit (S/N 100) at the fourth plate of the array or excessive yaw (S/N 104) entering the array. Four rounds of the group (S/N's 100, 102, 103, and 105) were not recovered due to their exiting the top of the plywood bundle. Rounds 101 and 105 entered the array at center of the top. No yaw was evident in either penetrator until Plate K (S/N 101) and Plate O (S/N 105). Figure 2 shows the plate order and call letters of the plate array. Round 102 entered the array at the apex of Plate A, yawed through the target and tumbled after exit of the last plate. Round 103

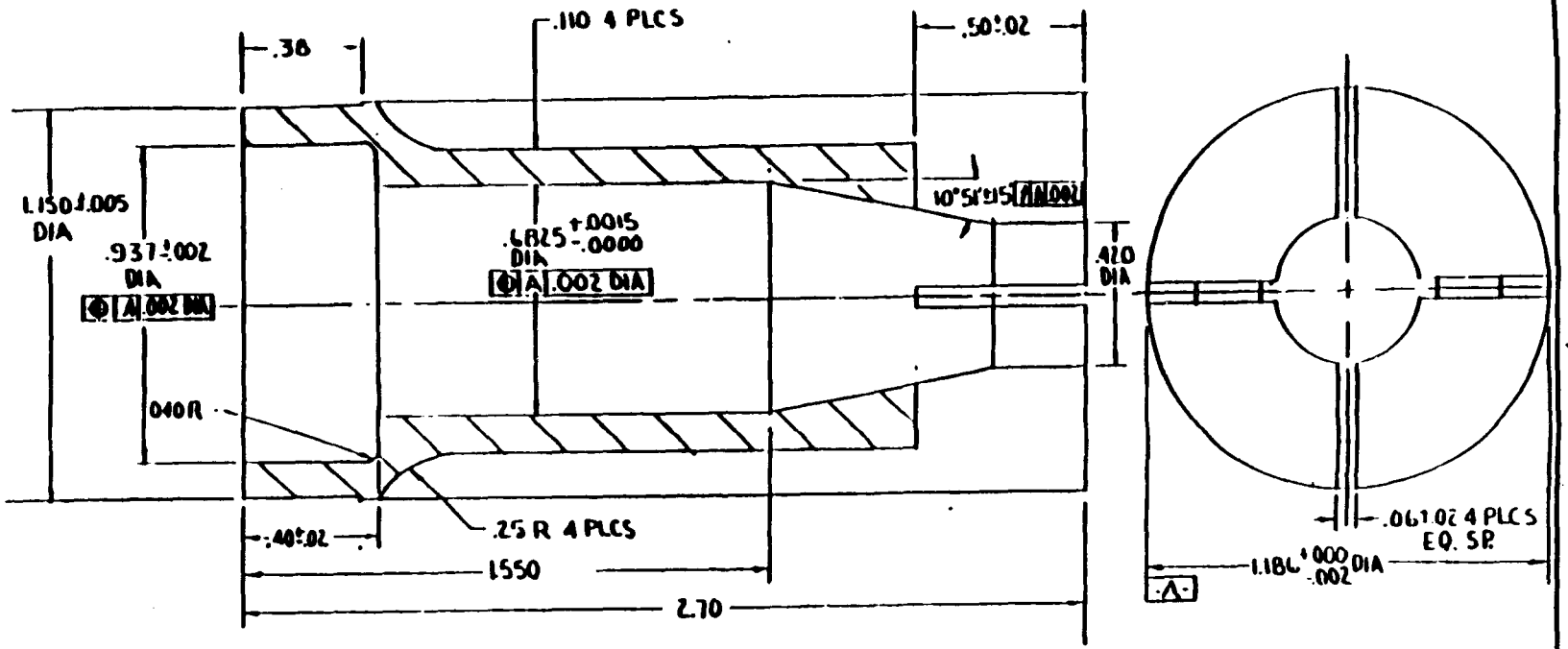

FIGURE 4

QTY REQD	NOMENCLATURE OR DESCRIPTION	IDENTIFYING NUMBER	DOCUMENT NUMBER	FSCM NUMBER	MATERIAL OR NOTE	ITEM NO
	ASSY	PARTS LIST				

UNLESS OTHERWISE SPECIFIED — CONTRACT NO

DR C.O.

CHK

DIMENSIONS ARE IN INCHES

DO NOT SCALE DRAWING

MATERIAL: NYLON 6/6 12%GLASS

NEXT ASSY | USED ON

APPLICATION

APPROVED | DATE

Olin ORDNANCE PRODUCTS MARION IL 62959

MACHINED SABOT, DISCARDING
30MM APDS
(685 DIA)

SIZE	FSCM NO	DRAWING NO	REV
C	14578	8008116	

SCALE 4/1 SHEET 1 OF 1

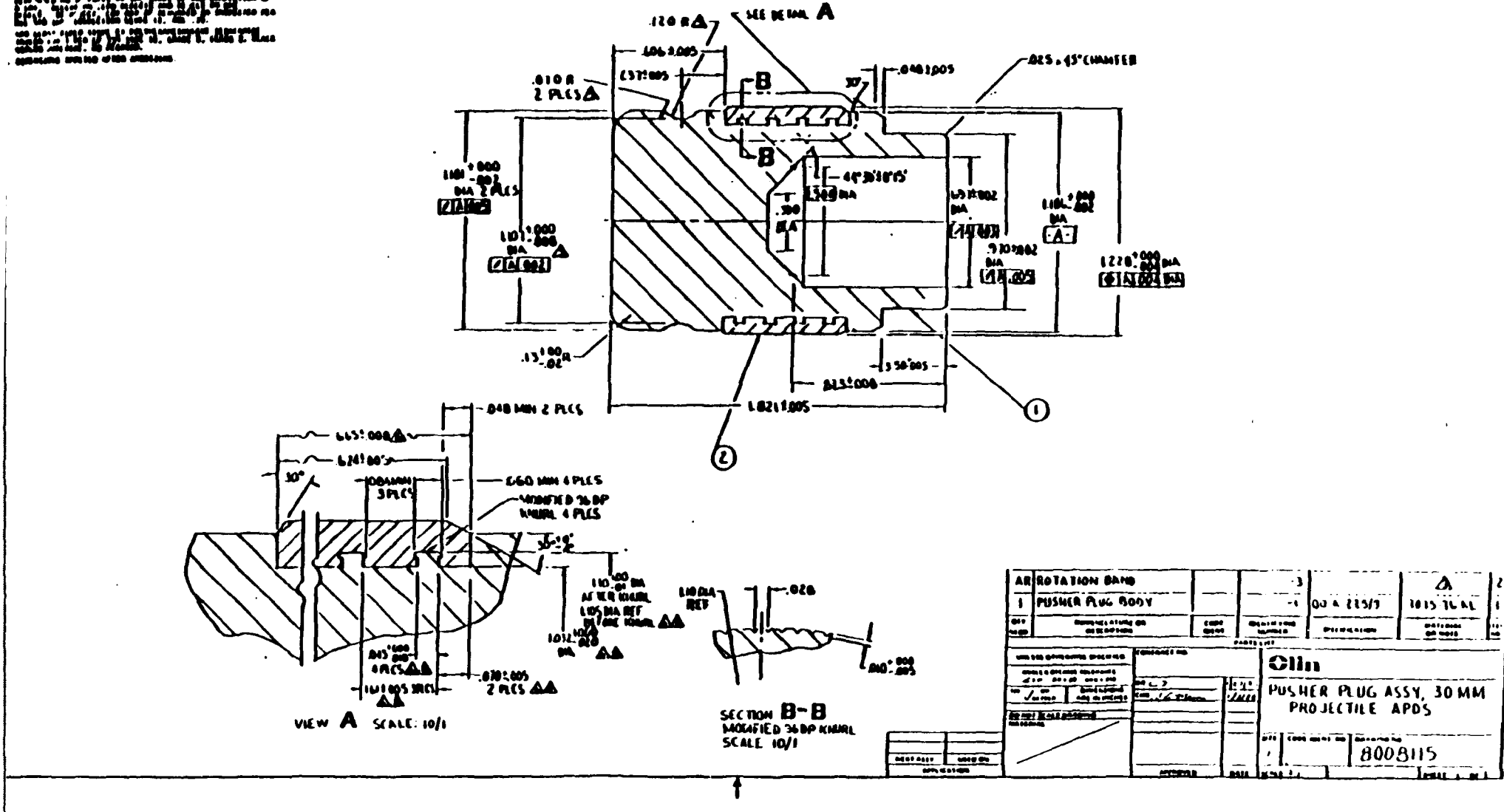

Pusher Plug Assembly

FIGURE 5

$$\Theta = \text{TAN}^{-1} \frac{F}{C}$$

$$= \text{TAN}^{-1} \sqrt{\frac{E^2+D^2}{C}}$$

$$= \text{TAN}^{-1} \sqrt{\frac{C^2\text{TAN}^2\,\beta + C^2\text{TAN}^2\,\alpha}{C}}$$

$$\Theta = \text{TAN}^{-1} \sqrt{\text{TAN}^2\,\beta + \text{TAN}^2\,\alpha}$$

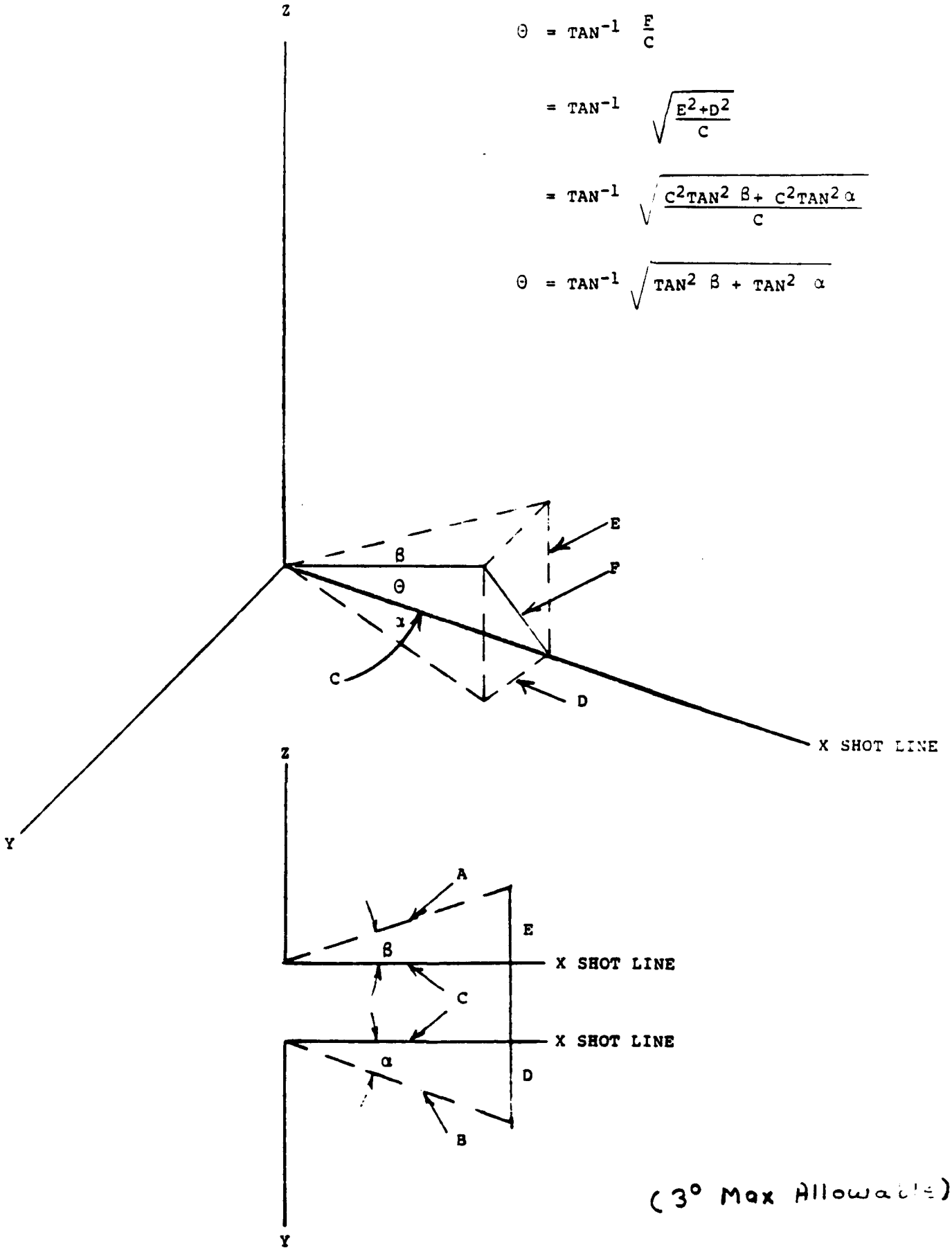

(3° Max Allowable)

FIGURE 6. YAW ANGLE CALCULATIONS

Table II. P/N 924321-1
Type WHA-1069

SERIAL NUMBER	PENETRATOR MASS, GMS	IMPACT VELOCITY, FPS	ENTRANCE YAW, DEG.	EXIT VELOCITY*, FPS	RESIDUAL MASS GMS	COMMENT
100	269.92	4217	3.93	-	227.50**	Hit Frame
101	270.02	4182	2.56	3217	242.60	
102	270.04	4248	1.64	3425	254.25**	
103	269.70	4116	1.17	2188	235.59**	Yawed Exiting Plate Array
104	270.21	4085	10.99		241.12	Exited Array At Plate O
105	269.93	4249	1.68	3034	254.45**	

* Exit Velocity Measured From X-Ray Film
** Estimate Calculated From X-Ray Film

also entered the array at the apex after gun adjustment. This less than desireable dispersion is probably a result of the late pusher separation. Flash x-ray showed the pusher and penetrator were separating at the entrance of the target. Rounds 100 to 103 were tested using the sabots as manufactured. All other rounds used the modified sabots as described previously.

3.2 S/N 200-205, TYPE WHA-1078

During this test phase, four of the six shots were declared no-tests as a result of excessive yaw at impact (S/N's 201 and 202), frame impact (S/N 203), or missing the target array (S/N 205) (see Table III). The impact points on Plate A are shown in Figure 7. Five penetrators were not recovered due to exiting the top of the bundle (S/N 201, 202 and 203), exiting the back of the bundle (S/N 204), or missing the target array (S/N 205). Rounds 200 and 204 penetrated the array with no drifting of the penetrator location and exited with no noticeable yaw. Rounds 201 and 202 exhibited some yaw throughout the plate array.

3.3 S/N 300-303, TYPE WHA-1071

The tests results for four of the nine penetrators from this series are summarized in Table IV. Two fo the four shots were declared no-tests as a result of missing the array (S/N 300) or excessive yaw (S/N 301). The impact points on Plate A are shown in Figure 8. Two penetrators (S/N's 301 and 302) entered the array and broke on exit. The third penetrator (S/N 303) broke in two at Plate K of the array and crossed the path of Round 302 on three plates.

3.4 S/N 400-401, TYPE WHA-1053

Two of the ten penetrators from this series have been tested. The results are summarized in Table V. The first round (S/N 400) was declared a no-test as a result of a yaw angle greater than 11° entering the array. The second round (S/N 401) entered the target on the top plate penetrating the array with very little yawing. The penetrator was not recovered due to exit out the back of the plywood bundle. Figure 9 shows the impact points on Plate A.

Table III. P/N 924321-2
Type WHA-1078

SERIAL NUMBER	PENETRATOR MASS, GMS	IMPACT VELOCITY, FPS	ENTRANCE YAW, DEG.	EXIT VELOCITY*, FPS	RESIDUAL MASS GMS	COMMENT
200	279.43	4231	2.78	2917	253.05	
201	279.05	3930	>11	807	244.03**	Exited Top Of Plywood Bundle
202	278.08	4108	4.32	2917	267.38**	Yawed Exiting Plate Array
203	278.04	4081	-	-	-	Hit Frame
204	278.21	4113	0.4	3411	263.60**	Exited Back Of Plywood Bundle
205	278.13	4061	-	-	-	Missed Array

* Exit Velocity Measured From X-Ray Film
** Estimate Calculated From X-Ray Film

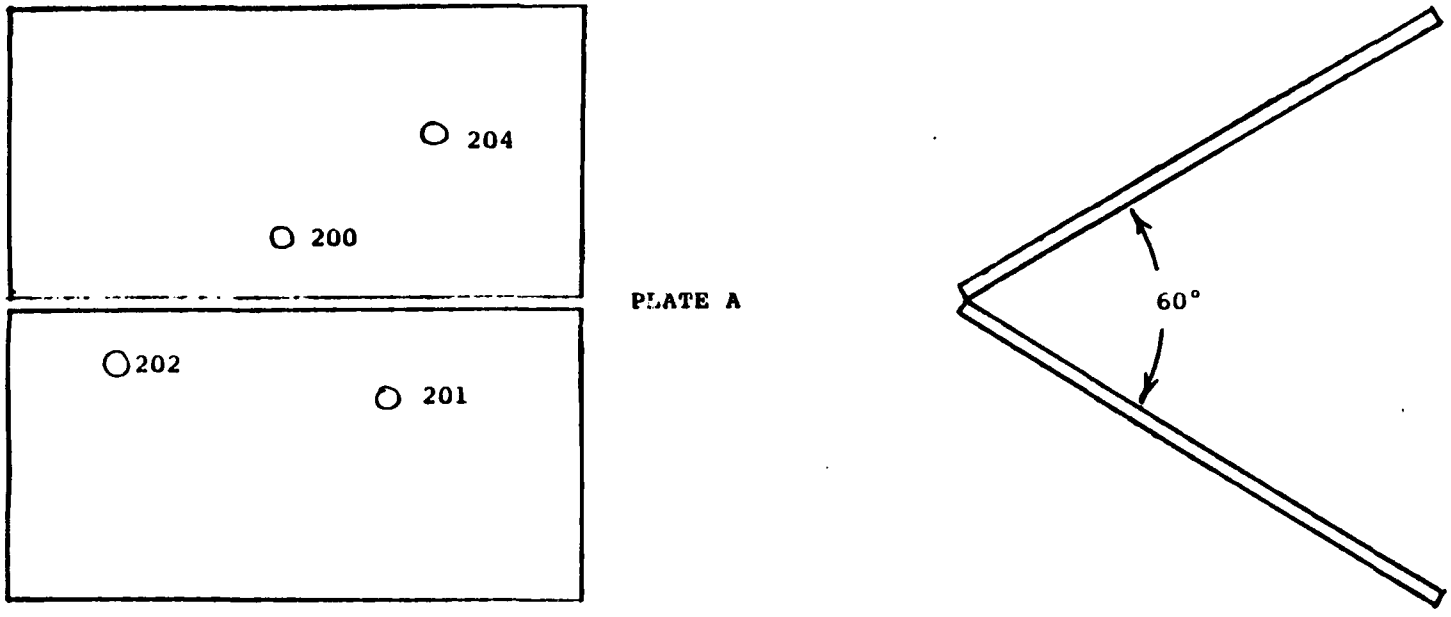

FIGURE 7. PLATE A
IMPACT POINTS FOR TYPE WHA-1078

Table IV. P/N 924321-3
Type WHA-1071

SERIAL NUMBER	PENETRATOR MASS, GMS	IMPACT VELOCITY, FPS	ENTRANCE YAW, DEG.	EXIT VELOCITY*, FPS	RESIDUAL MASS GMS	COMMENT
300	288.54	4166	-	-	-	Missed Array
301	287.94	4260	6.32	2995	65.83	Penetrator Broke
302	287.95	4040	1.10	3359	163.03 62.13	Penetrator Broke
303	288.52	4074	1.40	3255	94.58 31.71	Penetrator Broke Path Crossed #302 On 3 Plates

* Exit Velocity Measured From X-Ray Film

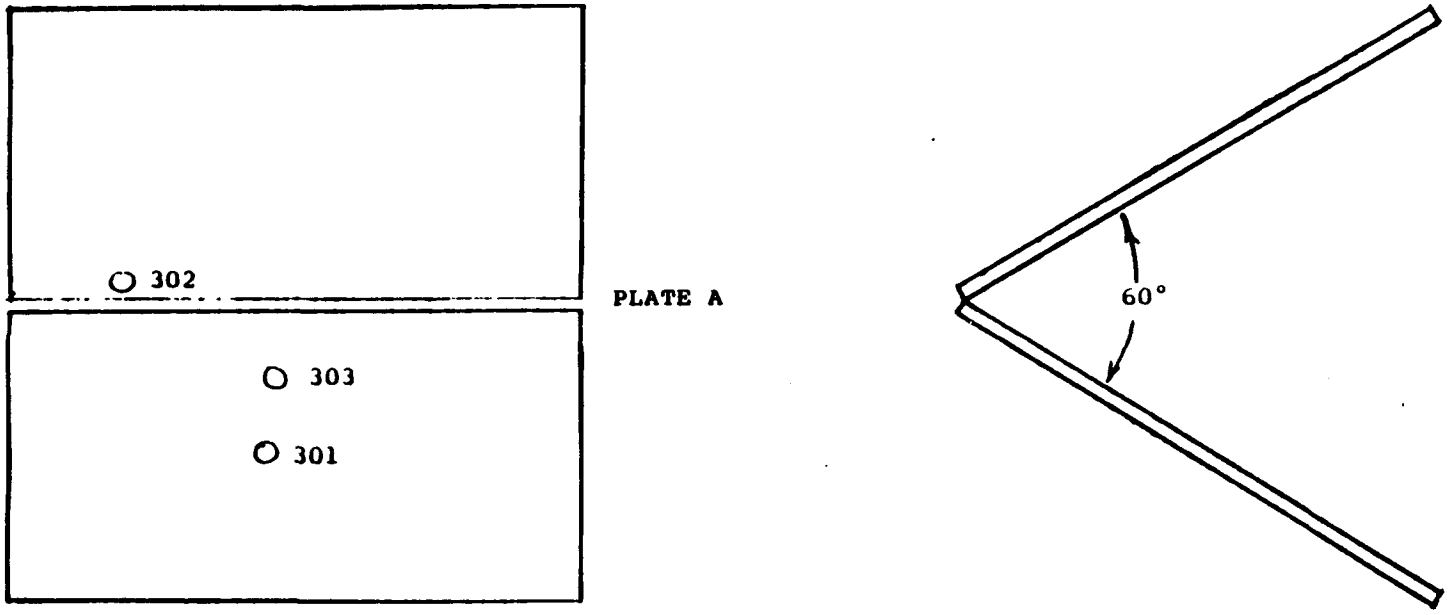

FIGURE 8. PLATE A
IMPACT POINTS FOR TYPE WHA-1071

Table V. P/N 924321-4
Type WHA-1053

SERIAL NUMBER	PENETRATOR MASS, GMS	IMPACT VELOCITY, FPS	ENTRANCE YAW, DEG.	EXIT VELOCITY, FPS	RESIDUAL MASS GMS	COMMENT
400	277.38	3847	>11	-	172.74	Exited Array At Plate O
401	277.52	4139	4.34	-	-	Exit X-Ray Did Not Trigger

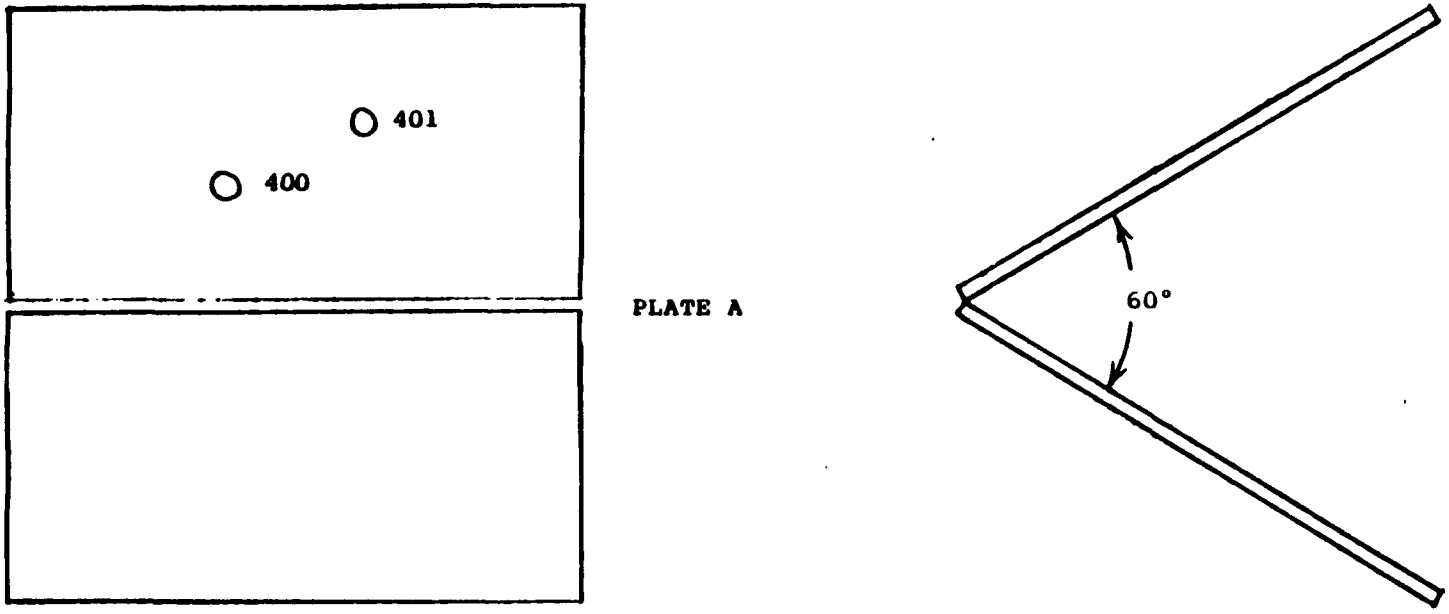

FIGURE 9. PLATE A
IMPACT POINTS FOR TYPE WHA-1053

3.5 S/N 500-501, TYPE WHA-1069

The test data from this series is summarized in Table VI for two penetrators. Round 500 was a no-test due to an entrance yaw angle of 4.01°. Round 501 had evidence of yaw at Plate O but no yaw was seen in the exit x-rays. The impact points on Plate A are shown in Figure 10.

3.6 S/N 600-601, TYPE WHA-1069

Two penetrators of this series were submitted for preliminary evaluation. Round 600 was a no-test due to a frame hit. Round 601 entered the array and penetrated the array with no noticeable yaw, see Table VII. Figure 11 shows the impact point of round 601 on Plate A.

4.0 CONCLUSION

The test data previously summarized for each round is included in Table VIII along with a velocity prediction to defeat 1-5/8 inch armor, 250 BHN. This prediction used BAL66 with the residual mass of each penetrator (recovered and estimated). As shown in the table, most of the penetrators have a good change of penetrating the 1-5/8 inch, 250 BHN plate with 40° obliquity. The P/N 924321-3 (300 series) would not be a likely candidate to defeat the armor plate due to the consistent breakage.

5.0 PLANS

The preliminary test results for this effort were not entirely acceptable considering the total number of no-tests resulting from dispersion and yaw.

These defects appear to be the result of excessive penetrator/sabot clearance and late separation of the pusher from the penetrator.

The tests have been suspended until the sabot/pusher is redesigned and evaluated for elimination of these characteristics.

The design will be included in the next progress report currently planned for 27 May 1988.

Table VI. P/N 924321-5
Type WHA-1069

SERIAL NUMBER	PENETRATOR MASS, GMS	IMPACT VELOCITY, FPS	ENTRANCE YAW, DEG.	EXIT VELOCITY*, FPS	RESIDUAL MASS GMS	COMMENT
500	269.97	4158	4.01	3398	247.05	
501	270.00	4128	1.70	3346	247.42	

* Exit Velocity Measured From X-Ray Film

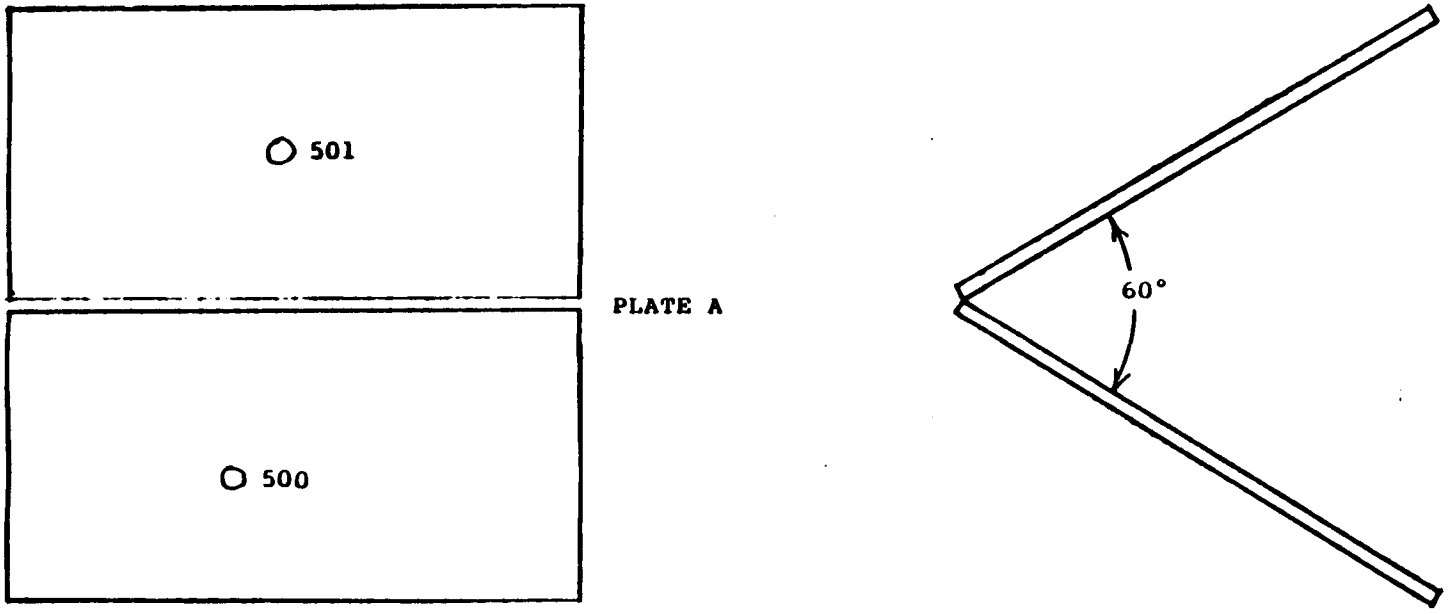

FIGURE 10. PLATE A
IMPACT POINTS FOR TYPE WHA-1069

Table VII. P/N 924321-6
Type WHA-1069

SERIAL NUMBER	PENETRATOR MASS, GMS	IMPACT VELOCITY, FPS	ENTRANCE YAW, DEG.	EXIT VELOCITY*, FPS	RESIDUAL MASS GMS	COMMENT
600	269.53	4159	-	-	215.66	Hit Frame
601	269.55	4101	1.70	3476	256.68	

* Exit Velocity Measured From X-Ray Film

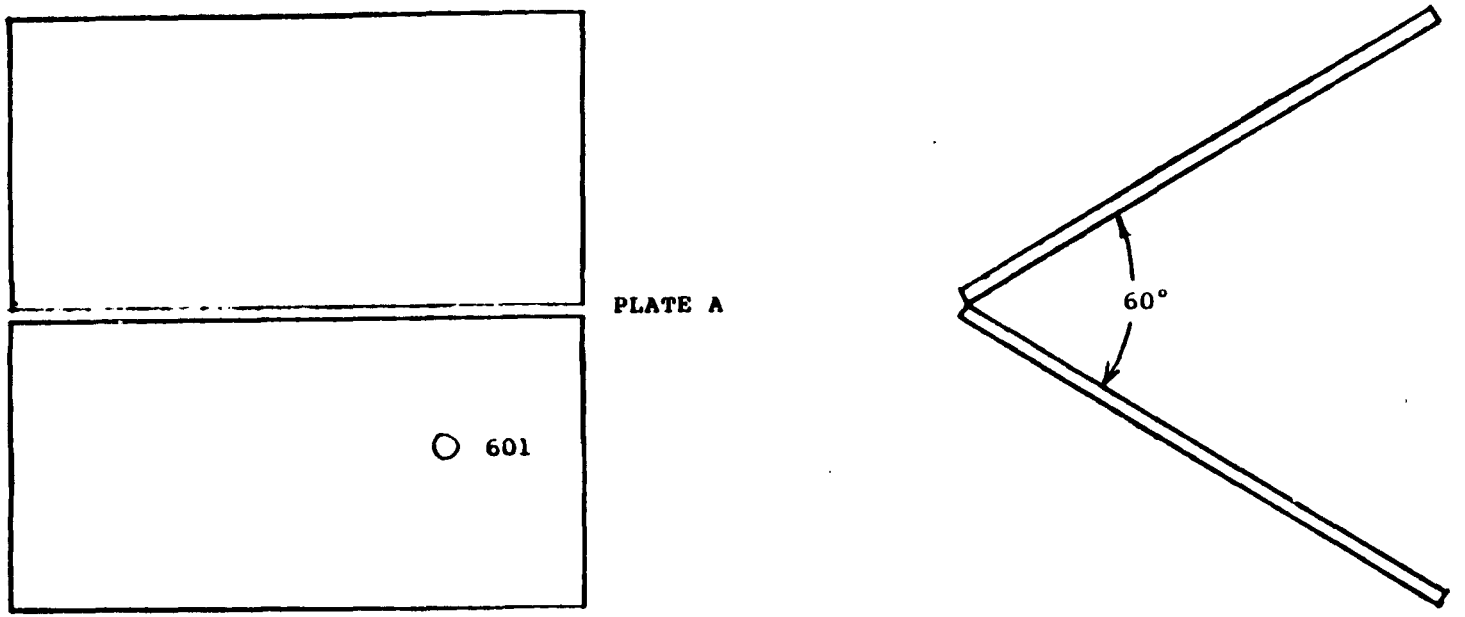

FIGURE 11. PLATE A
IMPACT POINTS FOR TYPE WHA-1069

Table VIII. Test Data Summary

SERIAL NUMBER	TYPE	MATERIAL	PENETRATOR MASS GMS	TEST/ NO TEST	ENTRANCE VELOCITY, FPS	ENTRANCE YAW, DEG	EXIT* VELOCITY, FPS (FOIL SCREENS)	EXIT VELOCITY, FPS (X-RAYS)
100	WHA-1069	WN008FU	269.92	No Test	4217	3.93	-	-
101	WHA-1069	WN008FU	270.02	Test	4182	2.56	3184	3217
102	WHA-1069	WN008FU	270.04	Test	4248	1.64	3294	3425
103	WHA-1069	WN008FU	269.70	Test	4116	1.17	2702	2188
104	WHA-1069	WN008FU	270.21	No Test	4085	10.99	-	-
105	WHA-1069	WN008FU	269.90	Test	4249	1.68	3044	3034
200	WHA-1078	WN308FU	279.43	Test	4231	2.78	3267	2917
201	WHA-1078	WN308FU	279.05	No Test	3930	>11	1051	807
202	WHA-1078	WN308FU	278.08	No Test	4108	4.32	3210	2917
203	WHA-1078	WN308FU	278.04	No Test	4081	-	-	-
204	WHA-1078	WN308FU	278.21	Test	4113	0.4	3623	3411
205	WHA-1078	WN308FU	278.13	No Test	4061	-	-	-

RESIDUAL MASS, GMS	RESIDUAL MASS, GMS (X-RAYS)	VELOCITY PREDICTION, FPS (TO DEFEAT 1-5/8" ARMOR, 250 BHN)	COMMENT
-	227.50	2853	Hit Frame
242.60	-	2789	
-	254.25	2742	
-	235.59	2817	Yawed Exiting Plate Array
241.12	-	2795	Exited Array At Plate O
-	254.45	2743	
253.05	-	2748	
-	244.03	2783	
-	267.38	2694	Yawed Exiting Plate Array
-	-	-	Hit Frame
-	263.60	2708	
-	-	-	Missed Array

300	WHA-1071	WN608FU	288.54	No Test	4166	-	-	-
301	WHA-1071	WN608FU	287.94	No Test	4260	6.32	3041	2995
302	WHA-1071	WN608FU	287.95	Test	4040	1.10	3095	3359
303	WHA-1071	WN608FU	288.52	Test	4074	1.40	3407	3255
400	WHA-1053	WN307FU	277.38	No Test	3847	>11	-	-
401	WHA-1053	WN307FU	277.52	Test	4139	4.34	3571	-
500	WHA-1069	WN008FH	269.97	No Test	4158	4.01	2985	3398
501	WHA-1069	WN008FH	270.00	Test	4128	1.70	3355	3346
600	WHA-1069	WN008FH	269.53	No Test	4159	-	-	-
601	WHA-1069	WN008FH	269.55	Test	4101	1.70	-	3476

* Reference: Information Only

-	-	-	Missed Array
65.83	-	4425	Penetrator Broke Exiting Array
163.03 62.13	-	3210 4517	Penetrator Broke Exiting Array
94.58 31.71	-	3893 5731	Penetrator Broke At Plate K
172.74	-	3146	Exited Array At Plate O
-	-	-	Exited Back Of Plywood; X-Ray Did Not Trigger
247.05	-	2771	
247.42	-	2770	
215.66	-	2907	Hit Frame
256.58	-	2734	

PRELIMINARY

REPORT NUMBER 2

FOR

GTE TUNGSTEN PENETRATOR

EVALUATION

PREPARED FOR:

GTE SYLVANIA

PURCHASE ORDER NO. 21160

BY:

KATHY GOWINS

SEPTEMBER 1988

OLIN CORPORATION - MARION OPERATIONS

RESEARCH AND DEVELOPMENT

MARION, ILLINOIS

ABSTRACT

This report describes the second and third test and evaluation of the GTE-Sylvania tungsten penetrators submitted to Olin Corporation in accordance with Sylvania Purchase Order No. 21160. Fifty penetrators were tested during these iterations, five were tested against the XW-1 plate array, the remaining 45 were against the X-1 plate array. Total rounds to date tested against the X-1 plate array is 67.

1.0 INTRODUCTION

This report describes the second and third iteration testing of GTE-Sylvania tungsten penetrators. These penetrators were submitted to Olin Corporation in accordance with the GTE-Sylvania Purchase Order No. 21160.

Olin's scope of work under this purchase order includes the following:

1. Assembly of the penetrators in Olin supplied test sabots.
2. Testing against the X-1 plate array at entrance velocities greater than 1220 meters per seconds with penetrators soft recovery.
3. Data acquisition, summary, analysis, and reporting.

The remainder of the first shipment of penetrators along with the second shipment of penetrators, received 5 May 1988, were tested during the two test iterations. The penetrators were manufactured to Olin Drawing No. 8001466, see Figure 1. Table I is a description of the penetrators along with the Olin assigned serial numbers.

TABLE I.

MATERIAL	TYPE	2/17/88 SHIPMENT QUANTITY	5/20/88 SHIPMENT QUANTITY	P/N	OLIN S/N
WN008FU	WHA-1069	3	-	92431-1	106-108
WN308FU	WHA-1078	4	2	924321-2	206-209 211-212
WN608FU	WHA-1071	2	-	924321-3	304-305
WN307FU	WHA-1053	8	7	924321-4	402-409 411-417
WN008FH	WHA-1069	8	4	924321-5	502-509 511-514
WN008FH	WHA-1069	8	4	924321-6	602-609 611-617

The material properties of each series is in Appendix A.

A total of 50 penetrators were tested, five of these were against the XW-1 plate array, the remainder were against the X-1 plate array, see Figures 2 and 3.

Material Supplied to Olin

Material	Blend	Alloy	Ni/Fe	Thermo-Mechanical Treatment
WN-008FU	WHA-1069	90W-8Ni-2Fe	8/2	As Sintered
WN-308FU	WHA-1078	93W-5.6Ni-1.4Fe	8/2	As Sintered
WN-608FU	WHA-1071	96W-3.2Ni-0.8Fe	8/2	As Sintered
WN-307FU	WHA-1053	93W-4.9Ni-2.1Fe	7/3	As Sintered
WN-008FH	WHA-1069	90W-8Ni-2Fe	8/2	Swaged 15%
WN-008FH	WHA-1069	90W-8Ni-2Fe	8/2	Swaged 15% - Aged 4hrs at 400°C

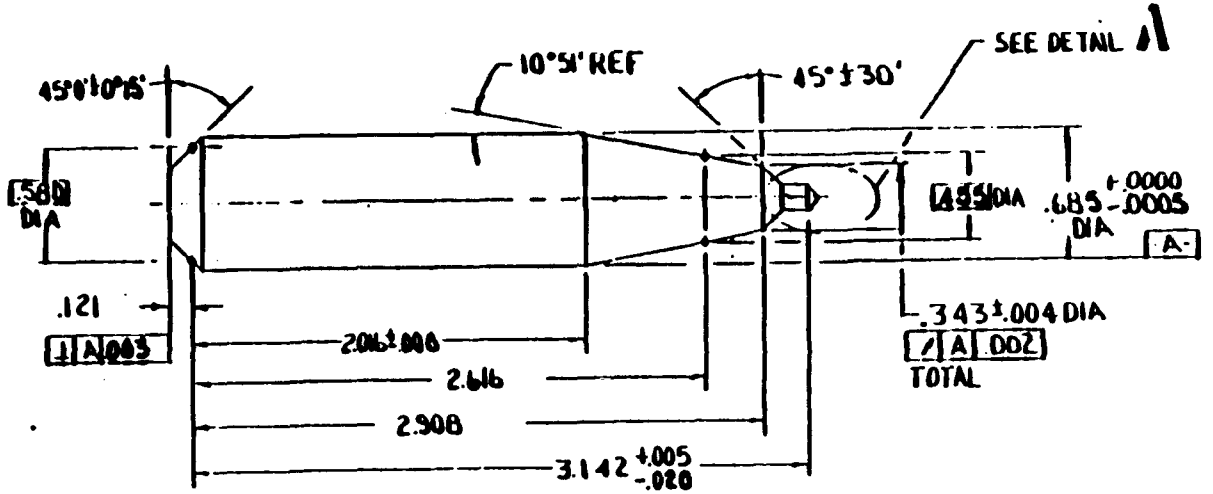

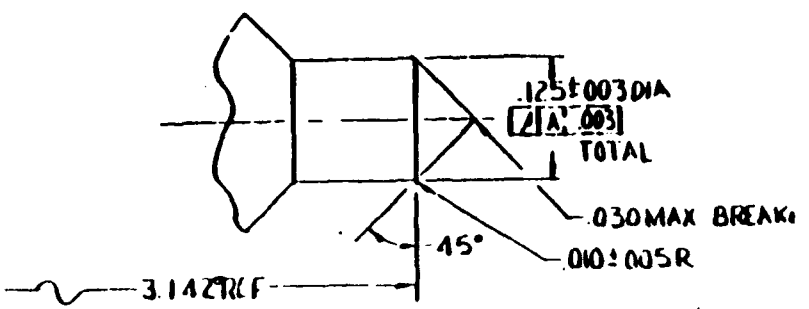

VIEW A
SCALE: 10/1

QTY REQD	NOMENCLATURE OR DESCRIPTION	IDENTIFYING NUMBER	DOCUMENT NUMBER	FSCM NUMBER	MATERIAL OR NOTE	ITEM NO
1		-1				2
						1

ASSY — PARTS LIST

UNLESS OTHERWISE SPECIFIED

CONTRACT NO

Olin ORDNANCE PRODUCTS MARION, IL 62959

PENETRATOR, 30 MM
APDS

SIZE	FSCM NO	DRAWING NO	REV
C	14578	8001466	

SCALE 1/1 WT SHEET 1 OF 1

NEXT ASSY | USED ON

DO NOT SCALE DRAWING

MATERIAL

APPROVED DATE

XW-1 PLATE ARRAY

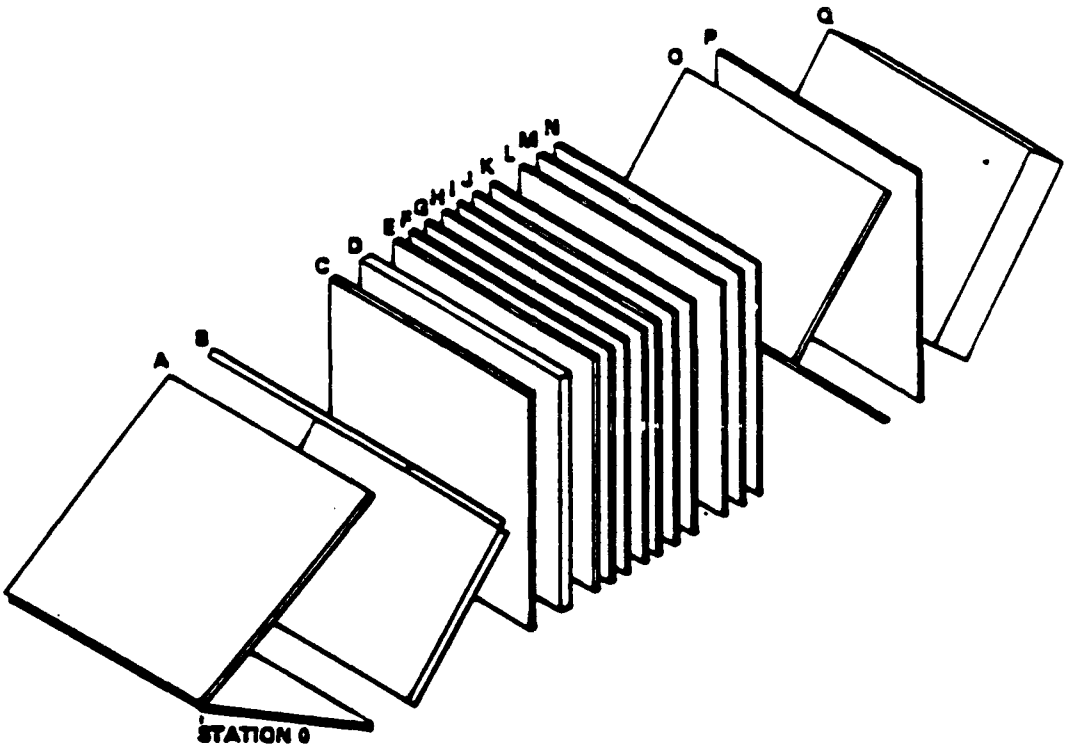

PLATE	THICKNESS in.	THICKNESS mm	STATION NUMBER in.	STATION NUMBER mm	OBLIQUITY deg	MATERIAL
A	0.300	7.620	0.000	0.000	60.000	G-10 GRP*
B	0.500	12.700	18.400	467.360	45.000	2024-T3 Al**
C	0.250	6.350	20.400	518.160	0.000	MILD STEEL
D	0.500	12.700	22.400	568.960	0.000	2024-T3 Al
E	0.250	6.350	24.400	619.760	0.000	2024-T3 Al
F	0.250	6.350	25.400	645.160	0.000	2024-T3 Al
G	0.250	6.350	26.400	670.560	0.000	2024-T3 Al
H	0.250	6.350	27.400	695.960	0.000	2024-T3 Al
I	0.250	6.350	28.400	721.360	0.000	2024-T3 Al
J	0.250	6.350	29.400	746.760	0.000	2024-T3 Al
K	0.250	6.350	30.400	772.160	0.000	2024-T3 Al
L	0.250	6.350	32.400	822.960	0.000	2024-T3 Al
M	0.250	6.350	33.400	848.360	0.000	2024-T3 Al
N	0.250	6.350	34.400	873.760	0.000	2024-T3 Al
O	0.250	6.350	35.400	924.560	45.000	MILD STEEL
P	0.250	6.350	44.400	1127.760	0.000	2024-T3 Al
Q	1.625	41.275	48.257	1251.121	45.000	250 BHN† STEEL

*GRP = GLASS-REINFORCED PLASTIC
**Al = ALUMINUM
†BHN = BRINELL HARDNESS NUMBER

FIGURE 2

X-1 PLATE ARRAY

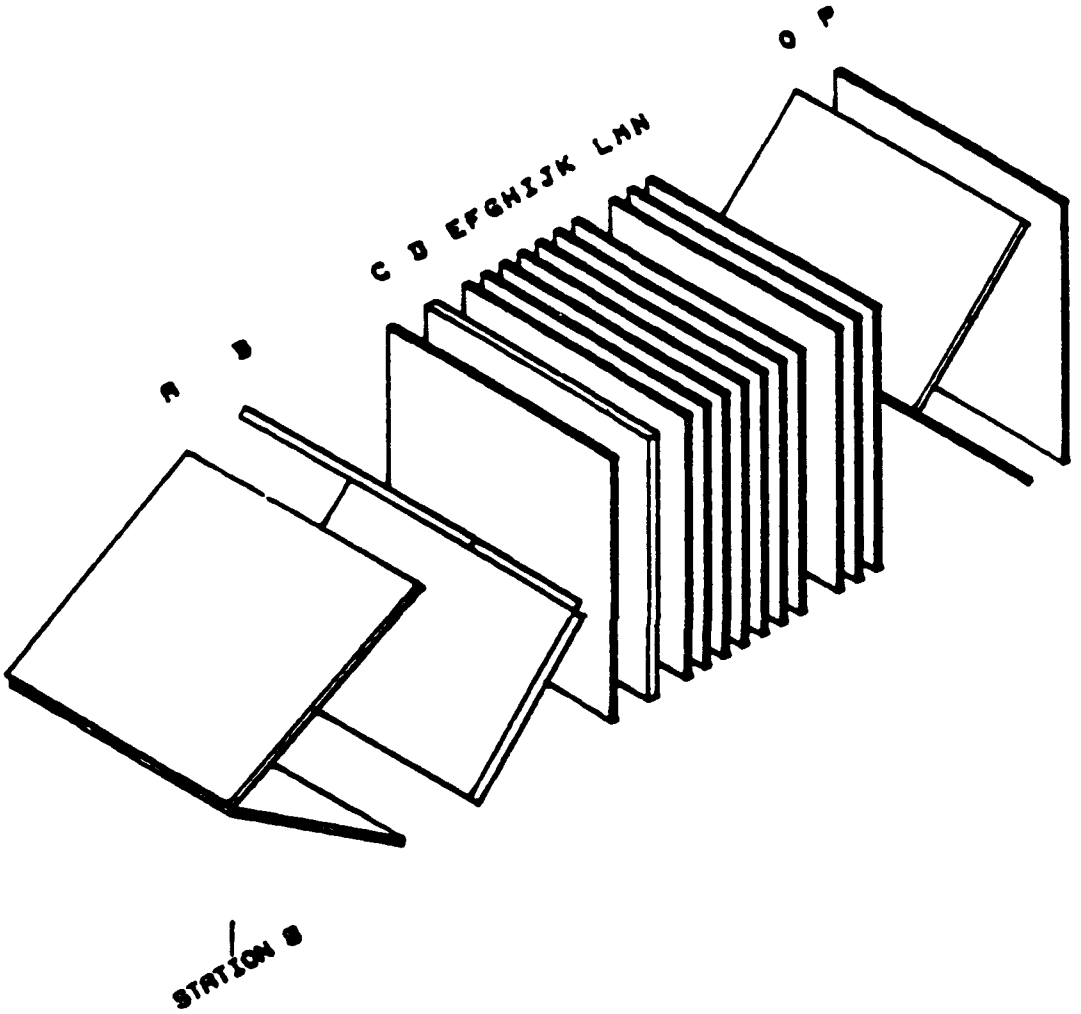

PLATE	THICKNESS IN.	THICKNESS MM	STATION NUMBER IN.	STATION NUMBER MM	OBLIQUITY DEGREES	MATERIAL
A	.300	7.620	0.000	0.000	60.000	G-10 GRP
B	.500	12.700	18.400	467.360	45.000	2024-T3 AL
C	.250	6.350	20.400	518.160	0.000	MILD STEEL
D	.500	12.700	22.400	568.960	0.000	2024-T3 AL
E	.250	6.350	24.400	619.760	0.000	2024-T3 AL
F	.250	6.350	25.400	645.160	0.000	2024-T3 AL
G	.250	6.350	26.400	670.560	0.000	2024-T3 AL
H	.250	6.350	27.400	695.960	0.000	2024-T3 AL
I	.250	6.350	28.400	721.360	0.000	2024-T3 AL
J	.250	6.350	29.400	746.760	0.000	2024-T3 AL
K	.250	6.350	30.400	772.160	0.000	2024-T3 AL
L	.250	6.350	32.400	822.960	0.000	2024-T3 AL
M	.250	6.350	33.400	848.360	0.000	2024-T3 AL
N	.250	6.350	34.400	873.760	0.000	2024-T3 AL
O	.250	6.350	36.400	924.560	45.000	MILD STEEL
P	.250	6.350	44.400	1127.760	0.000	2024-T3 AL

FIGURE 3

2.0 TEST SETUP

The test setup was unchanged from the previous tests (see Figure 4). Velocity light screens were setup at 183 ft. from the muzzle to measure entrance velocity. The array frame was placed at 197 feet from the muzzle. Plywood bundles were positioned behind the array for recovery of the penetrator upon exit of the X-1 plate array. Orthogonal flash x-ray was used at plate array entrance, for yaw measurements prior to target impact. Flash x-ray was also taken at the point between plates N and O and at the plate array exit. Foil velocity screens were also placed between the plate array and the plywood for exit velocity readings. (3° max yaw allowed)

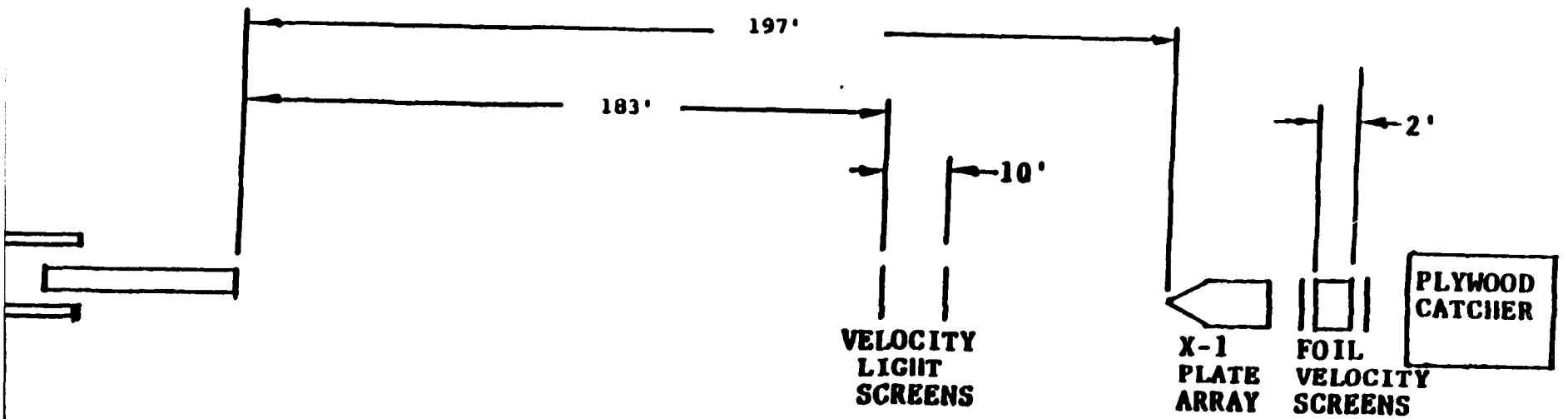

Typical Test Set-Up

FIGURE 4

3.0 PERFORMANCE

The test sabot and pusher plug for these two iterations were modified to the decrease yaw experienced in earlier tests. The sabot material was changed to Lexan, in accordance with Olin Drawing No. 8008116, Figure 5. The first iteration pusher plug was modified from the existing design with the cavity diameter enlarged and a flat bottom added, see Figure 6. The final iteration used this modification with an aluminum plug threaded into the cavity decreasing the cavity depth from .965 inch to .200 inch. The sabot overall length was measured from 1.25 inch to 2.00 inch.

To insure spin for the array tests, a coining groove was added to the base of the penetrator. The interfaces between the penetrator and sabot and sabot and pusher plug were designed as zero clearance to a light press fit.

3.1 S/N 106-108, TYPE WHA-1069

Three rounds from this group were tested during these two iterations. The first was fired at the XW-1 plate array. It defeated the target with no yaw and a residual mass of 251.5 grams.

Rounds 107 and 108 were fired against the X-1 plate array using the last sabot and pusher plug design. Round 107 had visible yaw on plates E through G but exited the X-1 plate array with no yaw. Round 108 hit the left edge of the plate array and was a no-test. Figure 7 shows the entry of these rounds, and Table II gives the data for each round.

3.2 S/N 206-209, 211-212, TYPE WHA-1078

Rounds 206 and 207 were fired against the XW-1 plate array. Round 206 hit the frame. Round 207 defeated the X-1 array but did not penetrate the armor plate. Rounds 208, 209, 211 and 212 all defeated the X-1 array with good exit velocities and residual masses. Exit data for Round 211 was not obtained due to fragments cutting the wires prior to the round's exit from the array. Figure 8 shows the entry locations on Plate A, and Table III summarizes the data of this group.

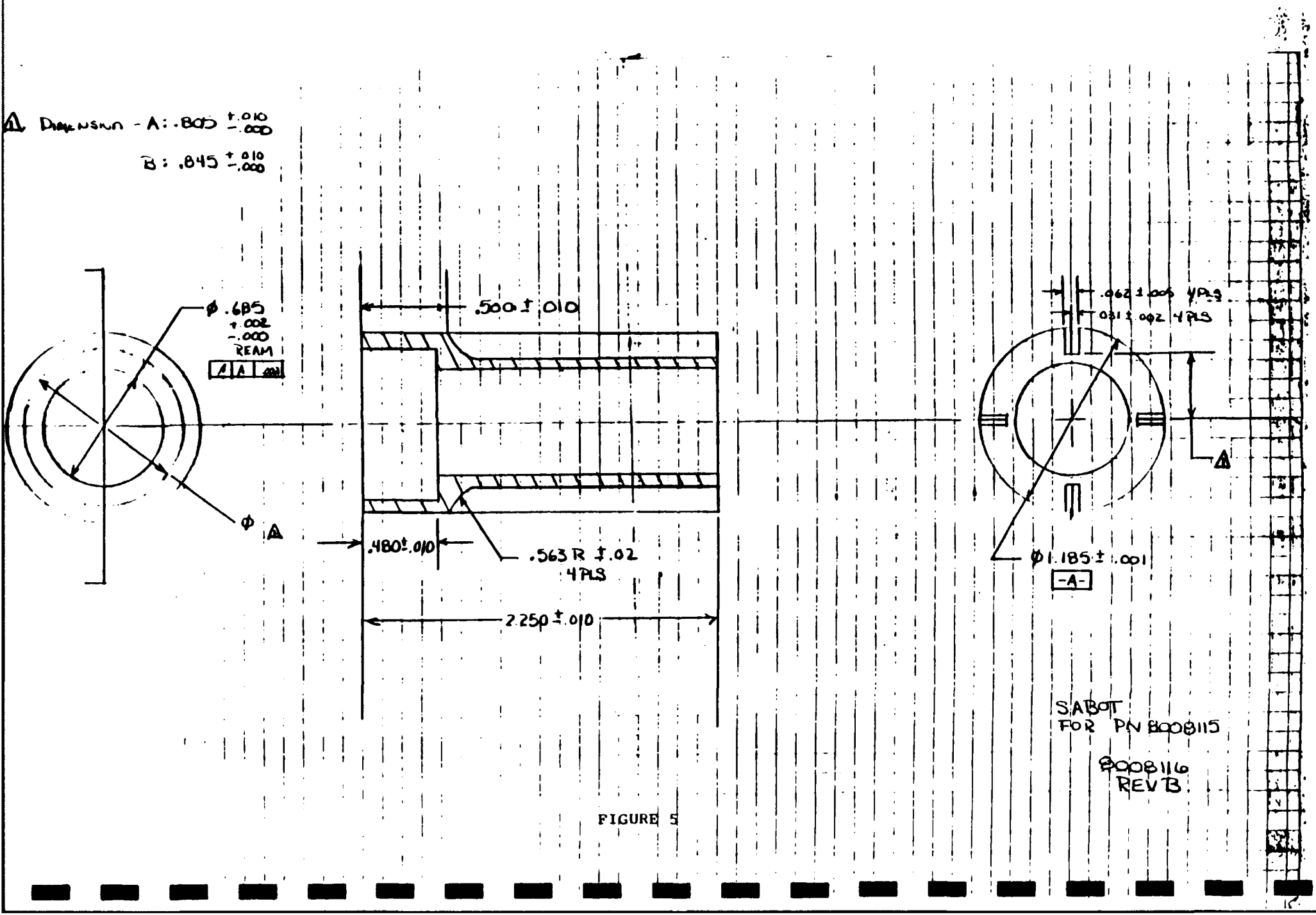
1 DIMENSION - A: .805 +.010 -.000
B: .845 +.010 -.000
ø .685 +.002 -.000 REAM
A A
ø A
.500 ± .010
.480 ± .010
.563 R ± .02 4PLS
2.250 ± .010
.062 ± .005 4PLS
.031 ± .002 4PLS
ø 1.185 ± .001
-A-
1
SABOT FOR PN B00B115
B00B116 REV B

FIGURE 5

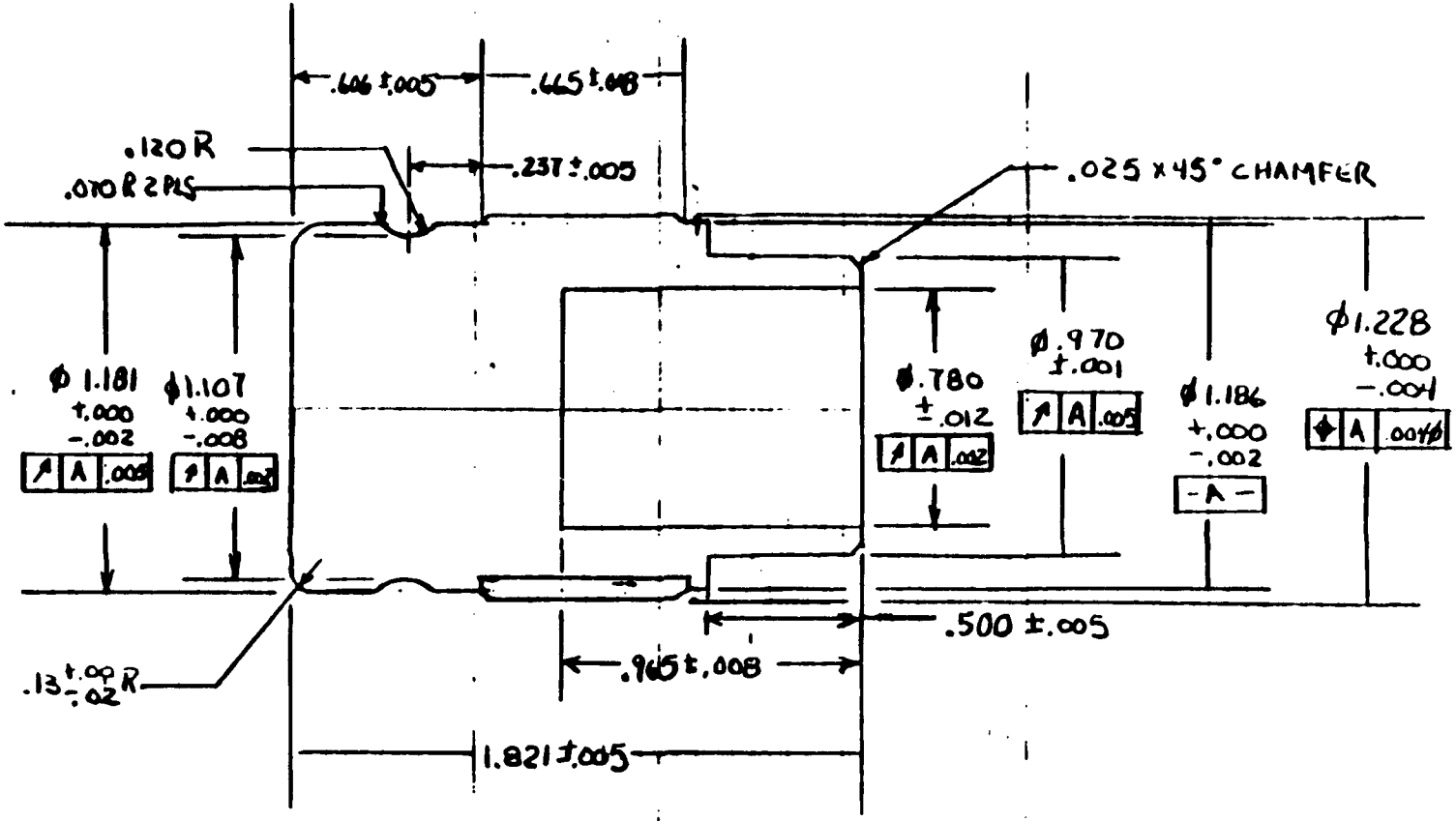

ALIN CORP
PUSHER PLUG

8008115
REV. B
7/14/88
KBG

FIGURE 6

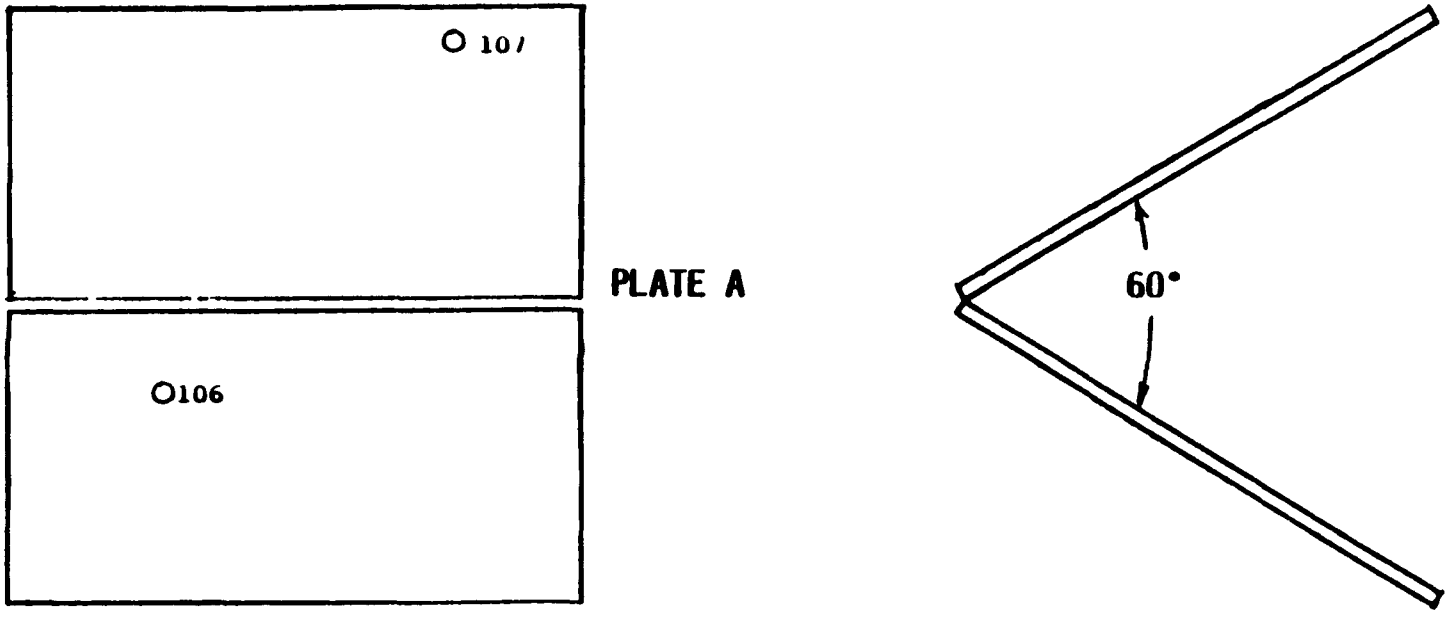

FIGURE 7

TABLE II. P/N 924321-1
TYPE WHA-1069 - MATERIAL: WN008FU

S/N	DATE FIRED	PENETRATOR MASS GMS	X-1 ARRAY ENTRANCE VELOCITY, FPS	X-1 ARRAY ENTRANCE YAW, $\leq 3^{o}$	X-1 ARRAY EXIT VELOCITY, FPS	X-1 ARRAY RESIDUAL MASS, GMS	XW-1 ARRAY VELOCITY PREDICTION, FPS	COMMENT
106*	7/28/88	269.43	4163	YES	3116	251.5	2753	Penetrated Armor
107	8/31/88	270.11	4189	YES	3866	264.8	2706	
108	8/31/88	269.55	4185	YES	-	-	-	Missed Array

* Fired Against XW-1 Plate Array

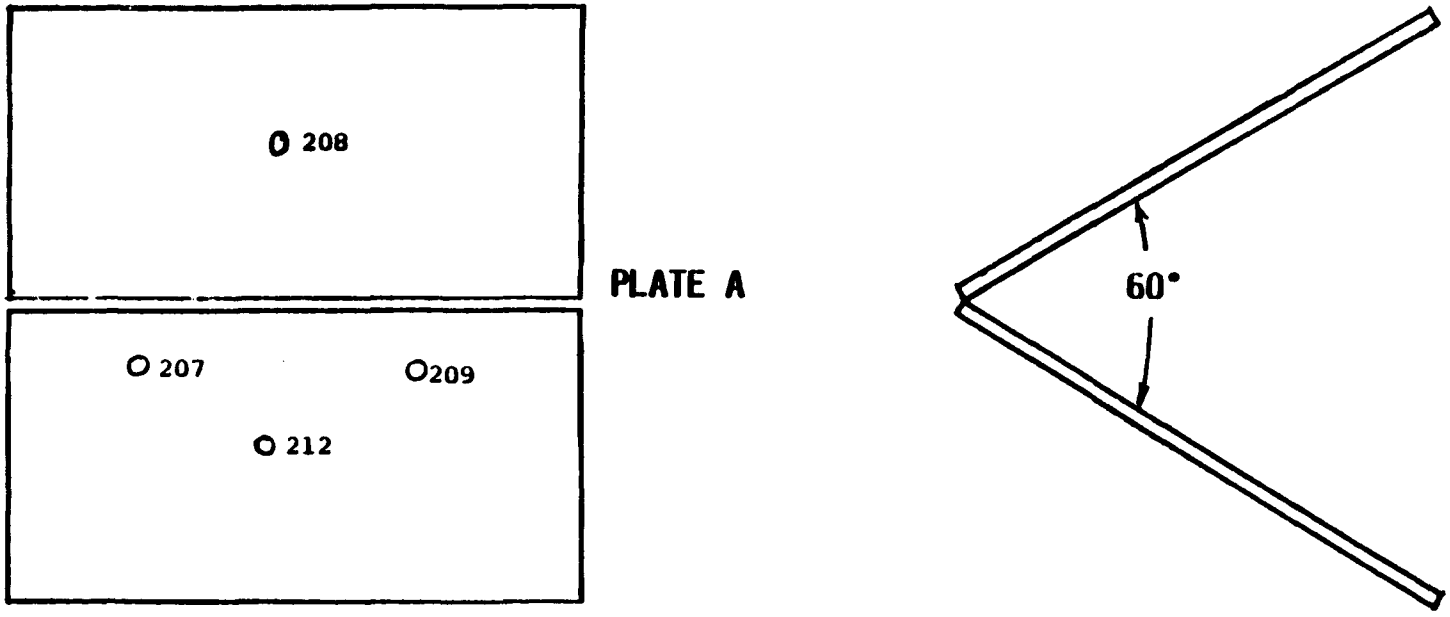

FIGURE 8

TABLE III. P/N 924321-2
TYPE WHA-1078 - MATERIAL: WN308FU

S/N	DATE FIRED	PENETRATOR MASS GMS	X-1 ARRAY ENTRANCE VELOCITY, FPS	X-1 ARRAY ENTRANCE YAW, ≤ 3°	X-1 ARRAY EXIT VELOCITY, FPS	X-1 ARRAY RESIDUAL MASS, GMS	XW-1 ARRAY VELOCITY PREDICTION, FPS	COMMENT
206*	7/28/88	277.88	4170	YES	-	-	-	Hit Frame
207*	7/28/88	278.49	4182	YES	-	140.91	3380	No Penetration
208	8/30/88	277.87	4151	YES	2921	259.1	2724	
209	8/30/88	277.92	4128	YES	3466	257.3	2731	
211	8/31/88	278.01	4144	YES	-	-	-	Wires Cut Prior To Penetrator Exit
212	8/31/88	278.00	4152	YES	3633	236	2831	

* Fired Against XW-1 Plate Array

3.3 S/N 304-305, TYPE WHA-1071

Both rounds, 304 and 305, were fired against the X-1 plate array. Round 305 broke on exit from the plate array. The exit x-rays did not trigger on Round 304. This round did not show evidence of breakup in the x-rays. The round exited the back of the plywood and entered the sand. Figure 9 shows Rounds 304 and 305 entrance locations into the plate array, and Table IV gives this group's data.

3.4 S/N 402-407, 408-409, AND 411-417, TYPE WHA-1053

Rounds 402 through 405 and 408, 409, 411 through 417 were fired against the X-1 plate array. Rounds 408 and 414 hit the target frame. Round 402 was tumbling on exit of the array, the recovered penetrator showed a lower than average residual mass. Rounds 409 and 417 also yawed on exit of array. Rounds 406 and 407 were fired against the XW-1 plate array. Neither succeeded in penetrating the armor plate. Exit data shows both rounds yawing on exit of the X-1 plate array, exit velocities are lower than average for this series. Entrance locations are plotted on Figures 10 and 11 with the data summarized in Table V.

3.5 S/N 502-509, 511-514, TYPE WHA-1069

Figure 12 shows the entrance location of the rounds of this group on Plate A of the plate array. Table VI is the data for each round. Two rounds either missed the plate array or hit the frame, these were Rounds 504 and 507. Round 512 broke the top right corner of the array plates. Six rounds displayed yaw on exit of the array resulting in low exit velocities lower than the average for this series.

3.6 S/N 602-609, 611-614, TYPE WHA-1069

Table VII summarizes the data from this group. Each round's entrance location is plotted on Figure 13. Two rounds from this series hit the target frame, 605 and 606, and Round 603 exited the plate array at Plate O. Two penetrators, 613 and 614, had breakage on exiting the plate array. Round 612 had yaw exiting the array and a low exit velocity.

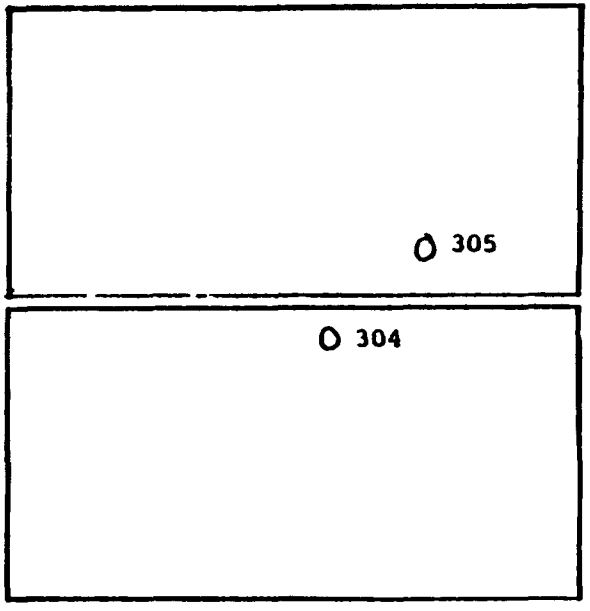

PLATE A

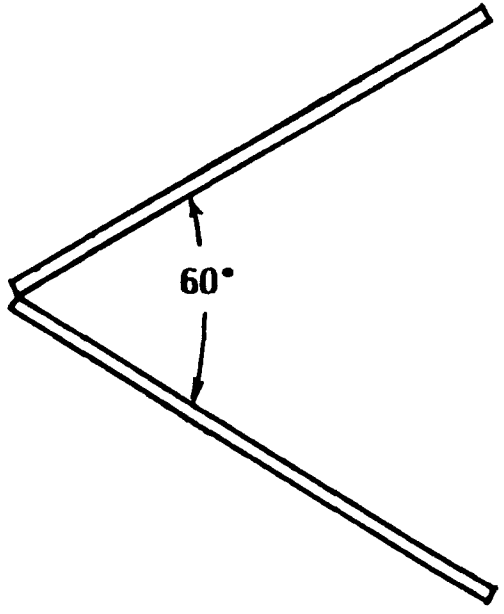

FIGURE 9

TABLE IV. P/N 924321-3
TYPE WHA-1071 - MATERIAL: WN608FU

S/N	DATE FIRED	PENETRATOR MASS GMS	X-1 ARRAY ENTRANCE VELOCITY, FPS	X-1 ARRAY ENTRANCE YAW, ± 3°	X-1 ARRAY EXIT VELOCITY, FPS	X-1 ARRAY RESIDUAL MASS, GMS	XW-1 ARRAY VELOCITY PREDICTION, FPS	COMMENT
304	7/27/88	287.52	-	YES	2812	-	-	Penetrator Entered Sand, Wires Cut
305	7/27/88	287.68	4171	YES	3121	157.7	3248	Penetrator Breakage

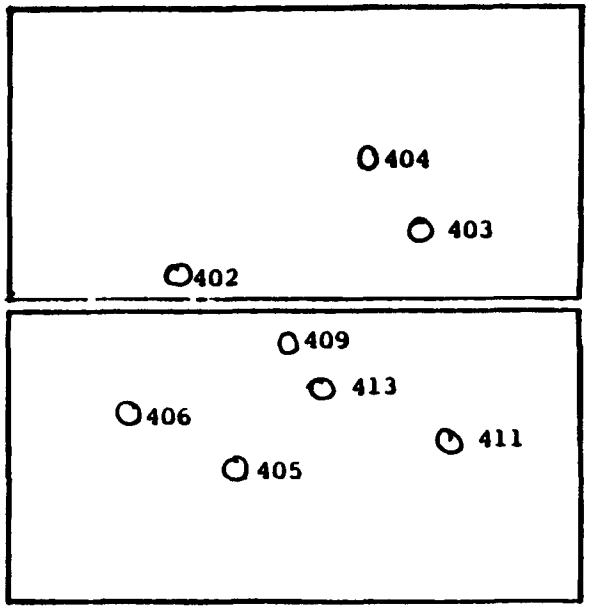

PLATE A

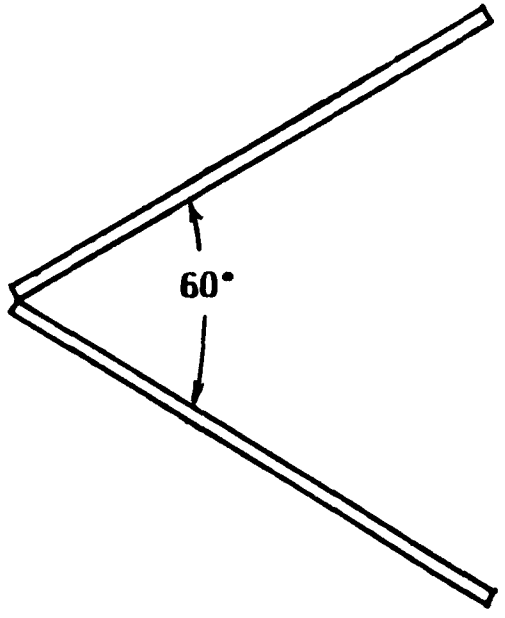

FIGURE 10

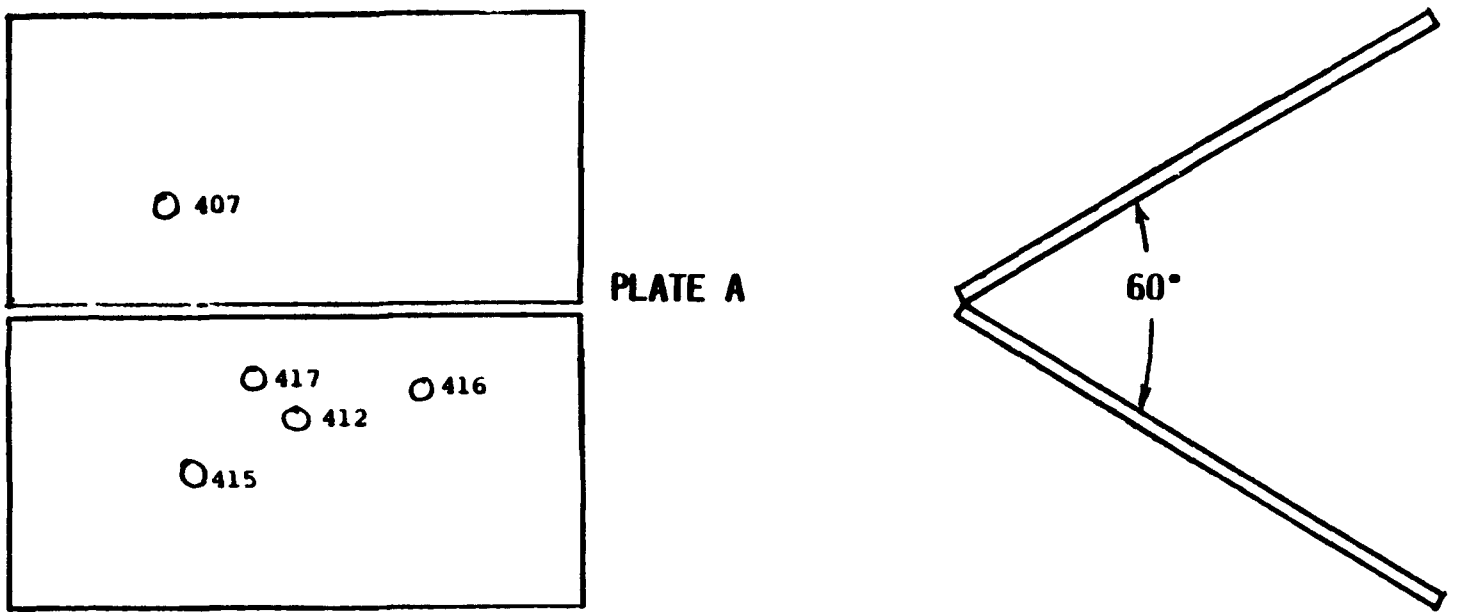

FIGURE 11

TABLE V. P/N 924321-4
TYPE WHA-1053 - MATERIAL: WN307FU

S/N	DATE FIRED	PENETRATOR MASS GMS	X-1 ARRAY ENTRANCE VELOCITY, FPS	X-1 ARRAY ENTRANCE YAW, ≤ 3°	X-1 ARRAY EXIT VELOCITY, FPS	X-1 ARRAY RESIDUAL MASS, GMS	XW-1 ARRAY VELOCITY PREDICTION, FPS	COMMENT
402	7/27/88	277.09	4178	YES	2758	140.37	3390	Yawed Exiting Array
403	7/27/88	277.12	4132	YES	3108	234.06	2824	
404	7/27/88	276.93	4120	YES	3551	261.80	2714	
405	7/17/88	277.20	4139	YES	3405	251.46	2753	
406*	7/28/88	277.00	4149	YES	2292	245.92	2775	No Penetration Final Residual Mass: 223.56 gms
407*	7/28/88	277.13	4175	YES	2252	228.8	2847	No Penetration
408	8/29/88	277.24	4066	YES	2607	101.3/118.4	-	Hit Frame
409	8/29/88	276.96	4048	YES	1976	276.31	2663	Yaw Exiting Array
411	8/29/88	277.18	4084	YES	2477	232.7	2830	
412	8/29/88	277.27	4115	YES	3277	208.8	3041	
413	8/29/88	277.23	4108	YES	3544	228.1	2850	
414	8/29/88	277.25	4115	YES	-	-	-	Hit Frame
415	8/29/88	277.16	4096	YES	-	-	-	Exit Wires Cut
416	8/29/88	277.00	4130	YES	2946	255.4	2738	
417	8/29/88	277.67	4084	NO	2192	232.9	2784	Yawed Exiting Array

* Fired Against XW-1 Plate Array

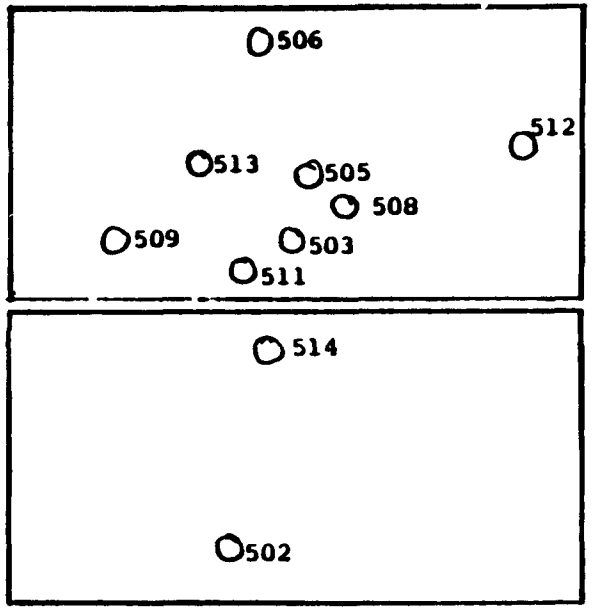

PLATE A

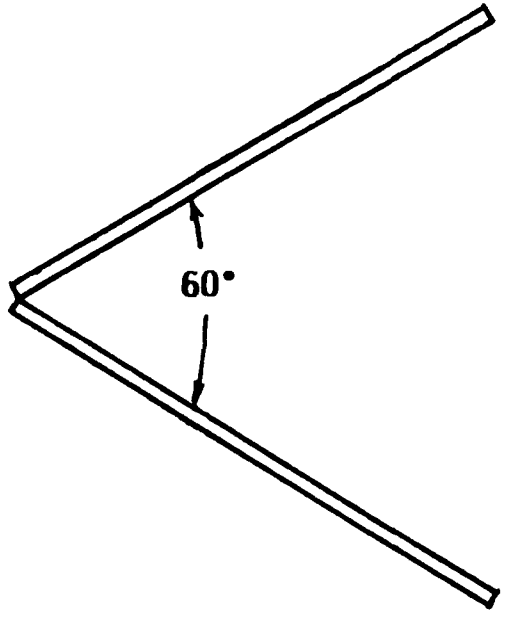

FIGURE 12

TABLE VI. P/N 924321-5
TYPE WHA-1069 - MATERIAL: WN008FH

S/N	DATE FIRED	PENETRATOR MASS GMS	X-1 ARRAY ENTRANCE VELOCITY, FPS	X-1 ARRAY ENTRANCE YAW, ≤ 3°	X-1 ARRAY EXIT VELOCITY, FPS	X-1 ARRAY RESIDUAL MASS, GMS	XW-1 ARRAY VELOCITY PREDICTION, FPS	COMMENT
502	7/27/88	269.58	4184	YES	2300	229.2	2845	
503	7/27/88	269.81	4142	NO	1335	241.6	2792	Excessive Entrance Yaw
504	7/27/88	270.11	4177	YES	-	-	-	Hit Frame
505	7/27/88	269.17	4151	NO	2200	252.9	2748	
506	8/30/88	270.09	4118	YES	2697	251.6	2702	
507	8/30/88	269.85	4135	YES	-	-	-	Missed Array
508	8/30/88	269.56	4100	YES	2344	210.65	2931	
509	8/30/88	269.43	4132	YES	2972	217.47	2844	
511	8/30/88	269.43	4144	YES	2457	-	-	
512	8/30/88	269.82	4135	YES	4087	258.69	2726	
513	8/30/88	269.76	4191	YES	3076	247.79	2768	
514	8/30/88	269.37	4156	YES	2506	246.75	2772	

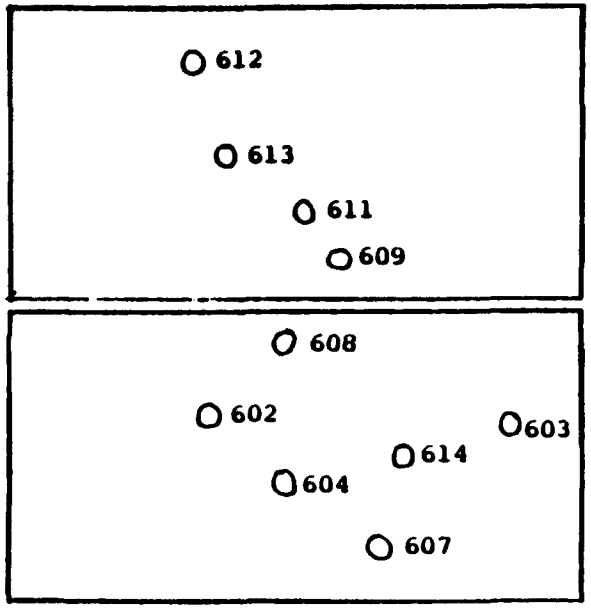

PLATE A

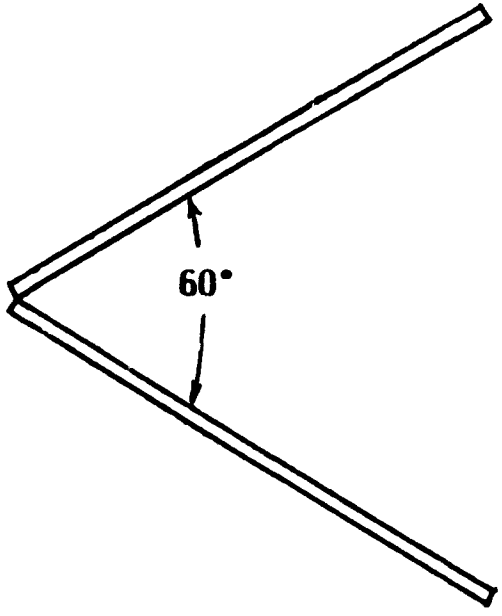

FIGURE 13

TABLE VII. P/N 924321-6
TYPE WHA-1069 - MATERIAL: WN008FH

S/N	DATE FIRED	PENETRATOR MASS GMS	X-1 ARRAY ENTRANCE VELOCITY, FPS	X-1 ARRAY ENTRANCE YAW, ≤ 3°	X-1 ARRAY EXIT VELOCITY, FPS	X-1 ARRAY RESIDUAL MASS, GMS	XW-1 ARRAY VELOCITY PREDICTION, FPS	COMMENT
602	7/27/88	269.52	4161	YES	3437	184.6	3071	
603	7/27/88	268.93	-	YES	-	123.84	-	Exited Array At Plate O
604	7/27/88	269.80	4177	YES	3035	188.5	3049	
605	7/27/88	269.27	4154	YES	-	172.87	-	Hit Frame
606	8/31/88	269.64	4171	YES	-	259.45	-	Hit Frame
607	8/31/88	269.39	4171	YES	3236	246.87	2771	
608	8/31/88	269.55	4196	YES	3786	221.9	2878	
609	8/31/88	269.40	4196	YES	2661	235.7	2764	
611	8/31/88	287.16	4142	YES	3477	257.6	2730	
612	8/31/88	269.30	4171	NO	2038	246.3	2722	Excessive Entrance Yaw
613	8/31/88	269.75	4199	YES	3361	116.32/58.32	3617/4618	Penetrator Broke
614	8/31/88	269.49	4170	YES	2559	121.69	3560	Penetrator Broke

4.0 CONCLUSIONS

Data for each group has been summarized and is found in Table VIII. The first group, the 924321-1 series, shows good entrance and exit velocities, low entry angles and residual masses average 92% of the original. These penetrators do not show induced yaw or position shifts through the plate array. The second group also has good entrance and exit velocities, a slightly higher entry angle average and residual masses average 80% of the original. A small amount of yaw is evident in the array but does not increase throughout the plate array. As stated in the previous report, the third series, 924321-3, shows consistent breakage of penetrators. One out of two shots during these tests broke on exit from the plate array. The 924321-4 series, the fourth group, shows a drop in exit velocities, 72% of the entrance velocity and shows a higher entry angle average. Residual mass averages 84% of the original mass and induced yaw in Plates N through P is quite evident. The fifth group, series 924321-5, also shows a drop in exit velocities although they are slightly above the predicted values required to defeat the XW-1 plate array. The residual mass average is high, approximately 88% of original mass. The entry angle average is right below 3°. Some rounds show induced yaw and position shifts through the plate array. Others are consistent and steady. The last group, series 924321-6, has good exit velocities and good residual masses. There is less induced yaw seen through the plate array than in the 924321-5 series, most have little or no induced yaw with position held steady throughout the plate array. The last two penetrators from this series broke into two pieces on exiting the plate array. Round 611 had a higher original mass than the rest of this series. This mass is closer to that seen in the 924321-3 series. As it was labelled as 924321-6, it remained in that group. Table IX summarizes the data from each round shot during these tests.

TABLE VIII.

S/N	AVERAGE PENETRATOR MASS, GMS	AVERAGE ENTRANCE VELOCITY, FPS	AVERAGAE ENTRANCE YAW, DEGREES	AVERAGE EXIT VELOCITY, FPS	AVERAGE RESIDUAL MASS, GMS
106-108	269.86	4179	1.8	3491	247
206-212	278.02	4154	2.3	3340	223
304-305	287.6	4171	3.0	2966	157
402-417	277.16	4115	2.9	2903	233
502-514	269.66	4147	3.0	2804	239
602-614	270.9	4173	2.1	3194	210

TABLE IX

S/N	DATE FIRED	TYPE	MATERIAL	MATERIAL PROPERTIES	PENETRATOR MASS, GMS	X-1 ARRAY ENTRANCE VELOCITY, FPS	X-1 ARRAY ENTRANCE YAW ≤ 3°	X-1 ARRAY TEST/ NO TEST	X-1 ARRAY EXIT VELOCITY, FPS	X-1 ARRAY RESIDUAL MASS, GMS	COMMENT X-1 ARRAY	XW-1 ARRAY VELOCITY PREDICTION, FPS	XW-1 ARRAY RESIDUAL, MASS, GMS	COMMENT XW-1 ARRAY
06	7/28/88	WHA-1069	WN008FU	UTS = 139 KSI YS = 83 KSI EL = 38% ρ = 17.17 g/cc Impact = 92 ft/lb Hardness = 29.5 Rc	269.92	4163	YES	TEST	3116	251.5		2753	-	Penetrated
07	8/31/88	WHA-1069	WN008FU		270.11	4189	YES	TEST	3866	264.8		2706		
08	8/31/88	WHA-1069	WN008FU		269.55	4185	YES	NO TEST	-	-	Missed Array	-		
06	7/26/88	WHA-1078	WN308FU	UTS = 132 KSI YS = 86 KSI EL = 37% ρ = 17.7 g/cc Impact = 57 ft/lb Hardness = 30 Rc	277.88	4170	YES	NO TEST	-	-	Hit Frame	-	-	No Penetration
07	7/26/88	WHA-1078	WN308FU		278.69	4182	YES	TEST	-	160.9		3380	-	No Penetration
08	8/30/88	WHA-1078	WN308FU		277.87	4151	YES	TEST	2921	259.1		2724		
09	8/30/88	WHA-1078	WN308FU		277.92	4128	YES	TEST	3466	257.3		2731		
11	8/31/88	WHA-1078	WN308FU		278.81	4144	YES	TEST	-	-	Wires Cut Prior To Penetrator Exit	-		
12	8/31/88	WHA-1078	WN308FU		278.00	4152	YES	TEST	3633	236.1		2831		
04	7/27/88	WHA-1071	WN608FU	UTS = 140 KSI YS = 89 KSI EL = 26% ρ = 18.37 g/cc Impact = 10 ft/lb Hardness = 31.1 Rc	287.52	-	YES	TEST	2812	-	Wires Cut Before Trigger, Penetrator Entered Sand	-		
05	7/27/88	WHA-1071	WN608FU		287.68	4171	YES	TEST	3121	157.7	Breakage of Penetrator	3248		
02	7/27/88	WHA-1053	WN307FU	UTS = 139 KSI YS = 90 KSI EL = 32% ρ = 17.71 g/cc Impact = 18 ft/lb Hardness = 29.6 Rc	277.09	4178	NO	NO TEST	2758	160.6	Yawed Exiting Array	3390		
03	7/27/88	WHA-1053	WN307FU		277.12	4132	YES	TEST	3108	234.1		2824		
04	7/27/88	WHA-1053	WN307FU		276.93	4120	YES	TEST	3551	261.8		2714		
05	7/27/88	WHA-1053	WN307FU		277.20	4139	YES	TEST	3405	251.6		2753		
06	7/28/88	WHA-1053	WN307FU		277.08	4149	YES	TEST	2292	245.9		2775	223.5	No Penetration
07	7/28/88	WHA-1053	WN307FU		277.13	4173	YES	TEST	2252	228.8		2847		No Penetration
08	8/29/88	WHA-1053	WN307FU		277.24	4066	YES	NO TEST	2607	101.3/118.0	Hit Frame	-		
09	8/29/88	WHA-1053	WN307FU		276.96	4048	YES	TEST	1976	27 .3	Yawed Exiting Array	2663		
11	8/29/88	WHA-1053	WN307FU		277.18	4080	YES	TEST	2677	232.7		2830		
12	8/29/88	WHA-1053	WN307FU		277.27	4115	YES	TEST	3277	208.8		3041		
13	8/29/88	WHA-1053	WN307FU		277.23	4108	YES	TEST	3504	228.1		2850		
14	8/29/88	WHA-1053	WN307FU		277.23	4115	YES	NO TEST	-	-	Hit Frame	-		
15	8/29/88	WHA-1053	WN307FU		277.16	4096	YES	TEST	-	-	Exit Data Wires Cut	-		
16	8/29/88	WHA-1053	WN307FU		277.00	4130	YES	TEST	2906	255.0		2738		
17	8/29/88	WHA-1053	WN307FU		277.67	4084	YES	TEST	2192	232.9	Yawed Exiting Array	2784		

TABLE IX

DATE FIRED	TYPE	MATERIAL	MATERIAL PROPERTIES	PENETRATOR MASS, GMS	X-I ARRAY ENTRANCE VELOCITY, FPS	X-I ARRAY ENTRANCE YAW ≤ 3°	X-I ARRAY TEST/ NO TEST	X-I ARRAY EXIT VELOCITY, FPS	X-I ARRAY RESIDUAL MASS, GMS	X-I ARRAY COMMENT X-I ARRAY	XW-I ARRAY VELOCITY PREDICTION, FPS	XW-I ARRAY RESIDUAL, MASS, GMS	XW-I ARRAY COMMENT XW-I ARRAY
7/27/88	WHA-1069	WN008FH	UTS = 159 KSI YS = 140 KSI EL = 20% ρ = 17.17 g/cc Impact = 26 ft/lb Hardness = 37.7 Rc	269.58	6184	YES	TEST	2300	229.2		2845		
7/27/88	WHA-1069	WN008FH		269.81	6142	NO	NO TEST	1333	241.6		2792		
7/27/88	WHA-1069	WN008FH		270.11	6177	YES	NO TEST	-	-	Hit Frame	-		
7/27/88	WHA-1069	WN008FH		269.17	6151	NO	NO TEST	2200	252.9		2702		
8/30/88	WHA-1069	WN008FH		270.09	6118	YES	TEST	2697	251.6		2768		
8/30/88	WHA-1069	WN008FH		269.85	6135	YES	NO TEST	-	-	Missed Array	-		
8/30/88	WHA-1069	WN008FH		269.56	6100	YES	TEST	2340	210.6		2931		
8/30.88	WHA-1069	WN008FH		269.63	6132	YES	TEST	2972	217.07		2849		
8/30/88	WHA-1069	WN008FH		269.63	6100	YES	TEST	2957	-		-		
8/30/88	WHA-1069	WN008FH		269.82	6135	YES	TEST	2952	258.69		2726		
8/30/88	WHA-1069	WN008FH		269.76	6191	YES	TEST	3076	267.79		2768		
8/30/88	WHA-1069	WN008FH		269.37	6156	YES	TEST	2506	246.75		2772		
7/27/88	WHA-1069	WN008FH	UTS = 166 KSI YS = 151 KSI EL = 22% ρ = 17.17 g/cc Impact = 29 ft/lb Hardness = 39.0 Rc	269.52	6161	YES	TEST	3037	184.6		3071		
7/27/88	WHA-1069	WN008FH		268.93	-	YES	NO TEST	-	123.8	Exited Array at Plate O	-		
7/27/88	WHA-1069	WN008FH		269.80	6177	YES	TEST	3033	188.5		3049		
7/27/88	WHA-1069	WN008FH		269.27	6134	YES	NO TEST	-	172.87	Hit Frame	-		
8/31/88	WHA-1069	WN008FH		269.64	6171	YES	NO TEST	-	259.05	Hit Frame	-		
8/31/88	WHA-1069	WN008FH		269.39	6171	YES	TEST	3236	246.87		2771		
8/31/88	WHA-1069	WN008FH		269.55	6196	YES	TEST	3786	221.9		2878		
8/31/88	WHA-1069	WN008FH		269.60	6196	YES	TEST	2661	235.7		2764		
8/31/88	WHA-1069	WN008FH		287.16	6162	YES	TEST	3677	257.6		2730		
8/31/88	WHA-1069	WN008FH		269.30	6171	NO	NO TEST	2038	246.3	Yawed Exiting Array	2722		
8/31/88	WHA-1069	WN008FH		269.75	6199	YES	TEST	3361	116.3/58.3	Penetrator Broke Exiting Array	3617/4618		
8/31/88	WHA-1069	WN008FH		269.69	6170	YES	TEST	2559	121.69	Penetrator Broke Exiting Array	3560		

5.0 PLANS

New pusher plugs per Olin Drawing No. 8008115 Revision C, have been ordered. These will be banded using PES (polyether sulfone), 20% glass filled. These will be used with the sabots per Olin Drawing No. 8008116 Revision C. The pusher plugs are scheduled for completion by 15 October 1988. A test with tungsten blanks will be fired to verify accuracy and separation prior to the next iteration of GTE-Sylvania penetrator tests.

APPENDIX A

GTE PRODUCTS CORPORATION
TOWANDA, PA 18848

ENGINEERING SAMPLE

TEST NUMBER: 924321-1/37
CUSTOMER: Olin Corp.
ATTN: Frank Bone
Central Receiving
RTE 148 South
Marion, IL 62959

DATE: February 12, 1988
DEPARTMENT: 285
CHARGE: NO CHARGE: X
CUST ORDER NO:
SALES ORDER NUMBER:
SHIPPING METHOD: UPS-2 day

MATERIAL	TYPE	AMOUNT
WN008FU	WHA-1069	9 pcs.

PROGRAM NUMBER: DAAL04-85-C-0023

TEST DESCRIPTION: P/N 924321-1, Print No. 8001466, WN008FU
30 mm Phalanx Penetrators - Unworked.
NOTE: Some pieces have a flat at the front.

PROCESS COMMENTS:

DATA:

UTS (ksi)	139
YS (ksi)	85
EL (%)	38
Density (g/cc)	17.17
Impact (ft/lbs)	42
Hardness (R/C)	29.5

cc: E. L. Bok
D. P. Buttleman
D. R. Grover
F. B. Nair.
J. R. Spencer
V. P. Sylvester
S. R. Weigel - L.A

WRITTEN BY:

J. A. Mullendore

lw/1477.1-6

GTE PRODUCTS CORPORATION
TOWANDA, PA 18848

ENGINEERING SAMPLE

TEST NUMBER: 924321-2/38
CUSTOMER: Olin Corp.
ATTN: Frank Bone
Central Receiving
RTE 148 South
Marion, IL 62959

DATE: February 12, 1988
DEPARTMENT: 285
CHARGE: NO CHARGE: X
CUST ORDER NO:
SALES ORDER NUMBER:
SHIPPING METHOD: UPS-2 day

MATERIAL	TYPE	AMOUNT
WN308FU	WHA-1078	10 pcs.

PROGRAM NUMBER: DAAL04-85-C-0023

TEST DESCRIPTION: P/N 924321-2, Print No. 8001466, WN308FU
30 mm Phalanx Penetrators - Unworked.
NOTE: Some pieces have a flat at the front.

PROCESS COMMENTS:

DATA:

UTS (ksi)	132
YS (ksi)	84
EL (%)	37
Density (g/cc)	17.70
Impact (ft/lbs)	37
Hardness (R/C)	30

cc: E. L. Bok
D. P. Buttleman
D. R. Grover
F. B. Nair.
J. R. Spencer
V. P. Sylvester
S. R. Weigel - L.A

WRITTEN BY:

J. A. Mullendore

lw/1477.2-6

GTE PRODUCTS CORPORATION
TOWANDA, PA 18848

ENGINEERING SAMPLE

TEST NUMBER: 924321-3/39
CUSTOMER: Olin Corp.
ATTN: Frank Bone
Central Receiving
RTE 148 South
Marion, IL 62959

DATE: February 12, 1988
DEPARTMENT: 285
CHARGE: NO CHARGE: X
CUST ORDER NO:
SALES ORDER NUMBER:
SHIPPING METHOD: UPS-2 day

MATERIAL	TYPE	AMOUNT
WN608FU	WHA-1071	9 pcs.

PROGRAM NUMBER: DAAL04-85-C-0023

TEST DESCRIPTION: P/N 924321-3, Print No. 8001466, WN608FU
30 mm Phalanx Penetrators - Unworked.
NOTE: Some pieces have a flat at the front.

PROCESS COMMENTS:

DATA:

UTS (ksi)	140
YS (ksi)	89
EL (%)	26
Density (g/cc)	18.37
Impact (ft/lbs)	10
Hardness (R/C)	31.1

cc: E. L. Bok
D. P. Buttleman
D. R. Grover
F. B. Nair.
J. R. Spencer
V. P. Sylvester
S. R. Weigel - L.A

WRITTEN BY:

J. A. Mullendore

lw/1477.3-6

GTE PRODUCTS CORPORATION
TOWANDA, PA 18848

ENGINEERING SAMPLE

TEST NUMBER: 924321-4/40
CUSTOMER: Olin Corp.
ATTN: Frank Bone
Central Receiving
RTE 148 South
Marion, IL 62959

DATE: February 12, 1988
DEPARTMENT: 285
CHARGE: NO CHARGE: X
CUST ORDER NO:
SALES ORDER NUMBER:
SHIPPING METHOD: UPS-2 day

MATERIAL	TYPE	AMOUNT
WN307FU	WHA-1053	10 pcs.

PROGRAM NUMBER: DAAL04-85-C-0023

TEST DESCRIPTION: P/N 924321-4, Print No. 8001466, WN307FU
30 mm Phalanx Penetrators - Unworked.

PROCESS COMMENTS:

DATA:

UTS (ksi)	139
YS (ksi)	90
EL (%)	32
Density (g/cc)	17.71
Impact (ft/lbs)	18
Hardness (R/C)	29.6

cc: E. L. Bok
D. P. Buttleman
D. R. Grover
F. B. Nair.
J. R. Spencer
V. P. Sylvester
S. R. Weigel - L.A

WRITTEN BY:

J. A. Mullendore

lw/1477.4-6

GTE PRODUCTS CORPORATION
TOWANDA, PA 18848

ENGINEERING SAMPLE

TEST NUMBER: 924321-5/41
CUSTOMER: Olin Corp.
ATTN: Frank Bone
Central Receiving
RTE 148 South
Marion, IL 62959

DATE: February 12, 1988
DEPARTMENT: 285
CHARGE: NO CHARGE: X
CUST ORDER NO:
SALES ORDER NUMBER:
SHIPPING METHOD: UPS-2 day

MATERIAL	TYPE	AMOUNT
WN008FH	WHA-1069	10 pcs.

PROGRAM NUMBER: DAAL04-85-C-0023

TEST DESCRIPTION: P/N 924321-5, Print No. 8001466, WN008FH
30 mm Phalanx Penetrators - worked.

PROCESS COMMENTS:

DATA:

UTS (ksi)	159
YS (ksi)	144
EL (%)	20
Density (g/cc)	17.17
Impact (ft/lbs)	26
Hardness (R/C)	37.7

cc: E. L. Bok
D. P. Buttleman
D. R. Grover
F. B. Nair.
J. R. Spencer
V. P. Sylvester
S. R. Weigel - L.A

WRITTEN BY:

J. A. Mullendore

lw/1477.5-6

GTE PRODUCTS CORPORATION
TOWANDA, PA 18848

ENGINEERING SAMPLE

TEST NUMBER: 924321-6/42
CUSTOMER: Olin Corp.
ATTN: Frank Bone
Central Receiving
RTE 148 South
Marion, IL 62959

DATE: February 12, 1988
DEPARTMENT: 285
CHARGE: NO CHARGE: X
CUST ORDER NO:
SALES ORDER NUMBER:
SHIPPING METHOD: UPS-2 day

MATERIAL	TYPE	AMOUNT
WN008FH	WHA-1069	10 pcs.

PROGRAM NUMBER: DAAL04-85-C-0023

TEST DESCRIPTION: P/N 924321-6, Print No. 8001466, WN008FH
30 mm Phalanx Penetrators - worked.

PROCESS COMMENTS:

DATA:

UTS (ksi)	166
YS (ksi)	151
EL (%)	22
Density (g/cc)	17.17
Impact (ft/lbs)	29
Hardness (R/C)	39.4

cc: E. L. Bok
D. P. Buttleman
D. R. Grover
F. B. Nair.
J. R. Spencer
V. P. Sylvester
S. R. Weigel - L.A

WRITTEN BY:

J. A. Mullendore

lw/1477.6-6

U.S. Army Materials Technology Laboratory
Watertown Massachusetts 02172-0001
RELATIONSHIP BETWEEN COMPOSITION, STRUCTURE, PROPERTIES, THERMO-MECHANICAL PROCESSING AND BALLISTIC PERFORMANCE OF TUNGSTEN HEAVY ALLOYS
James R. Spencer & James A. Mullendore
GTE Products Corporation
Chemical and Metallurgical Division
Towanda, Pennsylvania 18848

AD____________________
UNCLASSIFIED
UNLIMITED DISTRIBUTION

Key Words
Tungsten alloys
Composites
Microstructure
Impurities
Mechanical properties
Thermo-mechanical processing

Technical Report MTL TR 91-44 Nov. 1991 222pp
Contract DAAL04-86-C-0023
Final Report - March 1986 - July 1991

A through study of the W-Ni-Fe heavy alloy system was made relating composition, structure, impurity content and thermo-mechanical processing to mechanical properties. Also explored were additions of cobalt, rhenium and ruthenium to the W-Ni-Fe system. Ballistic testing was done on a wide range of alloys and processing conditions. Ballistic tests included a 20mm in house range, 30mm Phalanx, M791(25mm Bushmaster) and XM-881(long rod Bushmaster).

U.S. Army Materials Technology Laboratory
Watertown Massachusetts 02172-0001
RELATIONSHIP BETWEEN COMPOSITION, STRUCTURE, PROPERTIES, THERMO-MECHANICAL PROCESSING AND BALLISTIC PERFORMANCE OF TUNGSTEN HEAVY ALLOYS
James R. Spencer & James A. Mullendore
GTE Products Corporation
Chemical and Metallurgical Division
Towanda, Pennsylvania 18848

AD____________________
UNCLASSIFIED
UNLIMITED DISTRIBUTION

Key Words
Tungsten alloys
Composites
Microstructure
Impurities
Mechanical properties
Thermo-mechanical processing

Technical Report MTL TR 91-44 Nov. 1991 222pp
Contract DAAL04-86-C-0023
Final Report - March 1986 - July 1991

A through study of the W-Ni-Fe heavy alloy system was made relating composition, structure, impurity content and thermo-mechanical processing to mechanical properties. Also explored were additions of cobalt, rhenium and ruthenium to the W-Ni-Fe system. Ballistic testing was done on a wide range of alloys and processing conditions. Ballistic tests included a 20mm in house range, 30mm Phalanx, M791(25mm Bushmaster) and XM-881(long rod Bushmaster).

U.S. Army Materials Technology Laboratory
Watertown Massachusetts 02172-0001
RELATIONSHIP BETWEEN COMPOSITION, STRUCTURE, PROPERTIES, THERMO-MECHANICAL PROCESSING AND BALLISTIC PERFORMANCE OF TUNGSTEN HEAVY ALLOYS
James R. Spencer & James A. Mullendore
GTE Products Corporation
Chemical and Metallurgical Division
Towanda, Pennsylvania 18848

AD____________________
UNCLASSIFIED
UNLIMITED DISTRIBUTION

Key Words
Tungsten alloys
Composites
Microstructure
Impurities
Mechanical properties
Thermo-mechanical processing

Technical Report MTL TR 91-44 Nov. 1991 222pp
Contract DAAL04-86-C-0023
Final Report - March 1986 - July 1991

A through study of the W-Ni-Fe heavy alloy system was made relating composition, structure, impurity content and thermo-mechanical processing to mechanical properties. Also explored were additions of cobalt, rhenium and ruthenium to the W-Ni-Fe system. Ballistic testing was done on a wide range of alloys and processing conditions. Ballistic tests included a 20mm in house range, 30mm Phalanx, M791(25mm Bushmaster) and XM-881(long rod Bushmaster).

U.S. Army Materials Technology Laboratory
Watertown Massachusetts 02172-0001
RELATIONSHIP BETWEEN COMPOSITION, STRUCTURE, PROPERTIES, THERMO-MECHANICAL PROCESSING AND BALLISTIC PERFORMANCE OF TUNGSTEN HEAVY ALLOYS
James R. Spencer & James A. Mullendore
GTE Products Corporation
Chemical and Metallurgical Division
Towanda, Pennsylvania 18848

AD____________________
UNCLASSIFIED
UNLIMITED DISTRIBUTION

Key Words
Tungsten alloys
Composites
Microstructure
Impurities
Mechanical properties
Thermo-mechanical processing

Technical Report MTL TR 91-44 Nov. 1991 222pp
Contract DAAL04-86-C-0023
Final Report - March 1986 - July 1991

A through study of the W-Ni-Fe heavy alloy system was made relating composition, structure, impurity content and thermo-mechanical processing to mechanical properties. Also explored were additions of cobalt, rhenium and ruthenium to the W-Ni-Fe system. Ballistic testing was done on a wide range of alloys and processing conditions. Ballistic tests included a 20mm in house range, 30mm Phalanx, M791(25mm Bushmaster) and XM-881(long rod Bushmaster).

U.S. Army Materials Technology Laboratory
Watertown Massachusetts 02172-0001
RELATIONSHIP BETWEEN COMPOSITION, STRUCTURE, PROPERTIES, THERMO-MECHANICAL PROCESSING AND BALLISTIC PERFORMANCE OF TUNGSTEN HEAVY ALLOYS
James R. Spencer & James A. Mullendore
GTE Products Corporation
Chemical and Metallurgical Division
Towanda, Pennsylvania 18848

AD______________
UNCLASSIFIED
UNLIMITED DISTRIBUTION
Key Words
Tungsten alloys
Composites
Microstructure
Impurities
Mechanical properties
Thermo-mechanical processing

Technical Report MTL TR 91-44 Nov. 1991 222pp
Contract DAAL04-86-C-0023
Final Report - March 1986 - July 1991

A through study of the W-Ni-Fe heavy alloy system was made relating composition, structure, impurity content and thermo-mechanical processing to mechanical properties. Also explored were additions of cobalt, rhenium and ruthenium to the W-Ni-Fe system. Ballistic testing was done on a wide range of alloys and processing conditions. Ballistic tests included a 20mm in house range, 30mm Phalanx, M791(25mm Bushmaster) and XM-881(long rod Bushmaster).

U.S. Army Materials Technology Laboratory
Watertown Massachusetts 02172-0001
RELATIONSHIP BETWEEN COMPOSITION, STRUCTURE, PROPERTIES, THERMO-MECHANICAL PROCESSING AND BALLISTIC PERFORMANCE OF TUNGSTEN HEAVY ALLOYS
James R. Spencer & James A. Mullendore
GTE Products Corporation
Chemical and Metallurgical Division
Towanda, Pennsylvania 18848

AD______________
UNCLASSIFIED
UNLIMITED DISTRIBUTION
Key Words
Tungsten alloys
Composites
Microstructure
Impurities
Mechanical properties
Thermo-mechanical processing

Technical Report MTL TR 91-44 Nov. 1991 222pp
Contract DAAL04-86-C-0023
Final Report - March 1986 - July 1991

A through study of the W-Ni-Fe heavy alloy system was made relating composition, structure, impurity content and thermo-mechanical processing to mechanical properties. Also explored were additions of cobalt, rhenium and ruthenium to the W-Ni-Fe system. Ballistic testing was done on a wide range of alloys and processing conditions. Ballistic tests included a 20mm in house range, 30mm Phalanx, M791(25mm Bushmaster) and XM-881(long rod Bushmaster).

U.S. Army Materials Technology Laboratory
Watertown Massachusetts 02172-0001
RELATIONSHIP BETWEEN COMPOSITION, STRUCTURE, PROPERTIES, THERMO-MECHANICAL PROCESSING AND BALLISTIC PERFORMANCE OF TUNGSTEN HEAVY ALLOYS
James R. Spencer & James A. Mullendore
GTE Products Corporation
Chemical and Metallurgical Division
Towanda, Pennsylvania 18848

AD______________
UNCLASSIFIED
UNLIMITED DISTRIBUTION
Key Words
Tungsten alloys
Composites
Microstructure
Impurities
Mechanical properties
Thermo-mechanical processing

Technical Report MTL TR 91-44 Nov. 1991 222pp
Contract DAAL04-86-C-0023
Final Report - March 1986 - July 1991

A through study of the W-Ni-Fe heavy alloy system was made relating composition, structure, impurity content and thermo-mechanical processing to mechanical properties. Also explored were additions of cobalt, rhenium and ruthenium to the W-Ni-Fe system. Ballistic testing was done on a wide range of alloys and processing conditions. Ballistic tests included a 20mm in house range, 30mm Phalanx, M791(25mm Bushmaster) and XM-881(long rod Bushmaster).

U.S. Army Materials Technology Laboratory
Watertown Massachusetts 02172-0001
RELATIONSHIP BETWEEN COMPOSITION, STRUCTURE, PROPERTIES, THERMO-MECHANICAL PROCESSING AND BALLISTIC PERFORMANCE OF TUNGSTEN HEAVY ALLOYS
James R. Spencer & James A. Mullendore
GTE Products Corporation
Chemical and Metallurgical Division
Towanda, Pennsylvania 18848

AD______________
UNCLASSIFIED
UNLIMITED DISTRIBUTION
Key Words
Tungsten alloys
Composites
Microstructure
Impurities
Mechanical properties
Thermo-mechanical processing

Technical Report MTL TR 91-44 Nov. 1991 222pp
Contract DAAL04-86-C-0023
Final Report - March 1986 - July 1991

A through study of the W-Ni-Fe heavy alloy system was made relating composition, structure, impurity content and thermo-mechanical processing to mechanical properties. Also explored were additions of cobalt, rhenium and ruthenium to the W-Ni-Fe system. Ballistic testing was done on a wide range of alloys and processing conditions. Ballistic tests included a 20mm in house range, 30mm Phalanx, M791(25mm Bushmaster) and XM-881(long rod Bushmaster).

DISTRIBUTION LIST

1 Office of the Secretary of Defense for Research and Engineering, The Pentagon, Washington, D.C. 20301

Commander, U.S. Army Laboratory Command, 2800 Powder Mill Road, Adelphi, MD 20783-1145
1 ATTN: AMSLC-IM-TL
1 ATTN: AMSLC-CT

Commander, Defense Technical Information Center, Cameron Station, Building 5, 5010 Duke Street, Alexandria, VA 22304-6145
2 DTIC-FDAC

1 MIAC/CINDAS, Purdue University, 2595 Yeager Road, West Lafayette, IN 47905

Commander, Army Research Office, P.O. Box 12211, Research Triangle Park, NC 27709-2211
1 ATTN: Information Processing Office
1 Dr. Andrew Crowson
Dr. Edward Chen

Commander U.S. Army Materiel Command (AMC), 5001 Eisenhower Avenue, Alexandria, VA 22333
1 ATTN: AMCSCI

Commander, U.S. Army Materiel Systems Analysis Activity, Aberdeen Proving Ground, MD 21005
1 ATTN: AMXSY-MP, Director

Commander, U.S. Army Missile Command, Redstone Scientific Information Center, Redstone Arsenal, AL 35898-5241
1 ATTN: AMSMI-RD-CS-R/Doc

Commander, U.S. Army Armament Research Development and Engineering Center, Dover, NJ 07801
1 ATTN: Technical Library
1 Mr. D. Kapoor
1 Dr. S. Cytron

Commander, U.S. Army Tank-Automotive Command, Warren, MI 48397-5000
2 ATTN: AMSTA-TSL Technical Library

Commander, U.S. Army Foreign Science and Technology Center, 220 7th Street, N.E., Charlottesville, VA 22901
3 ATTN: AIFRTC, Applied Technologies Branch, Gerald Schlesinger

Naval Research Laboratory, Washington, D.C. 20375
1 ATTN: Code 5830
1 Code 2627

Chief of Naval Research, Arlington, VA 22217
1 ATTN: Code 471

Naval Surface Weapons Center, Dahlgren Laboratory, Dahlgren, VA 22448
1 ATTN: Code G-32, Ammunition Branch, Mr. Brian Sabourin

Commander, Rock Island Arsenal, Rock Island, IL 61299-6000
1 ATTN: SMCRI-SEM-T

Battelle Columbus Laboratories, Battelle Memorial Institute, 505 King Avenue, Columbus, OH 43201
1 ATTN: Mr. Henry Cialone
1 Dr. Alan Clauer

Battelle Pacific Northwest Laboratories, P.O. Box 999, Richland, WA 99352
1 ATTN: Mr. William Gurwell
1 Dr. Gordon Dudder

GTE Sylvania, Inc. Chemical and Metallurgical Division, Hawes Street, Towanda, PA 18848
1 ATTN: Dr. James Mullendore
1 Mr. James Spencer

Director, Ballistic Research Laboratory, Aberdeen Proving Ground, MD 21005
1 ATTN: SLCBR-TSB-S (STINFO)
1 SLCBR-TB-P, Mr. Lee Magness

Teledyne Firth Sterling, 1 Teledyne Place, LaVergne, TN 37086
1 ATTN: Dr. Steven Caldwell
1 Dr. Thomas Penrice

Technology Associates Corp., 17911 Sampson Lane, Huntington Beach, CA 92647
1 ATTN: Dr. Gary Allen

Los Alamos National Laboratory, ATAC, MS F681, P.O. Box 1663, Los Alamos, NM 87545
1 ATTN: Dr. Bill Hogan

Philips Elmet, 1560 Lisbon Road, Lewiston, ME 04240
1 ATTN: Mr. James Anderson

Ultramet, Inc., 12173 Montague Street, Pacoima, CA 91331
1 ATTN: Dr. J.J. Stiglich
1 Mr. Brian Williams
1 Dr. Robert Tuffias

Ceracon, Inc., 1101 N. Market Boulevard, Suite 9, Sacramento, CA 95834
1 ATTN: Dr. Ramas Raman

Southwest Research Institute, 6220 Culebra Road, P.O. Drawer 28510, San Antonio, TX 78228-0510
1 ATTN: Dr. Animesh Bose
1 Dr. James Lankford

Metalworking Technology, Inc., 1450 Scalp Avenue, Johnstown, PA 15904
1 ATTN: Mr. C. Buck Skena
1 Mr. Timothy McCabe

Research Triangle Institute, P.O. Box 12194, Research Triangle Park, NC 27709-2154
1 ATTN: Dr. John B. Posthill

3C Systems, 620 Arglye Road, Wynnewood, PA 19096
1 ATTN: Mr. Murray Kornhauser

Advance Technology Coatings, 300 Blue Smoke Ct. West, Fort Worth, TX 76105
1 ATTN: Mr. Grady Sheek

Alliant Techsystems, 7225 Northland Drive, Brooklyn Park, MN 55428
1 ATTN: Dr. Stan Nelson
1 Mr. MArk Jones
1 Mr. Thomas Steigauf

CAMDEC, 3002 Dow Avenue, Suite 110, Tustin, CA 92680
1 ATTN: Dr. Richard Harlow

Chamberlain Manufacturing Co., 550 Esther St., P.O. Box 2545, Waterloo, IA 50704
1 ATTN: Mr. Tom Lynch

Defense Technology International, Inc., The Stark House, 22 Concord Street, Nashua, NH
1 ATTN: Mr. Douglas Ayer

Materials and Electrochemical Research Corporation, 7960 S. Kolb Road, Tucson, AZ 85706
1 ATTN: Dr. James Withers
1 Dr. Sumit Guha

Materials Modification, Inc., P.O. Box 4817, Falls Church, Va 22044
1 ATTN: Dr. T.S. Sudarshan

Micro Materials Technology, 120-D Research Drive, Milford, CT 06460
1 ATTN: Dr. Richard Cheney

Nuclear Metals, 2229 Main Street, Concord, MA 01742
1 ATTN: Dr. Willian Nachtrab

Olin Ordnance, 10101 9th Street N., St. Petersburg, FL
1 ATTN: Hugh McElroy

The Pennsylvania State University, Department of Engineering Science and Mechanics, 227 Hammond Building, University Park, PA 16802-1401
1 ATTN: Dr. Randall M. German, Professor, Brush Chair in Materials

Director, U.S. Army Materials Technology Laboratory, Watertown, MA 02172-0001
2 ATTN: SLCMT-TML
1 SLCMT-IMA-V
1 SLCMT-PRC
15 SLCMT-MEM, Mr. Robert Dowding, Dr. Kenneth Tauer, COR

SUPPLEMENTARY

INFORMATION

ERRATA AD-A245849

REFERENCES

1. Proceedings of the High Density Penetrator Materials Conf., AMMRC SP-3 April, 1977.

2. Delai, A. J., "Fabrication Of High Density Tungsten Penetrator Materials", Proceedings of the High Density Penetrator Materials Conf., AMMRC SP-3 April, 1977.

3. Katlin, J. M. and Nowak S. P., "Simulated Scale Model High Density Penetrators for the 105mm XM735 Projectile", Proceedings of the High Density Penetrator Materials Conf., AMMRC SP-3 April, 1977.

4. Nowak, S. P. and Katlin, J. M., "Ballistic Evaluation Of Tungsten Materials As Penetrators Pertinent to 25-30mm Weapon Systems", Proceedings of the High Density Penetrator Materials Conf., AMMRC SP-3 April, 1977.

5. Chiao, W. F., and Larsen, F. R., "Matrix Chemistry and Mechanical Properties of High Density Tungsten Alloys", Proc. Of The Second High Density K. E. Penetrator Materials Conf., AMMRC MS 82-2, April 1982.

6. Northcutt Jr., W. G. and Snyder Jr. W. B., "Process for Fabricating Articles of Tungsten-Nickel-Iron Alloy", USP 3,979,234, September 7, 1976.

7. Spencer, J. R., "Tungsten Alloy Fabrication of Penetrator Materials", AMMRC TR 81-40, Aug. 1981.

8. Edmonds D. V., and Jones P. N., "Interfacial Embrittlement in Liquid-Phase Sintered Tungsten Heavy Alloys", Metallurgical Transactions, Volume 10A, March 1979.

9. German, R. M., et al, "Toughness Variations with Test Temperature and Cooling Rate for Liquid-Phase Sintered W- 3.5Ni-1.5Fe", Metallurgical Transactions Volume 15A, 1984.

10. Bloore, E. W. et al, "Design and Development of the Silver Bullet APFSDS Penetrator for the 105mm M68 Gun." BRL MR2503 ADC010690, November 1976.and private communication.

11. Lux,B.,et al, "The Influence of Chemistry and Various Fabrication Parameters on the Properties of Tungsten Heavy Metals", DTIC TR AD AO 99799 ,Feb. 1981.

12. Dickinson, J. M., et al, "Strengthening of Liquid Sintered Tungsten Alloys", Modern Developments In Powder Metallurgy Volume 6, p329, ed H. Hausner, and W. E. Smith, MPIF, Princeton, N.J., 1974.

13. Northcutt Jr., W. G., "Reduced Sintering Distortion in Tungsten-Nickel-Iron Alloys by Use of Alloying Additions". Y/DA-7117, March 8, 1977.

14. Guillermet, A. F., and Ostlund, L., "Experimental and Theoretical Study of the Phase Equilibria in the Fe-Ni-W System", Metallurgical Transactions A, Volume 17A, October 1986.

15. Zukas, E. G., et al, "Spheroid Growth by Coalescence During Liquid-Phase Sintering", Z. Metallkde. Bd. 67(1976)H.9.